ZANCO (Print Version: ISSN 2218-0230)
(Online Version: ISSN 2412-3986)
(DOI : 10 . 21271 / ZJPAS)

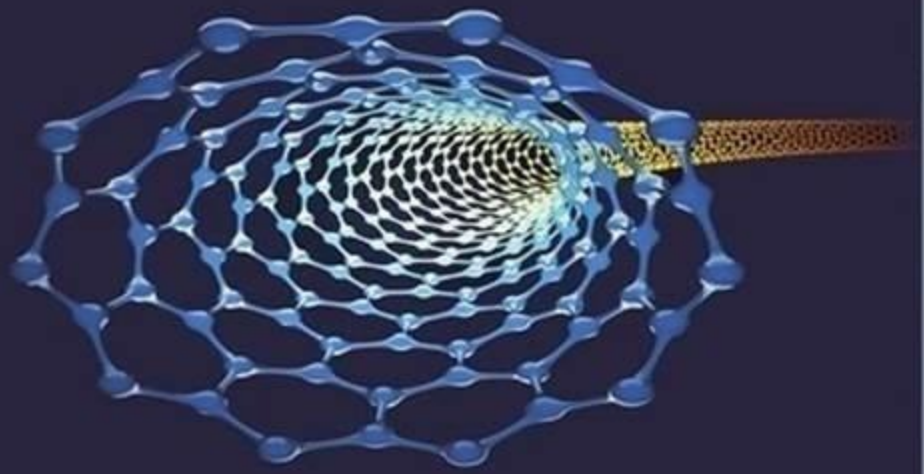

زانکۆی سەلاحەدین - هەولێر
Salahaddin University-Erbil

Volume 31,Number 4, 2019

ZANCO Journal of Pure and Applied Sciences

ZANCO

Journal of Pure and Applied Sciences

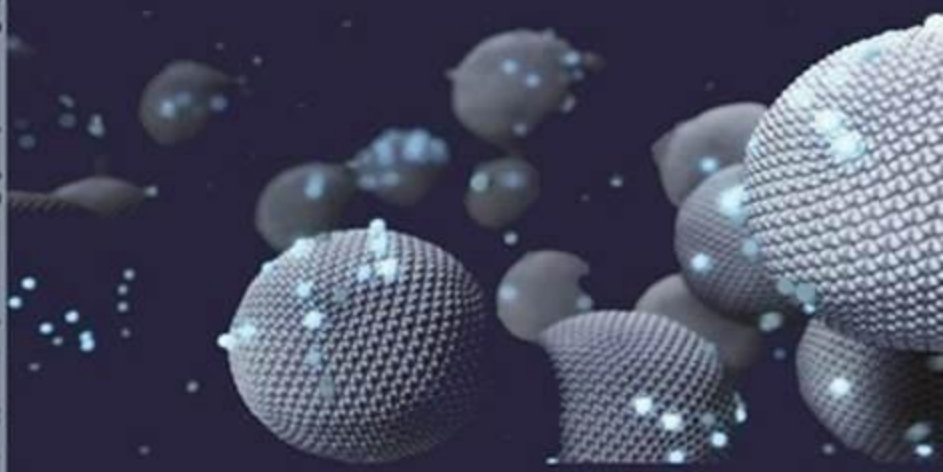

زانکۆی سەلاحەدین - هەولێر
Salahaddin University-Erbil

Volume 31,number 4, 2019

ZANCO Journal of Pure and Applied Sciences
The official scientific journal of Salahaddin University-Erbil
https://zancojournals.su.edu.krd/index.php/JPAS

ISSN (print):2218-0230**, ISSN (online):** 2412-3986**, DOI: http://dx.doi.org/10.21271/zjpas**

RESEARCH PAPER

Isolation, Identification and Antifungal Susceptibility Testing of *Candida* Species from Dermatologic Specimens in Duhok Province

Adar S. Saeed[1], Asia A. M. Saadullah[2]
[1&2,] Department of Biology, College of Sciences, University of Duhok, Kurdistan Region / Iraq

A B S T R A C T:

Candida species. is a member of the mucous membrane of the normal flora, gastrointestinal tract and skin. They are endogenous opportunistic pathogens that cause secondary infections with underlying immunocompromised condition. Candidiasis is a common fungal infection in human. This study was aimed to isolation and identification of *Candida* using germ tube, chlamydospore formation, and chromogenic agar testes and to asses antifungal susceptibility to some isolates. A total of 180 samples of skin swabs and skin particles, nail and hair were collected from patients in Duhok Province Hospitals, outpatient and a number of private clinic dermatologists in Duhok city. A Total of 63 *Candida* isolates was detected in this study. These isolates were subjected to germ tube test, chlamydospores formation and inoculation on commercially available CHROMagar. *Candida* albicans was the main yeast species isolated followed by *C. krusei*, *C. tropicalis* and *C. glabrata* CHROMO agar is a convenient and very fast method of identifications of *Candida* species even in resources poor settings. The result of antifungal sensitivity test revealed that itraconazole is the main active antifungal against all *Candida* species with the minimum inhibition concentration (MIC) of 25 µg /ml. followed by terbinafine, fluconazole and griseofulvin.

KEY WORDS: *Candida*, Non- albicans *Candida*, CHROM agar, Duhok province.
DOI: http://dx.doi.org/10.21271/ZJPAS.31.4.1
ZJPAS (2019) , 31(4);1-8 .

1. INTRODUCTION:

Candidiasis refers to fungal infection caused by several species related to genus *Candida*. The Incidence of Candidiasis is increasing worldwide. The infections by *Candida* increased dramatically in their prevalence during the past 20 years (Kim et al., 2016). *Candida* species are the main common causes of the fungal infections. The species of *Candida* produce infections ranges from superficial mucosal infections, cutaneous to invasive and non–life-threatening mucocutaneous infections that may involve substantially any organ that caused by alteration of immune defences (Dabas, 2013).

* **Corresponding Author:**
Adar S. Saeed1
E-mail: asiasaadullah73@yahoo.com
Article History:
Received: 23/01/2019
Accepted: 04/03/2019
Published: 10/09 /2019

Recently, *Candida albicans* is the most common opportunistic invaders in humans and is associated with nearly (60-80) % of the nosocomial fungal infection), that can increase mortality and morbidity in hospitalized patients (Pappas et al., 2004; Kim and Sudbery, 2011).

There are many conditions in which the normal balance between the host and *Candida* is change and leads to pathologic situation: elders, diabetes, pregnancy, malignancy, steroid therapy, extensive administration of antibiotics, and AIDS. *Candida* infections constitutes the main widely recognized fungal infection in AIDS patients. (Hasan et al., (2009); Fidel, (2006). During last decades an increase of prevalence of non-albicans *Candida* (NAC) species have been noticed (Mokaddas et al.,2007, Srinivasan et al.,2006)

Together with the *C. albicans* there has been a greater concern of the importance of the non-

albicans *Candida* species (NAC) in human disease mainly *C. glabrata* and *C. krusei*. These species have received awareness because it promotes resistance to different antifungal agents (Rajeswari et al., 2018).

The traditional methods for identification of *Candida* isolates to species level has done using germ tube test, fermentation tests, sugar assimilations and chlamydospore formation. Recently newer methods include CHROM agar, Viteks 2 / ID system, API (Analytical Profile Index) system, and molecular techniques have been widely employed (Jain et al., 2012). Since Vitek 2ID system, API system, and molecular techniques are expensive and time consuming, use of CHROM Agar for species identification would be of benefit and useful for rapid and easy differentiation (Abdel et al.,2007).

The CHROMagar contain chromogenic substances that reacts with *Candida* secreted enzymes and produces different pigmentation of colonies. These Enzymes are species specific, allowing fungus to be identified to a species level by their colony characteristics and color (Mehta and Anupama, 2016).

The identification of non- albicans *Candida* species is very important. CHROM agar as a selective medium is used to identify a clinically *Candida* species. according to growth color and other characteristics (Lymn et al., 2003). It is useful to detect mixed cultures of *candida* in clinical samples.

The present study aimed to isolation and identification of *Candida* species in Duhok hospitals using germ tube test, chlamydospores formation and CHROMagar to asses antifungal susceptibility of some isolates against various antifungal.

2. MATERIALS AND METHODS

2.1 Samples Collection

From Azadi Teaching Hospital, outpatient and a number of private dermatophyte clinics dermatologists in Duhok city, 180 samples including hair, nail, skin scraping and skin swabs were collected also from patients with suspected candidiasis in these tissues and ages from 1 to 61 and above years, samples were obtained during February 5th to June 5th/2018 by using sterilized fine scissors, forceps, nail clipper, scalpel blades, and 70% ethanol.

Appropriate material including skin scrapings, hair or nail clippings were taken from the infected tissues, which were treated with 70% ethanol prior of sample collection. Out of the material collected, part of it was used for direct potassium hydroxide (KOH) examination and remaining part was used to inoculate SDA, Potato Dextrose Agar (PDA) and Malt Extract Agar (MEA) medium for culture and isolation causative fungi.

2.2 Direct Examination

Direct microscopic examination was carried out for samples (skin scraping and nails) were placed on a clean glass slide; then a drop of 10% KOH was added to them. A clean cover slip was placed on the sample and with gentle pressure to prevent the air bubbles formation. The slide was examined by using light microscope. This allows complete visualization of pseudohyphae as well as the budding oval yeasts cells, (Dismukes et al., 2003; Shamim et al., 2005; Singh and Beena, 2003) which corresponds to various *Candida* species.

2.3 Cultures Media

All the collected samples of hair, nail and skin were inoculated directly, on Potato Dextrose Agar (PDA), Malt Extract Agar (MEA) and Sabouraud Dextrose Agar (SDA) containing chloramphenicol 0.5 g/ml was added to prevent bacterial contamination. To prevent the growth of saprophytic fungi, cycloheximide (Actidione) 0.05 g/l was added to SDA (Campbell et al., 2013). The inoculated plates were incubated for 48hrs. The three media (SDA (CONDA, Spain)), PDA (LAB-M, UK) and MEA (LAB-M, UK)) were prepared as per instructions provided by manufacturers.

2.4 Germ Tube test (GTT)

This test is a rapid method for differentiation between *Candida dubliniensis* and *Candida albicans* by its efficiency to produce short, tube, delicate like structure known as germ tubes when it is incubated in serum of human blood at 37 ℃ for two hours. Germ tubes differs from pseudo-hyphae because it is elongations of daughter cells from the mother cell without shrinkages at the origins (Aryal, 2015; Deorukhkar and Saini, 2014).

2.5 Chlamydospores formation

An isolated colony from the primary culture medium was obtained. The plate of cornmeal agar was inoculated by making three parallel streaks about half inch apart at a 45 angle to the culture medium. Formation of large, highly retractile, thick walled, terminal spore was called chlamydospore. The test was used for the identification of *C. albicans* (Yadav et al., 2018).

2.6 CHROM agar *Candida* / culture media

All colonies of *Candida* isolates on SDA, MEA and PDA were sub cultured by streaking a loop full of culture on to CHROMagar *Candida* medium and incubate at 37 ℃ for 48 hours. This is a selective and differential medium which assist rapid isolation and presumptive identifications of many clinically important *Candida* species on the bases of colonies color and characteristics types.

As per manufacturer's instructions (ACUMEDIA –LAB, NEOGEN –UK). (Table 1). CHROMagar medium contain chromogenic substrate which react with the secreted enzymes by *Candida* species to yield colonies of different pigmentation, which allow to species identification as described by Odds and Bernarets,1994; Mathavi et al., 2016).

2.7 Antifungal susceptibility

Antifungal susceptibility test is a method used to detect antifungal resistance and it used to detect the preferable treatment for a specific fungus. In vitro susceptibility tests are available for patient care determination, for drug discovery and development or used in epidemiological studies. Clinical microbiology depends on these methods to choose the agent for a fungal infection, and also to recognize the global and the local epidemiology of antifungal resistance.

However, microdilution methods are the reference techniques or gold standard. Two organizations, the Clinical Laboratory Standards Institute (CLSI) and the European Committee on Antibiotic Susceptibility Test (EUCAST) have standardized methods to proceed antifungal susceptibility testing (Alastruey-Izquierdo et al., 2015).

2.8 Agar well diffusion method

Agar well diffusion method was used to estimate the activity of antimicrobial agent. Which similar to disk-diffusion method procedure, this test is performed using Casitone Agar. The inoculation of agar plate surface is performed by spreading 0.1 ml of the inoculum of microbial over the entire agar surface. Consequently, a hole with a diameter of 6 millimetres is punched aseptically by an antiseptic cork borer, and then a volume of 100 µL of the antimicrobial agent is subjected to the well. Furthermore, under suitable conditions agar plates are incubated, bases on the tested microorganism. The antimicrobial agent distributes in the medium and prevent the growth of the tested isolate (Balouiri et al., 2016).

3. RESULTS AND DISCUSSION

A total of 63 *Candida* isolates was obtained from diverse dermatological specimens including nail, skin particles and skin swabs. The majority of the isolates were from skin particles 33 (52.4%) followed by nail samples 15 (23.8%) and skin swabs 15 (23.8%) shown in table 2. All the samples were directly cultured on Sabouraud Dextrose Agar (SDA) containing antibacterial antibiotics chloramphenicol and cycloheximide the identification of the *Candida* species was performed depending on growth characteristics, chlamydospores formation and germ tube formation as well as CHROMO agar.

On Sabouraud Dextrose Agar (SDA) media, the colonies of *Candida* species were slimy, white to creamy, soft, round, and wrinkled to smooth, with a characteristic yeast (figure 1) grow rapidly during 2-3 days. Lactophenol cottons blue stain examinations of *Candida* isolates showed oval to spherical, with a presence of some budding (figure 2).

The germ tube test (GTT) formed within two hour of incubation and this is a differential *Candida* dubliniensis and *Candida albicans* (figure 3) .The results of this study revealed all *Candida albicans* were positive for germ tube test and in agreement with that found by Sheppard et al., (2008), they mentioned all *C. albicans* isolates were positive for germ tubes test when tested directly from the colony, while all non- species of albicans were negative to germ tube test when tested directly.

Distribution of samples of *Candida* isolates in Table 3. *Candida albicans* 33 (52.4%) was the most common isolated species. Among the non-albicans *Candida*, *C. krusei* 13 (20.6%), *C. tropicales* 9 (14.3%) and *C. glabarata* 8 (12.7%). As shown in the present study *Candida albicans* is predominant among all isolated species, same prominence was seen also by Srinivasan, (2006) however, higher incidence of non-albicans *Candida* had been recorded in many studies. *Candida krusei* was reported to be as the most identified species followed by *C. tropicalies*. The lowest incidence rate was *C. glabrata*. Similar results had been seen by Yucesoy and Marol, 2003.

Non-albicans *Candida* species are on the rises because of the increasing immunocompromised conditions, patient receiving prolonged antibacterial and offensive cancer chemotherapy, organ transplantation or undergoing invasive surgical procedure. (Mohandas and Ballal, 2011). Several studies have shown a considerable increase of the non-albicans *Candida* infections.

Different species of *Candida* previously known to causes an epidemic disease of animals in laboratory and in humans onychomycosis, has emerged as an opportunistic fungal pathogen capable of causing outbreaks of fungemia (Jaya and Harita, 2013).

Conventional speciation of *Candida* isolates was performed by germ tube test and chlamydospore formation which shown in Figure 4. These tests are laborious and time consuming. CHROM agar is a fast method to spectate the various *Candida* species. It facilitates the detection and identification of *Candida* species from mixed culture and provides results within 24- 48 hours.

All *Candida* isolates were positive for the germ tube test and they all showed distinguished growth on both 37°C and 45°C, while Non-albicans *Candida* are all negative for the previous test therefore, the CHROM agar was used to set up their identification.

This medium was originally developed for presumptive identification and selective isolation for many important clinically yeasts species for example *C. tropicales, C. glabrata, C. albicans* and *C. krusei* depending on the basis of differences in surface of colonies and color as shown in Figure 5 (Tornai-Lehoczki and Dlauchy, 2003).

The recent study confirmed the previous investigations concerning the high accuracy of CHROMagar medium. We found assumed identification of 100% of *C. albicans* isolates, *C. tropicalies*, *C. glabrata* and *C. krusei* isolates. None of the remaining species was misidentified as one of the four species. The results of this study confirmed those of Odds and Bernarets, (1994).

To differentiate between *Candida* with no requirement for germ tube confirmation test the most successful detector is CHROMagar-*Candida* test which has been reported by Odd et al., 1994.

The result of our study is in agreement with many previous studies. Mathavi and Priyadarsini, 2016 have reported that although the CHROMagar *Candida* is not only a simple, cost/ effective and reliable method for the identification of chlamydospore-negative atypical *C. albicanes*, but it is also used to differentiate different groups of chlamydospores negative *Candida* species.

3.1 Antifungal Susceptibility Test

Antifungal susceptibility testing was performed using four common antifungal drugs in the current study (Terbinafine, Itraconazole, Fluconazole, and griseofulvin) by using well diffusion method to determine minimum inhibition concentration (MIC) for each antifungal

Four pathogenic isolates of yeasts include *C. albicans, C. krusei, C. tropicalis, C. glabrata* were tested for their in-vitro sensitivity to selected antifungal drugs.

3.1.1 Terbinafine

The results in table 4, shows that *Candida krusei* (Figure 6 A) and *Candida tropicalis* had MIC at (25μg /ml) as well as *Candida albicans* and *Candida glabrata* had MIC at (50 μg /ml) and both had resistance at 25 μg /ml. The results were compatible with the study of Abdullah and Saadullah, (2017) in Duhok who found that *C. glabrata* had MIC of terbinafine at 100 μg /ml.

Terbinafine is the major agents of allylamines. It inhibits the synthesis of ergosterol, a key sterol component in the plasma membrane of the fungal cell. Terbinafine inhibits its squalene epoxidase, the enzyme which catalyses the conversion of squalene to squalene-2,3 epoxide, a precursor of lanosterol, which in turn is a direct

precursor of ergosterol. It can be found topical and oral (Dismukes et al., 2003).

3.1.2 Itraconazole

The results of itraconazole against *Candida* species were shown in table 4. That all isolates had MIC at (25 µg /ml) successfully (figure 6 B). Our findings are in agreement with sabaly, (2014) in Duhok which found MIC of itraconazole at different concentration.

Itraconazole is a member of Azole family, are active against a wide spectrum of pathogenic fungi, encompassing *Candida* species and dermatophytes.

Whole azole antifungal agents share same primary, common mechanism of action, which inhibits cytochrome P450-dependent enzyme lanosterol 14 alpha-demethylase. This is essential enzyme to convert lanosterol to ergosterol, avital component of the fungl membrane, which lead to cell membrane disruption by rising in permeability, that result in cell lysis and death (Wormser et al., 2010).

3.1.3 Fluconazole

So, *Candida albicans* (figure 6 C), *Candida tropicalis* and *Candida glabrata* had showed MIC at (25 µg /ml). on the other hand, *Candida krusei* had MIC at (75 µg /ml) concentration only that is shown in Table 4. However, the results were contradictory to a study by Ali et al., (2018) in Baghdad which found fluconazole is ineffective against *Candida* species.

The antifungal spectrum of fluconazole is less than that of other azoles. It has excellent activity against most *Candida* species (Schaechter et al., 2007). Fluconazole is used for candidiasis, urinary tract infection, onychomycosis and peritonitis (Sheppard and Lampiris, 1998).

3.1.4 Griseofulvin

The table 4 shows the results of antifungal griseofulvin against *Candida* species isolates, which reveal all resistance to griseofulvin at different concentration (Figure 6 D). Nowadays, the use of griseofulvin has largely been supplanted by terbinafine and itraconazole (Schaechter et al., 2007).

Griseofulvin is an oral agent used only for treatment of superficial dermatophyte infections. And is not active in vitro against *Candida* species. Griseofulvin's mechanism of action prevent cellular mitotic division by effecting on microtubules, but it is deposited in newly forming skin where it binds to keratin, protecting the skin from new infection. Because its action is to prevent infection of these new skin structures, griseofulvin must be administered for 2–6 weeks for skin and hair infections to allow the replacement of infected keratin by the resistant structures (Schaechter et al., 2007, Katzung et al., 2015, Dismukes et al., 2003).

4. CONCLUSIONS

The present study reveals that the most frequently isolated *candida* species from dermatologic specimens was *C. albicans* followed by nonalbicans *Candida* these are confirmed using CHROMagar *Candida* medium. It is important to increase the awareness of the public concerning the infection by *Candida* and this can be achieved carried out by predominantly designed educational program.

Acknowledgements

I have to express my highly appreciate to incredible role of my supervisor for the persistent support to my master study. I am grateful to the staff of the Biology Department/College of Science. I owe an appreciation to Mevan Jacksi for his constant encouragement, great sacrifice and unconditional supports.

Conflict of Interest (1)

Table (1) Color of different *Candida* species. on CHROM agar for identifications

Name	Colour on CHROMO agar
Candida albicans	Green
Candida tropicales	Blue
Candida krusei	Purple-Pink
***Candida* glabrata**	White-Purple

Table (2) Distribution of *Candida* isolates in different dermatologic samples

Samples	Number of *Candida* isolate
Skin	33
Nail	15
Skin swap	15
Hair	None
Total	63

Table (3) Distributions of *Candida* isolates in different dermatologic sample

Samples (source)	*C. albicanes*	*C. glabrata*	*C. tropicales*	*C. Kruseei*
Skin	19 (57.6%)	5 (62.5%)	1 (11.1%)	7 (53.8%)
Nail	5 (15.2%)	2 (25%)	5 (55.6%)	4 (30.8%)
Skin swap	9 (27.3%)	1 (12.5%)	3 (33.3%)	2 (15.4%)
Hair	0 (0%)	0 (0%)	0 (0%)	0 (0%)
Total	33 (52.4%)	8 (12.7%)	9 (14.3%)	13 (20.6%)

Table (4) Total phenolic content of two medicinal bulb extracts in different solvents

Fungal isolates	MIC of terbinafine (µg /ml)	MIC of Itraconazole (µg /ml)	MIC of Fluconazole (µg /ml)	MIC of Griseofulvin (µg /ml)
C. krusei	25	25	75	-
C. albicans	50	25	25	-
C. glabrata	50	25	25	-
C. tropicalis	25	25	25	-

Figure 1: Creamed colored colonies on SDA.

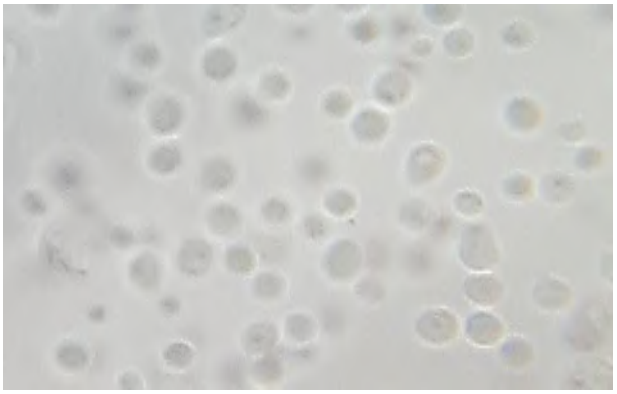

Figure 2: *Candida* Under Microscope

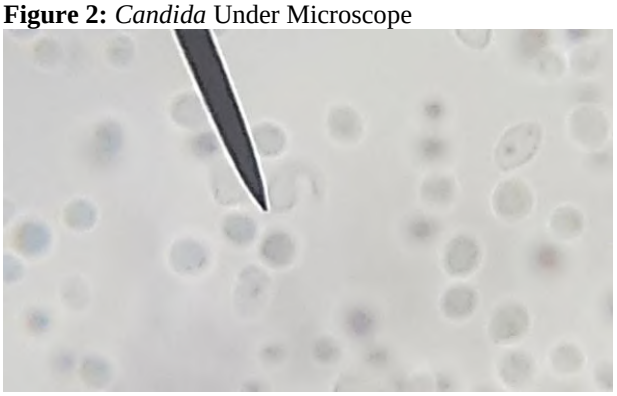

Figure 3: Germ tube test for *Candida*

Figure 4: Chlamydospore formation under 40X light mictoscopy

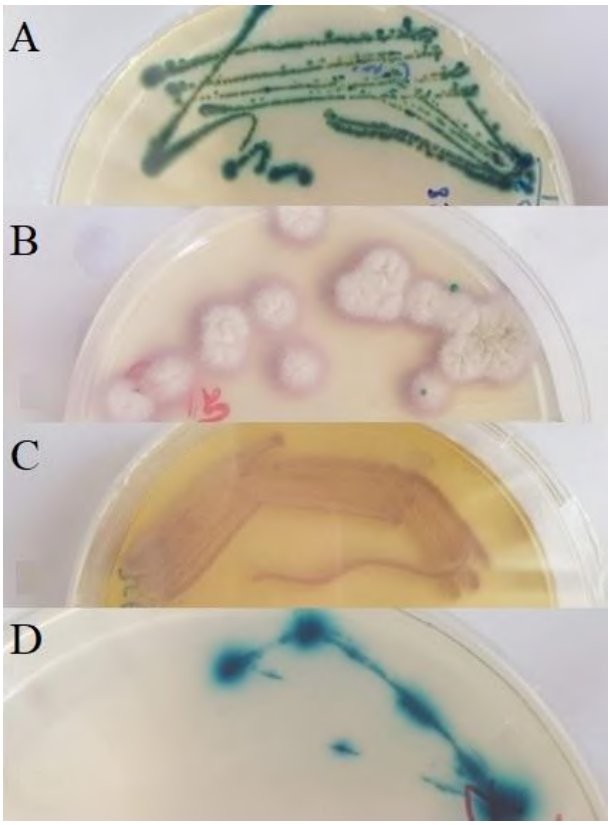

Figure 5: (A) C. albicans on CHROM agar (B) C. glabrata on CHROMagar (C) C. krusie on CHROMagar (D) C. tropicalis on CHROM agar

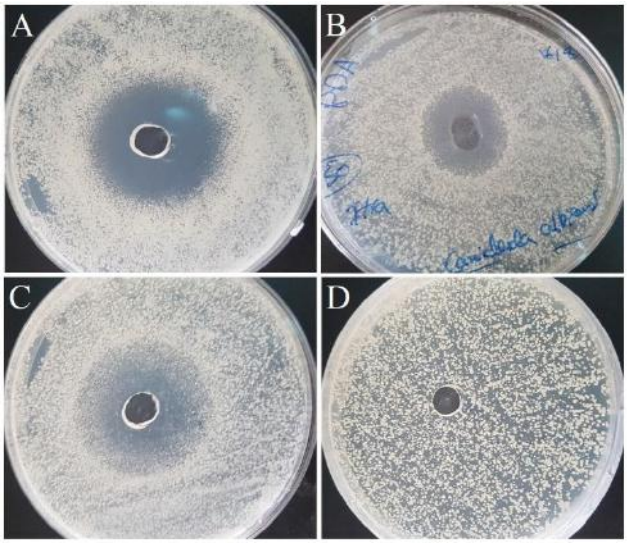

Figure 6: Susceptibility test results of (A) *Candida* krusei to antifungal Terbinafine at 100 µg /ml (B) *Candida* albican to antifungal Itraconazole at 50 µg /ml (C) *Candida* albicans to antifungal Fluconazole at 75 µg /ml (D) *Candida* krusei to antifungal Griseofulvin at 25 µg /ml

References

Abdel AM,; Taha AM, Mashal NE and Shabrawy, W.E .(2007). Antifungal susceptibility testing: New trends. Egyptian Dermatol Online J.3(1):1.

Aryal, S. (2015). Germ tube test-principle, procedure, results, interpretation and limitation. Online Microbiology Notes. Pp. 3. http://www.microbiologyinfo.com.

Balouiri, M., Sadiki, M., & Ibnsouda, S. K. (2016). Methods for in vitro evaluating antimicrobial activity: A review. Journal of pharmaceutical analysis, 6(2), 71-79.

Campbell, C. K.; Johnson, E. M. and Warnock, D. W. (2013). Identification of Pathogenic Fungi. Second edition. Health Protection AgencyBlackwell. UK.

Dabas, P. S. (2013). An approach to etiology, diagnosis and management of different types of candidiasis. Journal Of Yeast And Fungal Research, 4(6), 63-74.

Deorukhkar, S. and Saini, S. (2014). Laboratory approach for diagnosis of candidiasis through ages. Int. J. Microbiol. App. Sci. 3(1): 206-218.

Dismukes, W. E.; Pappas, P. G. and Sobel, J. D. (2003). Clinical Mycology.Oxford University Press, Inc. New York.

Fidel. PL. (2006). *Candida*-host interactions in HIV disease: relationships in oropharyngeal candidiasis. Adv Dent Res 19: 80-84.

Fotedar, R., and Al-Hedaithy, S.S.,(2003) "Identification of chlamydospores-negative *Candida* albicans using CHROM Agar-*Candida* medium" Mycoses, 46, 96-103.

Hasan F, Xess I, Wang X. (2009) Biofilm formation in clinical *Candida* isolates and its association with virulence. Microbes Infect 11: 753-761.

Jain N, Mathur P, Misra MC, Behera B, Xess I and Sharma SP. (2012). Rapid identification of yeast isolates from clinical specimens in critically ill trauma ICU patients. J Lab Physicians. 4(1):30-4.

Jaya, S and Harita ,V.,(2013) *Candida* Species Isolated from Various Clinical Samples and Their Susceptibility Patterns to Antifungals. JoMMID 2013, 1(1): 22-26

Katzung, B. G., & Trevor, A. J. (Eds.). (2015). Basic & clinical pharmacology (pp. 753-756). New York, NY: McGraw-Hill.ANALYSIS, 6(9).

Kim, J. and Sudbery, P. (2011). *Candida* albicans, a major human fungal pathogen. The Journal of Microbiology, 49(2), 171.

Kim, G. Y., Jeon, J. S., and Kim, J. K. (2016). Isolation frequency characteristics of *Candida* species from clinical specimens. Mycobiology, 44(2), 99-104.

Lymn LH, Duane RH, Eliriton KM and Dooley D. (2003). Direct isolation of *Candida* spp from blood culture on the chromogenic medium CHROM agar *Candida*. J Clin Microbiol. 41(6):2629-32.

Mathavi, S. , Sasikala, G. , Kavitha, A. and, R. I. (2016). CHROMagar as a primary isolation medium for

rapid identification of *Candida* and its role in mixed *Candida* infection in sputum samples. Indian J. Mirobiol. Res. 3(2):141-144.

Mehta, R., and Anupama, S. W. (2016). Evaluation of hicrome *candida* differential agar for species identification of *candida* isolates from various clinical samples. International Journal of Contemporary Medical Research, 3(4), 1219-22.

Mohandas V, BallalM. (2011). Distribution of *Candida* species in different clinical samples and their virulence:Biofilm formation, proteinase and phospholipase production: A study on hospitalized patients in Southern India. J Glob Infect Dis. 3(1): 4-8.

Mokaddas EM, Al-Sweith NA and Khan ZU.(2007). Species distribution and antifungal susceptibility of *Candida* bloodstream isolates in Kuwait: a 10-years study. J Med Microbiol.56:255-9.

Odds FC and Bernarets R.,(1994) CHROMagar *Candida*, a new differential isolation medium for presumptive identification of clinically important *Candida* species. J CIin Microbiol 32.1923-1929.

Pappas, P. G., Rex, J. H., Sobel, J. D., Filler, S. G., Dismukes, W. E., Walsh, T. J., & Edwards, J. E. (2004). Guidelines for treatment of candidiasis. Clinical Infectious Diseases, 38(2), 161-189.

Rajeswari. M.R. , Kalyani. M. , Hanumanthappa. A.R. , Vijayaraghavan. R., Lava. R. (2018). Detection of Virulence Factors in *Candida* Isolated from Different Clinical Specimens. IJBPAS, 7(3): 378-390

Schaechter, M., Engleberg, N. C., DiRita, V. J., & Dermody, T. (2007). Schaechter's mechanisms of microbial disease (p. 28). Lippincott Williams & Wilkins, Hagerstown, MD.

Shamim, S. U. M. B. U. L., Ahmed, S. W., Siddiqui, S. A., & Azhar, I. Q. B. A. L. (2005). Superficial mycoses: a study performed for the isolation and identification of fungal species from infected patients. Pakistan Journal of Pharmacology, 22(1), 41-46.

Sheppard, D. and Lampriis, H.W. (1998). Antifungal agents. Ini B.G. Katznny(Ed.). Basic and clinical pharmacology. 7th edn. Pp. 780-787. McGrew-Hill.Newyork.

Sheppard, Marie-Claude Locas, Christiane Restieri. (2008). Utility of the Germ Tube Test for Direct Identification of *Candida* albicans from Positive Blood Culture Bottles. J ClinMicrobiol 46: 3508-3509.

Singh, S. and Beena, P. (2003). Comparative Study of Different Microscopic Techniques and Culture Media for the Isolation of Dermatophytes.Indian Journal of Medical Microbiology. 21(1):21-24.

Srinivasan L, Kenneth J. (2006). Antibiotic susceptibility of *Candida* isolates in a tertiary care hospital in Southern India. Ind J Med Microbiol. 224:1-8.

Tornai-Lehoczki, J., Peter, G. and Dlauchy, D.,(2003) "CHROMAgar-*Candida* medium as a practical tool for the differentiation and presumptive identification of yeast species isolated from salads" Int. J. Food Microbiol., 86, 189-200,.

Wormser, G. P., & Kan, V. L. (2010). Antifungal Therapy Edited by Mahmoud A. Ghannoum John R. Perfect New York, NY: Informa Healthcare, 2010. 472 pp.

Yadav, R., Sujatha, R., & Kumar, A. (2018). Incidence of *Candida* Infection In Oral Cancer Patients Pre And Post Radiotherapy Treatment At A Tertiary Care Centre In Kanpur. Global Journal For Research analysis. 6(9).

Year, H., Poulain, D. and Lefebvre, A.,(2004) "Polymicrobial candidemia revealed by peripheral blood smear and chromogenic medium" J. Clin. Pathol., 57, 196-198,

Yucesoy, M. and Marol, S.,(2003) "Performance of CHROMagar and BIGGY agar for identification of yeast species" Ann. Clin. Microbiol. Antimicrob., 2(8), 1-7.

ZANCO Journal of Pure and Applied Sciences
The official scientific journal of Salahaddin University-Erbil
https://zancojournals.su.edu.krd/index.php/JPAS

ISSN (print):2218-0230**, ISSN (online):** 2412-3986**, DOI: http://dx.doi.org/10.21271/zjpas**

RESEARCH PAPER

Biofilm Forming Capability, Multidrug Resistance and Detection of Associated Genes in Uropathogenic *Escherichia coli* isolated from Catheterized Patients

Iman A. Muhammad[1] and Daristan J. Ghareb[2]

1&2 Department of Biology, College of Science, Salahaddin University-Erbil, Kurdistan Region, Iraq

A B S T R A C T:

Urinary tract infection (UTI) is one of the most widely recognized bacterial infections worldwide. Uropathogenic *Escherichia coli* (UPEC) is one of the main causative agents for nosocomial UTI. The microbial biofilms cause a public health problem to persons who require indwelling medical devices such as a urinary catheter. The pathogens in biofilms are protected from unfavorable conditions, antibiotic therapies and the host's immune system. The aim of the present study was to detect biofilm producer isolates, find out the correlation between biofilm production and associated virulence genes, and determination of antimicrobial susceptibility pattern of *E. coli* isolates isolated from the catheterized patient. In this study, we examined 43 isolates of *E. coli* collected from catheterized patients at three hospitals inside Erbil city during 25 of March to 23 of July 2018. All isolates were 100% biofilm producers using 96-well flat bottomed microtiter plate method. Also, molecular detection of *uspA* gene was performed as a species-specific PCR based marker for molecular identification of *E. coli*. *fimH* and *papC* genes were detected in 100% and 79% of the isolates respectively, as two adhesion genes responsible for biofilm formation. Minimal inhibitory concentrations (MIC_{50} and MIC_{90}) were defined as the lowest concentration of antimicrobials which show 50% and 90% inhibition of planktonic form and (BIC_{50}, BIC_{90}) were biofilm inhibitory concentration. All isolates were 100% resistant for Ceftriaxone, Ciprofloxacin, Levofloxacin and Cotrimoxazole. While the most effective antimicrobial agent used in the current study was Nitrofurantoin. Furthermore, most of isolates in the biofilm form were more resistant to antimicrobial agents than those of the planktonic form. Additionally, there was a positive relationship between the adhesion genes and the capacity to produce biofilm in UPEC.

KEY WORDS: UPEC, catheter , biofilm, adhesion gene, MIC, BIC.
DOI: http://dx.doi.org/10.21271/ZJPAS.31.4.2
ZJPAS (2019) , 31(4);9-22 .

1.INTRODUCTION :

Urinary tract infection is an important infection in humans, account for over 150 million cases worldwide (Terlizzi *et al*., 2017). Besides that UTI is the most distributed infections also reported as 36% of all health-care-associated infections (HAI) and 80% of them were expected to be catheter-associated (Parker *et al*., 2017) have an indwelling urinary catheter at the time or within 48 hours before infection (CDC, 2018). In addition to initial urinary infection, CAUTIs can cause some other infections such as asymptomatic bacteremia, at the point when an incident of CAUTI winds up symptomatic, the subsequent sequelae can go from slight (fever, urethritis, and cystitis) to serious (calculus formation, renal damaging, acute pyelonephritis). These complications result in longer hospitalization and may increase morbidity and mortality (Niël-Weise and van den Broek, 2005, Flores-Mireles *et al*., 2015).

* **Corresponding Author:**
Iman A. Muhammad
E-mail: iman.muhammad@su.edu.krd Or daristan.ghareb@su.edu.krd
Article History:
Received: 02/04/2019
Accepted: 12/05/2019
Published: 10/09 /2019

Escherichia coli is the most common etiologic agent of (UTIs) particularly in patients with long-term indwelling catheters. *Escherichia coli* is being reported to be the causative agent for more than 80% of all the UTIs and it cause both symptomatic and asymptomatic bacteriuria (Niveditha *et al*., 2012, Sabir *et al*., 2014). Pathogenicity of UPEC results from the existence and expression of many virulence factors which promote bacterial adherence and infectious expansion. Virulence genes are situated on the bacterial chromosome, plasmids or even bacteriophages and could be scattered horizontally or vertically between bacteria (Piatti *et al*., 2008).

Biofilm is a population of cells enclosed in an extracellular polysaccharides matrix, which make them grow to biotic and abiotic surfaces (Ganjo, 2018). The extracellular matrix facilitates communications among the cells through biochemical signals, acyl-homoserine lactone in Gram-negative bacteria and oligopeptides in Gram-positive bacteria, in a phenomenon called as quorum sensing (Kim *et al*., 2012). The ability to form biofilm in *E. coli* needs several genes to be expressed which enhancing its initiation, attachment, and consequent maturation (Lee *et al*., 2016). A variety of virulence factors are involved in biofilm formation in *E. coli*, including hemolysin, fimbriae, lipopolysaccharides (LPS), secreted proteins, capsules, and ironacquisition systems, which allow attachment and bacterial colonization in the mucosal epithelial cells lining the urinary tract (Oliveira *et al*., 2011). In order to initiate production of a biofilm, the microorganism should initially be attached to the medical device to encourage stable attachment. The accumulation of proteins and polysaccharides in the urine favours adhesion then attachment of bacteria on to the catheter surface. When the pathogens are constantly linked to the indwelling device surface, they create exopolysaccharides to starting biofilm growth (Ohkawa *et al*., 1990).

Two major virulence determinants of UPEC isolates are required in biofilm development: type 1 fimbriae (*fim*), coded by the *fim* gene cluster; and P-fimbriae coded by the *pap* (pyelonephritis-associated pili) gene (Oliveira *et al*., 2011). The resistance of biofilm cells to antimicrobial agents is a clinically significant feature. Bacteria forming biofilms are difficult to eliminate due to the antimicrobial resistance phenotype therefore early investigation of biofilm producers is crucial, to reduce the irrational antimicrobial burden proceeding antimicrobial resistance in the patient; then, it would be an auxiliary in controlling device-associated infections in medical clinics (Maharjan *et al*., 2018).

The purpose of this study was to detect biofilm producer isolates, find out the correlation between biofilm production and associated virulence genes, and determination of antimicrobial susceptibility pattern of *E. coli* isolates isolated from the catheterized patient.

2. MATERIALS AND METHODS

2.1. Samples collection:

A total of 211 urine samples were collected from catheterized patients in the following departments (urology, surgery, burn, intensive care unit, and respiratory care unit) at Rzgari Hospital, West Emergency Hospital and Republic Teaching Hospital in Erbil City. Samples were taken irrespectively of age and gender, for four months during 25 of March to 23 of July 2018. The samples were collected under complete aseptic conditions with a sterile syringe then transferred to a sterile plain tube.

2.2. Culture and Identification of bacteria

Catheter urine samples were cultured on blood and MacConkey agar, incubated under aerobic conditions at 37°C for 24 hours, after incubation the growth of the organism with an account of $\geq 10^2$ colony forming unit (CFU)/ml was considered as CAUTI (Hooton *et al*., 2010). Bacterial isolates were identified and typed according to microscopic examination (gram stain smear), colonial morphology, fermentation, pigment production and hemolysis on blood agar (Garcia, 2010). As well as API 20E (Bio Merieux, France) was used to identify members of *Enterobacteriaceae*. For more confermation molecular approach used for *E. coli* identification by PCR assay.

2.3. Preparation of stock solutions for antimicrobial agents

The antimicrobial agents which used in the determination of minimal inhibitory concentration (MIC) for planktonic cells and minimum biofilm inhibitory concentration (BIC) for biofilm producer isolates were obtained from Awamedica (Drug manufacturing company-Erbil) in pure powder form. The antimicrobials were (Levofloxacin dissolved in 1M NaOH, Trimethoprim in 0.1M lactic acid, Ciprofloxacin in acetone, Nitrofurantoin in dimethylformamide (DMF) +PBS 0.1M pH 8, Clotrimoxazole in 95% ethanol, Meropenem, Ceftriaxone, and Tetracycline were dissolved in distilled water). The stock solution for each tested antimicrobial agent was prepared at the concentration of 5120 µg /ml. Two-fold dilutions from the stock solutions were prepared from 256 – 4 µg/ml, (CLSI, 2015).

2.4. Antimicrobial susceptibility test for planktonic cells

The antimicrobial susceptibility test was performed by determining the MIC for planktonic cells using the broth microdilution method (two-fold dilution) in a 96-well microtiter plate. A bacterial suspension of 0.5 McFarland (1.5×10^8 CFU/ml) was prepared and matched to (0.08 - 0.13) absorbance at 625 nm using spectrophotometer (APEL, Japan). Each well contained 110µl as a final volume which included (100µl from Muller Hinton Broth with antimicrobials+10µl bacterial suspension with a final concentration in each well 5×10^5 CFU/ml) as mentioned in the guidelines of Clinical and Laboratory Standard Institute . Positive control (Bacteria + media) and negative control (only broth) were prepared. Results were obtained after 24hours incubation at 37◦C for determining MIC (CLSI, 2015). The *E. coli* ATCC 25922 was used as a reference strain in all procedures.

2.5. Biofilm formation assay

The detection of biofilm was achieved by using a 96-well flat bottomed polystyrene microtiter plate (MTP) method as described by (Stepanović *et al*., 2007). An overnight incubated culture for each isolate was subcultured in 5ml brain heart infusion (BHI) broth for 24houres at 37◦C. A bacterial suspension of 0.5 McFarland was prepared as mentioned previously, then diluted (1:100) with the same broth and 200 µL of the suspension was transferred into each well, the final concentration of the inoculum inside each well was (5×10^5 CFU/ml) except negative control wells, which were contained only broth with the same volume. Plates covered with lids to prevent dehydration during incubation. After 24hours of static incubation at 37◦C, wells were decanted and washed three times with 300 µL of phosphate-buffered saline (PBS) PH = (7.4) to remove planktonic and loosely bound cells then fixed at 60◦C for an hour. Following fixation, the adherent bacteria were stained with 150 µL of 2% (w/v) crystal violet for 15 mins, then rinsed with sterile distilled water and dryed at room temperature for 5 mins. 150 µL of (95%) ethanol was add to each well for resolubilization of the dye bounded to the bacterial cells in the biofilm layer, after 15 mins the absorbance was measured at 630 nm by an ELISA reader(BioTek, USA). Data achieved for each isolate in triplicate. The biofilm category was estimated based on the absorbance values obtained for individual isolate as described by (Mathur *et al*., 2006) as follows 0.04 - 0.05 no biofilm, 0.06 – 0.09 weak, 0.1 – 0.2 moderate, > 0.2 strong biofilms former.

2.6. Biofilm susceptibility assay

The anti-biofilm activity of antimicrobial agents was evaluated during incubation, while the biofilm was being formed (Bakkiyaraj *et al*., 2013). Antimicrobial agents concentration and bacterial inoculum were prepared as mentioned before in section (2.4). Microtiter plates were incubated at 37◦C for 24 hours. After incubation, the biofilm process (crystal violet assay) was performed as described above. The results were obtained by measuring the absorbance at 630nm with an ELISA reader. The BIC was determined as the lowest concentration of antimicrobial agent that produce inhibition of biofilm formation (Baldassarri *et al*., 2006).

2.7. DNA Extraction

Genomic DNA was obtained for each isolate. A single bacterial colony of 18-24 hours subculture plate was inoculated into a tube

containing 5 ml of Luria-Bertani (LB) broth and incubated overnight at 37℃. DNA extraction was performed using a DNA extraction kit for Gram-Negative bacteria (GeNet Bio, Taiwan).

2.8. PCR amplification

Specific primers which were provided in a lyophilized form by Integrated DNA Technologies (USA), dissolved in free-nuclease water to give a final concentration of (20 pmol/µl) as recommended by primer provider and stored in deep freezer until used in PCR amplification. The first set of primers; *uspA* which designed for the universal regulator stress protein, has been selected as a target gene to detect *E. coli* at the molecular level. While the last two sets of primers; *fimH* (type 1 fimbriae) and *papC* (Pyelonephritis-associated pili) used for detection and amplify sequences of *E. coli* adhesion factors. Details of primers used in this study are illustrated in the table (1). PCR Master Mix (Ampliqon, Denmark) was implemented to amplify the targeted DNA regions.

Table (1) PCR primers for amplification of target genes

Target gene	Primer sequence (5` - 3`)	Amplicon size (bp)	PCR program run	Reference
uspA	F: CCGATACGCTGCCAATCAGT R: ACGCAGACCGTAGGCCAGAT	884	95℃ for 5 mins, 95℃ for 30 sec, 57℃ for 45 sec, 72℃ for 1 min, 40 cycles	(Chen and Griffiths, 1998)
fimH	F: TGCAGAACGGATAAGCCGTGG R: GCAGTCACCTGCCCTCCGGTA	508	94℃ for 5 mins, 94℃ for 1 min, 60℃ for 1 min, 72℃ for 1 min, 30 cycles	(Johnson and Stell, 2000)
papC	F: GTGGCAGTATGATGAATGACCGTTA R: ATATCCTTTCTGCAGGGATGCAATA	200	95℃ for 5 mins, 94℃ for 30 sec, 54℃ for 30 sec, 72℃ for 40 sec, 40 cycles	(Salehzadeh and Zamani, 2018)

2.9. PCR assay

All 43 isolates of *E. coli* were analyzed by PCR. The amplification reaction for each targeted region was carried out in 20µl reaction mixture composed of; 2µl of each forward and reverse primers, 5µl of DNA samples, 10µl master mix, and the volume adjusted to 20µl by adding free nuclease water. The PCR amplification conditions for detection of *uspA*, *fimH*, and *papC* genes are detailed in table (1). The amplification was performed in a thermocycler machine (Alpha PCR, UK). A 10µl aliquot of the PCR product was investigated by electrophoresis on 1.5% agarose gel, contain safe dye. The sizes of the amplicons were verified by comparing them with a 100-bp DNA ladder (GeNet Bio, Taiwan) by UV-transilluminator.

Statistical analysis

Statistical analysis was performed by using GraphPad Prism 7, chi-square (fishers exact) test was used to obtain the correlation between the variables. Nonlinear regressions used to determine MIC_{50}, MIC_{90}, and nonparametric test (Mann-Whitney) test used to compare the susceptibility of the planktonic and the biofilm growth state. The level of significance was set at $p < 0.05$.

3. RESULTS

3.1. Incidence and prevalence of urinary tract infections

During the study period, 211 catheter urine samples were collected. Out of these, 130 (61.61%) positive bacterial growth for UTI were detected. From these positive cultures, 66 (62.85%) females and 64 (60.37) males observed. No significant association was found between CAUTI with gender (p= 0.711) as presented in the

table (2). *E. coli* was much more frequently isolated bacteria 43 (33.7%) followed by *Klebsiella pneumoniae* and *Staphylococcus aureus* 16 (12.3%), *Staphylococcus epidermides* 14 (10.7%), *Enterobacter cloace* 9 (6.9%), *Shigella spp.* 7 (5.3%), *Acinetobacter baumanii* and *Salmonella typhi* 6 (4.6%), *Enterococcus faecalis* 5 (3.8%), *Proteus spp.* 4 (3.07%), *Citrobacter spp.*, and *Pseudomonas aeruginosa* 2 (1.5%) as depicted in Table (3). Our investigation focused on pure isolates of *E. coli*, while other bacterial species have been excluded. In addition to morphologic, microscopic, cultural characteristic, and API 20E system, molecular approach used for identification of *E. coli* by *uspA* gene which performed by PCR and gave clear bands of 884bp of amplified gene on 1.5% agarose gel as compared with 100bp DNA marker as shown in figure (1)

Table (2) Prevalence of UTI in associations with gender

UTI	Female No. %	Male No. %	Total No. %	p-value
Positive	66 (62.85)	64 (60.37)	130 (61.61)	
Negative	39 (37.14)	42 (39.62)	81 (38.38)	0.711
Total	**105 (100)**	**106 (100)**	**211 (100)**	

Table (3) Incidence of causative uropathogenic isolates from catheterized patients according to gender

Bacterial species	Gender		Total
	Female No. %	Male No. %	No. %
E.coli	29 (43.9)	14 (21.8)	43 (33.07)
Klebsiella pneumoniae	7 (10.6)	9 (14.06)	16 (12.3)
Staphylococcus aureus	6 (9.1)	10 (15.6)	16 (12.3)
Staphylococcus epidermides	6 (9.09)	8 (12.5)	14 (10.7)
Enterobacter cloace	5 (7.5)	4 (6.2)	9 (6.9)
Shigella spp.	2 (3.03)	5 (7.8)	7 (5.3)
Acinetobacter baumanii	2 (3.03)	4 (6.2)	6 (4.6)
Salmonella typhi	4 (6.06)	2 (3.1)	6 (4.6)
Enterococcus faecalis	3 (4.5)	2 (3.1)	5 (3.8)
Proteus spp.	0 (0)	4 (6.2)	4 (3.07)
Citrobacter spp.	2 (3.03)	0 (0)	2 (1.5)
Pseudomonas aeroginosa	0 (0)	2 (3.1)	2 (1.5)
Total	66 (100)	64 (100)	130 (100)

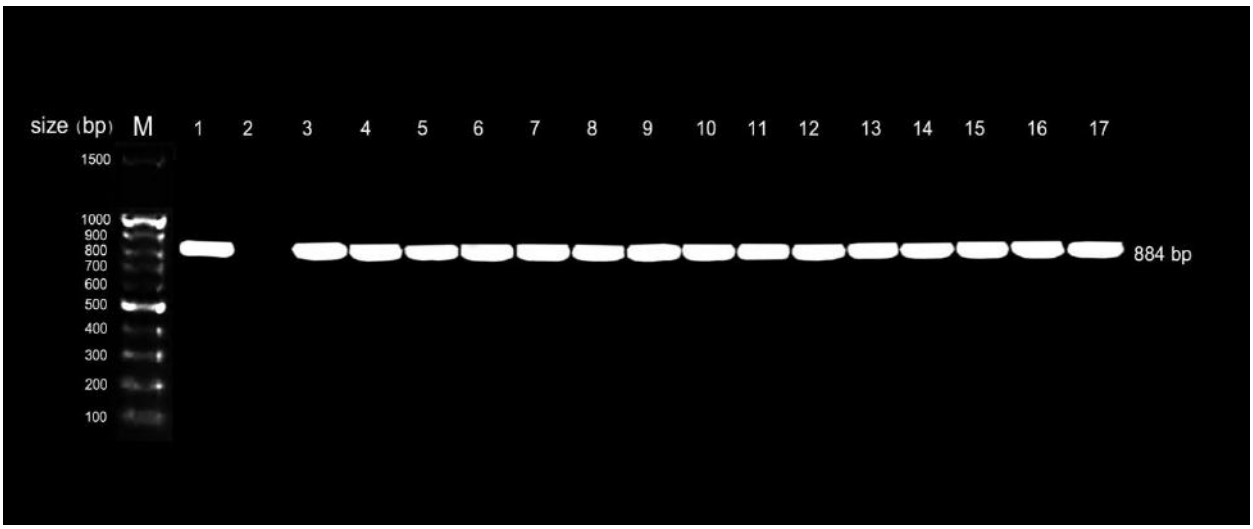

Figure (1) Amplification of *uspA* gene from 15 samples of *E. coli*. Agarose gel electrophoresis of PCR amplification of the target gene. M: 100-1500 bp DNA Marker, lane 1 is a positive control of *uspA* gene (*E. coli* ATCC 25922), lane 2 is a negative control for *uspA* gene (*K. pneumoniae*), and lane 3-17 are *E. coli* isolates.

3.2. Biofilm formation

In the current study, 43 *E. coli* isolates were underwent biofilm procedure. All the isolates (100%) were biofilm producers. From these, 13 (30.23%) showed strong biofilm formation while 25(58.13%) were moderate and 5(11.62%) were weak biofilm producer isolates as described in Table (4).

Table (4) Interpretation of biofilm producing *Escherichia coli*

Biofilm degree	No. isolates	Percentage (%)
Strong	13	30.23
Moderate	25	58.13
Weak	5	11.62
Total	43	100

Strong biofilm producer OD ≥ 0.240 ,Moderate OD = 0.120- 0.240 ,Weak < 0.120

3.3. Detection of virulence-associated genes

Table (5) demonstrates the predominance of *fimH* and *papC* genes between forty-three *E. coli* isolates. All *E. coli* isolates carried *fimH* 100%, and 79% *papC* gene. Gene detection obtained by PCR gave clear bands of the amplified *fimH*, and the *papC* gene on 1.5% agarose gel the size of amplified genes was 508bp and 200bp, respectively as compared with 100bp DNA Marker as shown in Figure (2) and (3). The relation between biofilm formation and adhesion genes was non-significant (p= 0.977).

Table (5) Correlation between biofilm and adhesion genes

Biofilm	*fimH* gene No. %	*papC* gene No. %	p-value
Strong No. (13)	13 (30.23)	11 (32.35)	0.977
Moderate No. (25)	25 (58.13)	19 (55.88)	
Weak No. (5)	5 (11.62)	4 (11.76)	
Total No. (43)	43 (100)	34 (79)	

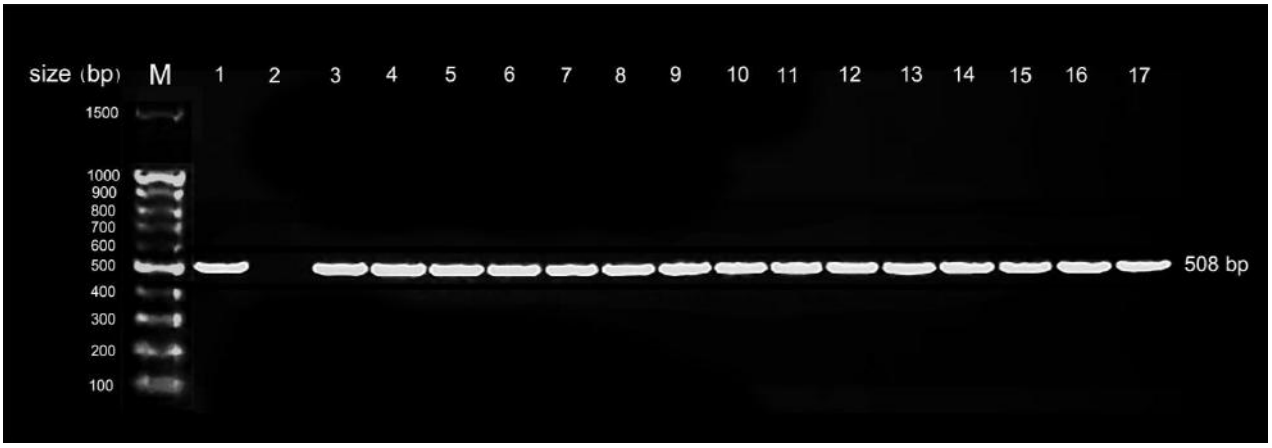

Figure (2) Amplification of the *fimH* gene from 15 samples of *E. coli*. Agarose gel electrophoresis of PCR amplification of the target gene. M: 100-1500 bp DNA Marker, lane 1 is a positive control of *fimH* gene (*E. coli* ATCC 25922), lane 2 is a negative control for the *fimH* gene (*K. pneumoniae*), and lane 3-17 are *E. coli* isolates.

Figure (3) Amplification of *papC* gene from 15 samples of *E. coli*. Agarose gel electrophoresis of PCR amplification of the target gene. M: 100-1500 bp DNA Marker, lane 1 is a positive control of *papC* gene (*E. coli* ATCC 25922), lane 2 is a negative control for the *papC* gene (*K. pneumoniae*), and lane 3-17 are *E. coli* isolates.

3.4. Antimicrobial susceptibility pattern

The MIC_{50}, MIC_{90} for planktonic cells and BIC_{50}, BIC_{90} for biofilm formation were calculated for eight antimicrobials (Meropenem, Ceftriaxone, Ciprofloxacin, Cotrimoxazole, Levofloxacin, Nitrofurantoin, Trimethoprim and Tetracycline). The values were calculated from the concentration of tested antimicrobials needed for 50% and 90% of plankton and biofilm inhibition agents by determining median and range that are represented in the table (6).

Table (6) The Minimal inhibitory concentration (MIC) and biofilm inhibitory concentration (BIC) for 43 isolates of *Escherichia coli*

Antimicrobial agents	Concentration(µg/ml)			
	Plankton (MIC)		Biofilm(BIC)	
	MIC_{50} Range*	MIC_{90} Range	BIC_{50} Range	BIC_{90} Range
Meropenem	3 (3 - 33)	4 (4 - 34)	4 (3 - 80)	5 (4 - 81)
Ceftriaxone	17 (5 - 80)	18 (6 - 81)	25 (4 -144)	26 (5 - 145)
Ciprofloxacin	16 (4 - 86)	18 (5 - 87)	18 (4 -129)	19 (5 - 130)
Cotrimoxazole	17 (8 - 88)	18 (10 -89)	33 (5 -137)	34 (6 - 138)
Levofloxacin	32 (4-128)	33 (5 -129)	33 (4 -143)	34 (5 - 144)
Nitrofurantoin	32 (8 - 64)	33 (9.1 -65)	32 (8 -136)	33 (9.3 -137)
Trimethoprim	16 (3 - 39)	18 (4 - 39)	17 (4 - 84)	18 (5 - 85)
Tetracycline	32 (4-128)	33 (5 -129)	17 (4 -134)	18 (5 - 135)

*Range = (minimum-maximum) of MIC for each antimicrobial agent.

3.5. Comparison between plankton and biofilm form according to MIC_{50} and MIC_{90}

Figures (4 & 5) showing a comparison between medians of MIC_{50} and MIC_{90} of antimicrobial agents for planktonic and biofilm form of UPEC. Although there are no significant differences between most of the antimicrobial agents statistically $p > 0.05$, there was a considerable difference found for affecting of these antimicrobial agents on bacterial isolates in planktonic and biofilm form especially in (B, C, D, and F). While there were significant differences between these two forms statistically as shown in (G, H) $p < 0.05$.

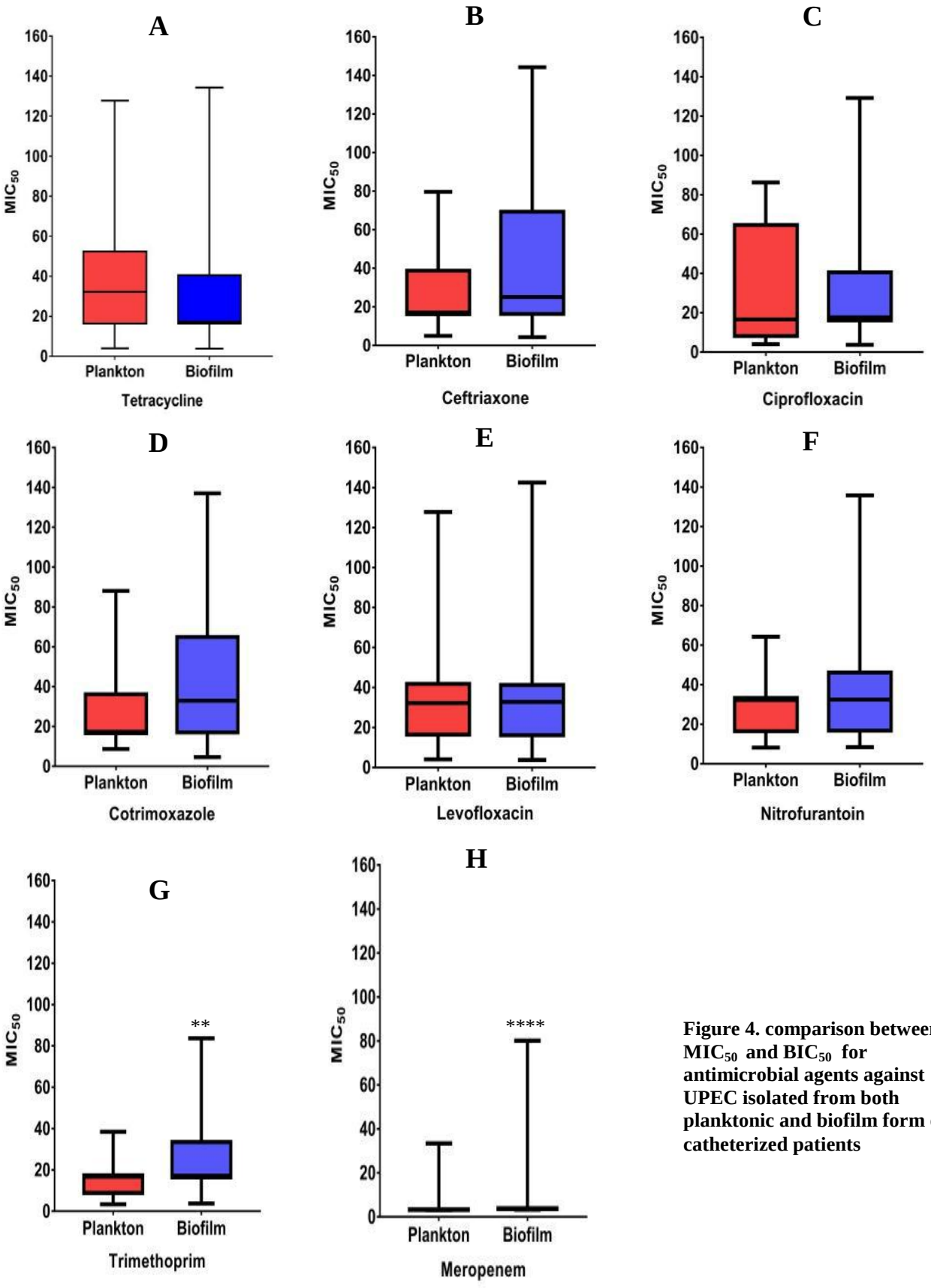

Figure 4. comparison between MIC_{50} and BIC_{50} for antimicrobial agents against UPEC isolated from both planktonic and biofilm form of catheterized patients

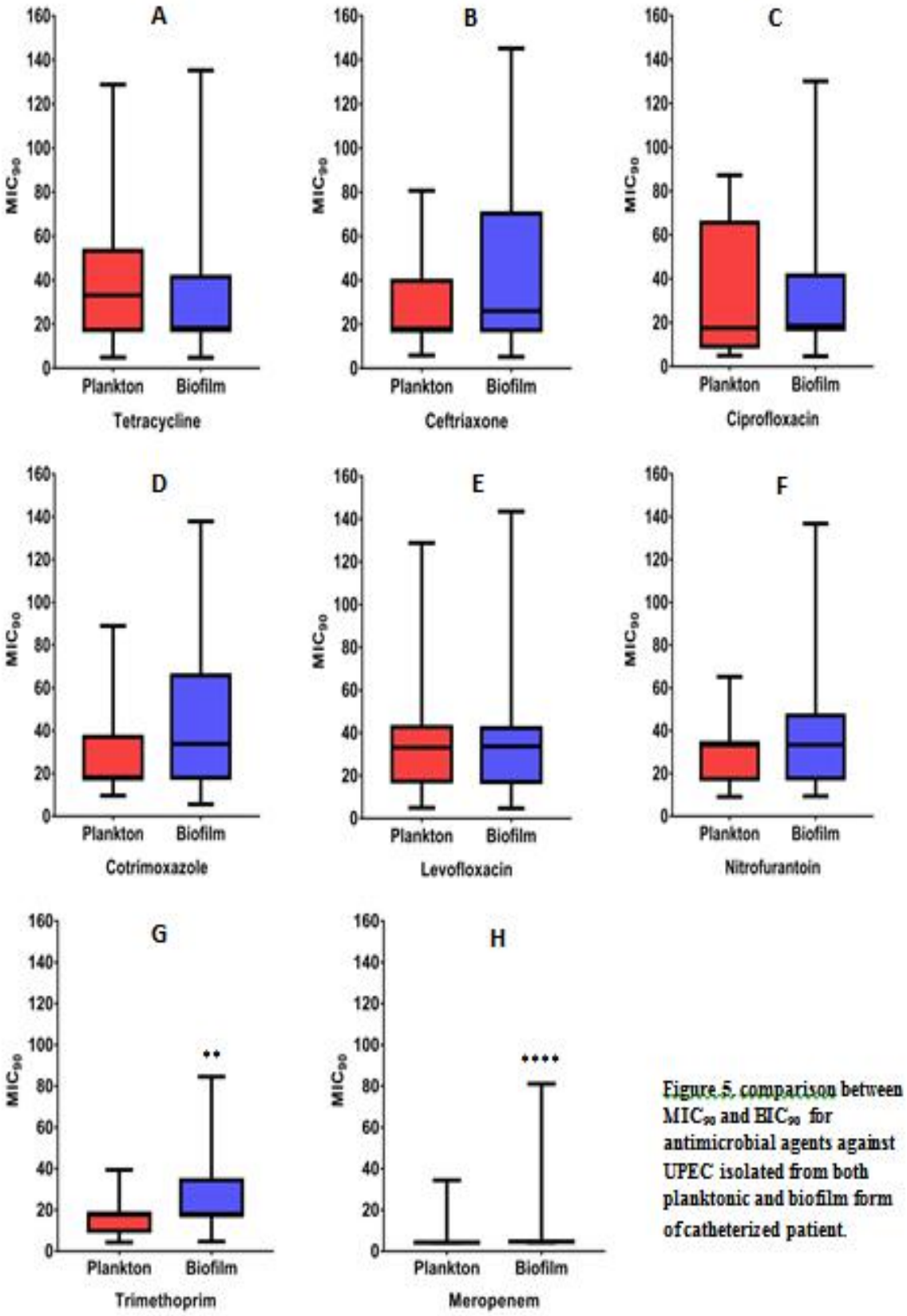

Figure 5. comparison between MIC_{90} and HIC_{90} for antimicrobial agents against UPEC isolated from both planktonic and biofilm form of catheterized patient.

4. DISCUSSION

Biofilm development on urinary catheters is a problem often underestimated. However, this factor greatly promotes UTI, which leads to high mortality rates, prolonged treatments and high costs in health care services (Dohnt *et al*., 2011). Although, in patients associated with diseases or under intensive care, the importance of recognition of biofilm makers is critical because CAUTIs is a typical nosocomial disease (Syed *et al*., 2010). In this study, The predominance of the infection was observed to be 61.61%. Despite lacking statistical significance, females suffers more predominantly 62.85%. This result was agreed with the finding of (Maharjan *et al*., 2018) in which his results for the prevalence of CAUTI were 61.9% and 66.2% for females. A similar incidence was recognized in a review of (Nicolle, 2014) from several developing countries. Females suffer more predominantly; this might be attributed to the anatomical differences of urogenital position, anal proximity and shorter urethra in female (Forbes *et al*., 2007).

Furthermore, the present study reported *E. coli* as the most common uropathogen contributing CAUTI with 33.07% nearly similar findings has been reported earlier by (Abdallah *et al*., 2011) who discovered that *E. coli* 31% was the causative agent. In a study (Seif Eldein *et al*., 2013) *E. coli* reported 50%, while (Maharjan *et al*., 2018) observed 57%.

Biofilm formation is a crucial period in the host infection process and thus contributes to pathogenicity (Parsek and Singh, 2003). In the current study, Biofilm phenomenon was stated in 100% of isolates, from this 30.23% were strong, 58.13% were moderate, and 11.62% were weak biofilm producers. A study from Iraq (Al-Taai *et al*., 2018) revealed that UPEC isolates were 100% biofilm formers, and this supports our findings. While the result of (Fattahi *et al*., 2015) referred that 92% of UPEC isolates were positive for biofilm and 38% of isolates were strong. Existence of a urinary catheter appeared to be a risk factor for biofilm creation (Niveditha *et al*., 2012).

In the present investigation, *fimH* and *papC* gene found 100% and 79% in UPEC isolates, our results supported by the findings of (Johnson and Stell, 2000) who found that *fimH* and *papC* genes detected from *E. coli* isolates from urosepsis 100% and 77% . As well as the result of (Al-Mayahie, 2013) reported that the *fimH* gene was 100% identified in pyelonephritis.

Studies had been recognized that biofilm behaves as a barrier, protect the microorganisms from the action of antimicrobials, and other virulence factors had an important role in preventing the bacteria from unfavorable conditions, and this made treatment difficult because of increased drug-resistant (Mittal *et al*., 2015). This investigation has revealed that all the isolates of *E. coli* in plankton and biofilm form were resistant 100% to (Ceftriaxone, Levofloxacin, Cotrimoxazole). This is an indicator for multidrug-resistant (MDR) of *E. coli.*

More than half 86% , 74.4% of the isolates were resistant to tetracycline and trimethoprim, and 93.1% of isolates showed an intermediate susceptibility pattern for meropenem, these were in planktonic form. On the other hand, isolates were more resistant for antimicrobial agents in biofilm form, The percentage of resistance for Tetracycline and Trimethoprim increased to 90.7%, 83.7%, while 20.9% of isolates were resistant to meropenem others 79.1% were intermediate. Meropenem is one of the most prescribed antimicrobial agent for catheterized patients especially in CAUTI in hospitals of Erbil city; this is a risk sign because meropenem is the last resort drug. While the only effective antimicrobial used in this study against UPEC was Nitrofurantoin in which 72.1% and 60.4% of isolates in planktonic and biofilm form were sensitive for this antimicrobial agent. Additionally, $MIC_{50,}$ MIC_{90} for planktonic growth and $BIC_{50,}$ BIC_{90} for biofilm form as described in the table (6) confirm this percentage of antimicrobial resistance.

Many scientists stated that bacteria living in biofilm exhibit high spread in their antibiotic tolerance in contrast to their planktonic form counterpart (Dufour *et al*., 2010). So this agreed with our results in which bacteria in biofilm form were more resistant to the tested antimicrobial agents than those in planktonic form. The drug-resistance strategy employed by sessile biofilm cells are different from The ones adopted by planktonic cell, such as acquisition of new

enzymes and mutation of the drug targets. On the other hand, as the sessile bacteria adopt a slow rate of growth, biofilm are relatively insensitive to antimicrobials (Chen and Wen, 2011). The double-membrane structure of Gram-negative bacteria (*E. coli*) and the intrinsic production of efflux pumps allow antimicrobials to be exported, thus reducing intracellular concentration allowing bacteria to survive at higher external concentrations of antimicrobial agents , leading to survival and resistance. New genetic material can be exchanged between organisms, This process can provide the host cell and its progeny with new genetic material encoding antimicrobial resistance and can occur through several mechanisms (transduction, transformation, conjugation) of which perhaps the most important is plasmid transmission (Parsley *et al*., 2010). Additionally, we observed a positive relationship between the capacity of biofilm formation and the virulence gene expression demonstrating that biofilm-forming bacteria are more pathogenic than the planktonic form in urinary tract infections, creating biofilm-based UTI very hard to cure. Furthermore reasons for antibiotic resistant phenomena, up to half of all antimicrobials recommended to people are expected unnecessary. However, the concentration of antibiotic prescribing might be highest in inpatient settings, with 30-40% of patients on antibiotics in European hospitals (Suetens *et al*., 2013). This overuse of antimicrobials is considered to be the main reason for antimicrobial resistance (WHO, 2012, Laxminarayan *et al*., 2013). Also overuse and misuse of antimicrobials in our hospitals are another important factor for spreading of this phenomena.

5. CONCLUSION

From our study we concluded that, *E. coli* was the main predominant organism isolated from CAUTI patients. All the isolates were biofilm formers, *fimH* gene detected in all isolates while *papC* gene was observed in 79% of the isolates. The isolates were multi drug resistant. The most effective antimicrobial agent was Nitrofurantoin. There was a positive relationship between biofilm formation and antimicrobial resistance. Study of the biofilm formation supports the decision for better management against persistent and recurrent UTI in catheterized patient.

References

ABDALLAH, N. M. A., ELSAYED, S. B., MOSTAFA, M. M. Y. & EL-GOHARY, G. M. 2011. Biofilm forming bacteria isolated from urinary tract infection, relation to catheterization and susceptibility to antibiotics. *International Journal of Biotechnology and Molecular Biology Research,* 2**,** 172-178.

AL-MAYAHIE, S. M. G. 2013. Vaginal colonization by papG allele II+ Escherichia coli isolates from pregnant and nonpregnant women as predisposing factor to pyelonephritis. *Infectious diseases in obstetrics and gynecology,* 2013.

AL-TAAI, H. R., AL-JEBOURI, Z. A., KHALAF, B. H. & MOHAMMED, Y. Q. 2018. Antibiotic resistance patterns and adhesion ability of uropathogenic Escherichia coli in children. *Iraqi Journal of Biotechnology,* 17**,** 18-26.

BAKKIYARAJ, D., NANDHINI, J. R., MALATHY, B. & PANDIAN, S. K. 2013. The anti-biofilm potential of pomegranate (Punica granatum L.) extract against human bacterial and fungal pathogens. *Biofouling,* 29**,** 929-937.

BALDASSARRI, L., CRETI, R., RECCHIA, S., IMPERI, M., FACINELLI, B., GIOVANETTI, E., PATARACCHIA, M., ALFARONE, G. & OREFICI, G. 2006. Therapeutic failures of antibiotics used to treat macrolide-susceptible Streptococcus pyogenes infections may be due to biofilm formation. *Journal of Clinical Microbiology,* 44**,** 2721-2727.

CDC 2018. NHSN Catheter-Associated Urinary Tract Infection Surveillance in 2018. 11.

CHEN, J. & GRIFFITHS, M. 1998. PCR differentiation of Escherichia coli from other Gram-negative bacteria using primers derived from the nucleotide sequences flanking the gene encoding the universal stress protein. *Letters in applied microbiology,* 27**,** 369-371.

CHEN, L. & WEN, Y. M. 2011. The role of bacterial biofilm in persistent infections and control strategies. *International journal of oral science,* 3**,** 66.

CLSI, C. A. L. S. I. 2015. Methods for Dilution Antimicrobial Susceptibility Tests for Bacteria that Grow Aerobically Approved Standard, 10th edition (M07 - A10).

DOHNT, K., SAUER, M., MÜLLER, M., ATALLAH, K., WEIDEMANN, M., GRONEMEYER, P., RASCH, D., TIELEN, P. & KRULL, R. 2011. An in vitro urinary tract catheter system to investigate biofilm development in catheter-associated urinary tract infections. *Journal of microbiological methods,* 87**,** 302-308.

DUFOUR, D., LEUNG, V. & LÉVESQUE, C. M. 2010. Bacterial biofilm: structure, function, and antimicrobial resistance. *Endodontic Topics,* 22**,** 2-16.

FATTAHI, S., KAFIL, H. S., NAHAI, M. R., ASGHARZADEH, M., NORI, R. &

AGHAZADEH, M. 2015. Relationship of biofilm formation and different virulence genes in uropathogenic Escherichia coli isolates from Northwest Iran. *GMS hygiene and infection control*, 10.

FLORES-MIRELES, A. L., WALKER, J. N., CAPARON, M. & HULTGREN, S. J. 2015. Urinary tract infections: epidemiology, mechanisms of infection and treatment options. *Nature reviews microbiology*, 13**,** 269.

FORBES, B. A., SAHM, D. F., WEISSFELD, A. & BARON, E. 2007. Bailey & Scott's diagnostic microbiology, Mosby, St. *Louis, MO***,** 10-840.

GANJO, A. R. 2018. In vitro biofilm formation and antimicrobial resistance pattern in Pseudomonas aeruginosa recovered from infected burn wounds in Erbil city. *ZANCO Journal of Pure and Applied Sciences*, 30**,** 67-75.

GARCIA, L. S. 2010. *Clinical microbiology procedures handbook*, American Society for Microbiology Press.

HOOTON, T. M., BRADLEY, S. F., CARDENAS, D. D., COLGAN, R., GEERLINGS, S. E., RICE, J. C., SAINT, S., SCHAEFFER, A. J., TAMBAYH, P. A. & TENKE, P. 2010. Diagnosis, prevention, and treatment of catheter-associated urinary tract infection in adults: 2009 International Clinical Practice Guidelines from the Infectious Diseases Society of America. *Clinical infectious diseases*, 50**,** 625-663.

JOHNSON, J. R. & STELL, A. L. 2000. Extended virulence genotypes of Escherichia coli strains from patients with urosepsis in relation to phylogeny and host compromise. *The Journal of infectious diseases*, 181**,** 261-272.

KIM, J., PARK, H.-D. & CHUNG, S. 2012. Microfluidic approaches to bacterial biofilm formation. *Molecules*, 17**,** 9818-9834.

LAXMINARAYAN, R., DUSE, A., WATTAL, C., ZAIDI, A. K., WERTHEIM, H. F., SUMPRADIT, N., VLIEGHE, E., HARA, G. L., GOULD, I. M. & GOOSSENS, H. 2013. Antibiotic resistance—the need for global solutions. *The Lancet infectious diseases*, 13**,** 1057-1098.

LEE, J., SUBHADRA, B., SON, Y. J., KIM, D., PARK, H., KIM, J., KOO, S., OH, M., KIM, H. J. & CHOI, C. 2016. Phylogenetic group distributions, virulence factors and antimicrobial resistance properties of uropathogenic Escherichia coli strains isolated from patients with urinary tract infections in South Korea. *Letters in applied microbiology*, 62**,** 84-90.

MAHARJAN, G., KHADKA, P., SIDDHI SHILPAKAR, G., CHAPAGAIN, G. & DHUNGANA, G. R. 2018. Catheter-associated urinary tract infection and obstinate biofilm producers. *Canadian Journal of Infectious Diseases and Medical Microbiology*, 2018.

MATHUR, T., SINGHAL, S., KHAN, S., UPADHYAY, D., FATMA, T. & RATTAN, A. 2006. Detection of biofilm formation among the clinical isolates of staphylococci: an evaluation of three different screening methods. *Indian journal of medical microbiology*, 24**,** 25.

MITTAL, S., SHARMA, M. & CHAUDHARY, U. 2015. Biofilm and multidrug resistance in uropathogenic Escherichia coli. *Pathogens and global health*, 109**,** 26-29.

NICOLLE, L. E. 2014. Catheter associated urinary tract infections. *Antimicrobial resistance and infection control*, 3**,** 23.

NIËL-WEISE, B. S. & VAN DEN BROEK, P. J. 2005. Urinary catheter policies for short-term bladder drainage in adults. *Cochrane Database of Systematic Reviews*.

NIVEDITHA, S., PRAMODHINI, S., UMADEVI, S., KUMAR, S. & STEPHEN, S. 2012. The isolation and the biofilm formation of uropathogens in the patients with catheter associated urinary tract infections (UTIs). *Journal of clinical and diagnostic research: JCDR*, 6**,** 1478.

OHKAWA, M., SUGATA, T., SAWAKI, M., NAKASHIMA, T., FUSE, H. & HISAZUMI, H. 1990. Bacterial and crystal adherence to the surfaces of indwelling urethral catheters. *The Journal of urology*, 143**,** 717-721.

OLIVEIRA, F., PALUDO, K., AREND, L., FARAH, S., PEDROSA, F., SOUZA, E., SUREK, M., PICHETH, G. & FADEL-PICHETH, C. 2011. Virulence characteristics and antimicrobial susceptibility of uropathogenic Escherichia coli strains. *Genet Mol Res*, 10**,** 4114-25.

PARKER, V., GILES, M., GRAHAM, L., SUTHERS, B., WATTS, W., O'BRIEN, T. & SEARLES, A. 2017. Avoiding inappropriate urinary catheter use and catheter-associated urinary tract infection (CAUTI): a pre-post control intervention study. *BMC health services research*, 17**,** 314.

PARSEK, M. R. & SINGH, P. K. 2003. Bacterial biofilms: an emerging link to disease pathogenesis. *Annual Reviews in Microbiology*, 57**,** 677-701.

PARSLEY, L. C., CONSUEGRA, E. J., KAKIRDE, K. S., LAND, A. M., HARPER, W. F. & LILES, M. R. 2010. Identification of diverse antimicrobial resistance determinants carried on bacterial, plasmid, or viral metagenomes from an activated sludge microbial assemblage. *Appl. Environ. Microbiol.*, 76**,** 3753-3757.

PIATTI, G., MANNINI, A., BALISTRERI, M. & SCHITO, A. M. 2008. Virulence factors in urinary Escherichia coli strains: phylogenetic background and quinolone and fluoroquinolone resistance. *Journal of clinical microbiology*, 46**,** 480-487.

SABIR, S., ANJUM, A. A., IJAZ, T. & ALI, M. A. 2014. Isolation and antibiotic susceptibility of E. coli from urinary tract infections in a tertiary care hospital. *Pakistan journal of medical sciences*, 30**,** 389.

SALEHZADEH, A. & ZAMANI, H. 2018. Characterization of (Uropathogenic) E. coli isolated from urinary tract infections: phylogenetic typing and distribution of virulence-associated traits. *British journal of biomedical science*, 75**,** 40-42.

SEIF ELDEIN, S. S., EL-TEMAWY, A.-E.-K. A., AHMED, E. H., EL-GAMMAL, M. A.-A. M., EL-SALAM, A. & NAGUIB, A. M. 2013. Biofilm Formation by E-Coli Causing Catheter Associated Urinary Tract Infection (CAUTI) in Assiut University Hospital. *The Egyptian Journal of Medical Microbiology,* 38**,** 1-9.

STEPANOVIĆ, S., VUKOVIĆ, D., HOLA, V., BONAVENTURA, G. D., DJUKIĆ, S., ĆIRKOVIĆ, I. & RUZICKA, F. 2007. Quantification of biofilm in microtiter plates: overview of testing conditions and practical recommendations for assessment of biofilm production by staphylococci. *Apmis,* 115**,** 891-899.

SUETENS, C., HOPKINS, S., KOLMAN, J. & DIAZ HÖGBERG, L. 2013. European Centre for Disease Prevention and Control. *Point prevalence survey of healthcare associated infections and antimicrobial use in European acute care hospitals. Sweden: ECDC*.

SYED, M. A., MANZOOR, U., SHAH, I. & BUKHARI, S. H. A. 2010. Antibacterial effects of Tungsten nanoparticles on the Escherichia coli strains isolated from catheterized urinary tract infection (UTI) cases and Staphylococcus aureus. *New Microbiologica,* 33**,** 329-335.

TERLIZZI, M. E., GRIBAUDO, G. & MAFFEI, M. E. 2017. UroPathogenic Escherichia coli (UPEC) infections: virulence factors, bladder responses, antibiotic, and non-antibiotic antimicrobial strategies. *Frontiers in microbiology,* 8**,** 1566.

WHO, W. H. O. 2012. *The evolving threat of antimicrobial resistance: options for action*, Geneva: World Health Organization.

ZANCO Journal of Pure and Applied Sciences
The official scientific journal of Salahaddin University-Erbil
https://zancojournals.su.edu.krd/index.php/JPAS

ISSN (print):2218-0230**, ISSN (online):** 2412-3986**, DOI: http://dx.doi.org/10.21271/zjpas**

RESEARCH PAPER

THE INFLUENCE OF CARBIMAZOLE ON SERUM LEPTIN HORMONE AND INSULIN RESISTANCE IN PATIENTS WITH HYPERTHYROIDISM

Bnar Saleh Ismael Shekhane[1], Muslih A. Ibrahim[2]

[1,2]Department of Pharmacology and Toxicology, College of Pharmacy, Hawler Medical University, Erbil, Kurdistan Region, Iraq

A B S T R A C T:

Carbimazole is one of the common antithyroid drugs for the treatment of hyperthyroidism. It interferes with the synthesis of thyroid hormones and results in the reducing of thyroid hormones level. Apart from determining the effects of carbimazole on serum TSH, T3, T4, insulin, HOMA-IR, HOMA-IS and leptin, the drug effects on corrected QT (QTc) interval duration in hyperthyroidism patients were examined concomitantly Female patients were recruited after obtaining informed consent. Venous blood samples were collected from control healthy subjects and hyperthyroid patients. Treatment with carbimazole results in the improvement of thyroid status and achievement of euthyroidism with a significant decrease in insulin level, and improvement in insulin resistance. The therapy also led to a significant increase in leptin levels. Nonetheless, the non-significant effect on QTc interval duration was observed. In conclusion, this treatment could be beneficial for hyperthyroidism who are at risks of insulin resistance syndrome.

KEY WORDS: Hyperthyroidism; carbimazole; insulin; insulin resistance; leptin; QTc interval.
DOI: http://dx.doi.org/10.21271/ZJPAS.31.4.3
ZJPAS (2019), 31(4);23-35.

1. INTRODUCTION :

Excess in production of thyroid hormones by thyroid gland or overactive thyroid gland is called hyperthyroidism or thyrotoxicosis (Golden et al., 2009, Ross et al., 2016).

The production and release of thyroid hormones are regulated by a sensitive negative feedback loop involving the hypothalamus, pituitary gland, and thyroid gland. The hypothalamus releases thyroid-releasing hormone (TRH), which stimulates the pituitary to release Thyroid stimulating and triiodothyronine (T3). The increased production of thyroid hormone normally causes inhibition of TRH and TSH release by the hypothalamus and pituitary respectively. Disruption of this delicate system leads to additional production and release of thyroid hormone and subsequent hyperthyroidism (Devereaux and Tewelde, 2014).

Hyperthyroidism predictable prevalence range is between 0.2% to 1.3%. The most common cause being Graves disease (GD) with an incidence of 20 to 50 cases per 100,000 persons which accounts for up to 70% of cases, followed by toxic multinodular goiter (TMNG) and toxic adenoma (TA) and less common cause include thyroiditis, increase in iodine intake, drugs(amiodarone). Women more affected by GD which mainly aged between 20 to 50 years. Male to female ratio of GD is (1: 4) it may occur at any age in both

* **Corresponding Author:**
Bnar Saleh Ismael Shexane
E-mail: bnars.shexane@gmail.com
Article History:
Received: 20/03/2019
Accepted: 14/05/2019
Published: 10/09 /2019

genders (Kravets, 2016). In Ranya town and Erbil city/Iraq the same prevalence of hyperthyroidism are observed (Al–Bustany, 2011, Wsso and Rasul, 2017).

Patients with thyrotoxicosis usually present with weight loss, heat intolerance, palpitations, tremor, increased sweating, diarrhea, fatigue, infertility and menstrual cycle abnormality which are the typical symptoms of hyperthyroidism (Cooper, 2003, Reid and Wheeler, 2005)

Treatment strategy and therapy choices for hyperthyroidism differ according to the cause. It includes antithyroid drugs (ATDs), radioactive iodine (RAI) therapy, and surgery. β blockers are used for controlling symptoms associated with thyrotoxicosis (Cooper, 2005, De Leo et al., 2016, Kravets, 2016). Carbimazole, a prodrug which is converted to the active form methimazole, is used for the treatment of hyperthyroidism by Interferes with the synthesis of thyroid hormones and as a result reduces the level of thyroid hormones (Mohan et al., 2015, Uduak et al., 2014).

In hyperthyroidism, decreased, normal, or even increased levels of plasma insulin have been reported. Thyrotoxicosis which has been associated with insulin resistance, the mechanism of insulin resistance induced by thyrotoxicosis has not been completely elucidated (Brenta, 2011, Chu et al., 2011). Association have been founded between Insulin and leptin. Leptin is a 167-amino-acid peptide , it is a potent anorexic hormone that is mainly expressed in white adipose tissue (WAT), but is also found in a variety of tissues including placenta, mammary gland, ovary, skeletal muscle, stomach, pituitary gland, and lymphoid tissue (Margetic et al., 2002). In compare between the euthyroid population with female hyperthyroid patients, decrease (Baig et al., 2003), and increase (Ozata et al., 1998) of leptin level have been reported.

Thyroid hormones have a significant impact on cardiac function and structure. Excess thyroid hormone affects cardiovascular hemodynamics (Osuna et al., 2017).The most common electrocardiogram (ECG) abnormality is sinus tachycardia (Ertek and Cicero, 2013).The second most common finding is arterial fibrillation (AF) with incidence increasing with age (Satpathy et al., 2013). Prolonged QT intervals have been reported in hyperthyroidism (Colzani et al., 2001, Kulairi et al., 2017, Lee et al., 2015).

Due to few studies regarding the association of hyperthyroidism and carbimazole treatment with leptin, insulin resistance and QTc interval duration. The present study was done to evaluate the alteration in thyroid hormones, insulin, leptin, Homeostasis Model Assessment of Insulin Resistance (HOMA-IR) and for insulin sensitivity (HOMA-IS) with QTC interval duration from ECG study pre- and post-treatment with carbimazole in hyperthyroid female patients and compared to healthy control group in Erbil city.

2. MATERIALS AND METHODS

2.1 Patients and design of the study

A prospective randomized clinical trial study was carried out at Rizgary teaching hospital department of internal medicine consultant and Hawler teaching hospital department of hormonal consultant in Erbil, Kurdistan Region from November 2017 to December 2018. The study design was approved by Regional Ethical Committee in the College of Pharmacy at Hawler Medical University. A verbal and consent form were obtained from each patient before the enrollment into the study. The patients were recruited from both hospitals, which attended the hospitals for management and follow-up of their disease Condition. A history is taken from patients using a previously prepared questionnaire. Each patient examined thoroughly by the consultant and then allocated to be enrolled in the study. Only female patients aged above 18 years who are recently diagnosed thyrotoxicosis and candidate to receive only carbimazole were included. Females with diabetes, liver and kidney disorders, cardiac failure and underlying infections were excluded. None of them was alcoholic or receiving medications known to affect the study parameters. The patients were followed up for a period of 12 weeks, blood samples and ECG were taken two times from the patients during this period; first at the start of the study, second after three months of follow up.

The subjects that were included in the study divided into two groups: Group 1 in which the total number of patients that were included is (35 females) newly diagnosed with thyrotoxicosis. Group 2 which is healthy control group includes (26 female).

2.2 Hormonal assay and QTc interval

A 10 to 12-hour overnight fasting 7-10ml of venous blood were obtained via venous puncture using a 10ml syringe from patients and collected into a test tube containing separator gel and Ethylene diamine tetra acetic acid (EDTA) tube. The serum separated within 20 minutes (coagulation time) after blood draw by centrifugation at 3000 rpm for 10 minutes. The samples were conserved at -80°C in medical research Centre/Hawler medical University. Serum Insulin, TSH, T3 andT4 were estimated using fully automated biochemical analyzer (Cobas-e 411 analyzer, Germany), leptin level estimated using enzyme-linked immunosorbent assay (ELISA) while fasting serum glucose was determined using Accent 200 analyzer. And QTc interval duration taken from ECG study in each patient which is measured in milliseconds(ms).

2.3 Statistical Analysis

Data analysis was performed using Graphpad Prism (version6) (California corporation, USA). The unpaired t-test performed for comparing the difference between control and patients group, using Mann-Whitney test regarding non-parametric data. Paired t-test performed for comparison within the patients group, using Wilcoxon matched paired t-test regarding non-parametric data. The results were considered statistically significant at P value ≤ 0.05. Parameters level accuracy for the diagnosis of hyperthyroidism was presented in terms of sensitivity and specificity. Receiver Operating Characteristic (ROC) curve is a graphical display of sensitivity on y-axis and (1-specificity) on the x-axis for varying cut-off points of test values. Spearman's Correlation coefficient (r) was also used to correlate the measured parameters (T_3, T_4, TSH, leptin, HOMA-IR and QTc).

3. RESULTS

The study group consisted of 46 patients with hyperthyroidism as (group 1), 35 females of them completed the study as seven patients excluded and four patients didn't attend follow up, with mean age of (42 ± 0.8117) years and mean body mass index of (25.98 ± 0.576) on monotherapy (carbimazole 5 mg); maximum starting dose of Carbimazole 45 mg and minimum dose 15 mg. The study also includes 26 healthy females as (group 2), with a mean age of (42.35 ± 1.296) years and mean body mass index of (25.57 ±0.7532). Almost all patients have gain weight after carbimazole therapy with an average of 3.5 kg. None of the participants were smoker, having any other diseases or taking other medications.

3.1 Baseline measurements and effect of carbimazole treatment on serum thyroid hormones (T3, T4 and TSH) level in hyperthyroidism patients and healthy control group.

The mean serum levels of T_3 and T_4, in hyperthyroidism subject's pre-treatment, was significantly higher compared to the control group (4.842 ± 0.3023 vs 1.681± 0.04436 nmol/l, $p<0.0001$) and (200.2 ±7.619 vs 105.1± 4.206 nmol/l, $p<0.0001$) respectively. While the serum level of TSH in hyperthyroid subject's pre-treatment treatment was significantly lower compared to the control group (0.01632 ± 0.0059 vs 2.317 ± 0.2027 uIU/ml, $p<0.0001$). After 3 months of treatment with carbimazole (median dose of 30 mg/day), all patients achieved an euthyroid state with a significant decrease in T_3 (1.867 ± 0.1014 nmol/l, $p<0.0001$), T_4 (92.46 ± 3.940 nmol/l, $p<0.0001$) and increase in TSH levels (2.176 ± 0.2848 uIU/ml, $p<0.0001$) (Figure 1).

3.2 Baseline measurements and the effect of carbimazole treatment on serum leptin level in hyperthyroidism patients and a healthy control group.

Serum leptin level in female patients with hyperthyroidism pre-treatment with carbimazole compared to the control group was non-significant (18.5 ± 2.28 ng/ml and 11.4 ±1.58 ng/ml respectively, $p>0.05$). Whereas after three months of therapy with carbimazole serum leptin level in hyperthyroid patients significantly increased compared to pre-treatment with carbimazole (24.6 ± 2.93 ng/ml and 18.5 ± 2.28 ng/ml respectively, $p<0.0001$) (Figure 2). Very-weak non-significant

positive correlation observed between T3 and T4 with leptin. Furthermore, a weak significant negative correlation seen between serum TSH with leptin (Figure 5). Moreover, the ROC curve of leptin and QTc doesn't verify a difference (sensitivity) between hyperthyroid patients and the healthy individuals (Figure 6).

3.3 Baseline measurements and the effect of carbimazole treatment on QTc interval duration in hyperthyroidism patients and a healthy control group.

Treatment with carbimazole shows non-significant effect on QTc interval in patients with hyperthyroidism pre-and post-treatment (425.11 ± 36.182 ms vs 422.894 ± 38.178 ms, $p > 0.05$) also non-significant difference in pre-treatment value compared to control group (411.2 ± 18.524 ms, $p > 0.05$) (Figure 3). Spearman's correlation shows a very weak non-significant positive correlation between serum T3 and T4 with QTc while a very weak significant negative correlation between serum TSH with QTc observed (Figure 5). Additionally, the ROC curve of QTc interval duration doesn't show discrimination between hyperthyroid patients and healthy individuals (Figure 6).

3.4 Baseline measurements and the effect of carbimazole treatment on serum insulin level and insulin resistance in hyperthyroidism patients and a healthy control group.

Serum insulin level and HOMA-IR value in control group was significantly lower than in hyperthyroid patients (10.2 ± 0.741 vs 23.1 ± 2.75 µU/ml, $p<0.0001$) and (2.58 ± 0.194 vs 6.02 ± 0.764, $p<0.0001$) respectively. While HOMA-IS in control group was significantly higher than in hyperthyroid patients (0.456 ± 0.0411 vs 0.253 ± 0.0276, $p<0.0001$).

Carbimazole significantly lowers insulin level and improves HOMA-IS in patients group (23.1 ± 2.75 vs 15 ± 1.87 µU/ml , $p<0.0001$) and (0.253 ± 0.0276 vs 0.396 ± 0.0436, $p<0.0001$) respectively after three months of treatment. Besides there was a significant decrease in HOMA-IR after treatment (6.02 ± 0.764 vs 3.86 ± 0.502, $p<0.0001$) (Figure 4). There was a significant positive correlation observed between serum T3 and T4 with HOMA-IR, whereas there was a significant negative correlation between serum TSH with HOMA-IR (Figure 5). Furthermore, the ROC curve of HOMA-IR, HOMA-IS verifies a difference (sensitivity) between hyperthyroid patients and healthy individuals (Figure 6).

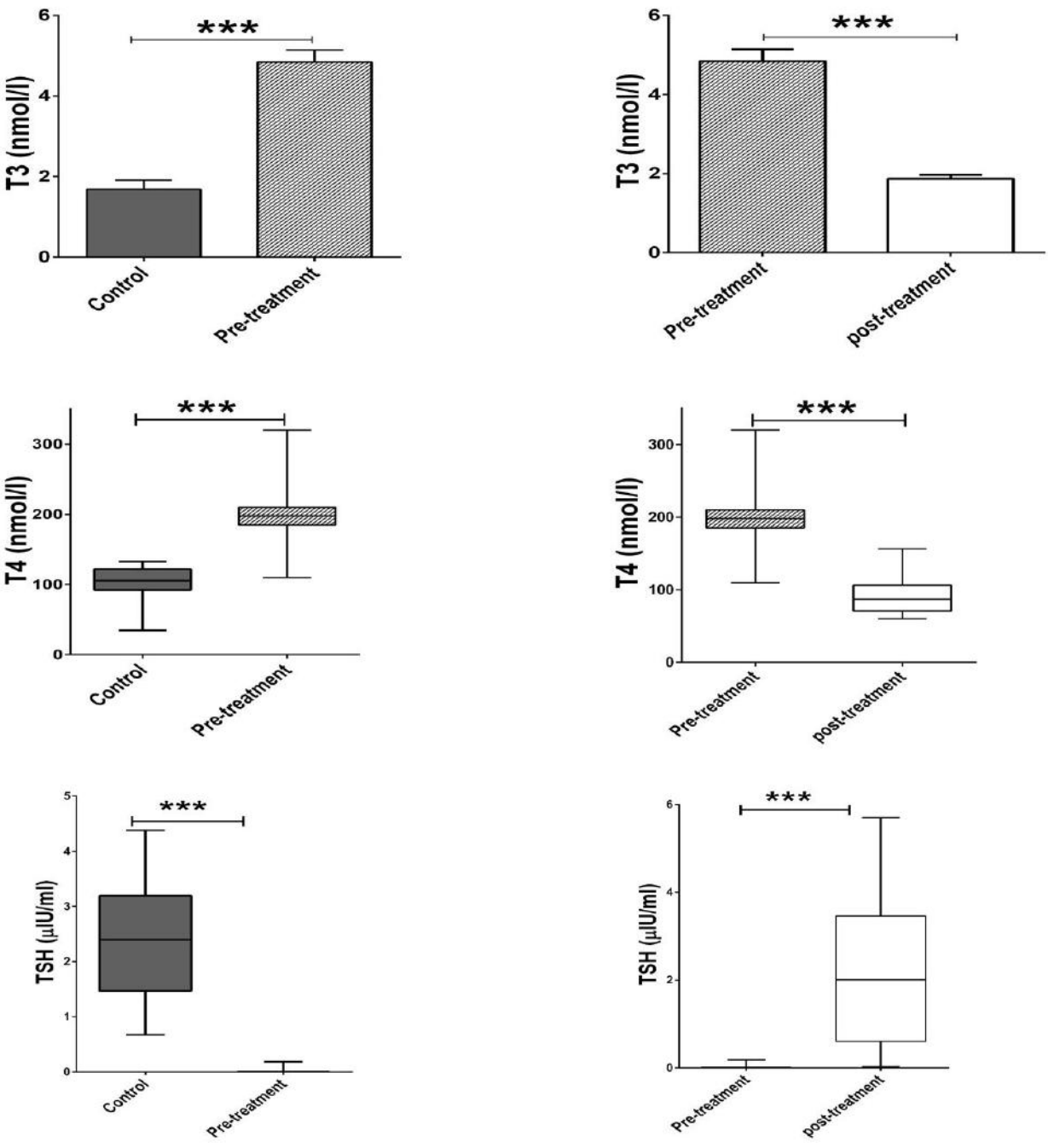

Figure 1. Effects of Carbimazole therapy on serum level of T3, T4 and TSH in female patients with hyperthyroidism and control subjects.

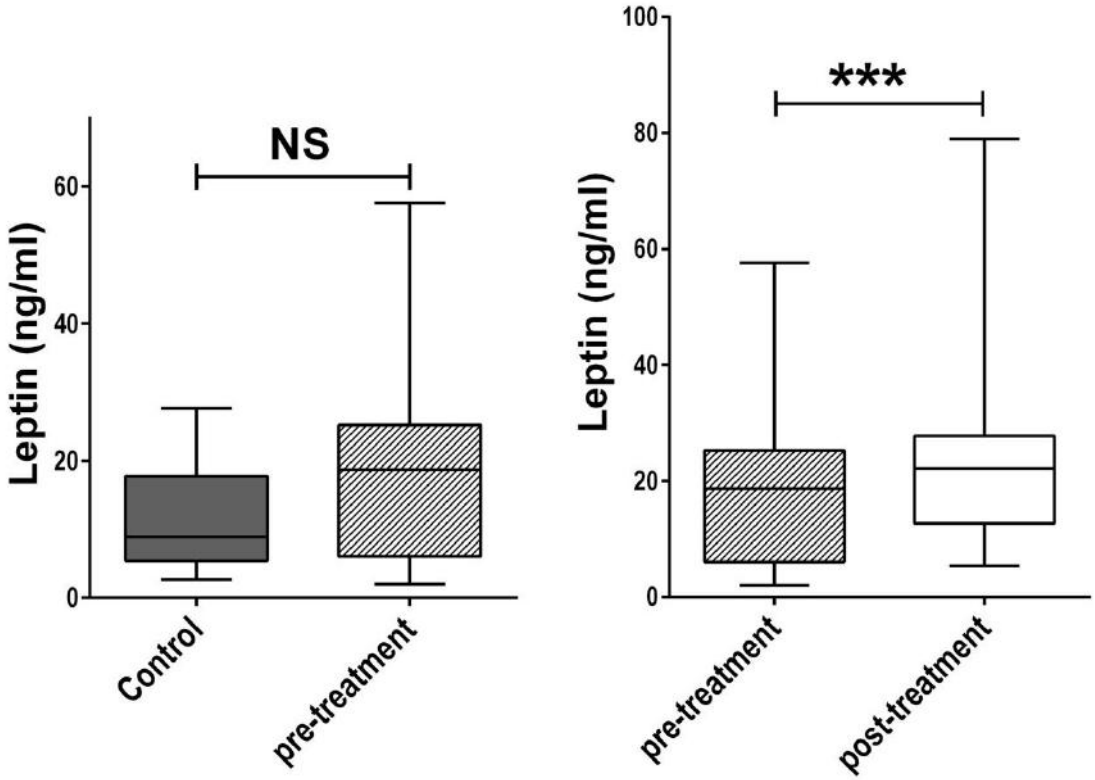

Figure 2. Effects of Carbimazole therapy on serum level of leptin in female patients with hyperthyroidism and control subjects.

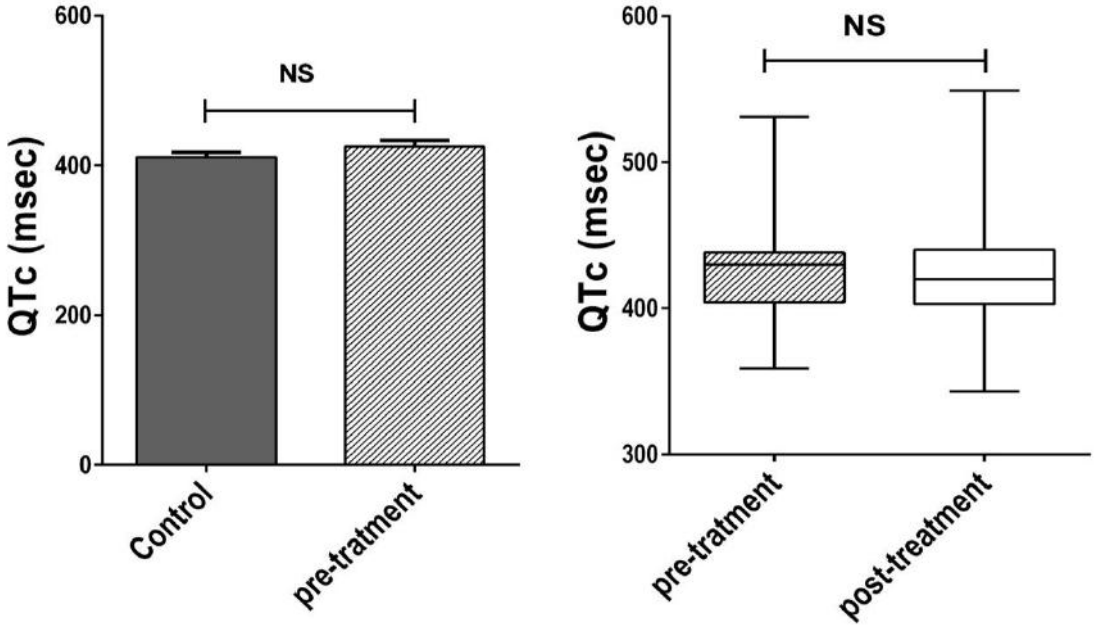

Figure 3. Effects of Carbimazole therapy on QTc interval in female patients with hyperthyroidism and control subjects.

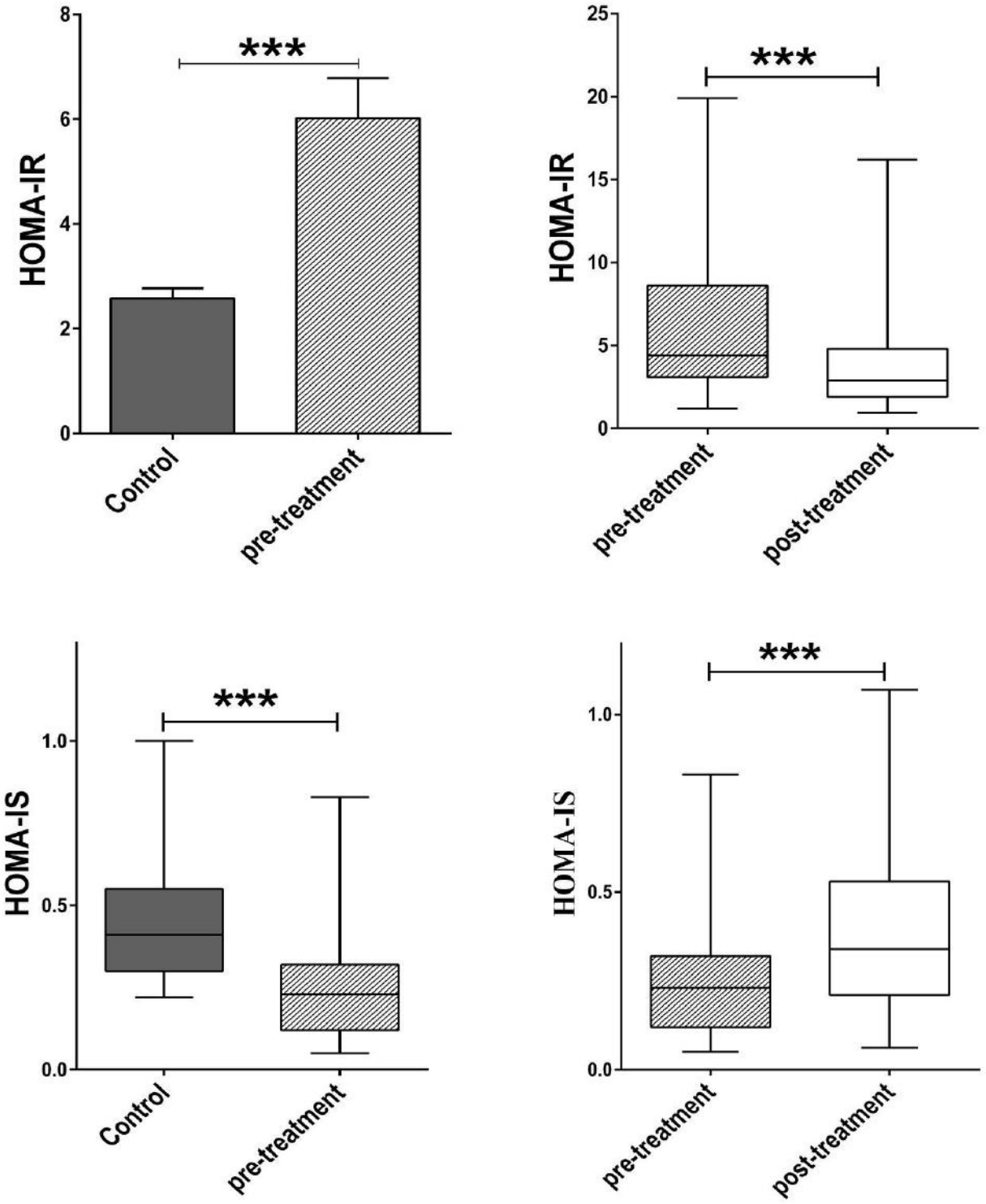

Figure 4. Impact of carbimazole on insulin resistance and insulin sensitivity in hyperthyroid patients and control subjects.

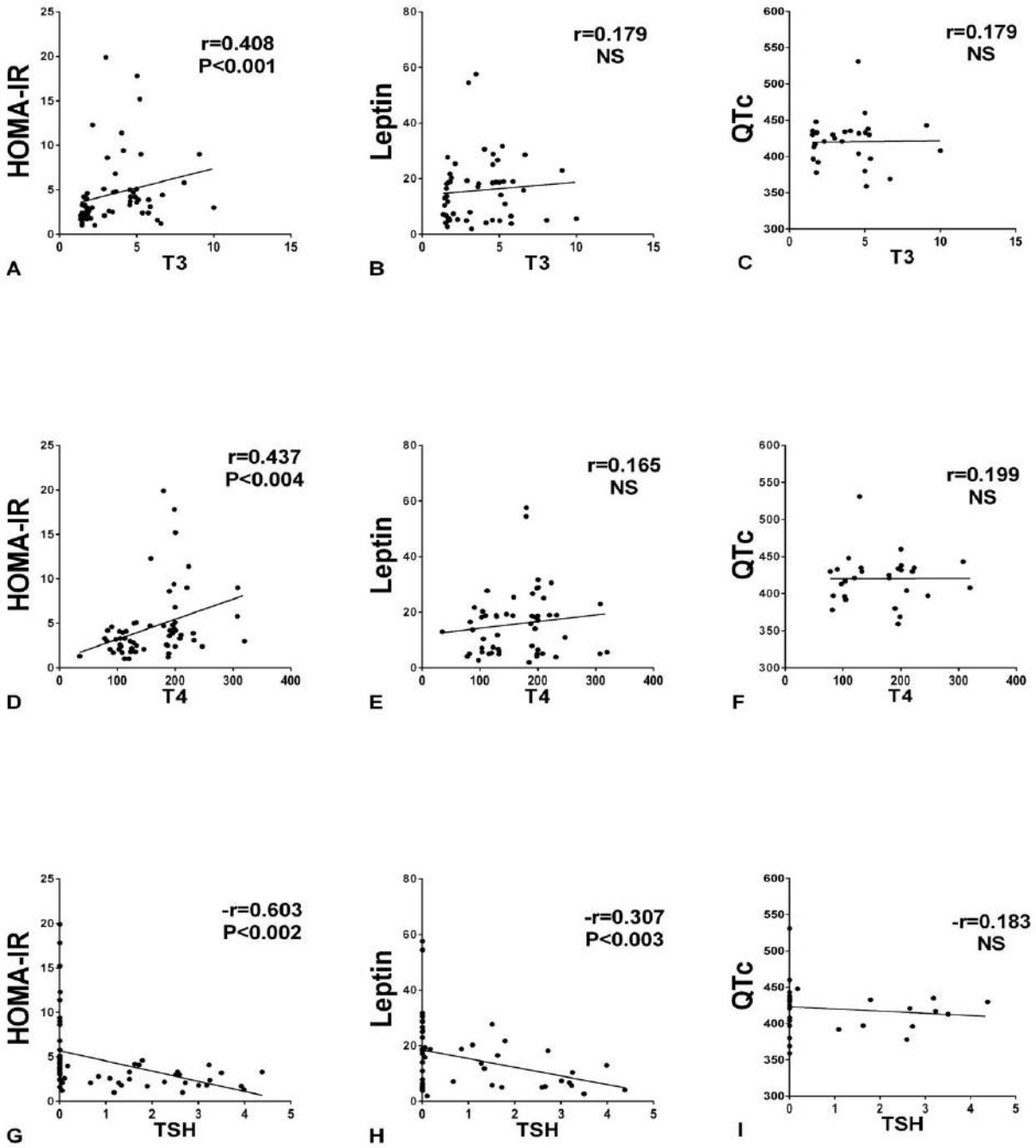

Figure 5. Spearman's correlations analysis between (A) Triiodothyronine (T3) and HOMA-IR, (B) Triiodothyronine (T3) and leptin, (C) Triiodothyronine (T3) and QTc, (D) Thyroxine (T4) and HOMA-IR, (E) Thyroxine (T4) and leptin, (F) Thyroid stimulating hormone (TSH) and QTc, (G) Thyroid stimulating hormone (TSH) and HOMA-IR, (H) Thyroid stimulating hormone (TSH) and leptin, (I) Thyroid stimulating hormone (TSH) and QTc.

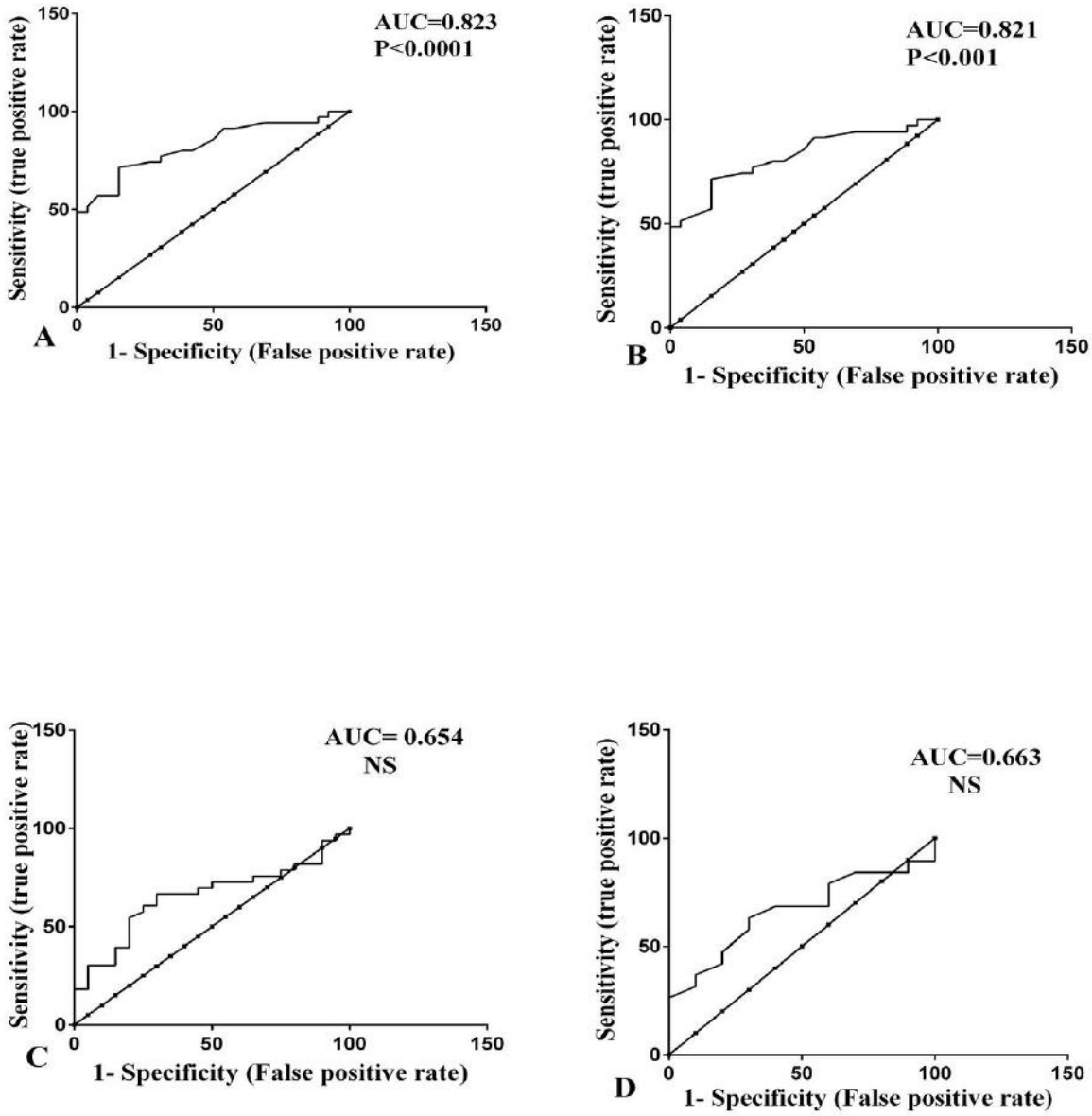

Figure 6. The ROC curves show: (A) The sensitivity and specificity of HOMA-IR, (B) The sensitivity and specificity of HOMA-IS, (C) The sensitivity and specificity of leptin and (D) The sensitivity and specificity of QTc in hyperthyroid patients. AUC: Area under the curve.

4. DISCUSSION

Antithyroid drugs are recommended for treatment of hyperthyroidism caused by overproduction of thyroid hormones in children, adults and pregnant women. They can be used as a long-term essential treatment for Graves' disease, with a duration of therapy that is considered to be 12 to 18 months, and can be given for longer durations up to 24 months in lower doses. A short-term ATD gave to prepare the patients with Graves' disease or toxic nodular goiter for thyroid surgery or radioactive ablation (Jastrzębska, 2015, Abraham et al., 2005).

It is documented that in hyperthyroidism disease, euthyroidism will be achieved after carbimazole therapy (Lizcano and Salvador, 2008, Dutta et al., 2012, Kansara et al., 2017) , similarly in our study all patients return to euthyroid state after carbimazole therapy.

Very few counted studies available that depend on carbimazole as ATD of choice for their study, opposite to that most studies depend on methimazole as ATD of choice. But, besides that carbimazole, which is a prodrug which gets converted into the active form methimazole, exerts same effects of methimazole with similar properties (Cooper, 2005), so we tried to mention studies that done on methimazole in our discussion.

In this clinical trial, there was a non-significant difference in serum leptin level in hyperthyroid patients compared to healthy control. Additionally, Spearman's correlation (weak correlation) show that decrease of TSH level associated with an increase in leptin level ($p<0.003$) while correlation between T_3 and T_4 and leptin was very weak and non-significant. However, reports available showing no alteration in serum leptin levels in thyroid dysfunction. Serum leptin concentrations either increased or unchanged in patients with hyperthyroidism. A study showed that thyroid hormone increases the expression of leptin mRNA and secretion of leptin in vitro adipocytes (Yoshida et al., 1998).

According to Baig *et al* (2003), serum levels of leptin in hyperthyroid female patients was lower than euthyroid control patients. (Al-Shoumer et al., 2000), also observed low leptin concentration of Arab women in Kuwait with hyperthyroidism, with an inverse relationship with T_3. Similarly, baseline leptin concentrations were significantly decreased in all hyperthyroid patients as compared with controls and non-significant correlation found between hyperthyroidism and leptin concentrations (Obermayer-Pietsch et al., 2001). Opposite to that, Studies show that serum leptin level increased in hyperthyroid patients compared to hypothyroid patients or healthy controls (Ozata et al., 1998, Nakamura et al., 2000, Dutta et al., 2012). Furthermore, some studies have found no correlation in serum leptin level in hyperthyroid patients when compared to control subjects (Valcavi et al., 1997, Sohn et al., 2015).The cause for this variability is unidentified, variation in leptin level may be due to different body weight or difference in thyroid hormone levels in hyperthyroid patients during the time of the study (Rosenbaum et al., 1996, Sreenan et al., 1997, Hsieh et al., 2002).

After 3 months of treatment with carbimazole leptin concentration significantly increased, as known Circulating leptin levels are directly in proportion to the amount of body fat (Park and Ahima, 2015), most of obese human subjects have elevated plasma levels of leptin associated to the size of their total adipose tissue mass (Hussain and Khan, 2017), and almost all female patients have weight gain after carbimazole therapy which may explain increase in leptin level post-treatment.

However, a study done by (Dutta et al., 2012) Dutta *et al* (2012), shows a decrease in leptin levels after 3 months of carbimazole therapy despite an increase in body weight after carbimazole therapy which they explain the decrease in leptin level may be due improvement in insulin resistance. Also serum leptin level in premenopausal females slightly decreased after methimazole therapy although a positive correlation found between serum leptin and %BF (body fat) (Braclik et al., 2008).

A study was done by Al-Shoumer et al., 2000, stated that after six months of therapy with carbimazole in female patients with hyperthyroidism there was non-significant change in serum leptin levels (Al-Shoumer et al., 2000). Another study that consists of 16 women and four men with hyperthyroidism treated with methimazole showed non-significant increase in leptin level post-therapy (Iglesias et al., 2003). Serum leptin in 21 female patients non-significantly decreased after two months of therapy with methimazole and 12 of these 21 patients were followed after 6 months of therapy and serum leptin was non-significantly increased compared to baseline measurements with significant increase in body weight (Nakamura et al., 2000), these findings suggest that antithyroid drugs in general has little or no effect on leptin level in humans, there may be another mechanism despite thyroid hormones that effect on serum leptin levels further investigations needed especially on genetic level.

In hyperthyroidism, decreased, normal, or even increased levels of plasma insulin have been reported. In the current study serum insulin levels and HOMA-IR were significantly higher than the healthy control group at baseline and significantly decreased after achievement of euthyroidism with carbimazole with improvement in insulin sensitivity , these results were consistent with other findings (Iglesias et al., 2003, Al-Shoumer et al., 2006, Chu et al., 2011, Dutta et al., 2012).

In our study, T_3 and T_4 were positively correlated with HOMA-IR, and TSH was negatively correlated with HOMA-IR, hyperthyroidism has been associated with insulin resistance, the mechanism of insulin resistance induced by thyrotoxicosis has not been completely explained. Furthermore, it is commonly recognized that leptin exerts an inhibitory effect on insulin secretion and leptin deficiencies are associated with hyperinsulinemia in humans. In which leptin directly affects pancreatic β-cell gene expression and leads to decrease insulin secretion (Seufert, 2004, Marroqui et al., 2012).

In the present study, there was non-significant change in QTc values in patients group pre-treatment compared to post-treatment with carbimazole and non-significant difference when compared to a healthy control group. And non-significant very weak correlation found between thyroid hormones and QTc interval (positive non-significant correlation between T3 and T4 with QTc interval while TSH shows a negative non-significant correlation), which hyperthyroidism may be associated with QTc interval prolongation.

QTc interval prolongation has been reported in many cases with hyperthyroidism along with positive correlation between QTc interval duration with FT_3 and FT_4 were founded while no correlation observed with TSH. Additionally, decreased the value of QTc interval after treatment with methimazole (Colzani et al., 2001, Owecki et al., 2006, van Noord et al., 2008, Lee et al., 2015).

Mechanism of hyperthyroidism induced QTc prolongation still not clear, there are hypothesis which states that increase in thyroid hormones may increase level of cardiac sodium/potassium adenosine tri-phosphatase (NA/K ATPase) leading to increase in intracellular K^+ level and causing membrane hyperpolarization and prolongation of the QTc interval (Awais et al., 2000, Colzani et al., 2001, Lee et al., 2015). These data's show us importance of evaluation of ECG during diagnosis of hyperthyroidism and throughout follow up and the evaluation of every electrocardiogram should also include interpretation of QT interval to determine arrhythmias and risk for their development and sudden death that may be associated with an abnormal QT interval.

However, during our study one hyperthyroid patient, QTc interval prolongation (531 ms) recorded in patient's ECG and after 3 months of carbimazole monotherapy there was significant decrease in QTc interval to normal values (436 ms) which may show the protective effect of carbimazole. A case report described by (Kulairi et al., 2017) Kulairi et al (2017), a 29-year-old male newly diagnosed with hyperthyroidism had a prolonged QTc interval of 509 ms after 3 months of treatment with propranolol and methimazole on ECG normal rhythm observed with normal QTC interval of 410 ms. However, no studies found to show effect of carbimazole on QTc interval in female hyperthyroid patients. Furthermore, studies that include a large number of populations are more necessary to determine effect of carbimazole on QTc interval.

5. CONCLUSIONS

From the results of the current study, following conclusions can be drawn: the level of serum insulin and HOMA-IR value increased significantly in hyperthyroid patients. Interestingly patients treated with carbimazole displayed a markedly reduction in the level of insulin and HOMA-IR value. The present new finding with respect to the ROC curve analysis of HOMA-IR suggested that it could be represent as a biomarker for hyperthyroid patients. Furthermore, a significant increase in leptin level observed after carbimazole therapy in female hyperthyroid patients and the ROC curve analysis of leptin suggested that it cannot be represent as a biomarker for hyperthyroid patients.

Conflict of Interest

The authors declare no conflict of interest.

References

ABRAHAM, P., AVENELL, A., PARK, C. M., WATSON, W. A. & BEVAN, J. S. 2005. A systematic review of drug therapy for Graves' hyperthyroidism. Eur J Endocrinol, 153, 489-98.

AL-SHOUMER, K. A., VASANTHY, B. A. & AL-ZAID, M. M. 2006. Effects of treatment of hyperthyroidism on glucose homeostasis, insulin secretion, and markers of bone turnover. Endocr Pract, 12, 121-30.

AL-SHOUMER, K. A., VASANTHY, B. A., MAKHLOUF, H. A. & AL-ZAID, M. M. 2000. Leptin levels in

Arabs with primary hyperthyroidism. Ann Saudi Med, 20, 113-8.

Al–Bustany, D.A., 2011. Clinical study of cases with hyperthyroidism in Erbil Governorate, Kurdistan Region-Iraq, *Zanco J. Med. Sci*, 15(1)

AWAIS, D., SHAO, Y. & ISMAIL-BEIGI, F. 2000. Thyroid hormone regulation of myocardial Na/K-ATPase gene expression. J Mol Cell Cardiol, 32, 1969-80.

Baig, M., A. Karira, K., Ahmed, A., Zaidi, P., Niaz, K., Kamal, S., 2003. Serum Leptin level in Hyperthyroid Female Patients, *Journal of the Pakistan Medical Association*, 53(5).

BRACLIK, M., MARCISZ, C., GIEBEL, S. & ORZEL, A. 2008. Serum leptin and ghrelin levels in premenopausal women with stable body mass index during treatment of thyroid dysfunction. Thyroid, 18, 545-50.

BRENTA, G. 2011. Why can insulin resistance be a natural consequence of thyroid dysfunction? J Thyroid Res, 2011, 152850.

CHU, C. H., LAM, H. C., LEE, J. K., LU, C. C., SUN, C. C., WANG, M. C. & CHUANG, M. J. 2011. Hyperthyroidism-associated insulin resistance is not mediated by adiponectin levels. J Thyroid Res, 2011, 194721.

COLZANI, R. M., EMDIN, M., CONFORTI, F., PASSINO, C., SCARLATTINI, M. & IERVASI, G. 2001. Hyperthyroidism is associated with lengthening of ventricular repolarization. Clin Endocrinol (Oxf), 55, 27-32.

COOPER, D. S. 2003. Hyperthyroidism. Lancet, 362, 459-68.

COOPER, D. S. 2005. Antithyroid drugs. N Engl J Med, 352, 905-17.

DE LEO, S., LEE, S. Y. & BRAVERMAN, L. E. 2016. Hyperthyroidism. Lancet, 388, 906-918.

DEVEREAUX, D. & TEWELDE, S. Z. 2014. Hyperthyroidism and thyrotoxicosis. Emerg Med Clin North Am, 32, 277-92.

DUTTA, P., BHANSALI, A., WALIA, R., KHANDELWAL, N., DAS, S. & MASOODI, S. R. 2012. Weight homeostasis & its modulators in hyperthyroidism before & after treatment with carbimazole. Indian J Med Res, 136, 242-8.

ERTEK, S. & CICERO, A. F. 2013. Hyperthyroidism and cardiovascular complications: a narrative review on the basis of pathophysiology. Arch Med Sci, 9, 944-52.

GOLDEN, S. H., ROBINSON, K. A., SALDANHA, I., ANTON, B. & LADENSON, P. W. 2009. Clinical review: Prevalence and incidence of endocrine and metabolic disorders in the United States: a comprehensive review. J Clin Endocrinol Metab, 94, 1853-78.

HSIEH, C. J., WANG, P. W., WANG, S. T., LIU, R. T., TUNG, S. C., CHIEN, W. Y., LU, Y. C., CHEN, J. F., CHEN, C. H. & KUO, M. C. 2002. Serum leptin concentrations of patients with sequential thyroid function changes. Clin Endocrinol (Oxf), 57, 29-34.

HUSSAIN, Z. & KHAN, J. A. 2017. Food intake regulation by leptin: Mechanisms mediating gluconeogenesis and energy expenditure. Asian Pac J Trop Med, 10, 940-944.

IGLESIAS, P., ALVAREZ FIDALGO, P., CODOCEO, R. & DIEZ, J. J. 2003. Serum concentrations of adipocytokines in patients with hyperthyroidism and hypothyroidism before and after control of thyroid function. Clin Endocrinol (Oxf), 59, 621-9.

JASTRZĘBSKA, H. 2015. Antithyroid drugs. Thyroid Research, 8, A12.

KANSARA, S., KOTWAL, N., KUMAR, K., SINGH, Y., UPRETI, V. & NACHANKAR, A. 2017. Effect of Antithyroid Therapies on Bone and Body Composition: A Prospective, Randomized, Clinical Study Comparing Antithyroid Drugs with Radioiodine Therapy. Indian J Endocrinol Metab, 21, 531-534.

KRAVETS, I. 2016. Hyperthyroidism: Diagnosis and Treatment. Am Fam Physician, 93, 363-70.

KULAIRI, Z., DEOL, N., TOLLY, R., MANOCHA, R. & NASEER, M. 2017. QT Prolongation due to Graves' Disease. Case Rep Cardiol, 2017, 7612748.

LEE, Y. S., CHOI, J. W., BAE, E. J., PARK, W. I., LEE, H. J. & OH, P. S. 2015. The corrected QT (QTc) prolongation in hyperthyroidism and the association of thyroid hormone with the QTc interval. Korean J Pediatr, 58, 263-6.

LIZCANO, F. & SALVADOR, J. 2008. Effects of different treatments for hyperthyroidism on the hypothalamic-pituitary-adrenal axis. Clin Exp Pharmacol Physiol, 35, 1085-90.

MARGETIC, S., GAZZOLA, C., PEGG, G. G. & HILL, R. A. 2002. Leptin: a review of its peripheral actions and interactions. Int J Obes Relat Metab Disord, 26, 1407-33.

MARROQUI, L., GONZALEZ, A., NECO, P., CABALLERO-GARRIDO, E., VIEIRA, E., RIPOLL, C., NADAL, A. & QUESADA, I. 2012. Role of leptin in the pancreatic beta-cell: effects and signaling pathways. J Mol Endocrinol, 49, R9-17.

MOHAN, A., JOSEPH, S., SIDHARTHAN, N. & MURALI, D. 2015. Carbimazole-induced agranulocytosis. J Pharmacol Pharmacother, 6, 228-30.

NAKAMURA, T., NAGASAKA, S., ISHIKAWA, S., HAYASHI, H., SAITO, T., KUSAKA, I., HIGASHIYAMA, M. & SAITO, T. 2000. Association of hyperthyroidism with serum leptin levels. Metabolism, 49, 1285-8.

OBERMAYER-PIETSCH, B. M., FRUHAUF, G. E., LIPP, R. W., SENDLHOFER, G. & PIEBER, T. R. 2001. Dissociation of leptin and body weight in hyperthyroid patients after radioiodine treatment. Int J Obes Relat Metab Disord, 25, 115-20.

OSUNA, P. M., UDOVCIC, M. & SHARMA, M. D. 2017. Hyperthyroidism and the Heart. Methodist Debakey Cardiovasc J, 13, 60-63.

OWECKI, M., MICHALAK, A., NIKISCH, E. & SOWINSKI, J. 2006. Prolonged ventricular repolarization measured by corrected QT interval (QTc) in subclinical hyperthyroidism. Horm Metab Res, 38, 44-7.

OZATA, M., OZISIK, G., BINGOL, N., CORAKCI, A. & GUNDOGAN, M. A. 1998. The effects of thyroid status on plasma leptin levels in women. J Endocrinol Invest, 21, 337-41.

PARK, H. K. & AHIMA, R. S. 2015. Physiology of leptin: energy homeostasis, neuroendocrine function and metabolism. Metabolism, 64, 24-34.

REID, J. R. & WHEELER, S. F. 2005. Hyperthyroidism: diagnosis and treatment. Am Fam Physician, 72, 623-30.

ROSENBAUM, M., NICOLSON, M., HIRSCH, J., HEYMSFIELD, S. B., GALLAGHER, D., CHU, F. & LEIBEL, R. L. 1996. Effects of gender, body composition, and menopause on plasma concentrations of leptin. J Clin Endocrinol Metab, 81, 3424-7.

ROSS, D. S., BURCH, H. B., COOPER, D. S., GREENLEE, M. C., LAURBERG, P., MAIA, A. L., RIVKEES, S. A., SAMUELS, M., SOSA, J. A., STAN, M. N. & WALTER, M. A. 2016. 2016 American Thyroid Association Guidelines for Diagnosis and Management of Hyperthyroidism and Other Causes of Thyrotoxicosis. Thyroid, 26, 1343-1421.

SATPATHY, P., DIGGIKAR, P., SACHDEVA, V., LADDHA, M., AGARWAL, A. & SINGH, H. 2013. Lipid profile and electrocardiographic changes in thyroid dysfunction. Medical Journal of Dr. D.Y. Patil University, 6, 250-253.

SEUFERT, J. 2004. Leptin effects on pancreatic beta-cell gene expression and function. Diabetes, 53 Suppl 1, S152-8.

SOHN, S. Y., JOUNG, J. Y., CHO, Y. Y., PARK, S. M., JIN, S. M., CHUNG, J. H. & KIM, S. W. 2015. Weight Changes in Patients with Differentiated Thyroid Carcinoma during Postoperative Long-Term Follow-up under Thyroid Stimulating Hormone Suppression. Endocrinol Metab (Seoul), 30, 343-51.

SREENAN, S., CARO, J. F. & REFETOFF, S. 1997. Thyroid dysfunction is not associated with alterations in serum leptin levels. Thyroid, 7, 407-9.

UDUAK, O. A., ANI, E. J., ETOH, E. C. & MACSTEPHEN, A. O. 2014. Comparative effect of Citrus sinensis and carbimazole on serum T4, T3 and TSH levels. Niger Med J, 55, 230-4.

VALCAVI, R., ZINI, M., PEINO, R., CASANUEVA, F. F. & DIEGUEZ, C. 1997. Influence of thyroid status on serum immunoreactive leptin levels. J Clin Endocrinol Metab, 82, 1632-4.

VAN NOORD, C., VAN DER DEURE, W. M., STURKENBOOM, M. C., STRAUS, S. M., HOFMAN, A., VISSER, T. J., KORS, J. A., WITTEMAN, J. C. & STRICKER, B. H. 2008. High free thyroxine levels are associated with QTc prolongation in males. J Endocrinol, 198, 253-60.

Wsoo M. A. and Rasul Kh. H., 2017. Epidemicity of Thyroid Gland Disorders Among Ranya Town Dwellers: A Hospital-Based Survey, *ZJPAS*,29 (5), 1-9.

YOSHIDA, T., MOMOTANI, N., HAYASHI, M., MONKAWA, T., ITO, K. & SARUTA, T. 1998. Serum leptin concentrations in patients with thyroid disorders. Clin Endocrinol (Oxf), 48, 299-302.

ZANCO Journal of Pure and Applied Sciences
The official scientific journal of Salahaddin University-Erbil
https://zancojournals.su.edu.krd/index.php/JPAS
ISSN (print):2218-0230**, ISSN (online):** 2412-3986**, DOI: http://dx.doi.org/10.21271/zjpas**

RESEARCH PAPER

The minimum inhibitory concentration of different antifungal agents against *Candida species*

Vian B. Nehmatullah
Department of Microbiology, College of Medicine, Hawler Medical University, Kurdistan Region, Iraq

A B S T R A C T

Five antifungal drugs (terbinafine, griseofulvin, nystatin, ketoconazole and itraconazole) were tested *in vitro* against three *Candida* species which were: (*Candida albicans, C. tropicalis and C. parapsilosis*) for detection their Minimum Inhibitory Concentration (MIC). First the Antifungal inhibitory activity was tested by disc diffusion for the tested *Candida* spices, the result shows that the *C. parapsilosis* was the most sensitive yeast, especially to ketoconazole which have the most inhibitory activity with zone of inhibition of (2.26cm), followed by nystatin with zone of inhibition of (2.05cm), while *C. albicans* was more sensitive to nystatin with zone of inhibition of (2.01cm) followed by ketoconazole with zone of inhibition of (1.86 cm), The result showed that nystatin was the most effective antifungal drug against *C. albicans* and *C. parapsilosis* with (MIC) range (0.383 and 0.443 µg/ml) respectively, while ketoconazole showed the most inhibitory effect on *C. tropicalis* with MIC range (0.248 µg/ml)., while *C. tropicalis* has MIC of ketoconazole at 5th fold of dilution which was 0.248, followed by terbinafine and itraconazole which was (0.383 and 0.376) respectively.

KEY WORDS: Antifungal agent, *Candida sp.*, Minimum inhibitory concentration.
DOI: http://dx.doi.org/10.21271/ZJPAS.31.4.4
ZJPAS (2019), 31(4);36-41.

1. Introduction

The *Candida* genus presents over 150 species of which 10 are responsible for infections in humans*Candida albicans* is part of its normal microbiota in the oral cavity in human beings, digestive, , urinary and reproductive tract of birds, and it is common to isolate few of these fungi from healthy animals (Mancianti *et al*., 2002). *Candida* species may cause systemic infection in immunocompromised situations, more than 90% of invasive infections are caused by *C albicans, C. glabrata, C. parapsilosis, C. tropicalis and C. krusei* (Pfaller and Diekema, 2007).

* Corresponding Author:
Vian Badraddin Nehmatullah
E-mail: vianbadr@yahoo.com
Article History:
Received: 19/09/2018
Accepted: 15/05/2019
Published: 10/09 /2019

Because the prevalence of fungal infections raised in recent decades and drug resistant to fungal infection are more occurs, need to use and pursue novel strategies to treat fungal infection (Zu, *et al*., 2016). Candidiasis routinely treated with antifungal drugs in clinical settings. the antifungal drugs.

commonly used to treat candidiasis are topical clotrimazole, topical nystatin, fluconazole, and topical ketoconazole, it is possible for C. *albicans* to develop a resistance to the drugs used to treat it, as seen from research done involving fluconazole, one of the drugs that is used to treat candidiasis and noted about the emergence of fluconazole resistant (Peter, *et al*., 2004). The aim of this study was to evaluate the *in vitro* antifungal activity of five antifungal agents (ketoconazole, itraconazole, nystatin, griseofulvin and terbinafine) against different *candida species* isolated from patients with different *candida* infections.

2. Materials and Methods: *In vitro* antifungal drug susceptibility testing.

2.1. Inoculum preparation:

The *Candida* spp. Were obtained from Biology dep., Science college Salahaddin University, preserved at Mycobank, the inoculum of *Candida spp*. (*C. albicans, C. tropicalis and C. Parapsilosis*) were prepared by suspending several colonies of grown cultures on Sabouraud's Dextrose Broth (SDB). Inoculum standardization was done using standard procedure in which the fungal suspensions were adjusted spectrophotometrically to an absorbance of 0.6 at 530 nm, which corresponds with the 0.5 McFarland standards (Siddiqui, *et al.,* 2013).

2.2. Disk diffusion method:

The commercially available following antifungal drugs: nystatin, itrconazole, ketaconazole, terbinafin and griseofulvin were used in this study. Each SDA plate was inoculated with the standard inoculum suspensions (0.1ml) by soaking a swab and rotating it over the agar plate. Six pore of diameter (6mm) were made on each agar plates with three replications for each, the pores were filled with appropriate antifungal suspensions. After 24 hours of incubation at 37℃ zone of inhibition of growth was measured and recorded. (Rex, et al., 1998).

2.3. Antifungal agent's preparation:

The antifungal agents stock solution (nystatin, itrconazole, ketaconazole, terbinafin and griseofulvin) were prepared according to the (Ismael, 2009).

2.3.1. Nystatin sensitivity test:

The stock solution (20 mg/ml) of Nystatin was prepared by dissolving a Nystatin disc (Al Kanawati medical products /Syria) which contained (500 000 I.U. of nystatin) in 10 ml of sterilized distilled water(SDW).

2.3.2. Itraconazole sensitivity test:

The stock solution (20 mg/ml) of the antimycotic was prepared by dissolving an Itraconazole disc (containing 100mg of Itraconazol antimycotic: JOSWE medical /Jordan) in 10 ml of SDW.

2.3.3. Ketaconazole sensitivity test:

The stock solution (20 mg/ml) of the antimycotic was prepared by dissolving a ketoconazole disc (containing 100mg of ketoconazole antimycotic: JOSWE medical /Jordan) in 10 ml of SDW.

2.3.4. Terbinafine sensitivity test:

The stock solution (20 mg/ml) of the antimycotic was prepared by dissolving a Terbinafine disc (250 mg: Jamjoom Pharma) in 10 ml of SDW.

2.3.5. Griseofulvin sensitivity test:

The stock solution (20 mg/ml) of the antimycotic was prepared by dissolving a griseofulvin disc (250 mg: Jamjoom Pharma) in 10 ml of SDW (Ismael, 2009).

2.4. Preparation of antifungal concentrations:

The concentrations (2, 4 and 6 mg/ml) prepared from the stock solution for each antimycotic were added to 500ml of SDA and poured onto sterilized Petri dishes and were inoculated by the fungi. A sterilized Petri dish with no addition of antifungal agents (SDA medium only), used as control, was also inoculated with fungi (Rios *et al*., 1987).

Yeast suspension prepared from 24-hour colony by using the Phosphate Buffer Saline (PBS) 0.1 ml of yeast suspension were inoculated on SDA then spread and later incubated at 37°C for 24-48 hour (Ismael, 2009).

2.5. Minimum Inhibitory Concentration (MIC):

The MIC was determined using the micro dilution technique. Ninety-six-well micro titer plates with a U-shaped bottom were used. Initially, 100 µL of Sabouraud's Dextrose Broth (SDB) (Difco, India) was distributed in the plate holes. Then, 100 µL of prepared antifungal solution was transferred to the first well and serially diluted by transferring an aliquot of 100 µL from the most concentrated well to the next cavity. Thus, antifungal concentrations from 112-fold dilution were obtained. Finally, 100 µL of inoculum corresponding to each strain was added to each cavity (de Castro, *et al*., 2015). The inocula were prepared in 0.9 % saline, and the turbidity of the fungal suspensions was compared with that of the solution in tube 0.5 of the McFarland nephelometric scale, which corresponds to an inoculum of approximately 106 CFU/mL, and adjusted as needed. Then, the suspension was diluted in SDB to obtain an inoculum concentration of 103 CFU/mL (CLSI, 2002).

Meanwhile, the viability of yeast strains (growth control) and medium sterility were controlled. Through serial dilution, nystatin concentrations from 1,000 µg/mL to 0.48 µg/mL were obtained (de Castro, et al., 2015).

The test was performed in triplicate, and the micro titer plates were incubated at 37 °C for 24 h. A visual reading was performed to determine the MIC of each antifungal agents on *Candida spp*. strains. The formation of cell clumps ("buds") on the bottoms of the wells was considered.

Thus, the lowest test product concentration that could visibly inhibit fungal growth was considered the MIC (CLSI, 2002). Spectrophotometric readings were based on the reduction of growth compared to that in a growth control well for each isolate. For this, micro titer plates were agitated and the optical densities of the wells were determined at 490 nm (de Castro, *et al*., 2015).

3. Results and Discussion:

Figure 1 and 2 shows the result of the activity of five tested antifungal agents which were (nystatin, itrconazole, ketaconazole, terbinafin and griseofulvin) against three tested *Candida* spp., as shown in the figure, Nystatin was the most effective antifungal agents, especially against *C. parapsilosis* the clear zone of nystatin were (2.01, 1.88, 2.05 cm) for *C. albicans, C. tropicalis* and *C. parapsilosis* respectively, followed by ketaconazole which also shows high inhibitory activity against tested *Candida*, which were 1.86, 1.78 and 2.26. *C. albicans, C. tropicalis* and *C. parapsilosis* respectively, followed by terbinafin (1.2, 0.96, 1.31 cm); and itraconazole (0.13, 0.78, 0.73 cm); against *C. albicans, C. tropicalis* and *C. parapsilosis* respectively, they show moderate inhibitory activity, while griseofulvin have lowest antifungal activity (0.4 cm) against *C. tropicalis*, and have no any inhibitory activity against another two tested *Candida* sp.

Nystain binds to ergosterols in the cell membranes, this interaction alters the membrane fluidity and perhaps produces pores in the membrane through which ions and small molecules are lost (Brooks, et al., 2004). Arikan, *et al*., (2002) stated that nystatin in general shows good activity against all *Candida* sp. That nystatin and liposomal nystatin have similarly active in vitro against a variety of *Candida* species.

These results are in agreement with those found by (Ismael, 2009) and (Al-Refai, 2006) whom stated that nystatin had an inhibitory effect on the growth *C. albicans, C. krusi, C. pseudotropicalis, and Rhodotorula sp*., and that *C. albicans* was the most sensitive where as *Rhodotorula sp*. was the least. This result is also in line with that found by (Bonifaz and Saul, 2000) there terbinafin was shown to be more efficacious after one week than ketoconazole was after two weeks of drug assimilation.

Table 1 presents the MIC obtained by spectrophotometric absorbance measurement and optical density determination based on turbidity due to growth of *Candida spp*. compared to the visual readings, the spectrophotometrically determined MIC values for the clinical isolates of *C. albicans, C. parapsilosis and C. tropicalis* were slightly lower: 3.7 IU/mL (0.625 µg/mL) at 24 hours, in contrast to the visual readings, only a few strains had a photometric MIC value of 7.4 IU/mL (1.25 µg/mL), as shown in table 1, *C. albicans* was sensitive to nystatin at 6^{th} fold of dilution which was 0.383, followed by terbinafine and ketoconazole which was (0.382 and 0.399 respectively), while *C. tropicalis* has MIC of ketoconazole at 5th fold of dilution which was 0.248, followed by terbinafine and itraconazole which was (0.383 and 0.376) respectively. While *C. topicalis* has MIC at 7^{th} fold of dilution to nystatin, followed by other tested antifungal agents.

As shown in the result nystatin shows the highest inhibitory activity against *C. albicans* which was (0.39 - 0.38) at 3rd - 6th fold of dilution, Nystatin was also the most effective antifungal drug against *C. parapsilosis* with (MIC) range (0.443 µg/ml) respectively, while Ketoconazole showed the most inhibitory effect on *C. tropicalis* with MIC range (0.248 µg/ml). While the griseofulvin shows the lowest rate of inhibition against all tested *Candida spp*.

The azoles interfere with the synthesis of ergosterol. They block the cytochrome P450-dependent 14 α demethylation of lanosterol, which is a precursor of ergosterol in fungi and cholesterol in mammalian cells (Brooks *et al*., 2004). This result is agreement with that found by (Nenoff, *et al*., 2016) who stated that the visual read-out of growth inhibition revealed MICs for nystatin in a range from 3.7 to 7.4 IU/mL (0.625 to 1.25 µg/mL) for all *Candida* species tested.

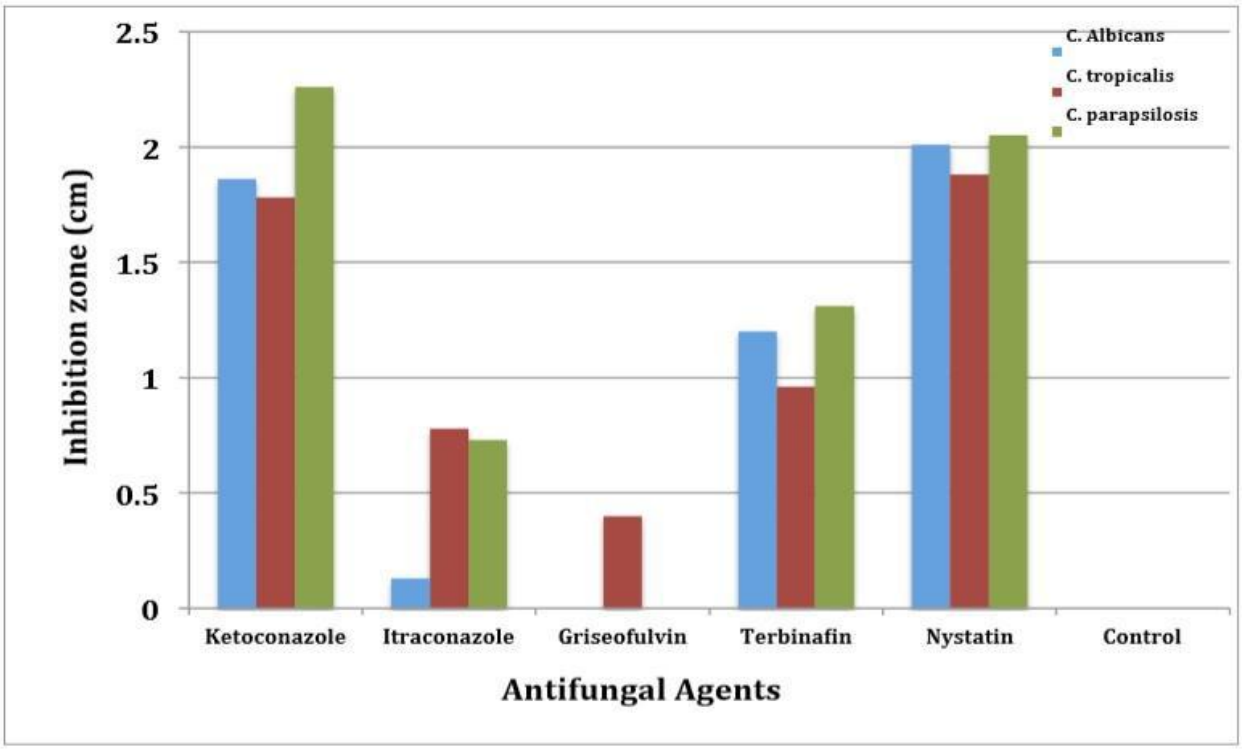

Figure 1: Means of inhibition growth diameter obtained by disc diffusion method using different antifungal agents against *Candida* spp.

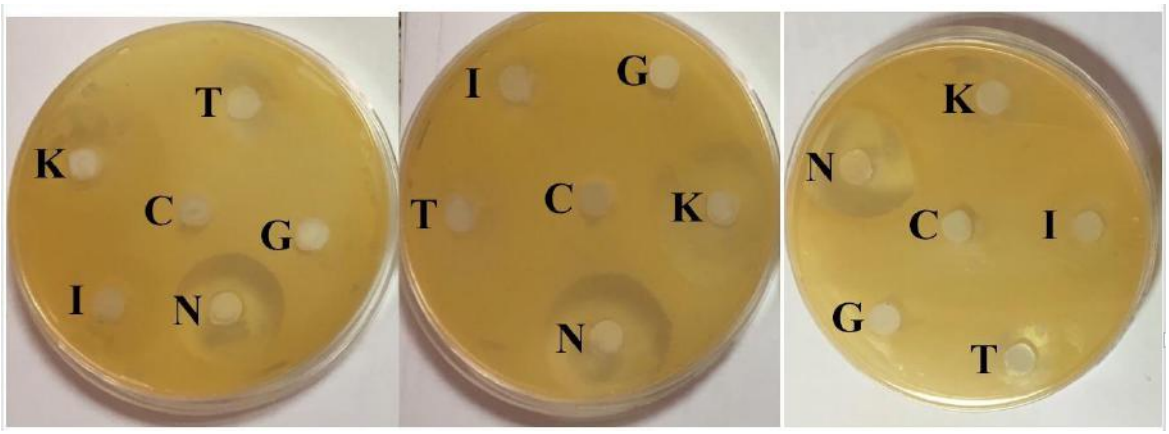

C. albicans ***C. tropicalis*** ***C. parapsilosis***

Figure 2: The Zone of inhibition of antifungal agents against *Candida spp*.

Table 1: In vitro Minimum Inhibitory Concentration Sensitivity test of five antifungal agents against three tested *Candida* spp.

Yeast	A	1	2	3	4	5	6	7	8	9	10	11	12	Control
C. albicans	N	0.921	0.576	0.392	0.389	0.371	0.383	0.531	0.58	0.589	0.592	0.589	0.608	0.62
	I	0.443	0.451	0.485	0.531	0.537	0.519	0.5	0.523	0.492	0.574	0.57	0.58	0.62
	K	0.558	0.465	0.452	0.399	0.424	0.405	0.406	0.416	0.437	0.42	0.426	0.426	0.61
	T	0.546	0.424	0.382	0.433	0.438	0.448	0.466	0.462	0.461	0.46	0.463	0.473	0.61
	G	1.596	1.035	0.729	0.612	0.566	0.578	0.578	0.588	0.582	0.582	0.572	0.603	0.61
C. tropicalis	N	0.485	0.47	0.378	0.249	0.475	0.44	0.455	0.45	0.331	0.495	0.489	0.486	0.51
	I	0.422	0.44	0.376	0.426	0.457	0.405	0.526	0.586	0.581	0.641	0.683	0.652	0.52
	K	0.744	0.364	0.29	0.278	0.248	0.357	0.462	0.62	0.557	0.693	0.587	0.592	0.5
	T	0.498	0.485	0.393	0.383	0.423	0.439	0.446	0.498	0.488	0.506	0.55	0.443	0.52
	G	1.619	0.878	0.669	0.602	0.649	0.518	0.629	0.658	0.659	0.659	0.639	0.639	0.51
C. parapsilopsis	N	1.082	0.796	0.526	0.588	0.473	0.465	0.443	0.524	0.468	0.497	0.545	0.522	0.649
	I	0.666	0.589	0.53	0.53	0.539	0.569	0.552	0.506	0.559	0.585	0.474	0.616	0.642
	K	1.049	0.668	0.462	0.544	0.444	0.634	0.577	0.499	0.493	0.42	0.463	0.452	0.649
	T	0.813	0.606	0.472	0.466	0.454	0.573	0.545	0.576	0.618	0.465	0.473	0.516	0.643
	G	1.696	1.135	0.688	0.605	0.483	0.564	0.613	0.504	0.509	0.617	0.576	0.451	0.644

References

Arikan, S., Ostrosky-zeichner, L., Lozano-Chiu., M., Paetznick, V., Gordon, D., Wallace T. and Rex., J (2002). Invitro activity of nystatin compared with those of liposomal nystatin, amphotericin B, and fluconazole against clinical Candida isolates, J Clin Microbiol, 40:1406-1412.

Brooks, G., Butel, J. and Morse, S. (2004). Jawets, Melnick, and Adelberg's Medical Microbiology. 20th ed. McGraw Hill, Boston. 818 pp.

Bonifaz A. and Saul, A (2000). Comparative study between terbinafine 15 emulsion-gel versus ketoconazole 2% creame in tinea cruris and tinea corporis. Eur J Dermatol 10:107

Clinical and Laboratory Standards Institute (CLSI) (2002). Protocol M27-A2. Reference method for broth dilution antifungal susceptibility testing of yeasts. 2nd ed. Pennsylvania: NCCLS.

de Castro, R. D., Pereira, Trícia M., de Souza, A., Bezerra, Louise M. D., Ferreira, G. LS., de Brito C., Edja, M. M. and Cavalcanti, A. L. (2015). Antifungal activity and mode of action of thymol and its synergism with nystatin against *Candida* species involved with infections in the oral cavity: an in vitro study. BMC Complementary and Alternative Medicine, 15:417.

Ismael, H. M. (2009). Prevalence of dermatophytes and non dermatophytic fungi in a rural village of Iraqi Kurdistan with special reference to their inhibition by some natural plant extract. Ph.D. Thesis. College of Science. SalahaddinErbil Univ. Iraq.

Mancianti, F., Nardoni, S., Cecchi, S., Corazza, M. and Taccini, F. (2002). Dermatophytes isolated from symptomatic dogs and cats in Tuscany, Italy during a 15-year-period. Mycopathologia 156: 13–18.

Neof, P., Kruger, C., Neumeister, C., Schwantes and Koch, D. (2016). In vitro susceptibility testing of yeasts to Nystatin low minimum inhibitory concentrations suggest no indication of in vitro resistance of *Candida albicans*, *Candida* species or non-*Candida* yeast species to Nystatin. Clin Med Invest, Volume 1(3): 7176.

Peter G.P., John H. R., Jack D. S., Scott G. F., William E. D., and John E. E. (2004). Guidelines for Treatment of Candidiasis, Clinical Infectious Diseases, 38(2): 161.

Pfaller A. and Diekema J. (2007). Azole antifungal drug cross-resistance: mechanisms, epidemiology, and clinical significance. J. Invasive Fungal Infect. 1:74–92.

Rajalakshmi R, Sangeetha D and Udhaya V (2017). Effect of antifungal drugs against candida isolates from diabetic women with vaginitis. , J Infect Dis. Ther. 5(4): 1-5.

Rex, J. H., P. W. Nelson, V. L. Paetznick, M. Lozano-Chiu, A. Espinel- Ingroff, and E. J. Anaissie. (1998). Optimizing the correlation between results of testing in vitro and therapeutic outcome in vivo for fluconazole by testing critical isolates in a murine model of invasive candidiasis. Antimicrob. Agents Chemother. 42: 129–134.

Rios, J. L., Recio, M. C. and Villar, A. (1987). Antimicrobial activity of selected plants employed in the Spanish mediterrranean area. J. Ethnopharmacology. 21: 135-144.

Siddiqui ZN, Farooq F, Musthafa TNM, Ahmad A, Khan AU. (2013). Synthesis, characterization and antimicrobial evaluation of novel halopyrazole derivatives. J Saudi Chem Soc.;17: 237– 243.

Zuo R, Garrison AT, Basak A, Zhang P, Huigens RW, Ding Y. (2016). In vitro antifungal and antibiofilm activities of halogenated quinoline analogues against *Candida albicans* and *Cryptococcus neoformans*. International journal of antimicrobial agents 48(2): 208-211.

ZANCO Journal of Pure and Applied Sciences
The official scientific journal of Salahaddin University-Erbil
https://zancojournals.su.edu.krd/index.php/JPAS

ISSN (print):2218-0230, ISSN (online): 2412-3986, DOI: http://dx.doi.org/10.21271/zjpas

RESEARCH PAPER

Antibiotic Resistance of Bacteria isolated in Urinary Tract Infections in Erbil City.

Ardalan Abdulhamid Osman (Khoshnaw)

Department of Pathological analysis, College of Science, University of Knowledge, Erbil, Kurdistan Region, Iraq

A B S T R A C T:

Urinary tract infections (UTIs) are the most unnoticed diseases worldwide. The resistant bacteria in UTI against commonly prescribed antimicrobials is coming forward with a daily demand for the management of antimicrobial treatment in health services. To estimate the resistance evolution of bacteria causing urinary tract infections to commonly used antimicrobials and to evaluate the options for treatment of UTIs. A total of 43 uropathogens of Gram- negative and Gram-positive bacteria were identified by using highly automated VITEK®2 System in Rizgare hospital; Erbil, Iraq; From January 2016 to December 2017. Four hundred eighty-two Urine samples from patients were cultured on appropriate bacteriological media and antibiotic sensitivity was determined by using disc diffusion method. From 482 urine specimens 80 % had positive results for bacterial cultures further more Among the 482 uropathogens, 184 samples tested for Extended-spectrum beta-lactamase (ESBL) which 94% was found to produce ESBLs. *E-coli* was the most common agent of UTIs (41.3 %) followed by *Staphylococcus* spp. (19.9%); *Klebsiella* spp. (11.6 %); *Streptococcus* spp. (7.3%); *Pseudomonas aeruginosa* (5%), *Sphingomonas paucimobilis* (4.1%); *Enterococcus* spp. (3.1%); *Proteus mirabilis* (2.9 %); other (4.8%). The disk diffusion assay proved that high degree of resistance among pathogens was to ampicillin; aztreonam; cephalothin; clindamycin; tetracycline. The lowest resistance was to amikacin; ciprofloxacin; imipenem and nitrofurantoin. Supervision for using favorable antibiotics and reducing the infection are very important.

KEY WORDS: Urinary tract infection; Antibiotic sensitivity; Antibiotic; Susceptibility; Resistance.
DOI: http://dx.doi.org/10.21271/ZJPAS.31.4.5
ZJPAS (2019), 31(4);42-49

INTRODUCTION:

Urinary tract infections (UTIs) are most ignored diseases in the world and responsible for twenty-five percent of the healthcare related infections (Rajivgandhi et al., 2018). It is considered to be the most common infectious disease-causing serious irregular medications. There are unstopped challenges in diagnosis and treatment procedures because of various infections are asymptomatic.

* **Corresponding Author:**
Ardalan Abdulhamid Osman (Khoshnaw)
E-mail: Ardalan.khoshnaw@gmail.com
Article History:
Received: 28/01/2019
Accepted: 19/05/2019
Published: 10/09/2019

Different species of bacteria which cause UTIs use different virulence mechanism for initial cell, tissue invasion and colonization of host mucosal surfaces and causing infections. These mechanisms include surface factors (fimbriae, adhesins, and P and type 1 pili) and extracellular factors (toxins, siderophores, enzymes, and polysaccharide coatings (Delcaru et al., 2016). Most of the UTIs bacteria enhancing the resistance against commonly used antibiotics to be resistance to multidrug (MDR) (Matsumoto and Muratani, 2004). Using of antibiotics agents often leads to increase of resistant microorganisms (Karam et al., 2016). In fact, one of the major

causes of increasing resistance is treatment failure in UTIs (Raeisi et al., 2017).

Escherichia coli has been identified by researchers to have a potent dominant in causing UTI. This followed by others like *Enterobacter* spp., *Klebsiella, Pseudomonas, Enterococcus,* and *Proteus* (Mohammed et al., 2016). During the last decade, the researches have observed that the antibiotic resistance in *E. coli* and *K. pneumoniae* increases (Sharma et al., 2007). One of the resistance mechanisms developed by Gram negative bacilli (GNB) is expression of Extended Spectrum Beta Lactamases (ESBL) which evolve bacteria to be multi drug resistance in UTIs ((K. Salih et al., 2016)) such as Acinetobacter spp., *Escherichia coli, Klebsiella pneumoniae, Proteus mirabilis* and *Pseudomonas* aeruginosa (Shaikh et al., 2015). The plasmids of GNB produce enzymes which enhance the bacterial resistance against beta lactam antibiotics, like cephalosporin, ceftazidime, piperacillin, furthermore the GNB have ability to make more antibiotic resistance genes against aminoglycosides, fluoroquinolones, chloramphenicol, tetracyclines and sulfamethoxazole (Rajivgandhi et al., 2018). The misuse antibiotic by patients, antibiotic quality, unhygienic environment responsible for drastic rise in resistance against different kinds of antibiotics including fluoroquinolones and all cephalosporin generations (Okeke et al., 2005).

The current study performed to evaluate the current antibiotic resistance in the common uropathogens isolated in Rizgare Hospital in Erbil- Iraq to guide the physicians through providing them sufficient information about choosing of the proper antibiotic for experiential treatment. Furthermore, to pursuit an evolutionary bacterial resistance making certain pathogens more resistant over time.

1. MATERIALS AND METHODS

A. Sample collection

A total of 482 Clean catch urine samples with suspected UTI patients were collected from both inpatients and outpatients of the Rizgare Hospital in Erbil - Iraq. The period of the study was 2 years (January 2016 to December 2017) and standard microbiological techniques were performed.

B. Culturing and Identification of Bacteria

Only patients with positive urine culture (≥100 000 CFU/mL) were studied to confirm the diagnosis and identification of the bacteria that causes the infection of urinary tract.

B.1 Culturing.

Each urine sample was inoculated into MacConkey Agar plates (used to distinguish the lactose fermenters bacteria from the others), Blood Agar Base plates (for the separation and cultivation of a variety of bacteria), and Muller-Hinton Agar plates (used to accomplish the antibiotics sensitivity test) also another culturing method used to identify unknown bacteria like Simmons Citrate Agar (This differential medium used to identify bacteria based on citrate utilization, especially for the *Enterobacteriaceae* spp.), Kligler Iron Agar (This differential medium used for specific bacteria which have the ability for fermentation of dextrose, lactose and produce hydrogen sulfide.), Urea Agar Base (for the isolation of bacteria that able to produce urease) and Eosin Methylene Blue Agar (for distinguish *E. coli* from *Klebsiella* spp).

All inoculated plates were incubated aerobically at 37°C for 18–24 hr. Sufficient population of bacteria were grown on the plate as well the bacteria isolated and sub cultured on selective media plates and the resulting cultures were subjected to microscopical and proper biochemical tests. The identified of bacteria species was done with various techniques including: examination of characteristics bacterial growth (color, texture, growth pattern, etc.) and Gram staining.

B.2 VITEK 2 System

The VITEK 2 is an automated microbiology system. A total of 482 bacterial isolates were identified by using highly automated VITEK®2 System which provided results on the same day (Bosshard et al., 2006). The VITEK 2 system use three identification cards to identify unknown microorganism (1). GN ID (Gram negative identification), (2). GP ID (Gram positive identification cards) and (3). YST ID (yeast and yeast like organism's identification cards) **(**Wallet et al., 2005). In the current study only, GP ID and GN ID were performed.

B.3. Antibiotic Sensitivity Test:

After that the species were identified, all isolated bacteria were recultured on Muller Hinton

Media and then antibiotic disks as shown in Table 1. were placed on the surface of the Muller Hinton Agar plates then incubated at 37°C for 24 h. After the incubation time, the diameter of the of inhibition zones for each disk were measured, determination of the bacterial population's sensitivity to a range of antibiotics were assessed by using disk diffusion assay Table (1).

Table 1: Antibiotics used for Gram-positive bacteria with its disc content

Gram positive bacteria	*Antibiotics*	*Abr.*	*disc content*
	Ciprofloxacin	CIP	5 µg
	Cefazolin	CZ	30 µg
	Cefotaxime	CTX	30 ug
	Clindamycin	CM	2 µg
	Erythromycine	E	15 µg
	Fusidic Acid	FA	10 µg
	Gentamicin	GM	10 µg
	Levofloxacin	LVX	5 µg
	Moxifloxacin	MXF	5 ug
	Mupirocin	MUP	5 µg
	Nitrofurantion	NIF	300 µg
Staphylococcus spp.	Oxacillin	OX	5 µg
*Streptococcu*s spp.	Penicillin	P	6 µg
Enterococcus faecalis	Rifampicin	RA	5 µg
	Tetracycline	TE	30 µg
	Teicoplanin	TEC	30 µg
	Tigecycline	TGC	15 µg
	Tobramycin	TM	10 µg
	Vancomycin	VAN	30 µg

Table 2: Antibiotics used for Gram-negative bacteria with its disc content

Gram negative bacteria	*Antibiotics*	*Abr.*	*disc content*
	Amikacin	AN	30 µg
	Amoxicillin + Clavulanic Acid	AMC	20 + 10 µg
Achromobacter denitrificans	Ampicillin	AMN	10 µg
Aeromonas sobria	Ampicillin + Sulbactam	SAM	10 + 10 µg
Acinetobacter lwoffii	Aztreonam	ATM	30 µg
Citrobacter spp.	Cefazolin	CZ	30 µg
Escherichia coli	Cefepime	FEP	30 µg
Enterobacter spp.	Cefotaxime	CTX	30 µg
Klebsiella pneumoniae	Ceftazidime	CTZ	30 µg
Pasteurella pneumotropica	Ceftriaxone	CRO	30 µg
Proteus spp.	Ciprofloxacin	CIP	5 µg
Providencia stuartii	Colistin	CS	10 µg
Pseudomonas spp.	Ertapenem	ETP	10 µg
Morganella spp	Imipenem	IPM	10 µg
Serratia spp.	Levofloxacin	LVX	5 µg
Salmonella typhi	Linezolid	LZD	30 µg
Sphingomonas paucimobilis	Meropenem	MEM	10 µg
	Piperacillin + Tazobactam	PTZ	30+6 µg
	Trimethoprim+ Sulfamethoxazole	SXT	1.25+23.75 µg

C. Statistical analysis

The latest version of Statistical Analysis Software (SPSS) used for calculating and analysis the results, likewise parameters between 2016 and 2017 were compared.

2. Result and discussion

The antibacterial sensitivity pattern from the collected samples, 199 *E. coli* (41.3%), 96. *Staphylococcus* spp. (19.9%), 56 *Klebsiella* spp. (11.6 %), 35 *Streptococcus* spp. (7.3%), 24 *Pseudomonas aeruginosa* (5%), 20 *Sphingomonas paucimobilis* (4.1%), 15 *Enterococcus* spp. (3.1%), 14 *Proteus mirabilis* (2.9 %), 23 others (4.8%) as shown in Table (3).

Table 3: Prevalence of bacterial isolates from urine samples of the patients.

	2016		2017	
Bacteria isolates	**Number of isolates**	**Incidence rate (%)**	**Number of isolates**	**Incidence rate (%)**
Citrobacter spp.	3	1	0	0
Enterococcus faecalis	9	3	4	2
Escherichia coli	109	39	90	44
Enterobacter spp.	1	0	3	2
Klebsiella pneumoniae	25	9	28	14
Klebsiella oxytoca	2	1	1	1
Proteus mirabilis	9	3	5	2
Pseudomonas aeruginosa	7	3	9	4
Pseudomonas spp.	3	1	5	2
Serratia spp.	0	0	4	2
Sphingomonas paucimobilis	7	3	13	6
Staphylococcus aureus	5	2	1	1
Staphylococcus epidermidis	6	2	4	2
Staphylococcus haemolyticus	48	17	18	9
Staphylococcus spp.	7	3	7	3
Streptococcus pyogenes	2	1	4	2
Streptococcus agalactiae	22	8	3	1
Streptococcus spp.	3	1	1	1
Other	9	3	5	2
Total	277	100%	205	100%

The antibiotic sensitivity pattern of the common Gram-negative and Gram- positive bacteria were confirmed in Rizgare Hospital Laboratory. The confirmation was done by using highly automated VITEK®2 System Table 4, 5.

Table 4. The percentage of antibiotic sensitivity pattern of the common Gram-negative bacteria.

GNB	***E. coli***			***Kl. pneumoniae***			***Sp. paucimobilis***			***Ps. aeruginosa***			***P. mirabilis***		
	S	I	R	S	I	R	S	I	R	S	I	R	S	I	R
AN	93	0	7	93	0	7	100	0	0	100	0	0	100	0	0
AMC	43	27.5	29.5	36.5	30	33.5	83.5	16.5	0	23	0	77	58	42	0
AMN	3.5	1.5	95	0	0	100	33.5	42	24.5	7	7	86	33	0	67
SAM	19.5	15.5	65	20.5	8	71.5	87.5	12.5	0	25	0	75	70	15	15
ATM	0	0	100	22.5	22	55.5							100	0	0
CZ	11.5	0.5	88	21	0	79	79.5	4	16.5	25	0	75	21.5	7	71.5
FEP	7.5	0.5	92	34	0	66	90	0	10	81	0	19	36	0	64
CTX				100	0	0									
CTZ	6	0.5	93.5	33	4.5	62.5	65	19	16	93	7	0	43	9	57
CRO	7.5	0	92.5	31	3	66	80	10	10	0	0	100	36	0	64
CIP	42.5	2	55.5	60	12.5	27.5	65.5	4.5	30	69	19	12	42	21	36
CS				100	0	0				0	0	100			

ETP	88	0.5	11.5	90	5	5				80	0	20	85	15	0
GM				65	0	35	81	0	19	85	15	0	50	14	36
IPM	94	0.5	5.5	100	0	0	93	0	7	84	0	17	100	0	0
LVX	48	1.5	50.5	64.5	2.5	33	65	25	10	62.5	6.5	31	50	7	43
MEM	92.5	0	7.5	93	0	7				67	33	0	100	0	0
NIF				36.5	35	28.5	75	5	20	21	0	79	8	0	92
P				12.5	12.5	75									
PTZ	72.5	10	17.5	68	21.5	10.5	91.5	8.5	0	100	0	0	92	8	0
TGC				100	0	0				80	20	0	0	0	100
TM	40.5	11	48.5	46	19	35	83.5	0	16.5	33	7	60	43	7	50
SXT	41.5	0	58.5	34.5	0	65.5	61.5	0	38.5	57	0	43	7	0	93

Table 5. The percentage of antibiotic sensitivity pattern of the common Gram-positive bacteria.

GPB	***Ent. faecalis***			***St. haemolyticus***			***Str. agalactiae***		
	S	I	R	S	I	R	S	I	R
BenP				1	0	99			
CTX							100	0	0
CRO							100	0	0
CM	5.5	0	94.5	8	0	92	11	0	89
E	0	29	71	6.5	0	93.5	0	0	100
FA				13	7.5	79.5			
GM				64	7.5	28.5			
LVX	65.5	0	34.5	55	22	23	85	0	15
LZD	65.5	0	34.5				100	0	0
MXF	71	12.5	16.5	73.5	17	9.5			
MUP				95.5	0	4.5			
NIF	83	0	17						
OX				2	0	98			
RA				27	0	73			
TEC	83.5	0	16.5	15	6	79			
TE	16.5	0	83.5	29.5	9.5	61	11.5	0	88.5
TGC	100	0	0	90	3	7			
TM				62.5	19	18.5			
TMP	50	0	50	67	0	33	95	0	5
VAN	34.5	0	65.5	17.5	0	82.5	97	0	3

From the turn of the 20th century, antibiotics resistance phenomenon has been growing quickly among uropathogens worldwide (Prestinaci, Pezzotti and Pantosti, 2015). isolated uropathogens presented high grade of resistance to commonly used antibiotics in the curing of variety of contagious diseases in Erbil - Iraq. Analysis of the results in Table 4 and 5 showing that.

Group 1. Fluoroquinolones

These group includes Ciprofloxacin, Moxifloxacin, Enoxacin, Fleroxacin, Gatifloxacin, Lomefloxacin, Levofloxacin, Norfloxacin, Ofloxacin and Pefloxacin used to treat UTIs. However, bacterial resistance to fluoroquinolones antibiotics enhanced by the production of ESBLs. Analysis of the results in Table 4 and 5 showing that 55.5% of *E. coli* and 27.5% of *K. pnumoniae*, 30% of *S. paucimobilis*. 33% of *P. mirabilis* were resistant to ciprofloxacin. In addition, ciprofloxacin showed less activity against *E. aerogenes*, *P. aeruginosa*, *A. lwoffii*, Levofloxacin High resistance rate observed among the isolates Gram-positive and negative pathogens in our study, the resistance rate was (34.5%) *E. faecalis*, (23%) *S. haemolyticus*, (15%) *S. agalactiae*, (50.5%) *E. coli*, (30%) *K. pneumoniae*, (10%) *S. paucimobilis*. Moxifloxacin. highly active against

Gram-positive pathogens such as *E. faecalis, S. haemolyticus* as shown in Table (4).

Group 2. Penicillin.

Include Ampicillin/sulbactam, Ampicillin, Amoxycillin, Azidocillin, Amoxycillin/clavulanic acid, Bacampicillin, Cloxacillin, Dicloxacillin, Flucloxacillin, Mezlocillin, Oxacillin, Penicillin G, Penicillin V, Propicillin, Piperacillin, Piperacillin tazobactam, sulbactam are family of these group. Ampicillin, have very weak activity against *E. coli, K. pnumoniae*. Despite that, resistance may happen. Aminopenicillins are touchy to beta -lactamases. Thus, they are not adequately active against specific species of bacteria, such staphylococci, and many enterobacteria. Our findings of high resistance rates to ampicillin highlights the fact that the above antibiotics should no longer be used for treatment.

Piperacillin-Tazobactam, they are described by their elevated activity against GNB such as *E. coli, K. pnumoniae, S. paucimobilis, E. aerogenes, P. aeruginosa*. Oxacillin has a narrow range of activity which showed high resistance rate in *S. haemolyticus*.

Group 3. Cephalosporins.

Include Axetile, Cefalexin, Ceftazidime, Cefadroxil, Cefaclor, Cefuroxime, Cefetamet, Ceftibuten, Cefixime, Cefazolin, Cefamandole, Cefotiam, Cefotaxime, Ceftriaxone, Cefoperazone, Cefepime, Loracarbef, and Pivoxil, they have very weak activity against Gram-negative microorganisms except in *S. paucimobilis* showed eight-fold higher activity. Cefepime, has very weak activity against Gram-negative bacteria like *E. coli, K. pnumoniae* except *S. paucimobilis* was 90 % sensitive to cefepime and a superior action against Gram-positive bacteria (Table 5). Cefotaxime, highly sensitive rate (100 %) observed in *Str. agalactiae* and *Kl. pneumoniae* rendering them as suitable choice for empiric treatment. Ceftriaxone, high resistance rate observed in *E. coli, K. pnumoniae* except for *S. paucimobilis* and *Str. agalactiae* was very sensitive to ceftriaxone. Our findings of high resistance rate to cephalosporines are significantly and agreeing with other studies in Iran (Ranjbar et al., 2009), and Turkey (Gökçe et al., 2017).

Group 4. Monobactams.

Among the monobactams, only aztreonam is available. according to other study it is active just against Gram-negative bacteria but in our study showed high resistance rate in *E. coli, K. pnumoniae.*

Group 5. Carbapenems.

Include Imipenem, meropenem, ertapenem have good activity against Gram-negative bacteria also *P. aeruginosa.*

Group 6. Aminoglycosides.

Include Amikacin, Gentamicin, tobramycin, Streptomycin. They have adequate activity against Gram-negative bacteria specifically Amikacin the sensitivity rate was between 93%- 100%. Sensitivity for tobramycin, gentamicin against GNB and GPB are moderate except that they are very active against *Sph. paucimobilis*.

Group 7. Glycopeptides.

Include Vancomycin, teicoplanin. They are active against Gram-positive pathogens, i.e. Vancomycin are very active against *Str. agalactiae* unless *Ent. faecalis, Sta. haemolyticus* showed high resistance rate. other than teicoplanin is mainly active against *Ent. faecalis* with limited activity against *Sta. haemolyticus*.

Group 8. Oxazolidones.

The exclusive item of this group is linezolid. It has good effectiveness against Gram-positive cocci, such as staphylococci, enterococci and streptococci.

Group 9. Macrolides.

include Erythromycin, clarithromycin, azithromycin only Erythromycin used in this study and observed high resistance rate in GPB.

Group 10. Tetracyclines.

Include Doxycycline, minocycline and tetracycline, which Shows high range of resistance against tetracycline of streptococci, enterococci and staphylococci.

Group 11. Nitrofuran.

The only substance of this group is ***Nitrofurantoin.*** has low activity against Gram-negative and Gram-positive bacteria.

Group 12. Trimethoprim- sulphamethoxazole.

Has Moderate influence against Gram-negative and Gram-positive bacteria without Streptococcus *agalactiae* was very sensitive.

This study was prepared to focus some light on MDR in UTI isolates from patients who visited Rizgary Hospital Laboratory in Erbil, Iraq during 2016 1nd 2017.

Our data showed that among the isolated Gram-positive bacteria *Staphylococcus* spp. was the most abundant (19.9%), and Staphylococci Coagulase Positive was the least detected one (0.2%). Later on, antibiotic susceptibility test identified *St. haemolyticus* as the most resistant GPB (55.09%) especially to: Cefotaxime, Ceftriaxone, Linezolid, Trimethoprim and Vancomycin, and *Str. agalactiae* as the most sensitive one (66.61%) especially to: Cefotaxime, Ceftriaxone, Linezolid, Trimethoprim and Vancomycin.

In regard to isolated Gram-negative bacteria, *E. coli* was the most abundant (41.3%), and *P. pneumotropica, A. sobria, Pr. stuartii, A. denitrificans* And *S. typhi* were the rarest (0.2%). For antibiotic sensitivity test, *E. coli* was the most resistant bacteria (53.97) especially to: Ampicillin, Aztreonam, Cefazollin, Ceftriaxone and *Sp. paucimobilis* was the most sensitive one (77.19) especially to: Amikacin, Ampicillin, Cefazollin, Cefepime, Ceftriaxone, Gentamicin, Imipenem, Nitrofurantoin, Piperacillin + Tazobactam and Tobramycin. Ahmed et al. (2018) reported similar results to ours in regard to the percentile of uropathogenic, GNB and GPB (Al-Naqshbandi, Chawsheen and Abdulqader, 2019).

Finally, our data also show that isolated GNB, were highly resistant to: Amoxicillin + Clavulanic Acid, Cefazollin, Cefepime and ethoxazole and GPB were highly resistant to: Benzylpenicillin, Clindamycin, faropenem, Oxacillin, Rifampicin, Teicoplanin, Vancomycin and Tetracycline.

3. Conclusion:

While antibiotic resistance rates in bacterial pathogens causing UTI increase; The results of this study confirm the increasing resistance to antibiotics. The best activity against uropathogens achieved with imipenem, amikacin, tigecycline, linezolid, cefotaxime, ceftriaxone, ciprofloxacin, meropenem as shown in table (4,5). Those antibiotics are suitable choice for difficulties treatment of UTI. Thus; Finally, it is the responsibility of all healthcare providers to selecting the correct drug, dose, avoid misdiagnosis of UTI and physicians should prescribe antimicrobials prudently, thoughtfully and rationally to improve quality of healthcare, since this is a significant issue which should to be censored and considered by Government as well Government should support researcher to make more research about UTI because the pattern of bacterial resistance to antibiotics remain vital, important and interested for many further studies. In addition, there is a need for greater education among local population in Erbil for proper hygienic practice regarding the prevention of UTI.

Acknowledgments

First of all, I would like to express my sincere thanks to the lord of the universe, Allah, the almighty, who enables me to achieve this work. My deep appreciation and gratitude go to my wife (Banaz Muhamad) for her continuing support and encouragement. Deepest thanks are due to the Ministry of Higher Education and presidency of the knowledge university in Erbil for giving me the opportunity to continue this research. Finally, I would like also express my great gratitude and faithful thanks to everyone working at the Rizgary Hospital for so kind guidance, sharing the instruments during the entire period of this work.

References

Al-Naqshbandi, A., Chawsheen, M. and Abdulqader, H. (2019). Prevalence and antimicrobial susceptibility of bacterial pathogens isolated from urine specimens received in rizgary hospital, Erbil. *Journal of Infection and Public Health*, 12(3), pp.330-336.

Bosshard, P., Zbinden, R., Abels, S., Boddinghaus, B., Altwegg, M. and Bottger, E. (2006). 16S rRNA Gene Sequencing versus the API 20 NE System and the VITEK 2 ID-GNB Card for Identification of Nonfermenting Gram-Negative Bacteria in the Clinical Laboratory. *Journal of Clinical Microbiology*, 44(4), pp.1359-1366.

Delcaru, C., Alexandru, I., Podgoreanu, P., Grosu, M., Stavropoulos, E., Chifiriuc, M. and Lazar, V. (2016). Microbial Biofilms in Urinary Tract Infections and Prostatitis: Etiology, Pathogenicity, and Combating strategies. *Pathogens*, 5(4), p.65

Gökçe, İ., Çiçek, N., Güven, S., Altuntaş, Ü., Bıyıklı, N., Yıldız, N. and Alpay, H. (2017). Changes in

Bacterial Resistance Patterns of Pediatric Urinary Tract Infections and Rationale for Empirical Antibiotic Therapy. *Balkan Medical Journal*, 34(5), pp.432-435.

K. Salih, M., Alrabadi, N., M. Thalij, K. and Hussien, A. (2016). Isolation of Pathogenic Gram-Negative Bacteria from Urinary Tract Infected Patients. *Open Journal of Medical Microbiology*, 06(02), pp.59-65.

Karam, G., Chastre, J., Wilcox, M. and Vincent, J. (2016). Antibiotic strategies in the era of multidrug resistance. *Critical Care*, 20(1).

Matsumoto, T. and Muratani, T. (2004). Newer carbapenems for urinary tract infections. *International Journal of Antimicrobial Agents*, 24, pp.35-38.

Mohammed, M., Alnour, T., Shakurfo, O. and Aburass, M. (2016). Prevalence and antimicrobial resistance pattern of bacterial strains isolated from patients with urinary tract infection in Messalata Central Hospital, Libya. *Asian Pacific Journal of Tropical Medicine*, 9(8), pp.771-776.

Okeke, I., Laxminarayan, R., Bhutta, Z., Duse, A., Jenkins, P., O'Brien, T., Pablos-Mendez, A. and Klugman, K. (2005). Antimicrobial resistance in developing countries. Part I: recent trends and current status. *The Lancet Infectious Diseases*, 5(8), pp.481-493.

Prestinaci, F., Pezzotti, P. and Pantosti, A. (2015). Antimicrobial resistance: a global multifaceted phenomenon. *Pathogens and Global Health*, 109(7), pp.309-318.

Raeisi, M., Mihankhah, A., Khoshbakht, R. and Raeisi, V. (2017). Prevalence and antibiotic resistance pattern of bacteria isolated from urinary tract infections in Northern Iran. *Journal of Research in Medical Sciences*, 22(1), p.108.

Rajivgandhi, G., Maruthupandy, M., Ramachandran, G., Priyanga, M. and Manoharan, N. (2018). Detection of ESBL genes from ciprofloxacin resistant Gram-negative bacteria isolated from urinary tract infections (UTIs). *Frontiers in Laboratory Medicine*, 2(1), pp.5-13.

Ranjbar, R., Jafari, N., Haghi-Ashtiani, M., Abedini, M. and Izadi, M. (2009). The Study of Prevalence and Antimicrobial Susceptibility of Tracheal Bacterial Strains Isolated from Pediatric Patients. *Pakistan Journal of Biological Sciences*, 12(5), pp.455-458.

Shaikh, S., Fatima, J., Shakil, S., Rizvi, S. and Kamal, M. (2015). Antibiotic resistance and extended spectrum beta-lactamases: Types, epidemiology and treatment. *Saudi Journal of Biological Sciences*, 22(1), pp.90-101.

Sharma S, Bhat GK, Shenoy S. Virulence factors and Drug Resistance in Escherichia coli isolated from extra- intestinal infections. Indian J Med Microbiol. 2007; 25:369-73.

Wallet, F., Loiez, C., Renaux, E., Lemaitre, N. and Courcol, R. (2005). Performances of VITEK 2 Colorimetric Cards for Identification of Gram-Positive and Gram-Negative Bacteria. *Journal of Clinical Microbiology*, 43(9), pp.4402-4406.

ZANCO Journal of Pure and Applied Sciences
The official scientific journal of Salahaddin University-Erbil
https://zancojournals.su.edu.krd/index.php/JPAS

ISSN (print):2218-0230**, ISSN (online):** 2412-3986**, DOI: http://dx.doi.org/10.21271/zjpas**

RESEARCH PAPER

Detection of Enterotoxigenic *Staphylococcus aureus* Strains in Raw Milk of Cows Reared in Erbil Province/Iraq

Nishtiman S. Hasan[1] and Dana F. Hoshyar[2]

[1&2]Department of Biology, College of Science, Salahaddin University-Erbil, Kurdistan Region, Iraq

A B S T R A C T:

Raw milk is usually contaminated with enterotoxin-producing Staphylococcus ¬aureus, which is regularly associated with staphylococcal food poisoning. The present study was conducted to investigate the occurrence of Staphylococcus aureus and enterotoxin producing strains in cow raw milk in Erbil province and to assess genotypic (multiplex PCR) versus phenotypic by reversed passive latex agglutination (RPLA) assays for staphylococcal enterotoxin detection. A total of 150 samples of caw raw milk (75 from direct milk and 75 bulk tank milk) were collected randomly from milk collectors and different farms in Erbil city. The Staphylococcus aureus isolates were identified conventionally and confirmed by PCR. Then, staphylococcal enterotoxins(SEs) from A to D were examined by RPLA, and types of related genes (sea-sed) were detected by multiplex PCR. S. aureus was recovered from 14 (18.6%) samples from direct milk and 32 samples (42.6%) from bulk tank milk. Of the total strains studied, 65.2% were determined to have some staphylococcal enterotoxin genes; however, only 34.7% produced a detectable amount of the staphylococcal enterotoxins. The most frequently produced enterotoxin gene was type A (60%), followed by sec (30%), sea+sec (10%) and genes seb and sed did not occur. A relatively high discrepancy was observed between the results of RPLA and multiplex PCR, especially with SEA. Our findings showed that cow raw milk in Erbil city is contaminated with toxigenic strains of S.aureus.

KEY WORDS: Enterotoxigenic *Staphylococcus aureus*, raw milk, enterotoxin genes, multiplex PCR, reversed passive latex agglutination.
DOI: http://dx.doi.org/10.21271/ZJPAS.31.4.6
ZJPAS (2019) , 31(4);50-60 .

INTRODUCTION :

The microorganism, Staphylococcus (S.) aureus is a gram-positive, facultative anaerobic coccal bacterium. The individuals of this infectious agent frequently reside on the skin and nasal mucous membranes of human and different species of animals (Otto, 2010, Salah et al., 2017).

* **Corresponding Author:**
Nishtiman Saeed Hasan1
E-mail: nishtiman.hasan@su.edu.krd
Article History:
Received: 14/02/2019
Accepted: 26/05/2019
Published: 10/09 /2019

Having said, some virulent toxins are produced by this bacterium such as staphylococcal enterotoxin (SE), Panton-Valentine leukocidin and toxic shock syndrome toxin-1. The bacterial toxin, SE is habitually implicated as the cardinal etiological agent of food poisoning in humankind (Bergdoll *et al.*, 1981, Hennekinne *et al.*, 2012). In humans, *S. aureus* is the main contributor to several infections including food intoxication (Silva *et al.*, 2003), wound contaminations after surgical operations and pulmonary pneumonia. Moreover, inflammation of urinary tract, joint infections and clinical mastitis are common ailments caused by this aggressive microorganism in animals comprising small and large ruminants (Lowy, 1998, Hennekinne *et al.*, 2012).

Usually, various bacteria proliferate in raw milk that contains many vital balanced dietary materials such as vitamins, proteins, immunoglobulin and minerals. Milk and its derivatives provide a convenient habitat for proliferation of *S. aureus* and enterotoxin production, which in turn, convey them to the consumers (Zecconi and Hahn, 1999, Kadariya *et al.*, 2014). Milk and its secondary products acquire bacterial contaminations by several routes like contaminated milking machines, dirty containers, improper handling, unhygienic environment of farm, infected mammary glands and other methods (Jørgensen *et al.*, 2005a, Kümmel *et al.*, 2016).

Staphylococcus food poisoning (SFP) is a mild intoxication that occurs when there are enough amounts of SE, usually 20 ng to1 µg in the food, which conduce to the appearance of clinical manifestations in humans (Normanno *et al.*, 2007, Argudín *et al.*, 2010). Clinical signs of SFP develop within a few hours (1-6 hrs.) after the consumption of foods contaminated by the bacterium. Depending on consumed toxic dosages and susceptibility of individuals, the symptoms include nausea, vomiting, diarrhoea and abdominal cramps (Jørgensen *et al.*, 2005c, Normanno *et al.*, 2005).

Chemically, SE toxins are composed of proteins that possess a low molecular weight (26-30kDa) and high antigenic activity (Liu *et al.*, 2014). Additionally, these toxins are highly resistant to denaturation statuses such as low pH, heat treatment and proteolytic enzymes. Therefore, their potencies are restricted to the alimentary canal where food poisoning outbreaks occur (Hu and Nakane, 2014). Currently, 23 SE have five defined ‘‘classical’’ (SEA, SEB, SEC, SED, and SEE), with a particular significance in food-borne infections (Umeda *et al.*, 2017, Korpysa-Dzirba and Osek, 2018). All of the above mentioned classical enterotoxins have been related to outbreaks as a consequence of raw milk consumption (Jørgensen *et al.*, 2005b).

At present, there is restricted data concerning the epidemicity and the ability to synthesise classical enterotoxins by *S. aureus* in raw milk of dairy cattle in Erbil governorate. For that reason, the main goal was to investigate the prevalence of *S. aureus* and enterotoxigenic strains from cow raw milk located in Erbil city, and to evaluate genotypic (multiplex PCR) versus phenotypic (RPLA) assays for detection of the staphylococcal enterotoxins and corresponding genes.

2. MATERIALS AND METHODS

2.1 Sample collection:

A total of 150 cow raw milk samples were collected randomly from April to the end of June 2018 in Erbil province, n = 75 direct milk (DM; directly from manually milked individual animals) and n = 75 bulk tank milk (BTM; farm and local market milk bulk tank, and milk collect centres). Fifty ml from each milk sample was placed in disposable sterile screw-cap containers and directly transported in a cooler box with ice packs to the laboratory (4 to 8 ˚C) for analysis.

2.2. Isolation and identification of *S. aureus*

Primarily each milk specimen was cultured on to Bired-Parker agar medium with (5% egg yolk tellurite emulsion) supplement (LabM,UK) and incubated at 37°C for 24 hrs (ISO, 1999).The isolates were identified conventionally by Gram staining, coagulase, catalase reaction, hemolysis test, lipase, lecithinase, DNase production and mannitol fermentation(Tille, 2013) and were further confirmed using API Staph system (API Staph,bioMérieux, France). Finally, all isolates were subjected to molecular identification targeting 16S rRNA and *nuc* genes by PCR (Gücükoğlu *et al.*, 2012, Akindolire *et al.*, 2015). All identified colonies were stored at −70 °C in nutrient broth (Oxoid, England) with 25% glycerol for further investigation (Ludlam *et al.*, 1989).

2.3. ATCC standard strains

S.epidermidis ATCC 12228 and *S.aureus* ATCC 43300 were used as negative and positive controls for *nuc and* 16S rRNA genes respectively.Also, they used as a control for cultures and biochemical tests. The reference strains were provided kindly by Media Diagnostic Center, Erbil.

2.4. Immunological detection of Staphylococcal enterotoxins (SEs).

Six to eight colonies from each *S.aureus* isolate were examined for enterotoxin production (SEA-SED) by SET-RPLA® kit (Oxoid, TD0900). The colonies were transferred into 10 ml tryptic soya broth (LAB M, UK) and incubated for 24 hrs at 37°C. Then, the cultures were centrifuged at 900g for 20 minutes at 4°C (BECKMAN, SCOTLAND) and the enterotoxin was detected in the supernatant according to the manufacturer's directions.

2.5. Confirmation of *S.aureus* and enterotoxin genes using PCR assay.

S.aureus and its enterotoxin genes in all positive raw milk samples were confirmed by using the PCR technique.Wich selected by detection of *nuc,* 16S rRNA, *sea, seb, sec, sed* genes from culture samples.The primers that utelized for the detection of the above mentioned genes were chosen according to Johnson *et al.* (1991), Mehrotra *et al.* (2000), and Maes *et al.* (2002). All primer pairs are listed in Table 1.

2.4 2.6. DNA extraction.

DNA was extracted from bacterial isolates using the Presto™ Mini gDNA Bacterial Kit (Geneaid, Taiwan) according to the suitable protocols in the manufacturer's instructions. The isolated DNA analyzed by agarose gel 1.2% and then stored at 4°C until required for PCR.

2.7. Determination of DNA Concentration.

For assessing the concentration and purity of DNA, the Nano Drop 1000c spectrophotometer was used in which 1 µl of the DNA genome was used for define the concentration and purity of DNA samples. A proportion of 1.8 indicates pure DNA. A proportion above 2 means the presence of RNA in the DNA sample. A ratio of beneath 1.8 denotes the existence of protein in the DNA sample (Agrawal, 2008, Desjardins and Conklin, 2010).

2.8. Uniplex PCR for amplification of 16S rRNA gene.

The designated primers were used for amplification of an approximately 372 bp of 16S ribosomal RNA gene. PCR was done in a final volume of 25 μl in a thermal cycler (Alpha Cycler, UK). Each reaction contained 1μl of DNA, 1μl of each primer, and 10μl of 2X Amplicon Master Mix (RED AMPLICON, German). Then the nuclease free water was used to adjust the volume of this mix to 25 μl. Amplification conditions for PCR were as follows: 5 min at 94◦C to denature the DNA followed by 35 cycles of denaturation at 95◦C for 30 sec, primer annealing at 59◦C for 45 sec, standard extension at 72◦C for 40 sec and eventually a final extension step at 72◦C for 5 min.

2.9. Multiplex PCR for detection of the *nuc* and SE genes (A to D).

2.9.1. Conditions of multiplex PCR.

Multiplex PCR procedure was implemented according to previously described (Johnson *et al.*, 1991, Mehrotra *et al.*, 2000). 2x PCR master mix solution (RED AMPLICON, German) was used for DNA amplification. The PCR reaction was done in a reaction mixture with a final volume of 50 µl containing 25 µl of PCR premix, 1 µl of each forward and reverse primer for each of *sea, seb, sec, sed* and *nuc* genes and 2 µl of the template DNA. Then sterile,free nuclease water was used to complete the volume of the mixture to 50 µl. The mixtures were then processed in a thermocycler (Alpha Cycler, UK) according to the subsequent program: 5 min at 95°C to denature DNA initialy, followed by 35 cycles of denaturation at 94°C for 2 min, primer annealing at 55 ◦C for 2 min, standard extension for 1 min at 72 °C and a final extension at 72 ◦C for 7 min. The PCR products were checked by visual inspection under UV light (BIOTECH, German) in 2.0% agarose gel with safe dye (GENET, Korea) 10 µl /100 ml at 80 V for 1.5 h. A molecular weight marker (GENET, Korea) was run simultaneously.

2.10. Statistical analysis

GraphPad Prism v 6 was used for statistical analyses. Fisher's exact two-tailed and chi-square test analyses were performed for variables and $P<0.05$ values were regarded as significant differences. Specificity and sensitivity of both

methods were done through the Excel program.

Table 1: Primers used for the amplification of S. aureus and its enterotoxin genes.

Primers	Nucleotide sequence (5'- 3')	Size (bps)	References
16S rRNA	F GTTGACTGCCGGTGACAAAC	372	Designed
16S rRNA	R GCTGTTACGACTTCACCCCA		
nuc	F AGCCAAGCCTTGACGAACTAAAGC	279	(Maes *et al.*, 2002)
nuc	R GCGATTGATGGTGATACGGTT		
sea	F GGTTATCAATGTGCGGGTGG	102	(Mehrotra *et al.*, 2000)
sea	R CGGCACTTTTTTCTCTTCGG		
seb	F GTATGGTGGTGTAACTGAGC	164	(Mehrotra *et al.*, 2000)
seb	R CCAAATAGTGACGAGTTAGG		
sec	F AGATGAAGTAGTTGATGTGTATGG	451	(Mehrotra *et al.*, 2000)
sec	R CACACTTTTAGAATCAACCG		
sed	F CTAGTTTGGTAATATCTCCT	317	(Johnson *et al.*, 1991)
sed	R TAATGCTATATCTTATAGGG		

3. RESULTS

3.1. The incidence of *S. aureus*.

Table (2) presents the occurrence and entrotoxigenecity of *S. aureus* isolated from cow raw milk in Erbil city. We picked up 150 milk samples (75 samples from DM and 75 from BTM) and screened for detection of *S.aureus*; which was found in 14 (18.6%) of DM and 32(42.6%) of BTM.

As mentioned in Table 2, the positive results of all the isolates with S.aureus were confirmed with PCR by amplification of *nuc* (Fig. 4) and 16S rRNA genes (Fig. 1).And the results with PCR analysis were the same as the results of conventional tests.

In table (2) elucidated that the number of isolates was significantly higher in BMT than in DM ($\chi 2 = 10.16$ & $p = 0.0007$). it show
ed significant difference ($P<0.05$) in the statistical point of view.

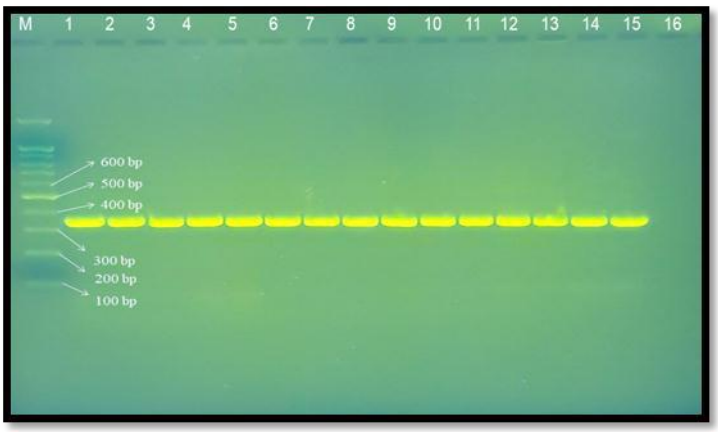

Figure 1: Uniplex PCR products on Agarose gel electrophoresis for detection of 16S rRNA gene. M: 100 bp DNA marker;lane 1: Positive control 16S rRNA (372bp) gene (*S. aureus* ATCC 43300);Lanes 2 to15:positive raw milk isolates; Lane 16: Negative control (*S. epidermidis* ATCC 12228).

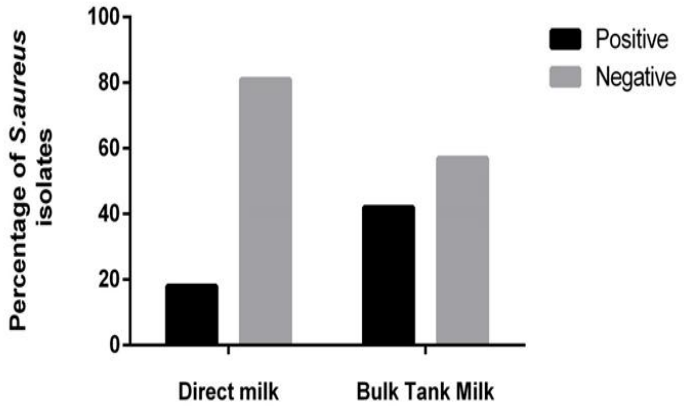

Figure 2: Incidence of *S.aureus* isolates from both sources of raw milk.

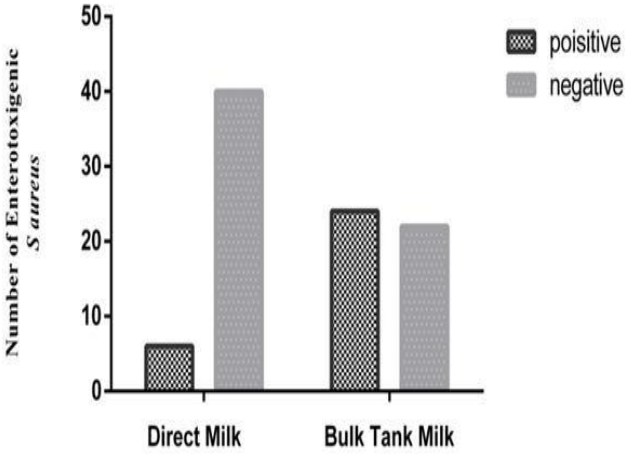

Figure 3: Frequency of enterotoxin producing *S. aureus* isolates in both sources.

3.2. Enterotoxigenicity of *S. aureus* isolates.

The capacity to synthesis classical enterotoxins was found in 16 of 46 (34.7%) *S.aureus* isolates by using the RPLA technique. The number of enterotoxin-producing isolate does not differ significantly between BTM (34%) and DM (16%) [$\chi 2 = 2.724$ &p = 0.0989].Nine isolates (56.2%) produced SEC, 7 isolates (43.7%) produced SEA, while type SEB, SED and SEA+SEC were not identified in raw milk samples. As revealed in the table (2).

In the table (2) demonstrated that enterotoxin genes were found in 30 out of 46 (65.2%) isolates by using Multiplex PCR. And the most common type was gene type A , then gene type C, but the least common type was gene type A+C which is isolated only from BTM. The *seb* and *sed* genes were not detected in any of these isolates. A greater diversity of SE genes was identified in isolates from BTM compared with isolates from DM with a highly significant difference between them ($p<0.0001$) (Fig.3). The Amplification products of multiplex PCR are shown in Figure 4.

3.3. Comparison of RPLA and multiplex PCR results.

The PCR strategy distinguished 30 (65.2%) strains maintaining genes of classical SEs (*sea* to *sed*) among 46 isolates. While, the RPLA method found just sixteen (34.7%) positive strains that expressing related toxins which includes SEA to SED. About 11 strains that carrying the sea gene were identified by PCR technique, but RPLA method didn't detect a toxin produced by these strains. Three isolates were *sea+sec* positive, however, SEA+SEC negative. The recurrence of detection of SEB, SEC and SED production was firmly fixed with the detection of their relating genes. As displayed in table (2) and figure (5).

As presented in table (3), contrasted with multiplex PCR, sensitivity of RPLA was 84% and the negative predictive value was 10%, whereas, specificity and predictive value positive were 100%.

3.3. 4. DISCUSSION

lobally cow raw milk is a familiar source of *S. aureus* (Oliver *et al.*, 2009). In this study, the focus is on the identification of *S. aureus* and enterotoxigenic strains in raw cow milk. In the present study, the overall presence of the pathogen was 30.6% among samples screened by PCR and microbiological methods,with the higher proportion of *S. aureus* (42.6%) in BTM than in DM (18.6%). Our results are matched with other researchers who found a *S. aureus* prevalence of 24% to 44% in cow's milk (Mansour *et al.*, 2017, Khudor, 2012, Ronco *et al.*, 2018, Peles *et al.*, 2007, Akindolire *et al.*, 2015).Ben Said *et al.*

(2016), in Tunisia, found that *S. aureus* was determined in 50% of BTM. However,Fagundes *et al.* (2010) and Rall *et al.* (2014), found *S. aureus* in 7.3% and 10.5% from bulk tank milk, mastitic and healthy cows respectively, which is a lower rate than that recorded in this study. Whereas, other reports isolated high rates than presented here (Rall *et al.*, 2008, Agban and Ahmed, 2013). The difference in rates is due to that the source of milk was from infected cows, or due to variations in sample size, techniques, milking utensils, storage environments, and transportation of the milk(Ruegg, 2003).

All separated strains that identified through standard microbiological methods were confirmed by amplification both 16S rRNA and *nuc* genes. The *nuc* gene encoding thermonuclease and 16S rRNA gene are broadly utilized for specific detection of *S. aureus* (Gücükoğlu *et al.*, 2012). Likewise,Akindolire *et al.* (2015), used PCR targeting above mentioned genes for the identification of *S. aureus*.

Regarding to staphylococcal enterotoxins determination, it has been discovered that out of 46 *S. aureus* isolates, 30(65.2%) revealed to be enterotoxigenic by multiplex PCR which is viewed as the standard gold technique in this examination. Similarly, various investigations identified a high level of enterotoxigenic *S. aureus* isolates in cow raw milk. For instance, a high rate 45.7% was reported in Italy(Riva *et al.*, 2015),50% in Brazil(Fagundes *et al.*, 2010) and 57.3% in Norway (Jørgensen *et al.*, 2005a). The high proportion of enterotoxin producers among *S. aureus* compel the preservation of the cold chain to inhibit the synthesize of the *S. aureus* stable enterotoxins (Hennekinne *et al.*, 2012). The techniques that are used, the geographical regions and the origin of the isolates describe the difference in the prevalence of enterotoxin production (Riva *et al.*, 2015, Rola *et al.*, 2016).

In our investigation, the highest percentage of toxigenic *S.aureus* was observed in BTM (75%), and the lowest rate was found in milk taken directly from the animal (42.8%), with statistically significant difference ($P < 0.0001$). The same result was discovered by (Fagundes *et al.*, 2010, Peles *et al.*, 2007). On the contrary, the most remarkable rates were detected in raw milk taken immediately from cows (75%) by Agban and Ahmed (2013). These results recommended that the sources of bacterial contamination of BTM were multiple, such as raw milk collected from several cows, production and processing environments, equipment,and personnel(Arcuri *et al.*, 2010).

Our information demonstrated that *sea* (60%) was the most repeated gene hold by the *S. aureus* isolates. This is confirmed by previous findings,which were done in Brazil and Ethiopia (Rall *et al.*, 2014, Tarekgne *et al.*, 2016).This could be attributed that enterotoxins A are once infrequently found among the strains of animal source than from human source. At that point these human source strains contaminate milk and dairy products during processing, transportation or even at the retail (Ahari *et al.*, 2009). In addition, SEA is one of the enterotoxin types that mostly found in *S. aureus*, and regularly associated with staphylococcal food poisoning related outbreaks(Johler *et al.*, 2015).

In the light of the present bacteriological and molecular investigations, about 65.2% of staphylococcal isolates are enterotoxigenic genotypically pursuant to the multiplex PCR, but 34.7% are enterotoxigenic phenotypically by SET-RPLA. LIM *et al.* (2004) and Morandi *et al.* (2007) reported that this discrepancy is back to the fact that PCR method determines only corresponding genes whilst, SET-RPLA detects the enterotoxin itself, under some conditions staphylococcal enterotoxins may not be generated or merely produced to undetectable level. The second interpretation for this circumstance is probably owing to the occurrence of point mutation in genes which converted to silent genes harboring defects in their expressions(Okoji *et al.*, 1993).

In this study, sensitivity of SET-RPLA was 84% and specificity was 100% in comparison with multiplex PCR. This is indicating that SET-RPLA has low sensitivity than but as specific as multiplex PCR. These results match with other examination (Jørgensen *et al.*, 2005a)

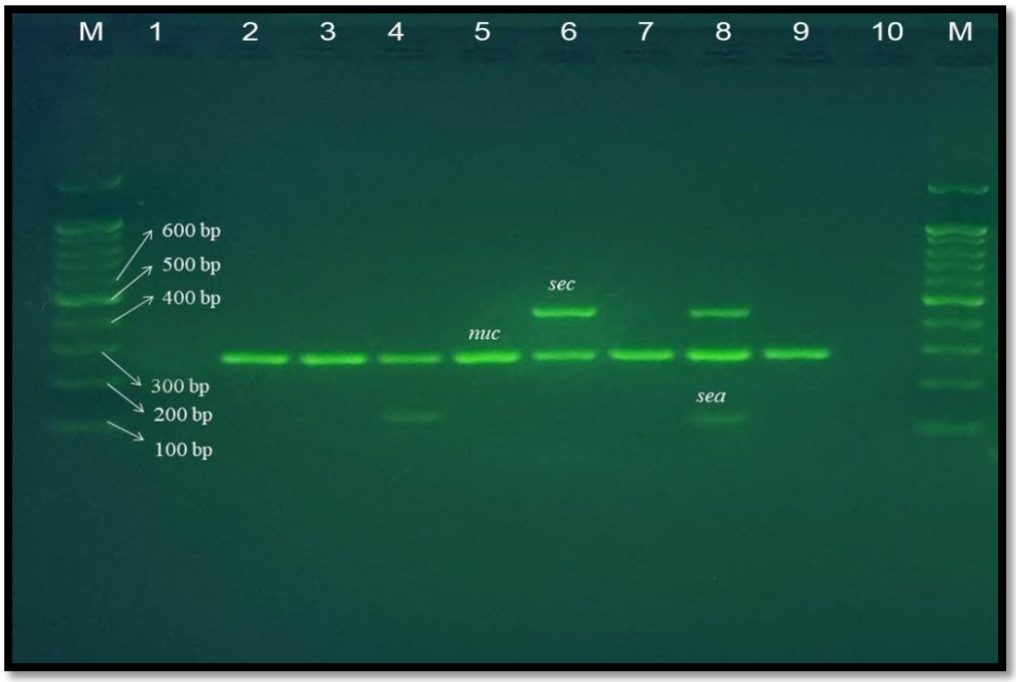

Figure 4: Multiplex PCR products on agarose gel electrophpresis for detection of *nuc* and staphylococcal enterotoxin genes(*ses*). M: 100 bp DNA marker; Lane 1: Negative control (*S. epidermidis* ATCC 12228);Lane 2: Positive control *nuc* (279 bp) gene (*S.aureus* ATCC 43300); Lane 3:raw milk isolates, *nuc* ; Lane 4: raw milk isolates, *nuc* and *sea (*102bp); Lane 5: raw milk isolates,*nuc* and negative *seb*;Lane 6: raw milk isolates, *nuc and sec(*451bp); Lane 7: raw milk isolates,*nuc* and negative *sed*; Lane 8: raw milk isolates, *nuc*,*sea and sec*; Lane 9: raw milk isolates, *nuc and* negative *ses*;Lane 10, negative control of sterile water.

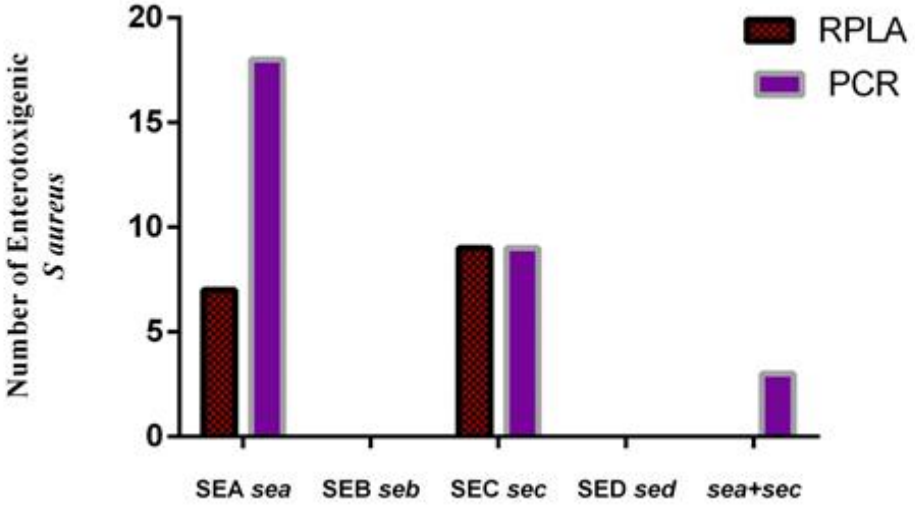

Figure 5: Detection of enterotoxigenic *S.aureus* by RPLA and multiplex PCR

Table 2: Prevalence and Enterotoxigenicity of *S.aureus* isolated from cow raw milk samples.

Number and source of analyzed Samples	NO. *(%)* of samples positive for *S. aureus* by culture technique	NO. *(%)* of samples positive for *s. aureus* by PCR (*16 S* rRNA-*nuc* genes)	Staphylococcal Enterotoxins by (RPLA)					Enterotoxin genes by multiplex PCR					
			NO. (%) of SE produces	SEA	SEB	SEC	SED	NO.(%) of SEs genes	*sea*	*seb*	*sec*	*sed*	*sea+sec*
Direct milk (n=75)	14(18.6)	14(18.6)	5(16)	3(60)	_	2(40)	_	6(42.8)	3(50)	_	3(50)	_	_
Bulk tank milk (n=75)	32(42.6)	32(42.6)	11(34)	4(36.3)	_	7(63.6)	_	24(75)	15(62.5)	_	6(25)	_	3(10)
P-value	P<0.0007***	P<0.0007***	P=0.0989 ns		_		_	P<0.001 ****		_		_	
Total (n=150)	46(30.6)	46(30.6)	16(34.7)	7(43.7)	_	9(56.2)	_	30(65.2)	18(60)	_	9(30)	_	3(10)

RPLA: Reverse Passive Latex Agglutination; SE: Staphylococcal Enterotoxin; *se:* Staphylococcal enterotoxin gene; - : not detected

Table 3: Specificity, sensitivity, predictive value negative and predictive value positive of RPLA versus multiplexPCR.

		Sensitivity (%)	Specificity (%)	PV^+ (%)	PV^- (%)
PRLA true positive	16	84	100	100	10
PRLA true negative	27				
PRLA false positive	0				
RPLA false negative	3				
PCR true positive	30	100	100	100	0
PCR true negative	16				
PCR false positive	0				
PCR false negative	0				

5. CONCLUSION

This study detected the existence of *S.aureus* and enterotoxin producers from cow raw milk. Approximately a third of all positive isolates demonstrated the presence of SE genes. A relatively low consistency happened between RPLA and multiplex PCR with the exemption for SEB, SEC and SED. Also, it concluded that multiplex PCR is a valuable and reliable strategy in finding of enterotoxigenic *S.aureus* isolates and it is more precise and sensitive than RPLA. Our results highlight the potential risk of consuming raw cow milk, particularly in the absence of strict hygiene to keep away the existence of *S. aureus* isolates and SEs production in milk

ACKNOWLEDGEMENT

I would like to direct my sincere gratitude to members of biology department, college of science, Salahaddin University especially Dr. Fikry A. Qadir, Mr.Abdulilah S. Ismaeil, Mrs.Akhter A. Ahmed and Mr.Rebwar M. Hamasalih for their help and supports.

REFERENCES

AGBAN, M. N. & AHMED, A. S. 2013. Detection and Identification of Staphylococcus Aureus Enterotoxins in Some Milk Products and their Handlers. *The Egyptian Journal of Medical Microbiology*, 38**,** 1-11.

AGRAWAL, S. 2008. Techniques in molecular biology. *International book distributing Co. Lucknow. India: 294.*, 1st ed.

AHARI, H., SHAHBAZZADEH, D. & MISAGHI, A. 2009. Selective amplification of SEA, SEB and SEC genes by multiplex PCR for rapid detection of Staphylococcus aureus. *Pakistan Journal of Nutrition*, 8**,** 1224-1228.

AKINDOLIRE, M. A., BABALOLA, O. O. & ATEBA, C. N. 2015. Detection of Antibiotic Resistant Staphylococcus aureus from Milk: A Public Health Implication. *Int J Environ Res Public Health*, 12**,** 10254-75.

ARCURI, E. F., ANGELO, F. F., GUIMARAES, M. F. M., TALON, R., DE FATIMA BORGES, M., LEROY, S., LOISEAU, G., LANGE, C. C., DE ANDRADE, N. J. & MONTET, D. 2010. Toxigenic status of Staphylococcus aureus isolated from bovine raw milk and Minas frescal cheese in Brazil. *Journal of food protection*, 73**,** 2225-2231.

ARGUDÍN, M. Á., MENDOZA, M. C. & RODICIO, M. R. 2010. Food poisoning and Staphylococcus aureus enterotoxins. *Toxins*, 2**,** 1751-1773.

BEN SAID, M., ABBASSI, M., BIANCHINI, V., SGHAIER, S., CREMONESI, P., ROMANÒ, A., GUALDI, V., HASSEN, A. & LUINI, M. 2016. Genetic characterization and antimicrobial resistance of Staphylococcus aureus isolated from bovine milk in Tunisia. *Letters in applied microbiology*, 63**,** 473-481.

BERGDOLL, M., REISER, R., CRASS, B., ROBBINS, R. & DAVIS, J. 1981. A new staphylococcal enterotoxin, enterotoxin F, associated with toxic-shock-syndrome Staphylococcus aureus isolates. *The Lancet*, 317**,** 1017-1021.

DESJARDINS, P. & CONKLIN, D. 2010. NanoDrop microvolume quantitation of nucleic acids. *Journal of visualized experiments: JoVE*.

FAGUNDES, H., BARCHESI, L., NADER FILHO, A., FERREIRA, L. M. & OLIVEIRA, C. A. F. 2010. Occurrence of Staphylococcus aureus in raw milk produced in dairy farms in São Paulo state, Brazil. *Brazilian Journal of Microbiology*, 41**,** 376-380.

GÜCÜKOĞLU, A., ONUR KEVENK, T., UYANIK, T., ÇADIRCI, Ö., TERZI, G. & ALIŞARLI, M. 2012. Detection of enterotoxigenic Staphylococcus aureus in raw milk and dairy products by multiplex PCR. *Journal of food science*, 77**,** M620-M623.

HENNEKINNE, J.-A., DE BUYSER, M.-L. & DRAGACCI, S. 2012. Staphylococcus aureus and its food poisoning toxins: characterization and outbreak investigation. *FEMS microbiology reviews*, 36**,** 815-836.

HU, D.-L. & NAKANE, A. 2014. Mechanisms of staphylococcal enterotoxin-induced emesis. *European journal of pharmacology*, 722**,** 95-107.

ISO, E. 1999. 6888-1 (1999): Microbiology of food and animal feeding stuffs. Horizontal method for the enumeration of coagulase-positive staphylococci (Staphylococcus aureus and other species). Part 1: Technique using Baird-Parker agar medium. *International Organization for Standardization, Geneva*.

JOHLER, S., WEDER, D., BRIDY, C., HUGUENIN, M.-C., ROBERT, L., HUMMERJOHANN, J. & STEPHAN, R. 2015. Outbreak of staphylococcal food poisoning among children and staff at a Swiss boarding school due to soft cheese made from raw milk. *Journal of dairy science*, 98**,** 2944-2948.

JOHNSON, W., TYLER, S., EWAN, E., ASHTON, F., POLLARD, D. & ROZEE, K. 1991. Detection of genes for enterotoxins, exfoliative toxins, and toxic shock syndrome toxin 1 in Staphylococcus aureus by the polymerase chain reaction. *Journal of Clinical Microbiology*, 29**,** 426-430.

JØRGENSEN, H., MØRK, T., HØGÅSEN, H. & RØRVIK, L. 2005a. Enterotoxigenic Staphylococcus aureus in bulk milk in Norway. *Journal of Applied Microbiology,* 99**,** 158-166.

JØRGENSEN, H., MØRK, T. & RØRVIK, L. 2005b. The occurrence of Staphylococcus aureus on a farm with small-scale production of raw milk cheese. *Journal of Dairy Science,* 88**,** 3810-3817.

JØRGENSEN, H. J., MATHISEN, T., LØVSETH, A., OMOE, K., QVALE, K. S. & LONCAREVIC, S. 2005c. An outbreak of staphylococcal food poisoning caused by enterotoxin H in mashed potato made with raw milk. *FEMS microbiology letters,* 252**,** 267-272.

KADARIYA, J., SMITH, T. C. & THAPALIYA, D. 2014. Staphylococcus aureus and staphylococcal food-borne disease: an ongoing challenge in public health. *BioMed research international,* 2014.

KHUDOR, M. H. 2012. DETECTION OF ENTEROTOXIN GENES OF STAPHYLOCOCCUS AUREUS ISOLATES FROM RAW MILK. *Basrah Journal of Veterinary Research.,* 11**,** 254-264.

KORPYSA-DZIRBA, W. & OSEK, J. 2018. Molecular Characterization of Enterotoxigenic Staphylococcus aureus Isolated from Raw Cow Milk in Poland. *Foodborne pathogens and disease*.

KÜMMEL, J., STESSL, B., GONANO, M., WALCHER, G., BEREUTER, O., FRICKER, M., GRUNERT, T., WAGNER, M. & EHLING-SCHULZ, M. 2016. Staphylococcus aureus entrance into the dairy chain: tracking S. aureus from dairy cow to cheese. *Frontiers in microbiology,* 7**,** 1603.

LIM, S.-K., JOO, Y.-S., MOON, J.-S., LEE, A.-R., NAM, H.-M., WEE, S.-H. & KOH, H.-B. 2004. Molecular typing of enterotoxigenic Staphylococcus aureus isolated from bovine mastitis in Korea. *Journal of veterinary medical Science,* 66**,** 581-584.

LIU, Y., CHEN, W., ALI, T., ALKASIR, R., YIN, J., LIU, G. & HAN, B. 2014. Staphylococcal enterotoxin H induced apoptosis of bovine mammary epithelial cells in vitro. *Toxins,* 6**,** 3552-3567.

LOWY, F. D. 1998. Staphylococcus aureus infections. *New England journal of medicine,* 339**,** 520-532.

LUDLAM, H., NWACHUKWU, B., NOBLE, W., SWAN, A. & PHILLIPS, I. 1989. The preservation of micro- organisms in biological specimens stored at–70° C. *Journal of applied bacteriology,* 67**,** 417-423.

MAES, N., MAGDALENA, J., ROTTIERS, S., DE GHELDRE, Y. & STRUELENS, M. 2002. Evaluation of a triplex PCR assay to discriminate Staphylococcus aureus from coagulase-negative staphylococci and determine methicillin resistance from blood cultures. *Journal of clinical microbiology,* 40**,** 1514-1517.

MANSOUR, A. S., WAGIH, G. E.-S., MORGAN, S. D., ELHARIRI, M., EL-SHABRAWY, M. A., ABUELNAGA, A. S. & ELGABRY, E. 2017. Detection of Staphylococcus aureus enterotoxigenic strains in bovine raw milk by reversed passive latex agglutination and multiplex polymerase chain reaction. *Veterinary world,* 10**,** 843.

MEHROTRA, M., WANG, G. & JOHNSON, W. M. 2000. Multiplex PCR for detection of genes forStaphylococcus aureus enterotoxins, exfoliative toxins, toxic shock syndrome toxin 1, and methicillin resistance. *Journal of clinical microbiology,* 38**,** 1032-1035.

MORANDI, S., BRASCA, M., LODI, R., CREMONESI, P. & CASTIGLIONI, B. 2007. Detection of classical enterotoxins and identification of enterotoxin genes in Staphylococcus aureus from milk and dairy products. *Veterinary microbiology,* 124**,** 66-72.

NORMANNO, G., FIRINU, A., VIRGILIO, S., MULA, G., DAMBROSIO, A., POGGIU, A., DECASTELLI, L., MIONI, R., SCUOTA, S. & BOLZONI, G. 2005. Coagulase-positive Staphylococci and Staphylococcus aureus in food products marketed in Italy. *International journal of food microbiology,* 98**,** 73-79.

NORMANNO, G., LA SALANDRA, G., DAMBROSIO, A., QUAGLIA, N., CORRENTE, M., PARISI, A., SANTAGADA, G., FIRINU, A., CRISETTI, E. & CELANO, G. 2007. Occurrence, characterization and antimicrobial resistance of enterotoxigenic Staphylococcus aureus isolated from meat and dairy products. *International journal of food microbiology,* 115**,** 290-296.

OKOJI, C. N., INGLIS, B. & STEWART, P. 1993. Potential problems in the use of oligonucleotide probes for staphylococcal enterotoxin genes. *Journal of applied bacteriology,* 74**,** 637-644.

OLIVER, S. P., BOOR, K. J., MURPHY, S. C. & MURINDA, S. E. 2009. Food safety hazards associated with consumption of raw milk. *Foodborne pathogens and disease,* 6**,** 793-806.

OTTO, M. 2010. Staphylococcus colonization of the skin and antimicrobial peptides. *Expert review of dermatology,* 5**,** 183-195.

PELES, F., WAGNER, M., VARGA, L., HEIN, I., RIECK, P., GUTSER, K., KERESZTÚRI, P., KARDOS, G., TURCSÁNYI, I., BÉRI, B. & SZABÓ, A. 2007. Characterization of Staphylococcus aureus strains isolated from bovine milk in Hungary. *International Journal of Food Microbiology,* 118**,** 186-193.

RALL, V., MIRANDA, E., CASTILHO, I., CAMARGO, C., LANGONI, H., GUIMARÃES, F., JÚNIOR, J. A. & JÚNIOR, A. F. 2014. Diversity of Staphylococcus species and prevalence of enterotoxin genes isolated from milk of healthy cows and cows with subclinical mastitis. *Journal of dairy science*, 97**,** 829-837.

RALL, V., VIEIRA, F., RALL, R., VIEITIS, R., FERNANDES JR, A., CANDEIAS, J., CARDOSO, K. & ARAÚJO JR, J. 2008. PCR detection of staphylococcal enterotoxin genes in Staphylococcus aureus strains isolated from raw and pasteurized milk. *Veterinary Microbiology*, 132**,** 408-413.

RIVA, A., BORGHI, E., CIRASOLA, D., COLMEGNA, S., BORGO, F., AMATO, E., PONTELLO, M. M. & MORACE, G. 2015. Methicillin-resistant Staphylococcus aureus in raw milk: Prevalence, SCC mec typing, enterotoxin characterization, and antimicrobial resistance patterns. *Journal of food protection*, 78**,** 1142-1146.

ROLA, J. G., CZUBKOWSKA, A., KORPYSA-DZIRBA, W. & OSEK, J. 2016. Occurrence of Staphylococcus aureus on farms with small scale production of raw milk cheeses in Poland. *Toxins*, 8**,** 62.

RONCO, T., KLAAS, I. C., STEGGER, M., SVENNESEN, L., ASTRUP, L. B., FARRE, M. & PEDERSEN, K. 2018. Genomic investigation of Staphylococcus aureus isolates from bulk tank milk and dairy cows with clinical mastitis. *Veterinary microbiology*, 215**,** 35-42.

RUEGG, P. 2003. Practical food safety interventions for dairy production. *Journal of dairy science*, 86**,** E1-E9.

SALAH, H., KHIDER, A. & MUNIANDY, S., 2017. *Detection of Methicillin Resistance, Staphylokinase Activity and Biofilm Formation in S. aureus Isolated from Clinical Samples*.

SILVA, W. P. D., SILVA, J. A., MACEDO, M. R. P. D., ARAÚJO, M. R. D., MATA, M. M. & GANDRA, E. A. 2003. Identification of Staphylococcus aureus, S. intermedius and S. hyicus by PCR amplification of coa and nuc genes. *Brazilian Journal of Microbiology*, 34**,** 125-127.

TAREKGNE, E. K., SKJERDAL, T., SKEIE, S., RUDI, K., PORCELLATO, D., FELIX, B. & NARVHUS, J. A. 2016. Enterotoxin gene profile and molecular characterization of Staphylococcus aureus isolates from bovine bulk milk and milk products of Tigray Region, Northern Ethiopia. *Journal of food protection*, 79**,** 1387-1395.

TILLE, P. M., 2013. *Bailey & Scott's Diagnostic Microbiology*. China, Elsevier-Mosby.

UMEDA, K., NAKAMURA, H., YAMAMOTO, K., NISHINA, N., YASUFUKU, K., HIRAI, Y., HIRAYAMA, T., GOTO, K., HASE, A. & OGASAWARA, J. 2017. Molecular and epidemiological characterization of staphylococcal foodborne outbreak of Staphylococcus aureus harboring seg, sei, sem, sen, seo, and selu genes without production of classical enterotoxins. *International journal of food microbiology*, 256**,** 30-35.

ZECCONI, A. & HAHN, G. 1999. Staphylococcus aureus in raw milk and human health risk. *International Dairy Federation*.

ZANCO Journal of Pure and Applied Sciences
The official scientific journal of Salahaddin University-Erbil
https://zancojournals.su.edu.krd/index.php/JPAS

ISSN (print):2218-0230**, ISSN (online):** 2412-3986**, DOI: http://dx.doi.org/10.21271/zjpas**

RESEARCH PAPER

Formulation of Alternative Culture Media from Natural Plant Protein Sources for Cultivation of Different Bacteria and Fungi

Susan A. Shareef
Department of General Science, College of Basic Education, Salahaddin University-Erbil, Kurdistan Region, Iraq.

A B S T R A C T

This study was carried out to find out some semisynthetic new media for routine microbiological tests in microbiology laboratories, with cheap natural protein source. Agar culture media were formulated using natural plant sources such as cowpea, lentil, split pea, chickpea, soy protein, mung beans and rice and used for cultivation of *Staphylococcus aureus*, *Escherichia coli*, *B. cereus*, *Pseudomonas aeruginosa*, *Penicillium sp.* and *Aspergillus sp.* All tested microorganisms grew well on most plant sources except on rice. *B. cereus* showed the best growth and large colonies on formulated media. *E. coli* and *P. aeruginosa* also showed good growth, and Pigmentation of *P. aeruginosa* was not affected. *S. aureus*, *P. aeruginosa* and *B. cereus* produced beta hemolysis on all formulated media. Each bacteria exhibit the same diameter of inhibition of antimicrobials used zone on all formulated media. Results showed that most protein sources used were suitable for cultivation, hemolysis detection and antimicrobial susceptibility test.

KEY WORDS: Alternative media; formulated; protein source; bacteria cultivation.
DOI: http://dx.doi.org/10.21271/ZJPAS.31.4.7
ZJPAS (2019) , 31(4);61-69 .

1. INTRODUCTION

Generally microorganisms grow naturally in almost all types of habitats. They need essential sources of nutrients to maintain growth and reproduction. Microorganisms generally, need sources of energy, carbon, nitrogen, phosphorus, sulfur and various minerals (Harvey *et al.*, 2007). Culture media is a nutrient material prepared for the growth of microorganisms in a laboratory. Nutrient agar medium is commonly used as general purpose medium for the cultivation of broad range of bacteria.

* **Corresponding Author:**
Susan A. Shareef
E-mail: suzan.sharif@su.edu.krd
Article History:
Received: 07/03/2018
Accepted: 26/05/2019
Published: 10/09 /2019

It is a basic medium composed of peptic digest of animal tissue, beef extract, yeast extract, sodium chloride and agar. Microbiological researches are carried out at high cost and scarcity of culture media (Adesemoye and Adedire, 2005). It is one of the serious problems for developing country. Microbial researches are hindered by high cost of culture media (Mekala *et al*., 2016).

The search for alternative, cheap media for use in laboratory agents for routine microbiological experiments is going on. Recent research has been focused on replacing the culture media with alternatives cheap materials (Mateen *et al*., 2012; Abbott and Chapman, 1981; Babbar and Jain, 1998; Babbar and Jain, 2004; Bromke and Furiga, 1991). Legume seeds serve as a good protein source and they are very cheap and widely available materials.

This study is aimed to find a cheap solid culture media used in routine microbiological experiments derived from plant products once the commercial ones are expensive and in most cases (most of the times) are not available.

2. MATERIALS AND METHODS

2.1. Culture Media Preparation

The tested alternative nutrient samples such as cowpea (*Vigna*), lentil (*Lens culinaris),* split pea (*Pisum sativum*), Chickpea (*Cicer arietinum*), soy protein, mung beans (*Vigna radiata*) and rice (*Oryza sativa*) were obtained from Erbil local markets.

The samples were ground into powder using electric blender (Tefal) and filtered by sieve and stored dry in air tight containers. Three grams of each sample and 2 gm of agar were dissolved in 100 ml of distilled water. The pH of the media were measured, which was between 6.4-6.8. Culture media were sterilized by exposing to microwaves (Gosonic- Model No. GOM-423) for 3 minutes (Shareef *et al*., 2019) and poured into sterilized petri dish. The appearance and the color of each prepared alternative media were reported. Nutrient agar (NA), Mueller-Hinton, blood agar and potato dextrose agar (PDA) were prepared and used as a control.

2.2. Collection of Tested Microorganisms

The tested bacteria were: *Staphylococcus aureus*, *Escherichia coli*, *Bacillus cereus* and *Pseudomonas aeruginosa*, while the tested fungi were: *Penicillium sp.* and *Aspergillus sp.* All tested bacteria and fungi were obtained from the Department of Biology / College of Science.

2.3. Inoculation of tested microorganisms

2.3.1. Bacteria

Serial dilution was done according to standard method to obtain a final concentration of $1.5x10^8$ cell/ml. Both NA and formulated media was inoculated in triplicate with 0.1 ml of a bacterial suspension broth. Solid media was inoculated on to the center and was spread uniformly by a sterile glass rod. All inoculated plates were incubated at 37^oC for 24h.

2.3.2. Fungi

Pure fungal cultures of *Penicillium sp. and Aspergillus sp.* were used. A fungal disc was cut by using sterile cork borer, placed upside down on the center surface of the formulated culture media. Another prepared fungal disc were inoculated on PDA media as control. All inoculated plates were incubated at 28±3 °C for 5 days.

After incubation fungal mycelia diameter was measured using a ruler in 3 directions and then average diameter was calculated for each fungus.

2.4. Blood Hemolysis test

Five ml of blood was added to 95 ml of alternative culture media to determine blood hemolysis. Blood base agar (LAB28) was used to prepare blood agar that used as control.

2.5. Antimicrobial susceptibility test

Antimicrobial susceptibility for four types of antibiotics (Amoxicillin, Amikacin, Gentamicin and Cloxacillin (Bioanalyse)) was tested for all species of tested bacteria on formulated culture media. The inoculum of each species of tested bacteria were, the suspensions broth were adjusted to an optical density of 0.5 McFarland. The antibiotic susceptibility testing was determined by using the Kirby–Bauer diffusion technique (Cheesbrough, 1987). Plates of formulated media and Mueller-Hinton were inoculated using

sterile cotton swabs. Tested antibiotic discs were placed on the inoculated media surfaces and incubated for 24 hours at 37^oC, the diameter of zone of inhibition were measured after incubation period and compared with the inhibition zone on Mueller-Hinton medium.

2.6. Statistical data analysis

A two way ANOVA was used to analyze the results.

3. RESULTS

Since the pH of different formulated culture media were ranged between 6.4-6.8, they were used without adjusting the pH.

The characteristics of formulated culture media were shown in the table (1), the color of most of the prepared media was white to creamy except for mung beans was light green and cowpea was light brown. The appearance of all prepared media was turbid and some contains particles, except that of protein soy agar was clear and transparent.

Table 1. Characteristics of formulated culture media

Formulated Medium	Color	Particles	Turbidity
Cowpea	Light brown	+	T
Lentil	Creamy	-	ST
Chickpea	Creamy	-	ST
Soy protein	Light amber	-	C
Mung beans	Light green	+	T
Split pea	Creamy	-	ST
Rice	White	-	ST

T=Turbid, ST=Slightly Turbid, C=Clear

All tested bacteria showed significantly ($p>0.05$) high growth rate on formulated media except rice. Among all tested bacteria; *B. cereus* showed the best growth on all formulated culture media (figure 1), there was no considerable differences in colony growth rates between the alternative media and NA. They exhibit swarming motility on chickpea and covered the surface of culture media, mean swarming was less on mung beans, cowpea, split pea and lentil. Swarming was controlled by increasing agar rate to 3% in the media (figure 2-4).

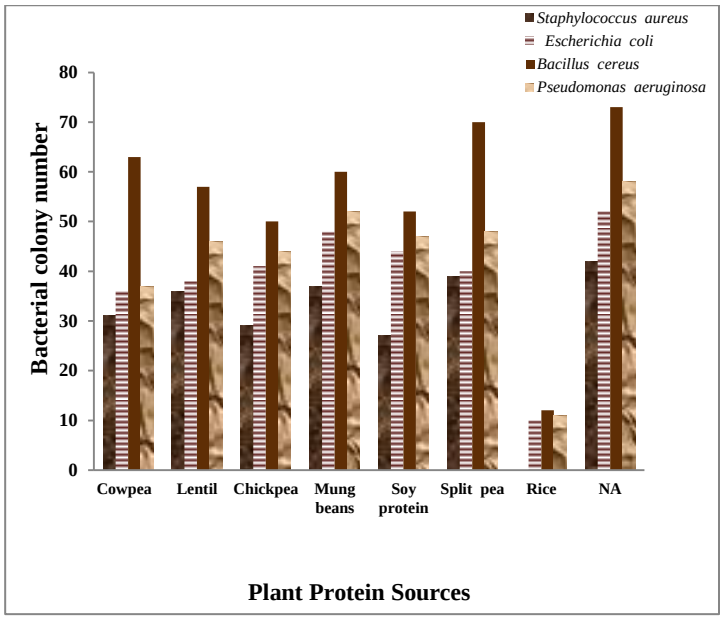

Fig 1. Bacterial growth on different formulated media

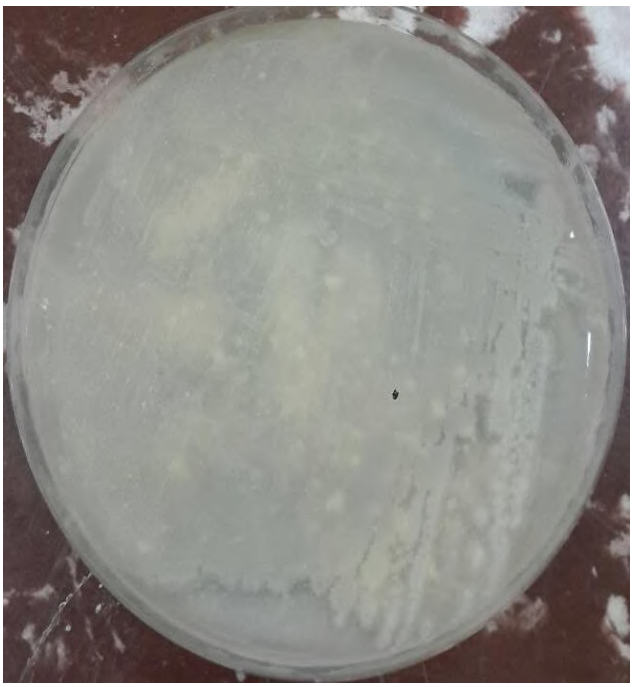

Fig 2. *B. cereus* colonies on Chickpea

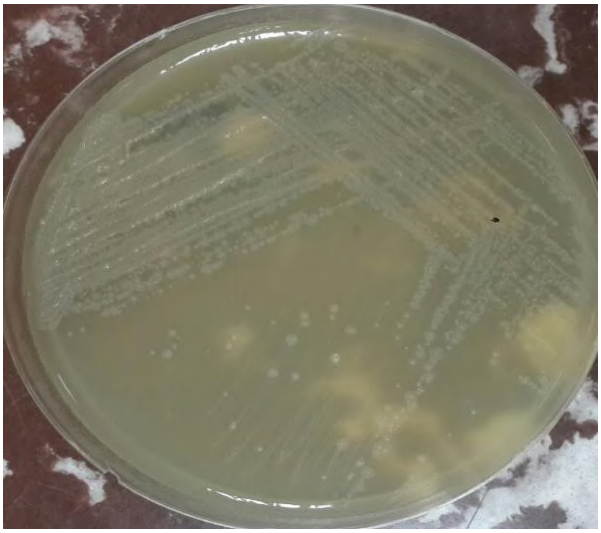

Fig 3. *B. cereus* growth on Soy protein agar

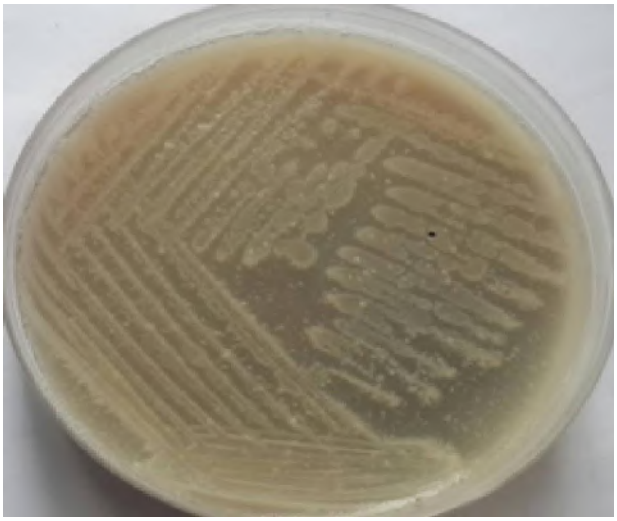

Fig 4. *B. cereus* growth on Cowpea agar

P. aeruginosa produced large opaque irregular colonies with sweet odor and characteristic pigments (figure 5). Pigmentation on formulated media was less obvious on soy protein agar. *E. coli* grew well on all formulated media except on rice, while *S. aureus* produced smaller colony size than on NA.

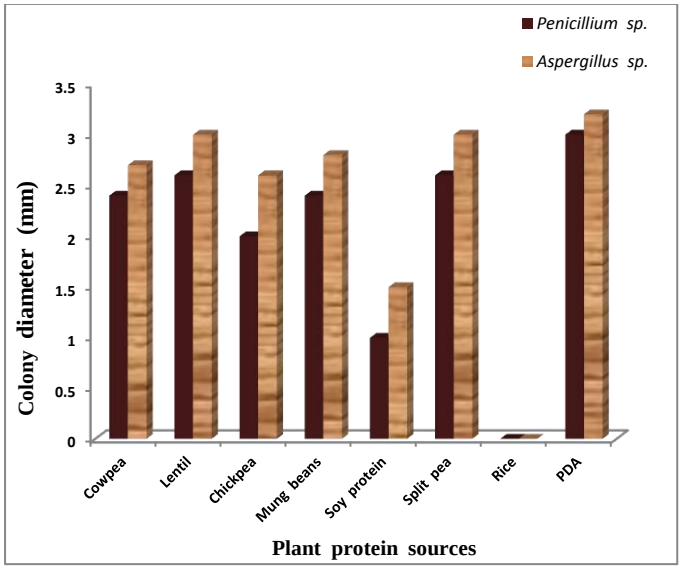

Fig 5. Fungal growth on formulated media

Both *Penicillium* and *Aspergillus* grew well on most prepared media except on rice (figure 6), while they produced small colonies on soy protein in comparison to their growth on PDA agar. Although these fungi showed better growth on PDA, the formulated media were suitable for routine culture of tested fungi (figure 7,8).

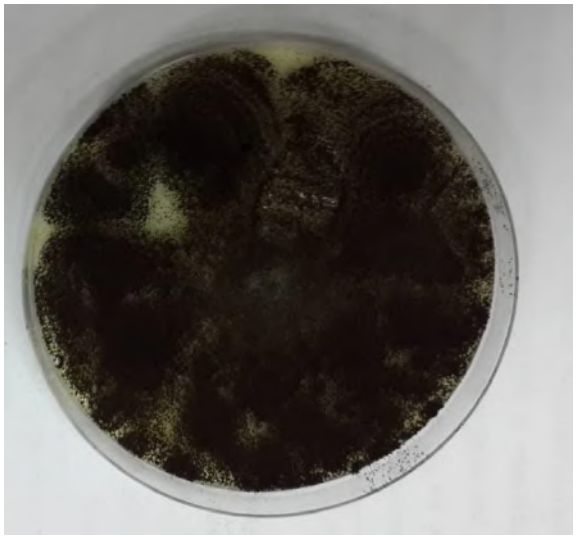

Fig 6. *Penicillium* colony on chickpeas

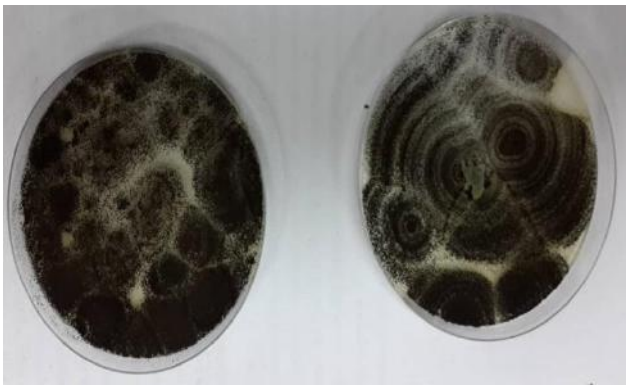

Fig. 7. *Aspergillus* and *Penicillium* colony on Split pea

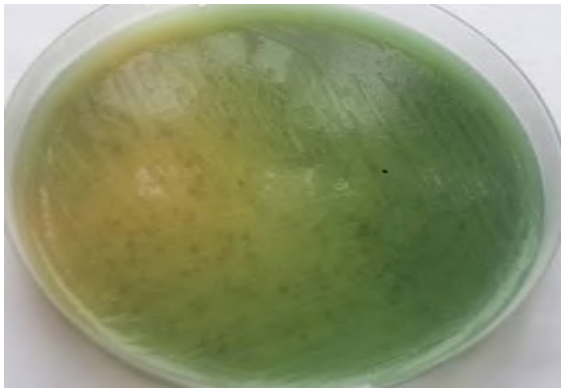

Fig 8. Pigmentation produced by *P. aeruginosa* on Lentil agar

taphyllococcus aureus, *B. cereus* and *P. aeruginosa* showed beta hemolysis on formulated blood agar. Hemolysis reactions of tested bacteria on formulated blood agar were shown in figure (9,10).

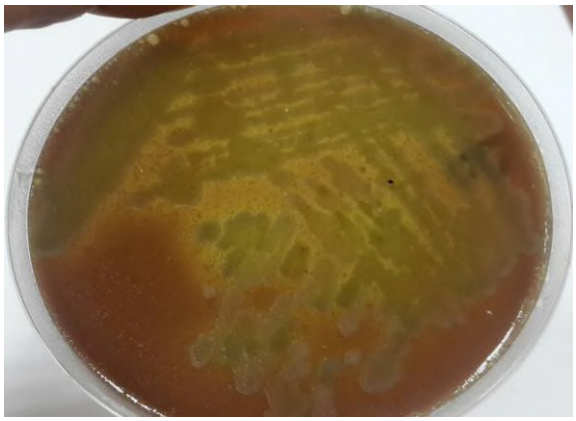

Fig 9. Beta hemolysis by *B. cereus* on Lentil agar

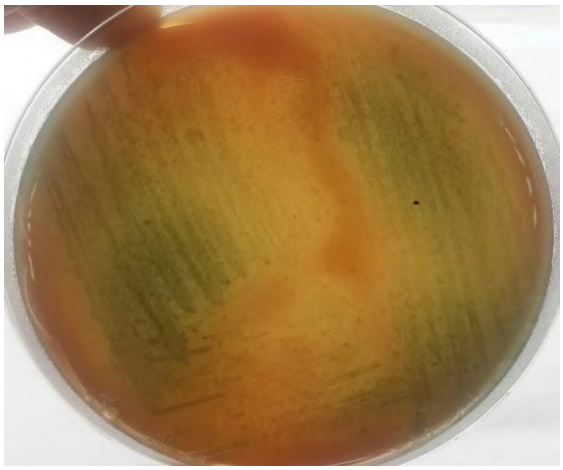

Fig 10. *Beta* hemolysis by *P. aeruginosa* on split pea agar

Staphyllococcus aureus hemolysis reaction on formulated blood agar media was less obvious than on blood agar while *B. cereus* and *P. aeruginosa* produced clear zone.

The susceptibility of bacteria against 4 antibiotics was tested on formulated media. Inhibition zone of each bacteria against antibiotics was measured and compared with inhibition zone of the same one on Mueller-Hinton agar as shown in table (2-4). All tested bacteria exhibited approximately the same inhibition zone against each antimicrobial agent on all formulated media. There were no significant differences between the inhibition zones on these media comparing with inhibition zones on Mueller-Hinton agar.

Table 2. Antibiotic activity against *S. aureus* on different formulated media (Inhibition zone (mm))

Antibiotic discs	Cowpea	Lentil	Chickpea	Soy protein	Mung beans	Mueller-Hinton
Amoxicillin	R	R	R	R	R	R
Amikacin	30	31	32	30	30	30
Gentamicin	33	34	36	36	40	36
Cloxacillin	R	R	R	R	R	R

R= resistant

Table 3. Antibiotic activity against *P. aeruginosa* on different formulated media (Inhibition zone (mm))

Antibiotic discs	Cowpea	Lentil	Chickpea	Soy protein	Mung beans	Mueller-Hinton
Amoxicillin	R	R	R	R	R	R
Amikacin	R	R	R	R	R	R
Gentamicin	R	R	R	R	R	R
Cloxacillin	R	R	R	R	R	R

Table 4. Antibiotic activity against *B. cereus* on different formulated media (Inhibition zone (mm))

Antibiotic discs	Cowpea	Lentil	Chickpea	Soy protein	Mung beans	Mueller-Hinton
Amoxicillin	16	15	14	13	13	14
Amikacin	34	33	36	35	36	36
Gentamicin	32	32	32	30	32	30
Cloxacillin	R	R	R	R	R	R

4. DISCUSSION

Because the pH of different formulated culture media were ranged between 6.4-6.8 they were used without adjusting the pH. This may be helpful in the laboratories that may not have pH meter especially in developing countries. In a study by Ravathie *et al* the pH of formulated culture media was between (6.12 - 6.89) (Ravathie *et al.*, 2012), they found no significant change in the number of colonies whether pH was adjusted to 7.0 or went on with the experiments as such.

The properties and appearance of all prepared media supported them to be suitable to use in microbiology laboratories.

The results showed that the formulated media contained sufficient amount of nutrients to support the growth of the tested bacteria (*S. aureus, E. coli, P. aeruginosa B. cereus*) as well as fungi (*Penicillium sp* and *Aspergillus sp.*) except for rice. The composition of culture media is an important factor for growth of microorganism. The alternative culture media such as cowpea, lentil, chickpea, soy protein, mung beans and split pea contain protein and other nutrient sources that microorganism need for growth. Agar has no nutrient value, it was used as solidifying agent to allow carrying out of common techniques such as streaking out cultures easy and then estimate microbial growth on solid media (Sambali and Mehrotra, 2010).

Many studies have been carried out to replace nutrient agar with alternative formulated culture media from natural protein source. In a study, Sago replaced nutrient agar for the growth of different bacteria (Kapilan and Thavaranjit, 2008). In another study by Annan Prah *et al* in 2010., cowpea agar was effectively replaced with NA. Berde and Berde (2015) used vegetable waste as alternative microbiological media. The legume seeds were also used as alternative culture media (Ravathie *et al.*, 2012).

Pseudomonas aeruginosa produced large opaque irregular colonies with sweet odor and characteristic pigments due to blue colored pyocyanin which spreads out over the formulated culture media. Pigmentation on formulated media was less obvious on soy protein agar. *Pseudomonas aeruginosa* produces many extracellular pigments that are excreted into the culture medium surrounding the colonies. Pigment production is depends on the composition of the medium (Garibaldi, 1967).

Pigment formation and elaboration rely on a dynamic metabolic equilibrium provided by medium constituents such as peptones, minerals, and various ions (Daly *et al*, 1984). Pigmentation by *P. aeruginosa* was not affected by the new media.

Although the tested fungi showed better growth on PDA, the formulated media were suitable for routine culture. In a study by Mekala *et al* (2016), when culture media were formulated from rice, chickpea, corn, dhal, thinai, natural soy flour and processed soy flour, they found that *Sclerotium* sp., *Aspergillus* sp., *Fusarium* sp. and *Penicillium sp*. showed significantly ($p>0.05$) high growth rate in PDA than other alternative culture media. Fungi require carbohydrate rich media to grow well and PDA contains large amount of carbohydrate that required for fungal growth and it also dextrose that serves as a growth stimulant (Beever and Bollard, 1970).

Hemolysis is the ability of bacteria to breakdown the red blood cells by the action of hemolysins, erythrocyte-lysing enzymes, that it produce. Colonies to induce hemolysis when grown on blood agar is used to classify certain microorganisms. Blood hemolysis detection requires a culture medium for bacterial growth and a source of blood as a culture medium supplement. In this study formulated media were used instead of blood base agar and supplemented with blood to obtain hemolysis.

There was no significant differences between the inhibition zone on these media in comparison to inhibition zone on Mueller-Hinton agar as shown in table (2-4). Based on this finding, formulated media can be used for antimicrobial susceptibility test for student experiment.

Results showed that all the plant natural protein sources used are an acceptable alternatives for the routine culture and subculture, hemolysis detection, antimicrobial

susceptibility test and fungi cultivation instead of NA, blood base agar, Mueller-Hinton agar and PDA, respectively for different species of bacteria and fungi specially for routine student experiments in practical microbiology.

In developing countries, with high costs of manufacturing dehydrated media, the use of protein formulated media is more practical and cheaper compared with commercial ones that are widely used in laboratories. Beside they can be prepared immediately.

There are a number of studies concentrated on alternative source of culture media to be used instead of NA, but there was no previous studies about using them for more purposes such as hemolysis detection and antimicrobial susceptibility test.

5. CONCLUSION

Many protein sources such as legume seeds were used in formulation of culture media for cultivation of different microorganisms including bacteria and fungi. Most of formulated media (except rice) were good and suitable for microbial growth. Nutrient agar, blood base agar, Mueller-Hinton agar and potato dextrose agar can be replaced with one of these cheap alternative media for routine experiments in microbiology schools specially in developing countries for culture, hemolysis detection and antimicrobial susceptibility tests in addition of fungi cultivation.

For this purpose only a bottle of agar that cost 30$ with 600g of one of the alternative nutrients that costs ~1.00$ is needed to prepare 20 litters of four important and essential culture media that used widely in microbiology laboratory.

Therefore the use of different natural plant protein sources as culture media in laboratories is very much possible and cheaper when compared to commercially prepared culture media. Although plant protein sources can be prepared easily, rapidly and they can be stored in air tight containers for a long time at room temperature.

REFERENCES

Abbott I.A., Chapman F.A. 1981. Kappa-Carrageenan: as a substitute for agar in microbiological media, *Arch. Micro.* 128: 355-359.

Adesemoye A.O., Adedire C.O. 2005. Use of Cereals as basal medium for the formulation of alternative culture media for fungi, *Wor. J. Micro. & Biotech.*, 21: 329-336.

Annan-Prah A., Akorli S.Y., Sedofia K.B. 2010. *Afr. J. Microb. Res.* 4 (23): 2626-2628. http://www.academicjournals.org/journal/AJMR/article-abstract/BFDF29816421.

Babbar S.B., Jain N. 1998. Isubgol: as an alternative gelling agent in plant tissue culture media. *Pla. Cel. Rep.* 17: 318-322.

Babbar S.B., Jain N., Walia N. 2004. Guar gum: as a gelling agent for plant tissue culture media. In Vitro Cell, *Dev. Biol. Plant*, 41: 258-261.

Beever R.E., Bollard E.G. 1970. The nature of the stimulation of fungal growth by potato extract, *J. Gen. Micro*. 60 (2): 273-279.

Bromke B.J., Furiga M. 1991. Carrageenan is a desirable substitute for agar in media for growing *Trichoderma vginali*, *Microb. Meth*. 13: 61-65.

Chanda V. B., Vikrant B. B. 2015. Vegetable Waste As Alternative Microbiological Media For Laboratory And Industry, *World. J. Pharm. & pharm. sci.* 4 (5): 1488-1494.

Cheesbrough M. 1987. Medical Laboratory Manual for Tropical Countries, Second ed., Butterworth-Heinemann, Cambridge, UK, 2–392.

Daly J.A., Boshard R., Matsen J.M. 1984. Differential primary plating medium for enhancement of pigment production by *Pseudomonas aeruginosa*, *J. Clin. Microbiol*. 19: 742–3.

Garibaldi J. A. 1967. Media for the Enhancement of Fluorescent Pigment Production by *Pseudomonas* Species, *J. Bacter.*, 5 (94): 1296-1299.

Harvey R.A., Champe P.C., Fisher B.D. 2007. Lippincott's Illustrated Reviews: Microbiology, Second ed., Lippincott Williams & Wilkins, Philadelphia.

Kapilan R., Thavaranjit A.C. 2008. Alternative culture media for bacterial growth using different formulation of protein source, *J. Sci. Uni. Kelaniya*, 4:11-14.

Mateen A., Hussain S., Rehman S.U., Mahmood B., Khan M.A., Rashid A., Sohail M., Farooq M., Shah S.J.A. 2012. Suitability of various plant derived gelling agents as agar substitute in microbiological growth media, *Afr. J. Biotech.* 11: 10362-10367. https://www.ajol.info/index.php/ajb/article/view/128475

Mekala U., Sevvel P., Nirmala R., Sutharshiny S. 2016. Formulation of alternative culture media for bacterial and fungal growth, *Der. Pharmacia. Lettre*., 8 (1): 431-436.

Ravathie A., Sevvel P., Nirmala R., Kularajany N. 2012. Alternative culture media for bacterial

growth using different formulation of protein sources, *J. Nat. pro. Pla. Reso*., 2: 697-700.

Sambali G., Mehrotra R.S. 2010. Growth, culture and maintenance of microorganisms. Principles of Microbiology, First ed., Tata McGraw-Hill Education, New Delhi, India, 71-124.

Shareef S.A., Hamasaeed P.A., Ismaeil A.S. 2019. Sterilization of Culture Media for Microorganisms Using a Microwave Oven Instead of Autoclave, *Raf. J. Sci.*, 28 (1): 1-6. https://www.iasj.net/iasj?func=fulltext&aId=158562.

ZANCO Journal of Pure and Applied Sciences
The official scientific journal of Salahaddin University-Erbil
https://zancojournals.su.edu.krd/index.php/JPAS

ISSN (print):2218-0230**, ISSN (online):** 2412-3986**, DOI: http://dx.doi.org/10.21271/zjpas**

RESEARCH PAPER

Appearance-based indoor place recognition for localization of the visually impaired person

Dlnya S. Salih, Abbas M. Ali

Department of Software and Informatics , College of Engineering, Salahaddin University-Erbil, Kurdistan Region, Iraq.

A B S T R A C T:

Indoor localization and mapping is an important issue in computer vision. Many approaches have been proposed and used to give an accurate process of localization. most of them have limitations and cannot precisely recognize places since this challenge involves many issues like a random representation of features not based on spatial domains let mismatch of finding the corresponding image in an accurate way. In addition, some other minor problems are related to the way of features extraction like octave , Haar,…etc. Hence, it still is regarded as an open problem. The proposed system uses and compares different machine learning techniques for feature extraction like BOW, HOG, and EOH for visual place recognition in a way that improves accuracy and robustness of indoor localization for the visually impaired person. Here we combined several powerful approaches, then applied them to two international datasets (COLD and IDOL) and found more accurate results as compared to using each method separately.

KEY WORDS: Visual place recognition BOW,HOG,EOH,indoor localization,visually impaire
DOI: http://dx.doi.org/10.21271/ZJPAS.31.4.8.
ZJPAS (2019) , 31(4);70-81 .

INTRODUCTION :

Indoor localization and Mapping system are very significant for assisting visually impaired person in order to localize themselves and also navigating indoor environments that are not familiar for them in their normal daily lives. Based on the information from the World Health Organization, there are 285 million people with disabilities in their vision where 39 million among them are blind (Hu *et al.*, 2016).

Currently, so many buildings are generally built for sighted people, thus localization and navigation tasks in the environment that normal people do it without any problem could be a great issue for the visually impaired person. Even various systems have designed for the purpose of assisting visually impaired person for robotic navigation, efficient solutions are not found yet (Hu et al., 2016). Here it is proposed to use and compare different types of approaches to accomplish the task; handling some issue which involves enhancing the accuracy and robustness of appearance-based recognition of locations this will aim to implement a visual localization system for the visually impaired person to demonstrate improvements in robustness and accuracy over existing methods.

The image in front of the visually impaired person will be compared with other images which are already stored in the computer database. This will lead us to think of transforming the images into another form of information and store it in the

* **Corresponding Author:**
Dlnya S. Salih
E-mail: Dlnya.salih@gmail.com
Article History:
Received: 07/12/2018
Accepted: 24/03/2019
Published: 10/09 /2019

database. Different types of algorithms will be used to complete this task and will be examined and compared (Ugave, 2014).

Here machine-learning techniques are combined for speeding up localization or visual appearance-based place recognition for the visually impaired person in a robust enough with fewer constraints in real time. This paper aims To design an efficient algorithm in machine learning for appearance-based place recognition using common datasets in this field could be applied to a sequence of live images and then be implemented in real-time modes.

2. LITERATURE REVIEW AND THEORETICAL BACKGROUND

2.1 Place Recognition and Simultaneous Localization and Mapping

A map is required for a robotic localization system, for recognizing a place where it is already visited. Simultaneous Localization and Mapping (SLAM) are the processes of creating a map about the environments and localization within the map. The process of simultaneously building a map about the surroundings and localizing itself within the map is called Simultaneous Localization and Mapping (SLAM), and it has been a very active field in the past four decades. To support visually impaired person for the purpose of possessing safe and quality life, researchers have developed aiding ways and machines.

SLAM is applied in several applications like VSLAM. Several vital features like strength, scalability in detailed mapping, semantic mapping representations and metric explained during a review regarding SLAM. This review utilizes novel sensors and concepts like deep learning to handle active SLAM and its new boundaries exploration (Cadena *et al.*, 2016). Different sorts of VSLAM implementations that uses no filter has been reviewed so far that describes some methods to find out ingredients of SLAM (Younes *et al.*, 2016), for estimating offline sub-maps and

aligning them to international map in efficient way an indirect monocular SLAM that uses no filter is proposed(Bourmaud and Mégret, 2015).

Though numerous inquiries were completed utilizing monocular and stereo vision primg harily based algorithms with applications, for instance, obstacle avoidance, localization, and following robots, only some of them concentrate on visually impaired person's navigation. Using a wired camera for sence enlargement and 3D map building a combination of mono SLAM and object recognition were utilized(Castle, Klein and Murray, 2010). Location of the object is discovered by the homography decomposition between the pair of current and former image. Device with hand-pushed mobility ability has been created utilizing dual cameras – one among them for recognizing the scence utilizing GIST features and estimating pose whereas the other is for enhancing Fast-Appearance-Based map (FAB-MAP) via marker detection.

Scene recognition includes a training procedure offline before the online approach is performed in a precise online direction(Nguyen et al., 2017).6DOF posture estimation technique concentrates on using a 3D camera that is firmed on the white cane with an active Rolling Tip (ART) at its termination that can lead itself in the desirable way of a tour. It utilizes Gaussian measurement Model (GMM) based on pattern recognition approach presenting good outcomes for stairway and obstacle detection (Hong, Qian and Wu, 2016). For interaction of human and device an interface for speech that uses a Bluetooth headphone and keyboard is planned to be used. In order to get the final pose utilizing VO and VSLAM, visual depth measurements are needed. With utilizing a static monocular camera the depth from an object can be measured values of object and height of the camera are known (Diamantas, Astaras, and Pnevmatikakis, 2016). Sparse-depth data depth gained from a RGBD camera 3D lidar with monocular camera for estimating posture and recovery utilized by Depth improved VO(Zhang, Kaess and Singh, 2014). An intelligent system was developed for localization associate degreed navigation for visually impaired utilizing a monocular camera in interior surroundings. The proposed system is tested for 2 datasets that are standard Karlsruhe and indoor environment recorded datasets (Ramesh et al., 2018).

A wireless system for indoor way finding developed to help visually impaired person so as to navigate the unknown environment with steady and dynamic obstacles. The most effective rout can be found by the system for connecting a starting and a goal point in an indoor framework whereas giving hints to the visually impaired person regarding moving on the surface by passing obstacles (Milici, et al 2018).

2.2 Speeded Up Robust Features (SURF)

SIFT feature descriptor which is most widely accepted shows the big cost of computations. H.Bay et al. presented a speeded up variant of SIFT named as SURF (Speeded Up Robust Features). For each key point, SIFT calculates a 128-dimensional feature descriptor of neighbors based on local gradients histogram while SURF produces a 64-dimensional feature descriptor relying on sums of Haar wavelet components. SURF is approximated. By using Laplacian of Gaussian with a box filter instead of the difference of Gaussian. The calculation time has decreased highly in SURF because of utilizing integral images which performs box type filter calculation very fast. Based on the Hessian matrix determinant the interest points are detected. The selection of interest point at each location in the image over different scales is computed based on local maxima of Hessian matrix determinant.to permit invariance of rotation orientation is associated for every key point. by calculating the Haar wavelet response of each key point in a circular neighborhood the orientation is computed. With the strength of horizontal and vertical responses, the wavelet responses are plotted as points on the two axes. Every response within the sliding window is computed and the leading orientation is chosen as the key point orientation. By considering a square box filter of size 20 around each key point oriented along its perspective orientation the SURF descriptors are computed. The area around each key point is split into 4×4 subregions then for each block, Haar wavelet response in the horizontal and vertical direction is calculated. Then each subregion is represented by using a four-dimensional descriptor that contains the wavelet responses summation ($d_x$and d_y) and the summation of absolute values of $d_x$and d_y as illustrated by equation (1) (Abedin, Dhar and Deb, 2017):

$$v = (\sum d_x, \sum d_y, \sum |d_x|, \sum |d_y|) \qquad (1)$$

2.3 Bag of Words (BOW)

for analyzing text document bag-of-words (BoW) technique was initially presented in the problem of text retrieval domain, it was also acclimatized for applications of computer vision. In the BoW model, a visual analogue of a word is utilized for analyzing the image, which depends on the process of quantizing the vector though clustering low-level visual features of local areas or points, like color, structure and so on. For extracting BoW features from images consist of the following four steps:

1. Interest area or point detection in an automatic way,
2. Local descriptor calculation over detected areas/points,
3. Creating visual vocabulary by quantizing the descriptors to words,
4. BoW feature construction by finding the appearance inside the image for every certain word in the visual vocabulary.

The BoW approach can be explained as the following. Having a dataset S including m images expressed by S = s1, s2, ..., and sn, where s represents visual features, a particular algorithm for unsupervised learning, like k-means, is utilized for grouping S depending on a constant number of visual words O expressed by O= o1,o2, ..., and oc, when C represent the cluster number. Then, the data can be summarized in a C×M concurrence table of counts Mij = m (oi, sj), where n (oi, sj) indicates how many times the image si contains the word oi (Tsai, 2012).

2.4 Edge Oriented Histogram (EOH)

Edge orientation histograms (EOH) is utilized in some tasks such as classification and detection as a feature descriptors. The local orientation or the directions of the edge are described by those descriptors. The histograms are constructed by starting with calculating the image edge. Here, after converting the image to greyscale the edge is calculated through filtering the image, the following kernels are utilized for the filtering process: $[-1,0,1]$ And $[-1,0,1]^T$.the obtained filtered images are indicated by d_x and d_y respectively. The direction (α) and magnitude (M) of the edge for the pixels within the image are calculated by Equation (2) and Equation (3) respectively. The producing α will be perpendicular to real direction of the edge in the image.

$$\alpha = \arctan(d_y/d_x) \qquad (2)$$

$$M = \sqrt{d_x^2 + d_y^2} \qquad (3)$$

The next phase is separating the image into small areas which are not overlapping, named cell. Here rectangular cells of $c_x \times c_y$ pixels is used.by

this step $n_x \times n_y$ cells are generated. If the size of the image is$x \times y$, then $n_x = \lfloor (x/c_x) \rfloor$ and $n_y = \lfloor (y/c_y) \rfloor$ .single orientation histogram will describe each cell. The bins of edge orientation histogram are equally spreaded through direction of the edge $0° - 180°$ where the gradient sign is neglected. If $d°$ is the histogram bin size, then number of histogram bins n_b is$180°/d°$. Based on the magnitude of edge,M the histogram is calculated depending on the weighted vote (Timotius and Setyawan, 2015).

Histogram of Gradient (HOG): HOG features give a summarized but robust representation of images for classification of the image in general (Peter A. Torrione et al, 2014). The fundamental concept beyond HOG features is that the allocation of gradients' intensity or the direction of edge describes the appearance of local object and shape in the image. HOG splits the image into cells which are small areas connected to each other, and for the pixels inside each cell, a histogram of gradient directions is compiled by HOG. Based on the founded value in the computation of gradient, every pixel inside the cell casts for the channel of orientation-based histogram a weighted vote. Along 0 to 180 degrees the histogram channels are equally spread, then the feature vector is represented by the collection of those cell histograms. It will be contrast normalized via calculation of an intensity measure through the greater image region, named block, afterward this value is utilized for normalizing every cell inside the block. More preferable invariant in lightening or shadowing results from this normalization (Ren, and Li 2014).**Figure 1** illustrates the HOG extraction process.

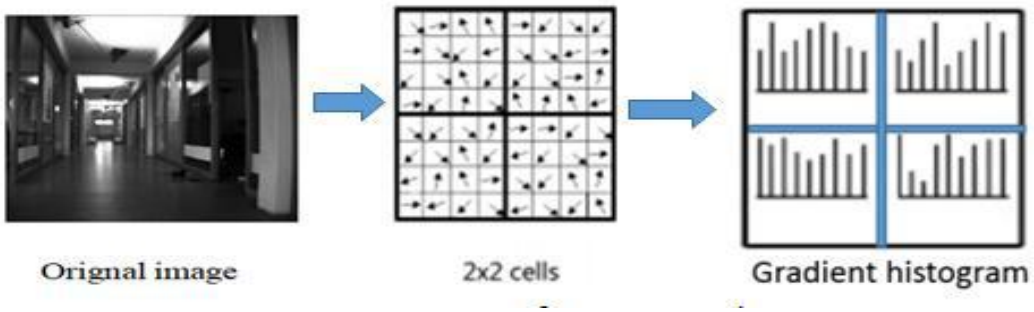

Figure 1: HOG feature

2.4 Support Vector Machine (SVM)

SVMs are originally classifiers with two class which is presented to be an appealing and more formal technique for linear or non-linear decision boundaries learning. Having a group of points, that to either of two classes belong, the hyperplane is found by SVM and it leaves the biggest possible number of fraction points on the same side of the same class while increasing the space from hyperplane of either class. This is equal to minimizing structural risk for obtaining generalization with good results from two classes supposing 1 example

$$(x_1,y_1),(x_2,y_2)\dots(x_l,y_l), x_i \in R^N,\ y_i \in \{-1,+1\} \qquad (4)$$

Quadratic programming is utilized to find the most preferable hyperplane implies fixing a constrained improvement issue. The margin width between classes is the criteria for optimization. Finding optimal hyper-plane implies solving a constrained optimization problem using quadratic programming. The margin width between classes is considered as the criteria of optimization. The distinguished hyperplane is illustrated by Equation (5).

$$f(x) = \sum_{i=1}^{l} y_i\, a_i k(x, x_i) + b \qquad (5)$$

Where kernel function is $k(x, x_i)$ and the membership of x is indicated by the $fx()$ sign. The optimal hyperplane construction is equal to finding every a_i that are nonzero. The optimal hyperplane support vector is every x_i data point that corresponds to nonzero a_i (Sun, Bebis and Miller, 2002).

3. METHODOLOGY AND DESIGN

3.1 Proposed Method

In general the proposed method consists of the following steps

1. Input stage: Initially the two international datasets that have been used for place recognition purpose in the literature are obtained from a reliable source of information such as machine learning websites and used here for enhancing the accuracy percentage which is COLD and IDOL datasets. Here all the images from datasets are going to be ready for the next step which is feature extraction using a powerful descriptor, this phase also includes data collection and other preprocessing activities such as removing noisy data and redundant information and image filtering such as converting a colored image to grayscale is performed in this stage as well.
2. Feature extraction: This step is the core phase of the system where local features are extracted using speeded up robust feature (SURF). There are two types of feature detection global and local feature here interest points are extracted using local features. Local feature extraction consists of two steps which are detection and description. In this thesis, a robust descriptor which is SURF is utilized for selecting the 100 strongest local features within each image of the whole three databases (COLD and IDOL). SURF size of 128 is used and the threshold of 600 is used as well. HOG descriptor which is an excellent descriptor for extracting local features is also used. In order to enhance recognition accuracy, another technique is used for feature extraction called EOH. Here some of these techniques are combined as well, for obtaining better results as shown in **Figure 2**.

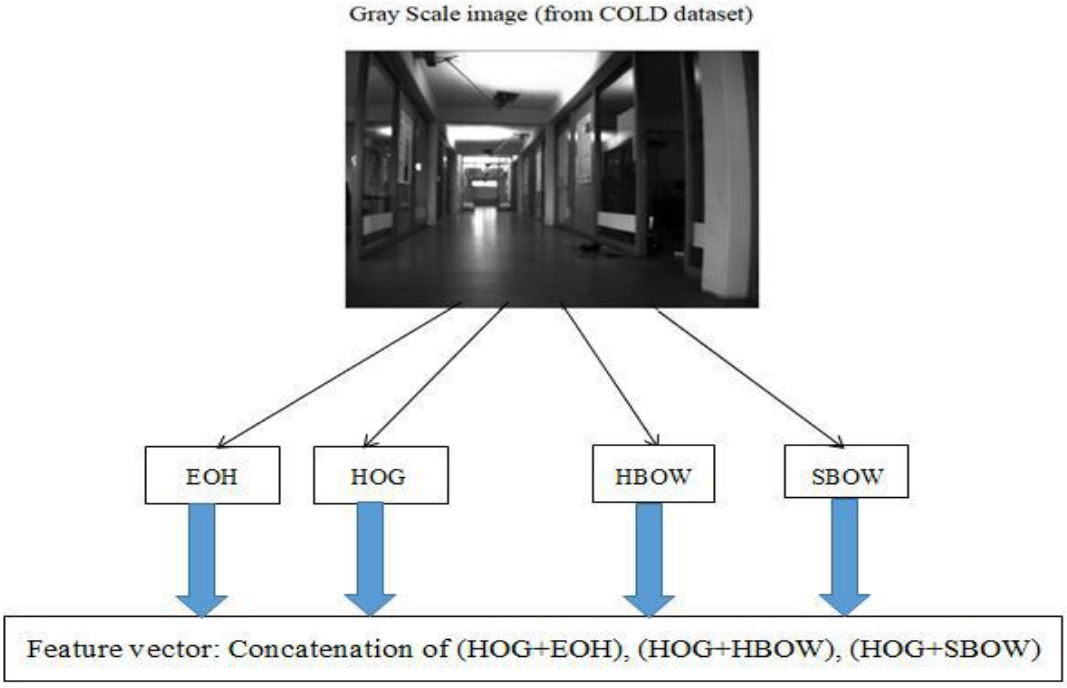

Figure 2: Features are first extracted from each image within the dataset then concatenated together to create a new feature vector for every image.

3. Localization process: This step also can be referred to as a recognition process. For recognition task clustering techniques and machine learning, classification methods are used. For clustering purpose, unsupervised learning technique which is known as k-mean is used for grouping similar features together. Training the dataset using a different number of centroids within the range [50-600] and figuring out which one obtains the best localization accuracy. BOW technique has been used for the result of every used centroid of the images inside the datasets. One row of BOW feature is obtained and saved together for all the images in an excel sheet then the result is saved in a readable format by Weka application in

order to be classified using SVM, random forest and naïve Bayes or any other classifier.

To specify the type of the image feature for example, for idol dataset the type field contains five labels (one-person office, two-person office, printer area, corridor, and kitchen), a tag is assigned for every feature vector that represents each image in the dataset as shown in **Figure 3**.

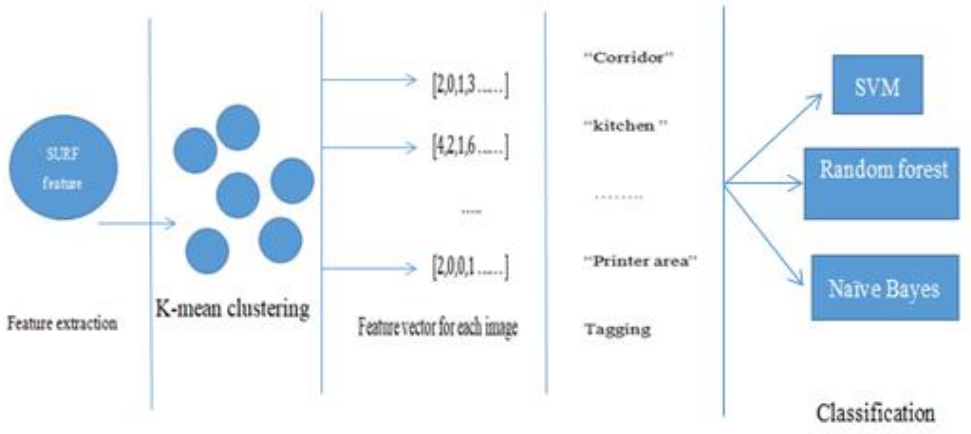

Figure 3 : graphical representation of the training and classification process

4. Reading next frame from the live images then returning back to step two to calculate features for new frames. The overall process is shown in **Figure 4**.

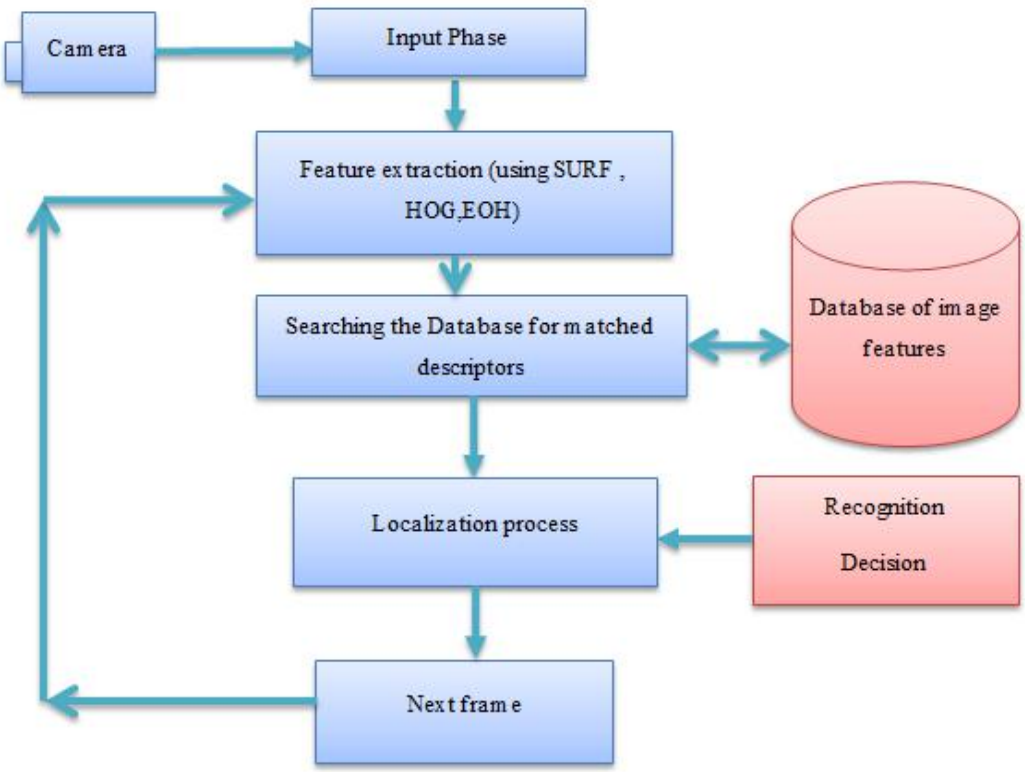

Figure 4: The general process

The following subsections give the explanation for both datasets that have been used in this paper.

3.2 COsy Localization Database (COLD)

The COLD is the abbreviation of COsy (Cognitive System for Cognitive Assistant) Localization Database. For assessing the localization system which is primarily vision-based for working on mobile platforms in a rational setting, this database is representing an attempt for providing an environment on a large scale and has flexibility in testing. This database has three types (COLD-Freiburg, COLD-Ljubljana, COLD-Saarbrücken) that acquired inside three labs in three different cities in Europe: in Germany at Freiburg University inside the laboratory of autonomous intelligent System; Slovenia,at Ljubljana University inside the laboratory of Visual Cognitive Systems; and the laboratory in Saarbrücken, Germany at the Artificial Intelligence research center.

Regular and omni-directional cameras with laser range scans and odometry data are utilized for capturing the images of the dataset. During several days under different weather and illumination conditions (cloudy, night and sunny weather) utilizing triple different mobile platforms and the same camera setup, the data were recorded. Within every three laboratories, the image capturing was carried out inside some different function rooms. Thus, for evaluating the strength of localization and recognition algorithms with respect to variations caused by human activities and changes in illumination conditions, COLD dataset considered as a perfect testing database for this purpose (Pronobis and Caputo, 2009). **Figure 7** shows some examples of camera images within the database for each of the three laboratories.

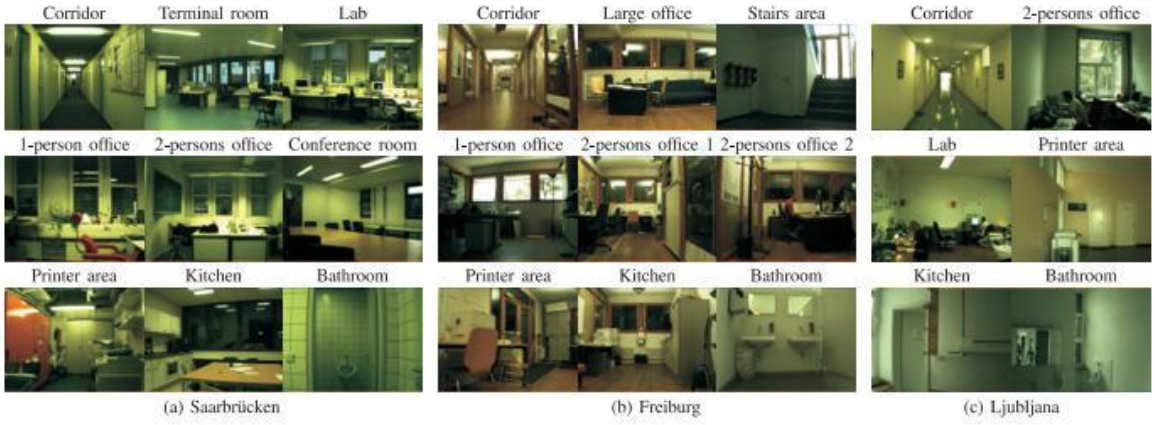

Figure 7: samples of COLD dataset images presenting some rooms for each of three types (Pronobis and Caputo, 2009).

3.3 Image database for rObot Localization (IDOL)

The word IDOL is the abbreviation of Image Database for robot Localization. The dataset contains 24 sequences of images accompanied by laser scans and odometry data obtained utilizing two mobile robot platforms. In the duration of 6 months, The data was acquired inside an indoor lab circumstance including five places with diverse working (one-person office, two-people office, corridor, kitchen, and printer area) under several illumination variations (in cloudy, night and sunny weather). Consequently, natural diversity is captured that exist in the real world surroundings caused by both human activity and illumination conditions. The KTH-IDOL1 database has an extension which is KTH-IDOL2 composed of 12 image sequences brought out from KTH-IDOL1 dataset and another 12 sequences captured after 6 months (Luo et al., 2006). **Figure 8** shows sample of images of the dataset.

Figure 8: sample of images from the IDOL database presenting each of five places (Luo et al., 2006)

4. RESULTS AND DISCUSSION

Here we have used several approaches to calculate Recognition accuracy which are Bag Of Word (BOW) combined with speeded up robust features (SURF) descriptor, Histogram Of gradient (HOG), Edge Oriented Histogram (EOH) and SVM classifier. Then we have combined HOG once with EOH and also combined it with the soft assignment of BOW using SVD in order to achieve more accurate results for two international datasets (COLD and IDOL).**Table1** includes accuracy percentage of COLD dataset when features of the images are extracted using SURF descriptor then K-mean clustering with a deferent number of centroids is used within the range [50-600], then BOW is calculated for each cluster the final result is achieved after SVM classifier is used. It can be noticeable that for cold sunny dataset it reaches a maximum accuracy of 68.710% when cluster 150 is used. The highest accuracy achieved is 81.369 for cold cloudy at a cluster of 100. The last column of the table1 includes accuracies of cold night dataset when it gains best results 76.037% with a cluster of 500. Here SMO classifier is used which is an improved application of SVM classifier.**Table2** contains correctly classified instances of IDOL dataset when the combination of SURF and BOW model is used for finding features and clustering then SVM classifier is applied to the result to gain overall accuracy. It can be seen that for IDOL dataset results are reduced. Both IDOL sunny and IDOL night reach the maximum accuracy of 65.995% and 65.388% respectively at a cluster of 150. Meanwhile, IDOL cloudy gains best result 64.885% accuracy at a cluster of 100. Soft assignment feature of BOW technique using SVD is calculated also in our paper for both COLD and IDOL dataset as shown in **Table 3** and **Table 4** respectively. The second way that we have used for accomplishing localization task is EOH which is a powerful machine learning technique. We applied this method to the same datasets that we have used previously COLD and IDOL. As shown in **Figure 5(a)** cold sunny, cold cloudy and cold night reach their peak accuracy of 93.617 %, 94.109%, and 93.983% respectively when the number of regions is 4 using random forest classifier. **Figure 5(b)** presents the accuracy results of IDOL dataset using random forest classifier. IDOL sunny, IDOL cloudy and IDOL night gain the peak accuracy of 90.380%, 89.640% and 88.601% at r=4. **Figure 6(a)** represents EOH accuracies for cold dataset using SVM classifier when cold sunny, cold cloudy and cold night reach their peak accuracy of 97.246 %, 96.164%, and 93.983 % respectively when number of regions is 8. As shown in **Figure 6(b)** IDOL Sunny reaches the top value 87.695% at r=4, while IDOL cloudy and IDOL night have the best result 88.222% and 86.321 % respectively at r=8. The third method applied to COLD and IDOL datasets to find recognition accuracy is HOG. Table5 contains percentage accuracy for both datasets when SVM classifier is used. Both EOH and HOG can obtain good results but we can still optimize the accuracy by using a combination of this two method (EOH+HOG) this combination obtains best results as shown in **Table 6**. We also combined HOG and soft assignment of BOW using SVD a notable improvement can be seen with this combination as shown in **Table 7.** It is worth noting that in all the obtained results no filter is used.

Table 1: Localization accuracy (in percentage) of COLD dataset when BOW and SVM classifier is used

No. of Cluster	50	100	150	200	250	300	350	400	450	500	550	600
COLD sunny	66.708	68.335	68.710	65.832	64.330	60.45	67.459	68.335	64.330	64.455	59.949	60.700
COLD cloudy	79.315	81.369	78.082	78.356	80.137	77.123	76.301	73.698	74.246	76.986	76.027	71.232
COLD night	68.049	73.755	74.481	70.435	70.746	70.954	71.991	68.879	72.199	76.037	74.792	73.029

Table 2: Localization accuracy (in percentage) of IDOL dataset when BOW and SVM classifier is used

No. of Cluster	50	100	150	200	250	300	350	400	450	500	550	600
IDOL sunny	63.758	63.758	65.995	60.962	59.172	57.941	54.474	57.382	58.053	55.704	53.803	53.355
IDOL cloudy	60.414	64.885	61.395	57.033	59.978	59.869	59.760	56.488	55.725	56.597	55.943	53.435
IDOL night	58.963	64.145	65.388	61.036	59.067	61.761	63.626	57.409	61.036	57.927	58.238	62.590

Table 3: Localization accuracy (in percentage) of COLD dataset for soft assignment of BOW using SVD when SVM classifier is utilized

No. of Cluster	50	100	150	200	250	300	350	400	450	500	550	600
COLD sunny	58.698	59.199	58.573	58.573	58.322	58.322	59.073	58.197	58.573	58.573	58.448	58.322
COLD cloudy	75	78.630	80.411	80.137	80.958	80.958	81.780	81.643	82.328	81.917	82.191	82.602
COLD night	64.211	63.070	61.825	62.551	62.033	62.759	62.240	61.929	62.344	62.240	62.551	62.136

Table 4: Localization accuracy (in percentage) of IDOL dataset for soft assignment of BOW using SVD when SVM classifier is utilized

No. of Cluster	50	100	150	200	250	300	350	400	450	500	550	600
IDOL sunny	60.962	60.962	62.080	61.073	60.850	62.639	59.172	60.962	61.073	61.745	61.745	59.955
IDOL cloudy	55.943	55.507	54.198	53.762	53.435	54.198	54.198	54.307	52.780	52.780	51.690	53.653
IDOL night	55.440	56.994	56.476	56.580	58.238	56.580	57.202	57.437	58.134	59.585	58.445	56.373

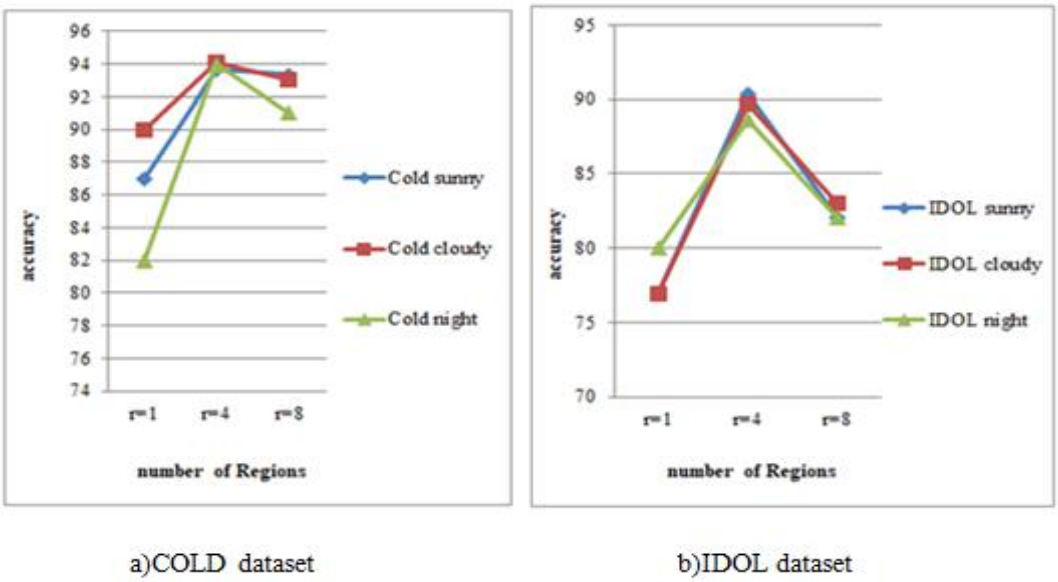

a)COLD dataset b)IDOL dataset

Figure 5: EOH classification accuracy for COLD and IDOL datasets using random forest classifier

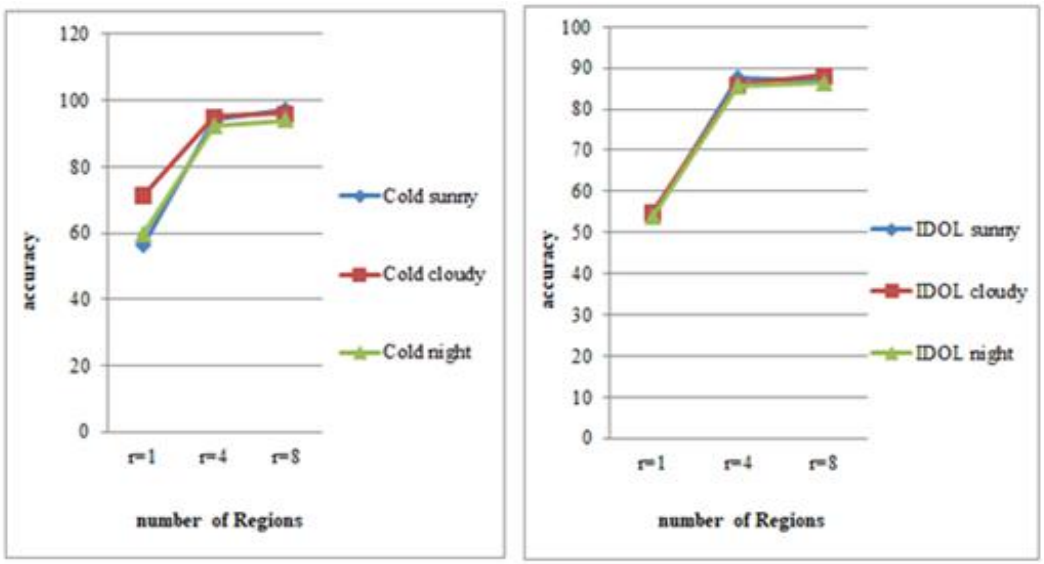

a)COLD dataset b)IDOL dataset

Figure 6: EOH classification accuracy for COLD and IDOL datasets using SVM classifier

Table 5: HOG classification result for COLD and IDOL datasets using SVM classifier

Dataset	**Accuracy(percentage)**
COLD sunny	88.235%
COLD cloudy	92.054%
COLD night	90.871%
IDOL sunny	86.800%
IDOL cloudy	85.278%
IDOL night	85.595%

Table 6: accuracy results of COLD and IDOL datasets for combination of EOH and HOG (EOH+HOG) using SVM classifier

Dataset	**Accuracy(percentage)**
COLD sunny	97.496%
COLD cloudy	98.082%
COLD night	98.962%
IDOL sunny	99.105%
IDOL cloudy	99.018%
IDOL night	98.238%

Table 7: accuracy results of COLD and IDOL datasets for the combination of soft assignment of BOW using SVD and HOG (SVD+HOG) classified by SVM.

Dataset	**Accuracy(percentage)**
COLD sunny	93.241%
COLD cloudy	96.712%
COLD night	93.879%
IDOL sunny	96.085%
IDOL cloudy	95.637%
IDOL night	93.367%

5. CONCLUSION

Three different methods have been used in this paper to find an accuracy percentage for two international datasets (COLD and IDOL). The first method is using a combination of SURF and BOW model where the obtained results by this method where not so accurate for COLD dataset maximum reached accuracy is 81.369%, while for IDOL it achieves its be best result of 65.995%. The second used method is EOH technique where COLD dataset reaches a peak of 97.246% accuracy which is a very good result and IDOL reaches top value 88.222% accuracy. A third technique that we have used is HOG for the COLD dataset best-obtained result is 92.054% while IDOL achieves the highest accuracy of 86.800%. Although EOH obtains good result we can still improve localization accuracy by using a combination of EOH and HOG. This combination gains most accurate results in all cases where it obtains results in the range of 97.496% and 99.105 %.HOG is also combined to soft assignment feature Of BOW using SVD where the results are more accurate than applying each of the two methods separately. This work can be improved using Deep learning for the purpose of localization.

REFERENCES

Abedin, Z., Dhar, P. and Deb, K. (2017) 'Traffic sign recognition using SURF: Speeded up robust feature descriptor and artificial neural network classifier', *Proceedings of 9th International Conference on Electrical and Computer Engineering, ICECE 2016*, pp. 198–201. doi: 10.1109/ICECE.2016.7853890.

Bourmaud, G. and Mégret, R. (2015) 'Robust large scale monocular visual SLAM', *Proceedings of the IEEE Computer Society Conference on Computer Vision and Pattern Recognition*, 07–12–June, pp. 1638–1647. doi: 10.1109/CVPR.2015.7298772.

Cadena, C. *et al.* (2016) 'Past, present, and future of simultaneous localization and mapping: Toward the robust-perception age', *IEEE Transactions on Robotics*, 32(6), pp. 1309–1332. doi: 10.1109/TRO.2016.2624754.

Castle, R. O., Klein, G. and Murray, D. W. (2010) 'Combining monoSLAM with object recognition for scene augmentation using a wearable camera',

Image and Vision Computing. Elsevier B.V., 28(11), pp. 1548–1556. doi: 10.1016/j.imavis.2010.03.009.

Diamantas, S., Astaras, S. and Pnevmatikakis, A. (2016) 'Depth estimation in still images and videos using a motionless monocular camera', *IST 2016 - 2016 IEEE International Conference on Imaging Systems and Techniques, Proceedings*, (October), pp. 129–134. doi: 10.1109/IST.2016.7738210.

Hong, S., Qian, X. and Wu, W. (2016) 'A Co-Robotic Cane', (August), pp. 33–42.

Hu, F. *et al.* (2016) 'Indoor Localization for the Visually Impaired Using a 3D Sensor', pp. 192–204.

Luo, J. *et al.* (2006) 'The KTH-IDOL2 Database', *Environment*, pp. 1–12.

Milici, Stefano; Esposito, Ambra; Staderini, E. M. (2018) 'A Wireless Indoor Navigation Aid for Visually Impaired People using UWB Localization Infra-structure and an Original Wayfinding Algorithm Stefano'. doi: 10.3929/ethz-b-000251651.

Nguyen, Q. H. *et al.* (2017) 'Developing a way-finding system on mobile robot assisting visually impaired people in an indoor environment', *Multimedia Tools and Applications*. Multimedia Tools and Applications, 76(2), pp. 2645–2669. doi: 10.1007/s11042-015-3204-2.

Pronobis, A. and Caputo, B. (2009) 'COLD: The CoSy localization database', *International Journal of Robotics Research*, 28(5), pp. 588–594. doi: 10.1177/0278364909103912.

Ramesh, K. *et al.* (2018) 'Real-time localization and navigation in an indoor environment using monocular camera for visually impaired', *2018 5th International Conference on Industrial Engineering and Applications, ICIEA 2018*. IEEE, pp. 122–128. doi: 10.1109/IEA.2018.8387082.

Ren, H. (2014) 'OBJECT DETECTION USING EDGE HISTOGRAM OF ORIENTED GRADIENT Haoyu Ren Ze-Nian Li Vision and Media Lab School of Computing Science Simon Fraser University', *International Conference on Image Processing(ICIP)*, pp. 4057–4061.

Sun, Z., Bebis, G. and Miller, R. (2002) 'On-road vehicle detection using Gabor filters and support vector machines', *International Conference on Digital Signal Processing, DSP*, 2, pp. 1019–1022. doi: 10.1109/ICDSP.2002.1028263.

Timotius, I. K. and Setyawan, I. (2015) 'Evaluation of Edge Orientation Histograms in smile detection', *Proceedings - 2014 6th International Conference on Information Technology and Electrical Engineering: Leveraging Research and Technology Through University-Industry Collaboration, ICITEE 2014*, pp. 2–6. doi: 10.1109/ICITEED.2014.7007905.

Tsai, C.-F. (2012) 'Bag-of-Words Representation in Image Annotation: A Review', *ISRN Artificial Intelligence*. Hindawi, 2012, pp. 1–19. doi: 10.5402/2012/376804.

Ugave, V. A. (2014) 'SMART INDOOR LOCALIZATION USING MACHINE LEARNING TECHNIQUES', pp. 1–149.

Younes, G. *et al.* (2016) 'Keyframe-based monocular SLAM: design, survey, and future directions', *Robotics and Autonomous Systems*, 98(July), pp. 67–88. doi: 10.1016/j.robot.2017.09.010.

Zhang, J., Kaess, M. and Singh, S. (2014) 'Real-time depth enhanced monocular odometry', *IEEE International Conference on Intelligent Robots and Systems*, (Iros), pp. 4973–4980. doi: 10.1109/IROS.2014.6943269.

ZANCO Journal of Pure and Applied Sciences
The official scientific journal of Salahaddin University-Erbil
https://zancojournals.su.edu.krd/index.php/JPAS

ISSN (print):2218-0230**, ISSN (online):** 2412-3986**, DOI: http://dx.doi.org/10.21271/zjpas**

RESEARCH PAPER

Radioactivity Investigation of the Anthropogenic ^{137}Cs Radionuclide in Soil Samples from the Marapasta Region in Iraqi Kurdistan.

Mohammed Ibrahim Mohammed Mustafa

Department of Physics, College of Science, University of Raparin, Rania- Sulaimania, Kurdistan Region, Iraq

A B S T R A C T:

Gamma ray spectroscopy analyses have been carried out on 32 soil samples from the Marapasta area for activity concentration comparisons and hazard effects due to the ^{137}Cs radionuclide for the first time in this region. The average activity concentration of the ^{137}Cs in the soil samples was measured using HPGe detector systems. The anthropogenic radioactivity levels of ^{137}Cs in the samples collected from the bottom-of-hole soil at Marapasta, in the undisturbed areas near the bottom of the mountain chain and for the cultivated agricultural areas were found to be of an average value of 12.07 ± 0.03 $Bqkg^{-1}$, 7.55 ± 1.68 $Bqkg^{-1}$ and 1.33 ± 0.6 $Bqkg^{-1}$ respectively. In order to evaluate the radiological hazards effects due to ^{137}Cs in the samples, the absorbed dose rate (D), the annual effective dose rate (AEDR), the excess lifetime cancer risk for outdoor and total exposures (ELCR) in the soil samples were also determined. The results have been compared with the worldwide average range of radioactivity measurements. The three different ranges obtained in this survey indicate that there are different levels of radioactive hazard related to man-made radionuclides in the area and could serve as a first baseline for ^{137}Cs.

KEY WORDS: Anthropogenic Radioactivity; Activity concentration; ELCR of ^{137}Cs radionuclide.
DOI: http://dx.doi.org/10.21271/ZJPAS.31.4.9.
ZJPAS (2019) , 31(4);82-93 .

1. INTRODUCTION :

The release history of the anthropogenic ^{137}Cs radionuclide to the atmosphere dates back to the first half of the last century, in 1945. Environmental contamination was produced by ^{137}Cs fallout due to fission processes and yielded mainly from atmospheric explosions in atomic bomb tests, with 948 PBq set free (Radiation, 2000). The Chernobyl accident in April 1986 caused an 85 PBq atmospheric release (Radiation, 2011) and the Fukushima Dai-ichi Nuclear Power Plant (FDNPP) accidents in March 2011 circulated an amount of 6–20 PBq into the atmosphere (Nagai and Kurihara, 2014).

Chino and colleagues estimated the amount of release to the atmosphere from the FDNPP incident was 13–15 PBq (Chino et al., 2011, Headquarters, 2011). Meanwhile, the atmospheric contribution of ^{137}Cs released from normal operation and reprocessing at nuclear power plants has not contributed to global fallout compared to the above nuclear accidents. For instance, the amounts of ^{137}Cs released to the atmosphere from La Hague and Sellafield up to 1997 were less than 1 GBq and less than 3.4 TBq respectively (Radiation, 2000). Released ^{137}Cs diffuses, is transported over the whole world by atmospheric circulation, falls to the ground in the form of dry and wet depositions, and is then strongly and rapidly absorbed by soil particles. The presence of ^{137}Cs in agricultural soil or natural plants leads to

* **Corresponding Author:**
Mohammed Ibrahim M. Mustafa
E-mail: m.m@uor.edu.krd
Article History:
Received: 26/11/2018
Accepted: 13/05/2019
Published: 10/09 /2019

transfer to food products and then to humans through the food chain. ^{137}Cs can be readily or uniformly absorbed by the human body with a biological half-life of about 110 days (Eisenbud and Gesell, 1997).

Water is considered another route of ^{137}Cs absorption. Because ^{137}Cs is more soluble in marine water than fresh water (Protection, 2006), it is taken up by seafood (fish) depending on the quantity of potassium ions in the water. Because caesium is chemically similar to potassium, it resembles potassium to the human body and is distributed similarly in all of its organs (Eisenbud and Gesell, 1997). Thus ^{137}Cs fallout leads to a risk of direct external and internal radiation exposure, giving rise to public concern (Zhu and Smolders, 2000). Therefore, soil surface contamination with long half-life (30.17 y) ^{137}Cs has an important impact on the human environment and research on the concentration of ^{137}Cs activities in the environment has become an indicator for environmental radioactive security assessment. The spatial distribution of ^{137}Cs in surface soil has not been reported in this region. Consequently, the aim of this study was to detect radioactive levels of ^{137}Cs, to establish the first baseline measurements for radioactivity concentration in the soil surface of the Marapasta region, and to present the factors influencing the presence of ^{137}Cs, as well as to assess the contamination hazard level.

2. GEOLOGY OF THE AREA

Marapasta is a famous mineralisation area located in the Qandile mountain range of the Zagrose suture zone northeast of Iraqi Kurdistan. It lies at latitude 36° 23' 37" north, longitude 45° 14' 6" east; at altitude 1710 m above sea level and it is about eight hours from Basta village on foot. The Marapasta area occupies approximately 4–6 km^2 of plateau at the top of the mountains. In this area, an extensive exploration was conducted by a Russian geological team between 1960 and 1964 (Jassim and Goff, 2006). Geological work in the area led to various holes with a depth of approximately 100–150 cm. Therefore, through excavation of the area, the soil surface has been distorted, leading to three kinds of soil: soil extracted and stockpiled for a long period of time (since 1976), soil from the bottoms of the holes, and the intact natural soil of the area at undisturbed surfaces (Al-Bassam, 2013).

3. MATERIALS AND METHODS

3.1. Sample collection and Processing

The preliminary tests in the present study identified the presence of a gamma ray spectral line at 661.7 keV in a specific soil sample from the three different types of soil samples collected in the Marapasta area. This led author to pay attention to anthropogenic sources of ^{137}Cs radionuclide, and to re-collecting ten specific samples from the region of interest for this study. Additionally, to collect soil samples from 22 sites in undisturbed areas near the bottom of the mountain chain and in cultivated agricultural areas at neighbouring sites affected by erosion by rainwater.

Total soil samples were collected randomly from 32 different locations according to the classified soil forms as shown in Figure 1. The soil samples were obtained at a typical depth of 10 to 15 cm from the top surface layer. The soil from each location was collected with a hand shovel and approximately 3–4 kg weighed for packing into its own tight, secure bag to prevent contamination. After collection, the samples were cleared of stones, crushed into fine powder using a pestle and dried in an oven at a temperature of 110 °C for 24 hours. The dried samples were pulverised into a fine powder and passed through a standard 2 mm mesh. The samples were then reweighed to an average of 2 kg of soil per sample, packed in a sealed, airtight Marinelli beaker and kept for a period of about 30 days to achieve the secular equilibrium between the ^{238}U and ^{232}Th series and with their respective

progenies decay products prior to analysis (Mollah et al., 1987).

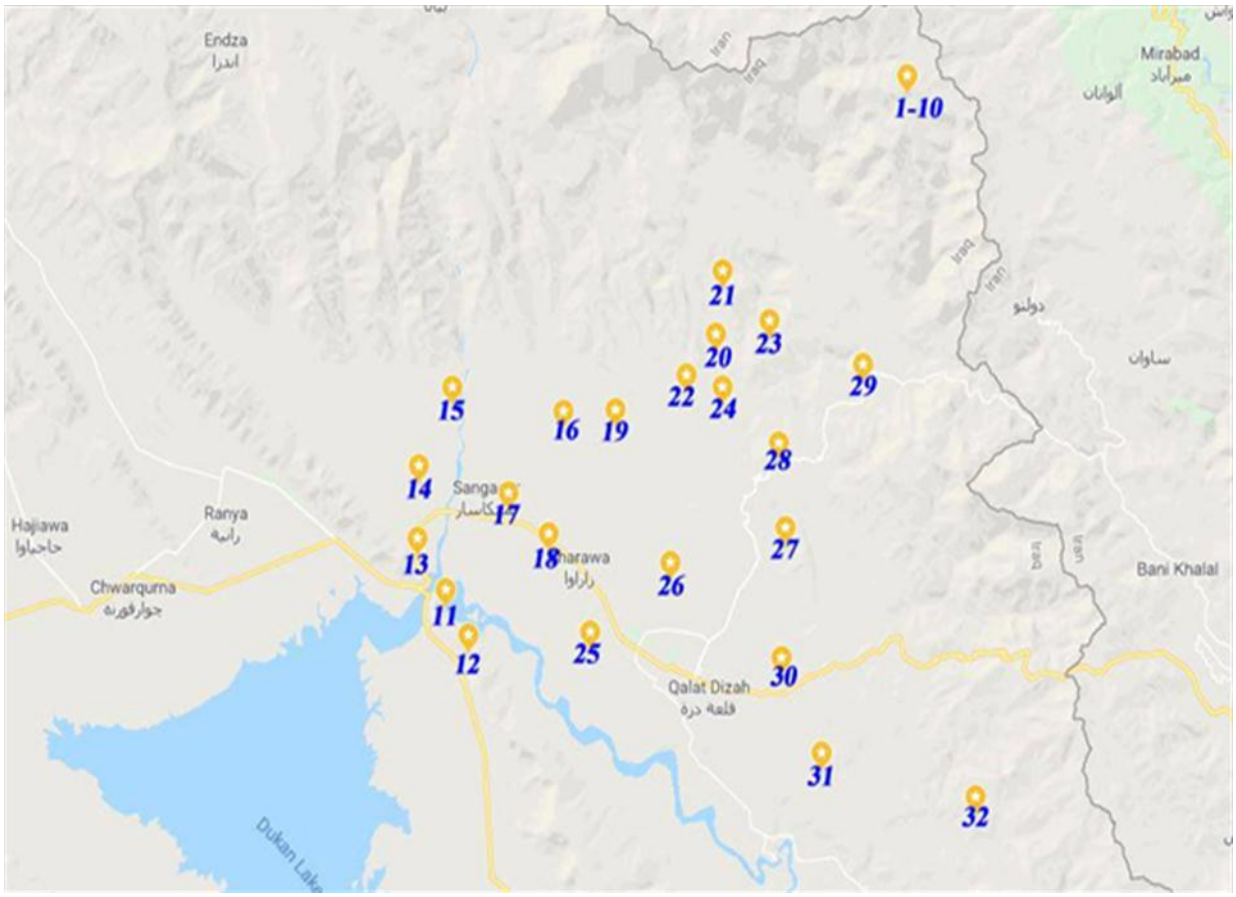

Figure 1: Geographical map of Marapasta region in Iraqi Kurdistan. The sampling location abbreviated on the map with numbers 1-32.

3.2. Experimental set up

The detection and activity concentration analysis of artificial ^{137}Cs radionuclide in the environmental soil samples was carried out by high-resolution gamma ray spectrometry using two different types of high-purity germanium (HPGe) detection system, Koya4039 (Ahmad, 2016) and Canberra GX5020 in the present research.

3.2.1. Koya 4039 HPGe Detection System

The gamma spectrometry measurements for the first ten samples from the bottom-of-hole soil) collected in the Marapasta region were implemented using HPGe at Koya University. The detector is a low Compton gamma spectrometer which was established recently with a PGT IGC70200 coaxial HPGe P-type detector of crystal length 70.7 mm, crystal diameter 70.6 mm and high relative efficiency (70% at 1332 keV). The detector has an energy resolution (FWHM) of 1.97 keV for the 133.2 keV gamma ray line of a ^{60}Co source.

The detector has a high peak-to-Compton ratio of 75:1, which is expressed as the ratio of maximum counts in the peak channel to the average number of counts in the Compton plateau region. The detector and preamplifier were placed inside a cylindrical lead shield (Kolga Model A340) of 10.1 cm thickness with an internal diameter of 28 cm and a height of 40 cm. The lead shield is lined with several layers of tin and copper, 0.5 and 1.6 mm thick respectively, to reduce the background

scattering in the measured spectrum and cooled by liquid nitrogen to reduce leakage current of the detector caused by thermal noise. The integrated signal processor consists of a pulse height analysis system to transform pulses, which are ultimately collected by System 8016, a computer-based multichannel analyser (Quantum MCA), and analysis performed with the Quantum Gold software of PGT. Standard gamma point sources with energies ranging from 59.5 to 1764.5 keV were used for energy and efficiency calibrations of the system.

3.2.2. GX5020 HPGe Detection System

The gamma ray spectrometry measurements for the other 22 samples in the current research were implemented at the Cekmece nuclear research and training centre in *Istanbul* using a coaxial HPGe model Canberra GX5020. The detector crystal is p-type and its geometry is closed-ended with dimensions of 68.5 mm diameter and 53 mm length. Its relative efficiency is 50% and its energy resolution is 2.0 keV at the 1332.5 keV line of FWHM from ^{60}Co. Its peak-to-Compton ratio is 60:1. For gamma ray shielding, a front-opening split-top shield was used to reduce the background. It features a 100 mm thickness of lead that is jacketed by a 9.5 mm steel outer housing. The graded liner comprises a 1 mm thick tin layer and a 1.5 mm thick copper layers to prevent interference by lead X-rays. To minimise scattered radiation from the shield, the detector was centred within it (Karataşlı et al., 2016). Gamma spectroscopy analysis was performed with the Genie-2000 software system interfaced with a multichannel analyser model DSA-1000, which is a full-featured 16K channel multichannel analyser with advanced digital signal processing techniques. The DSA-1000 operates through the Genie-2000 gamma spectroscopy software that includes functions such as peak searching, peak evaluation, energy and efficiency calibration modes, and nuclide identification. The calibration energy and relative efficiency of the GX5020 spectrometer were established using 1000 ml Marinelli calibration sources that contained ^{241}Am, ^{109}Cd, ^{57}Co, ^{139}Ce, ^{203}Hg, ^{113}Sn, ^{85}Sr, ^{137}Cs, ^{88}Y and ^{60}Co peaks for an energy range of 80 to 2500 keV (Stoulos et al., 2003).

3.3. ^{137}Cs Activity Concentration

3.3.1. Koya4039 Detection System

Radioactivity of radionuclides in the prepared environmental samples was determined by high-resolution gamma ray spectrometry with a high-purity germanium (HPGe) detector. Gamma ray emissions at energies of 661.7 keV corresponding to the ^{137}Cs radionuclide were detected in the present analysis of the activity concentration. The accumulative counting time of 43200 seconds (12 hrs) was set for measuring each soil sample and the background under the same condition to provide great counting efficiency with a PGT IGC70200 coaxial HPGe detector. The spectrum of the background count was used to correct the net peak area of gamma rays of the measured radionuclides. The counting errors for the samples ranged from 0.6 to 1.07%. The background subtracted spectrum of each sample was analysed directly for activity concentration with the Quantum Gold spectroscopy software of PGT (Princeton Gamma Tech.) produced by American Nuclear Systems of Oak Ridge National Laboratory. The activity concentration of ^{137}Cs in the detected soil samples was obtained using its 661.7 keV gamma ray line expressed as Bqkg^{-1} dry weight. The photo peak of 661.7 keV gamma ray energy was only detected in the samples were taken from the bottom of the holes in the Marapasta area soil samples (1–10) taken in June 2014 for the present study.

3.3.2. GX5020 HPGe Detection System

The GX5020 HPGe detection system was used to obtain the gamma ray spectra of samples 11–32 collected from the undisturbed areas near the bottom of the mountain chain and the cultivated agricultural areas from neighbouring sites in the current survey, after energy and efficiency calibration of the detector for the other soil

samples. Background counting was also performed. The accumulative counting for each sample was recorded for 50,000 seconds. The activity concentration (A) for the 661.7 keV gamma ray line (in $Bqkg^{-1}$) was calculated as follows (ICRP, 1991):

$$A = \frac{CR}{\varepsilon(E_\gamma) I_\gamma M} \quad \dots\dots\dots\dots\dots\dots\dots (1)$$

where CR is the net count rate of the 661.7 keV gamma ray line in the sample spectrum subtracted from the corresponding gamma ray line area in the background spectrum; ε (E_γ) is the absolute efficiency of the HPGe detector; I_γ is the gamma ray emission probability; and M is the mass of the sample (kg). After corrections for background and the Compton continuum, this gives the activity concentration for dry weight (in $Bqkg^{-1}$) of ^{137}Cs radio nucleus in each sample (IAEA, 2004).

4. RESULTS AND DISCUSSION

4.1. Activity concentration

Activity concentration analysis was carried out as described in the detection of activity section for samples taken from the bottoms of the holes in Marapasta (1–10), from the undisturbed areas near the bottom of the mountain chain (11–16), and from cultivated agricultural areas at neighbouring sites (17–32) for the aforementioned soil profile.

The anthropogenic radioactivity level of ^{137}Cs for the samples collected for the bottom-of-hole soil profile at Marapasta was found to be in the range of 8.14 ± 0.07 $Bqkg^{-1}$ to 17.18 ± 017 $Bqkg^{-1}$ with an average value of 12.07 ± 0.03 $Bqkg^{-1}$. For the samples collected in the undisturbed areas near to the bottom of the mountain chain, it ranged from 3.4 ± 0.50 $Bqkg^{-1}$ to 12.40 ± 2.2 $Bqkg^{-1}$ with an average value of 7.55 ± 1.68 $Bqkg^{-1}$. For the cultivated agricultural areas, it spanned 0.7 ± 0.09 $Bqkg^{-1}$ to 1.6 ± 0.12 $Bqkg^{-1}$ with an average value of 1.33 ± 0.6 $Bqkg^{-1}$. Table 1 presents the results of the ^{137}Cs analysis in the current research. The detection of the anthropogenic ^{137}Cs radionuclide ($T_{1/2}$ = 30.17 years) in the region under study may be attributed to global fallout released from nuclear fission in atomic bomb testing around the world or from explosions of nuclear power plants, such as those of Chernobyl on 26 April 1986 and of Fukushima-Daiichi nuclear power plant on 11 March 2011, which was distributed worldwide through the action of atmospheric winds. It is well documented in the literature that the ^{137}Cs radionuclide enters surface soil by dry deposition and precipitation scavenging. However, surface soil and clay particles absorb ^{137}Cs radionuclide and the horizontal migration of ^{137}Cs from the surface layer of soil occurs by lixiviation runoff and erosion (Squire and Middleton, 1966, Chikasawa et al., 2001, Ohta et al., 2012). Thus, the presence of the ^{137}Cs radionuclide in only the bottom holes soil profile in the Marapasta region, as mentioned in section on the geology of the area, could be explained by the accumulation of melted snow after those accidents causing deposition of ^{137}Cs radionuclide on the ground surface at those locations.

In addition, the effects of the latitude and rate of precipitation (Ritchie and McHenry, 1990) are the main factors affecting the distribution of ^{137}Cs on the Earth's surface (FDNPP: latitude 37° 25' 16.8" N, longitude 141° 1' 41.08" E; Marapasta: latitude 36° 23' 37" N, longitude 45° 14' 07" E; distance between locations: 8087 km). Therefore, high activity concentrations (8.14 ± 0.07 Bqkg-1 to 17.18 ± 017 Bqkg-1) in samples 1–10 are the result of the extreme amount of snow that fell during the period of those two nuclear fission accidents. Moreover, the annual snow season in the Qandile mountain range (in the Marapasta region) is long, from November to May. Figure 2; demonstrates significant fluctuations in the activity concentration of ^{137}Cs with soil sample location. This variation is attributed to the topographic differences, geomorphology and metrological conditions of the region (Al-Masri, 2006). The activity concentration is higher in the mountain area (samples 1–10) compared with the samples collected from the landscape below the mountains, samples 11–16 collected from the undisturbed areas near the bottom of the mountain chain and samples 17–32 from cultivated

agricultural areas of neighbouring sites. The average activity concentrations of ^{137}Cs were found to be 12.07 ± 0.03 $Bqkg^{-1}$, 7.55 ± 1.68 $Bqkg^{-1}$ and 1.33 ± 0.6 $Bqkg^{-1}$ respectively. These differences in the average activity concentration of the ^{137}Cs radionuclide in the soil samples in the current study confirm that the low content of clay and high content of organic matter in the soil of mountain area can be considered lead to a higher radiocaesium contamination level than at the other two locations, in addition to the transport of radiocaesium due to high amounts of rainfall in the latter two locations (Kiss et al., 1988).

The average activity concentration levels of ^{137}Cs (12.07 ± 0.03 $Bqkg^{-1}$; 7.55 ± 1.68 $Bqkg^{-1}$) in the investigated soil samples (1–10 and 11–16) in the Marapasta area are in agreement with the most significant obtained results for activity concentrations of ^{137}Cs (17. 92, 16.62 and 11.2 $Bqkg^{-1}$), with the average value of 8.17± 5.55 $Bqkg^{-1}$ in Nineveh province in the north of Iraq (Najam et al., 2015), and with the worldwide activity concentration limit, which is 14.8 $Bqkg^{-1}$ (Radiation, 2000). Consequently, the data acquired in the current investigation will be used as a reference for the ^{137}Cs radionuclide in the Kurdistan region (KRG-IRAQ) soil surface. Any alteration in these values can be attributed to a specific case, such as a nuclear accident or a future increase in the fallout level.

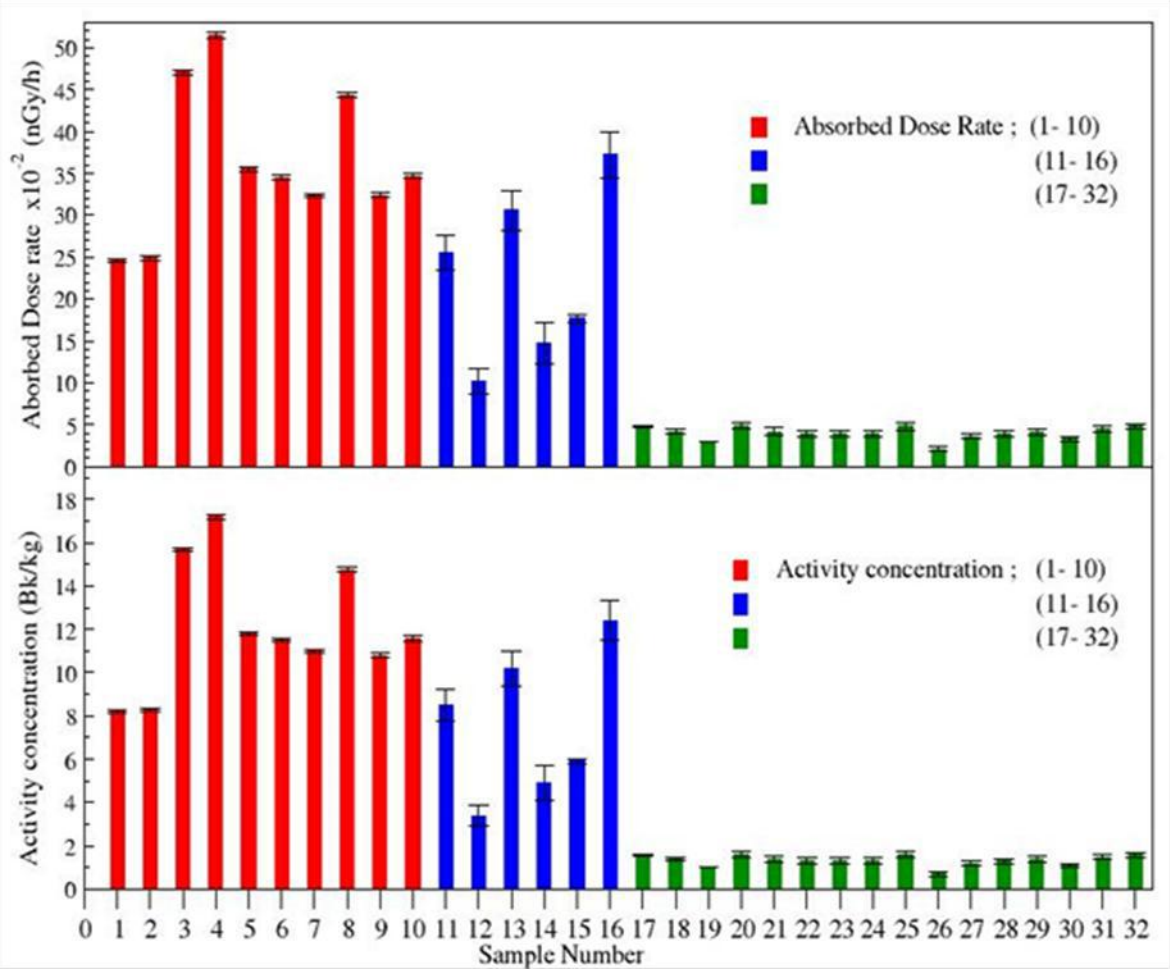

Figure 2: Bottom and top panels explain the variations of activity concentration and absorbed dose rate due to 137Cs respectively in the measured soil samples marked in Figure 1.

Table 1: Measured activity concentrations of ^{137}Cs and uncertainties and calculated absorbed gamma dose rates, with outdoor and total annual effective dose rate and excess lifetime cancer rate for in the soil samples collected samples in the current study.

Sample Number	North	East	Activity (Bq.kg^{-1})	D (nG.h^{-1}) × 10^{-2}	Outdoor AEDR (mSv.y^{-1}) × 10^{-5}	Total AEDR (mSv.y^{-1}) × 10^{-5}	Outdoor ELCR × 10^{-6}	Total ELCR × 10^{-6}
Soil 1	36° 23' 36"	45° 14' 7"	8.19 ± 0.07	24.6 ±0.21	30.1 ±0.26	150.7 ±1.0	1.05±0.01	5.27±0.04
Soil 2			8.29 ± 0.08	24.9 ±0.24	30.5 ±0.29	152.5 ±1.21	1.07±0.01	5.34±0.04
Soil 3			15.68 ± 0.10	47.1 ±0.30	57.7 ±0.37	288.4 ±1.52	2.02±0.01	10.06±0.05
Soil 4			17.18 ± 0.10	51.5 ±0.33	63.2 ±0.41	316.1 ±1.67	2.21±0.01	11.06±0.06
Soil 5			11.81 ± 0.09	35.5 ±0.27	43.5 ±0.33	217.3 ±1.37	1.52±0.01	7.6±0.05
Soil 6			11.49 ± 0.09	34.5 ±0.27	42.3 ±0.33	211.4 ±1.37	1.48±0.01	7.4±0.05
Soil 7			10.98 ± 0.07	32.29 ±0.21	40.4 ±0.26	202.0 ±1.06	1.41±0.01	7.07±0.04
Soil 8			14.75 ± 0.09	44.3 ±0.27	54.3 ±0.33	271.3 ±1.37	1.90±0.01	9.49±0.05
Soil 9			10.79 ± 0.09	32.4 ±0.27	39.7 ±0.33	198.5 ±1.37	1.39±0.01	6.95±0.05
Soil 10			11.57 ± 0.12	34.7 ±0.36	42.6 ±0.44	212.8 ±1.82	1.49±0.01	7.45±0.06
Soil 11	36° 13' 27"	44° 59' 1"	8.5 ± 0.7	25.5 ±2.10	31.3 ±2.57	156.4 ±10.6	1.09±0.09	5.47±0.37
Soil 12	36° 16' 47"	45° 0' 6"	3.4 ± 0.5	10.2 ±1.50	12.5 ±1.84	62.5 ±7.58	0.437±0.07	2.19±0.26
Soil 13	36° 16' 14"	45° 3' 32"	10.2 ± 0.8	30.6 ±2.40	37.5 ±2.94	187.6 ±12.1	1.31±0.1	6.57±0.42
Soil 14	36° 13' 34"	45° 3' 5"	4.9 ± 0.8	14.7 ±2.40	18.0 ±2.94	90.1 ±12.1	0.63±0.1	3.15±0.42
Soil 15	36° 16' 15"	45° 5' 7"	5.9 ± 0.14	17.7 ±0.42	21.7 ±0.51	108.5 ±2.12	0.76±0.02	3.79±0.07
Soil 16	36° 17' 57"	45° 8' 14"	12.4 ± 0.9	37.2 ±2.70	45.6 ±3.31	228.1 ±13.7	1.59±0.11	7.98±0.47
Soil 17	36° 12' 19"	44° 59' 55"	1.60 ± 0.04	4.8 ±0.12	5.89 ±0.15	29.4 ±0.61	0.206±0.05	1.03±0.02
Soil 18	36° 11' 19"	45° 0' 35"	1.4 ± 0.07	4.2 ±0.21	5.15 ±0.26	25.8 ±1.06	0.18±0.01	0.90±0.04
Soil 19	36° 15' 3"	44° 59' 1"	1.0 ± 0.01	3.0 ±0.03	3.68 ±0.04	18.4 ±1.52	0.13±0.01	0.63±0.05
Soil 20	36° 14' 26"	45° 1' 50"	1.6 ± 0.13	4.8 ±0.39	5.89 ±0.48	29.4 ±1.97	0.206±0.02	1.03±0.07
Soil 21	36° 19' 20"	45° 8' 25"	1.4 ± 0.15	4.2 ±0.45	5.15 ±0.55	25.8 ±2.28	0.18±0.02	0.90±0.08
Soil 22	36° 17' 2"	45° 7' 18"	1.3 ± 0.14	3.9 ±0.42	4.78 ±0.51	23.9 ±2.12	0.17±0.02	0.84±0.07
Soil 23	36° 18' 15"	45° 9' 52"	1.3 ± 0.14	3.9 ±0.42	4.78 ±0.51	23.9 ±2.12	0.17±0.02	0.84±0.07
Soil 24	36° 16' 47"	45° 8' 25"	1.3 ± 0.14	3.9 ±0.42	4.78 ±0.51	23.9 ±2.12	0.17±0.02	0.84±0.07
Soil 25	36° 11' 24"	45° 4' 20"	1.6 ± 0.15	4.8 ±0.45	5.89 ±0.55	29.4 ±2.28	0.206±0.02	1.03±0.08
Soil 26	36° 12' 56"	45° 6' 48"	0.7 ± 0.09	2.1 ±0.27	2.58 ±0.33	12.9 ±1.37	0.09±0.01	0.45±0.04
Soil 27	36° 13' 41"	45° 10' 23"	1.2 ± 0.11	3.6 ±0.33	4.42 ±0.41	22.1 ±1.67	0.15±0.01	0.772±0.06
Soil 28	36° 17' 32"	45° 10' 10"	1.3 ± 0.11	3.9 ±0.33	4.78 ±0.41	23.9 ±1.67	0.17±0.01	0.84±0.06
Soil 29	36° 17' 17"	45° 12' 46"	1.4 ± 0.13	4.2 ±0.39	5.15 ±0.48	25.8 ±1.97	0.18±0.01	0.90±0.07
Soil 30	36° 10' 50"	45° 10' 13"	1.1 ± 0.08	3.3 ±0.24	4.05 ±0.29	20.2 ±1.21	0.14±0.01	0.71±0.04
Soil 31	36° 8' 44"	45° 11' 28"	1.5 ± 0.11	4.5 ±0.33	5.52 ±0.41	27.6 ±1.67	0.19±0.01	0.97±0.06
Soil 32	36° 7' 46"	45° 16' 12"	1.6 ± 0.12	4.8 ±0.36	5.89 ±0.44	29.4 ±1.82	0.21±0.01	1.06±0.06

4.2. Absorbed Gamma Dose Rate

The contribution of ^{137}Cs radionuclide to the absorbed dose rate in the air due to gamma radiation at a height of 1 m above the ground surface depends on the activity concentration of ^{137}Cs (Bqkg^{-1}) and the dose rate per unit ^{137}Cs activity concentration coefficients (0.3 ×10^{-10} Gyh^{-1}/Bqkg^{-1}) (Radiation, 2000).

The above statement has been used to compute the outdoor absorbed gamma dose rates for the soil samples by assuming a gamma source uniformly distributed in the ground:

$$D\ (nGy.h^{-1}) = 0.03C_{Cs} \quad \ldots\ldots \quad (2)$$

Where, C_{Cs} denotes the activity concentrations of ^{137}Cs in Bqkg^{-1} (UNSCEAR, 2000).

The calculated outdoor absorbed dose rates in air for the soil samples are given in Table 1 and shown in Figure 2. The total absorbed gamma dose rates due to ^{137}Cs were found to vary from (24.6 ± 0.21) $\times10^{-2}$ to (51.5 ± 0.33) $\times10^{-2}$ nGyh^{-1} with an average value of (36.2 ± 0.09) $\times10^{-2}$ nGyh^{-1} for samples 1–10, from (37.2 ± 2.7) $\times10^{-2}$ to (10.2 ± 1.5) $\times10^{-2}$ nGyh^{-1} with an average value of (22.65 ± 0.84) $\times10^{-2}$ nGyh^{-1} for soil samples 11–16, and from (4.8 ± 0.12) $\times10^{-2}$ to (21 ± 0.27) $\times10^{-2}$ nGyh^{-1} with an average value of (3.99 ± 0.08) $\times10^{-2}$ nGyh^{-1} for samples 17–32. The contribution of ^{137}Cs in the current research to the outdoor absorbed gamma dose rate represents only 0.61-0.07% of the worldwide value for the average absorbed dose due to terrestrial gamma radiation (59 nGyh^{-1}) (Radiation, 2008). Thus, the direct influence of the anthropogenic ^{137}Cs radionuclide on outdoor radiation exposure of humans is almost negligible and the most significant outdoor radiation exposure is due to the contribution of natural radionuclides in the environment. This indicates that the measured activities of the ^{137}Cs radionuclide have not posed significant hazard effects to the people living in the vicinity of the locations where the soil samples were collected. However, it should be noted that the absorbed gamma dose rate does not directly represent radiation hazard effects on exposed people.

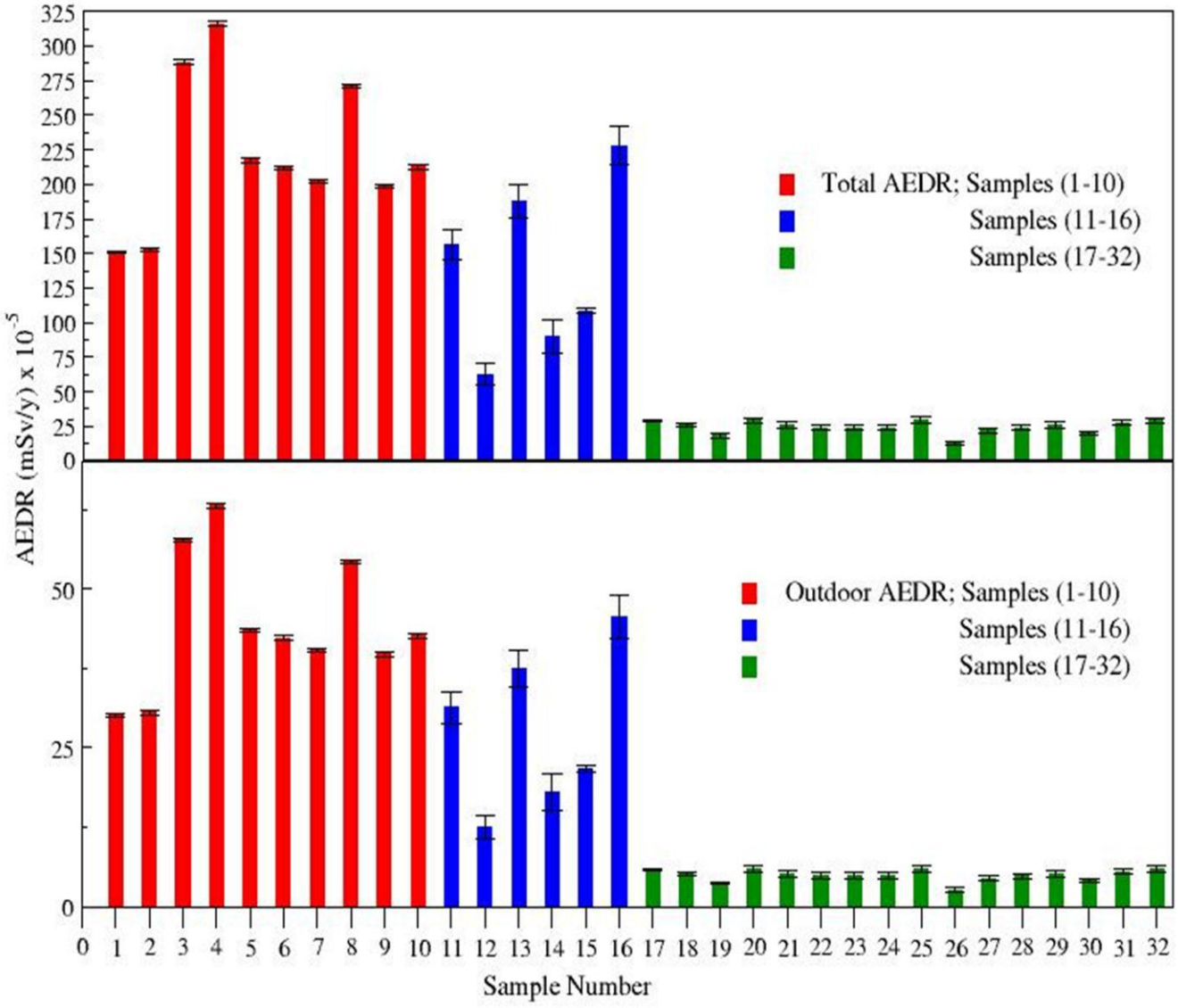

Figure 3: Variation of outdoor and total annual effective dose rates due to ^{137}Cs in the measured soil samples marked in Figure 1.

4.3. Annual Effective Dose

Estimation of the annual effective dose rate received by an adult in the air can be made by using the conversion coefficient for the effective dose received by an adult relative to the absorbed dose in the air (0.7 SvGy-1) and the outdoor occupancy factor of 0.2 or indoor occupancy factor of 0.8 (Radiation, 2000). The annual effective dose (AED) in $mSvy^{-1}$ can be calculated by the relation:

$$AEDR(mSvy^{-1}) = D(nGyh^{-1}) \times 8760(hy^{-1}) \times 0.2\ x\ 0.7\ (SvGy^{-1}) \times 10^{-6} \ldots\ldots (3)$$

The estimated values for the outdoor and annual effective dose rates are presented in Table 1 and Figure 3. The outdoor and total annual effective dose rates due to ^{137}Cs were found, for samples 1–10, to vary from (30.1 ± 0.26) $\times10^{-5}$ to (63.2 ± 0.41) $\times10^{-5}$ $mSvy^{-1}$, with an average value of (44.4 ± 0.11) $\times10^{-5}$ $mSvy^{-1}$, and (150.7 ± 1.06) ×10-5 to (316.0 ± 1.67) ×10-5 mSvy-1, with an average value of (222.1 ± 0.44) ×10-5 mSvy-1, respectively. For soil samples 11–16, they ranged from (12.5 ± 1.84) $\times10^{-5}$ to (45.6.1 ± 3.31) $\times10^{-5}$ mSvy-1, with an average value of (27.8 ± 8.1) $\times10^{-5}$ mSvy-1, and from (62.5 ± 7.57) $\times10^{-5}$ to (228.1 ± 13.7) $\times10^{-5}$ $mSvy^{-1}$, with an average value of (138.9 ± 0.43) $\times10^{-5}$ $mSvy^{-1}$, respectively. For samples17–32, they spanned (2.58 ± 0.33) $\times10^{-5}$ to (5.89 ± 0.15) $\times10^{-5}$ $mSvy^{-1}$, with an average value of (4.9 ± 0.24) $\times10^{-5}$ $mSvy^{-1}$, and (12.9 ± 1.37) $\times10^{-5}$ to (29.4 ± 0.61) $\times10^{-5}$ $mSvy^{-1}$ with an average value of (24.5 ± 0.43) $\times10^{-5}$ $mSvy^{-1}$, respectively. The above-mentioned values for the average outdoor and total annual effective dose rates (AEDR) are similar to or less than 0.55% of the worldwide average outdoor and total AEDRs due to terrestrial gamma radiation of 80 $\times10^{-3}$ $mSvy^{-1}$ and 500 $\times10^{-3}$ $mSvy^{-1}$ respectively (Radiation, 2000). Because the highest value for AED for one year is 1 $mSvy^{-1}$ (IAEA., 2018), clearly these average AEDR values are insignificant and show that there is no risk to humans at the locations of the soil samples collected for the current study due to ^{137}Cs radionuclide.

4.4. Excess Lifetime Cancer Risk

The excess lifetime cancer risk (ELCR) deals with the probability of developing cancer over a period of time due to ionising radiation emitted by radionuclides at a certain exposure level. Calculation of ELCR based on determined values of AEDR is expressed by the following equation:

$$ELCR = AEDR \times DL \times RF \ldots\ldots (4)$$

Where DL is the average duration of life (approximately 70 years) and RF is the fatal cancer risk factor in Sv^{-1}. For low-dose background radiation stochastic effects, ICRP 60 (Protection, 1991) uses a value of 0.05 for RF for public exposure (Protection, 1991). The ELCR values obtained from the outdoor and total AEDRs are presented in Table 1 and Figure 4. For samples 1–10, 11–16 and 17–32, the ELCR for outdoor exposure vary from (1.055 ± 0.01) $\times10^{-6}$ to (2.21 ± 0.01) $\times10^{-6}$ with an average value of (1.55 ± 0.004) $\times10^{-6}$, (0.44 ± 0.06) $\times10^{-6}$ to (1.6 ± 0.1) $\times10^{-6}$ with an average value of (0.97 ± 0.04) $\times10^{-6}$, and (0.09 ± 0.01) $\times10^{-6}$ to (0.2 ± 0.005) $\times10^{-6}$ with an average value of (0.17 ± 0.004) $\times10^{-6}$, respectively. Further, for samples 1–10, 11–16 and 17–32, the total annual (outdoor with indoor) exposure ranges from (5.27 ± 0.04) $\times10^{-6}$ to (11.06 ± 0.06) $\times10^{-6}$ with an average value of (7.77 ± 0.015) $\times10^{-6}$, (2.19 ± 0.26) $\times10^{-6}$ to (7.98 ± 0.47) $\times10^{-6}$ with an average value of (4.86 ± 0.15) $\times10^{-6}$, and (0.45 ± 0.05) $\times10^{-6}$ to (1.03 ± 0.02) $\times10^{-6}$ with an average value of (0.86 ± 0.015) $\times10^{-6}$, respectively.

The highest recorded average values for ELCR for outdoor and total exposures were for samples 1–10, at 1.55 $\times10^{-6}$ and 7.77 $\times10^{-6}$. Both of these highest values for average ELCR obtained in the

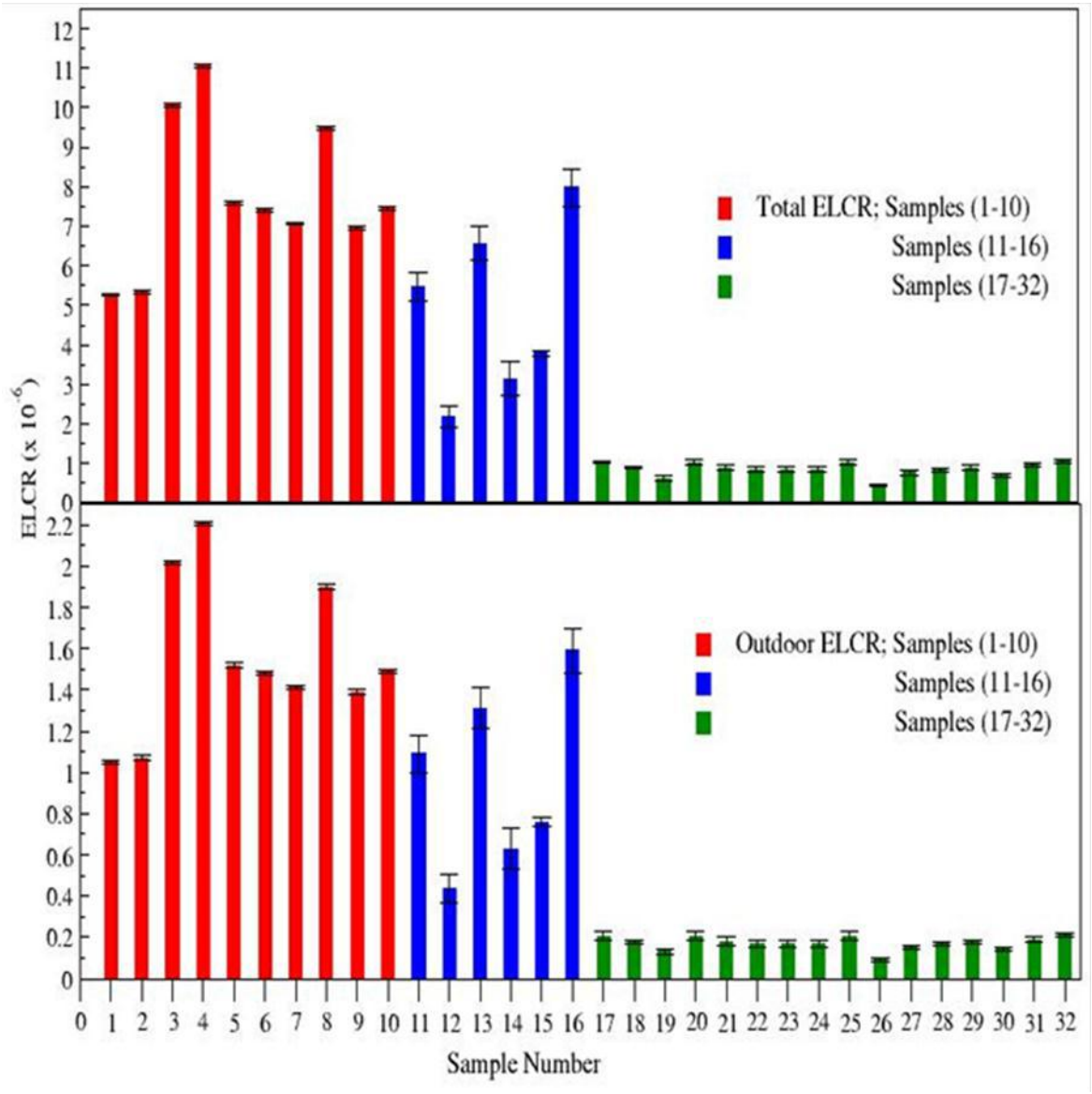

Figure 4: Variation of excess lifetime cancer risk for outdoor and total exposure due to ^{137}Cs in the measured soil samples marked in Figure 1.

present research are less than the average worldwide limit of 0.29 $\times 10^{-3}$ (Radiation, 2000), as shown in Figure 4. This indicates that the possibility of developing cancer among residents who spend all of their lives in the studied area, such as shepherds, who spend above 60% of their lives in that location, is not great considering only exposure to the anthropogenic^{137}Cs radionuclide.

5. CONCLUSIONS

Calculation of the activity concentration of anthropogenic ^{137}Cs radionuclide in soil samples collected from the Marapasta region have been performed using high-resolution gamma ray spectroscopy. The results are in agreement with the latest results of an average activity concentration value of 8.17 ± 5.55 Bqkg^{-1} in Nineveh province in the north of Iraq and with the worldwide activity concentration limit, which is 14.8 Bqkg^{-1}.

The average values for outdoor and total AEDR and ELCR were well below worldwide averages. The obtained results indicate that there is no risk to humans at the locations of the soil samples collected for this investigation due to the ^{137}Cs

radionuclide. The investigated soil samples were collected three years after the Fukushima Dai-ichi nuclear power plant accident. Thus, these findings may serve as a first baseline reference for the ^{137}Cs radionuclide in monitoring possible anthropogenic soil contamination in KRG- IRAQ. Due to the lack of precise statistics on death by cancer, further analysis and studies are needed to assess the real radiation hazard risks for people who are working in this region, especially shepherds and families whose living depends on domestic animals.

ACKNOWLEDMENTS

The Author acknowledges the help of Dr. Sadoon Taha Ahmed (Koya University) and Dr. M. Timuçin AYBERS (CNRTC) for providing the HPGe detection system for sample measurements.

REFERENCES

AHMAD, S. T. 2016. High purity Germanium Koya4039 Gamma detection system. *BOOK of PROCEEDING*, 268.

AL-BASSAM, K. S. 2013. Mineral resources of Kurdistan region, Iraq. *Iraqi Bulletin of Geology and Mining,* 9**,** 103-127.

AL-MASRI, M. 2006. Vertical distribution and inventories of 137Cs in the Syrian soils of the eastern Mediterranean region. *Journal of environmental radioactivity,* 86**,** 187-198.

CHIKASAWA, K., ISHII, T. & SUGIYAMA, H. 2001. Terrestrial gamma radiation in Kochi prefecture, Japan. *Journal of Health Science,* 47**,** 362-372.

CHINO, M., NAKAYAMA, H., NAGAI, H., TERADA, H., KATATA, G. & YAMAZAWA, H. 2011. Preliminary estimation of release amounts of 131I and 137Cs accidentally discharged from the Fukushima Daiichi nuclear power plant into the atmosphere. *Journal of nuclear science and technology,* 48**,** 1129-1134.

EISENBUD, M. & GESELL, T. F. 1997. *Environmental radioactivity from natural, industrial and military sources: from natural, industrial and military sources*, Elsevier.

HEADQUARTERS, N. E. R. 2011. Report of the Japanese Government to the IAEA Ministerial Conference on Nuclear Safety. *Japan: Government of Japan, Tokyo*.

IAEA. 2018. *Regulations for the safe transport of radioactive material*, IAEA.

JASSIM, S. Z. & GOFF, J. C. 2006. *Geology of Iraq*, DOLIN, sro, distributed by Geological Society of London.

KARATAŞLı, M., TURHAN, Ş., VARINLIOĞLU, A. & YEĞINGIL, Z. 2016. Natural and fallout radioactivity levels and radiation hazard evaluation in soil samples. *Environmental Earth Sciences,* 75**,** 424.

KISS, J., DE JONG, E. & MARTZ, L. 1988. The distribution of fallout cesium-137 in southern Saskatchewan, Canada. *Journal of Environmental Quality,* 17**,** 445-452.

MOLLAH, A., RAHMAN, M., KODDUS, M., HUSAIN, S. & MALEK, M. 1987. Measurement of high natural background radiation levels by TLD at Cox's Bazar coastal areas in Bangladesh. *Radiation protection dosimetry,* 18**,** 39-41.

NAGAI, H. & KURIHARA, O. 2014. Outline of UNSCEAR 2013 report (1). Radionuclide releases, dispersion and deposition. *Nippon Genshiryoku Gakkai-Shi,* 56**,** 791-795.

NAJAM, L. A., YOUNIS, S. A. & KITHAH, F. H. 2015. Natural radioactivity in soil samples in Nineveh Province and the associated radiation hazards. *Int. J. Phys,* 3**,** 126-132.

OHTA, T., MAHARA, Y., KUBOTA, T., FUKUTANI, S., FUJIWARA, K., TAKAMIYA, K., YOSHINAGA, H., MIZUOCHI, H. & IGARASHI, T. 2012. Prediction of groundwater contamination with 137Cs and 131I from the Fukushima nuclear accident in the Kanto district. *Journal of environmental radioactivity,* 111**,** 38-41.

PROTECTION, I. C. O. R. 1991. *ICRP Publication 60: 1990 Recommendations of the International Commission on Radiological Protection*, Elsevier Health Sciences.

PROTECTION, I. C. O. R. 2006. Human alimentary tract model for radiological protection. *ICRP Publication 100. Ann. ICRP,* 36.

RADIATION, U. N. S. C. O. T. E. O. A. 2000. *Sources and effects of ionizing radiation: sources*, United nations publications.

RADIATION, U. N. S. C. O. T. E. O. A. 2011. *Sources and Effects of Ionizing Radiation: Report to the General Assembly with Scientific Annexes. Volume 2. Annex D. Health Effects Due to Radiation from the Chernobyl Accident.(advanced Copy)*, UN.

RITCHIE, J. C. & MCHENRY, J. R. 1990. Application of radioactive fallout cesium-137 for measuring

soil erosion and sediment accumulation rates and patterns: a review. *Journal of environmental quality,* 19**,** 215-233.

SQUIRE, H. & MIDDLETON, L. 1966. Behaviour of Cs137 in soils and pastures a long term experiment. *Radiation Botany,* 6**,** 413-423.

STOULOS, S., MANOLOPOULOU, M. & PAPASTEFANOU, C. 2003. Assessment of natural radiation exposure and radon exhalation from building materials in Greece. *Journal of Environmental Radioactivity,* 69**,** 225-240.

ZHU, Y. G. & SMOLDERS, E. 2000. Plant uptake of radiocaesium: a review of mechanisms, regulation and application. *Journal of Experimental Botany,* 51**,** 1635-1645.

ZANCO Journal of Pure and Applied Sciences
The official scientific journal of Salahaddin University-Erbil
https://zancojournals.su.edu.krd/index.php/JPAS

ISSN (print):2218-0230**, ISSN (online):** 2412-3986**, DOI: http://dx.doi.org/10.21271/zjpas**

RESEARCH PAPER

Artificial Neural Network Based on Optimal Operation of Economic Load Dispatch in Power System

Ismael Kareem Saeed
Department of Electrical Engineering, College of Engineering, Salahaddin University-Erbil, Kurdistan Region, Iraq.

A B S T R A C T:

The LaGrange iterative method was construct to solve the problem of power losses reduction case to minimize the total fuel cost generation. It difficult to optimize nonlinearity cost functions of fuel generators in power systems with equality and inequality constraints. This paper presents an approach method of optimization for solving the economic load dispatch (ELD) problem with generator constraints and satisfying the load demand irrespective of transmission line losses. To verify the proposed work, an artificial neural network (ANN) based Lambda iterative optimization method with Matlab R2018a program is being apply to the test system. The numerical studies have been accomplished to IEEE model system (30-bus 6-generator, 41-line and 20-load). The results have manifests the effectiveness of the supposed algorithms because it can provide accurate dispatch solutions with wide range of load demand in minimum total cost. Further analyses indicate the total power losses in the system.

KEY WORDS: ANN; Economic load dispatch; Power system stability; Quadratic cost function; and Lambda iterative method.
DOI: http://dx.doi.org/10.21271/ZJPAS.31.4.10
ZJPAS (2019) , 31(4);94-102 .

1. INTRODUCTION :

The economic load dispatch (ELD) problem seeks the best generation schedule for the generating plants to supply the required demand plus transmission losses with the minimum production cost. Conventionally, the emphasis on performance optimization of fossil–fuel power systems was on economic operation only, using the ELD approach, as better solutions would result in significant economic benefits (Zhihang et al., 2013). The total electrical energy losses of transmission line have a negative effect on environment; also decrease the overall efficiency of the systems.

* **Corresponding Author:**
Ismael Kareem Saeed
E-mail: Ismael.Saeed@su.edu.krd
Article History:
Received: 05/04/2019
Accepted: 21/05/2019
Published: 10/09 /2019

Conversely, in local high voltage or low voltage distribution networks to satisfy the load demand distributed energy resources composed of distributed generations and energy storage devices are incorporated (Gomez et al., 2014). Optimal economic dispatch problems in electrical power systems should be solve minimization operation of the total fuel costs by setting the output power of each generator so as satisfy the load demand and related operational constraints. Since 1920, many experts and researchers conducted in the field of energy engineering related research. Optimal theories and circuits are base of economic dispatch problem. The power flow algorithm applied on real-time system states to compute the all bus voltages and line flows of power systems. However solutions computing by those methods are accurate, but more iterations and time-consuming processes to convergence problem (Acha and Kazemtabrizi, 2013; Chai et al., 2015;Kim, 2016; Raygani et al, 2012). Open

literature describe many computer programs of power system during the last three decades, (Neyer et al., 1990). Several of these software's were designing to provide a variety of engineering analysis ranging from load flow to transient stability. Others have been developed to plan and control the power system in real-time (Foley and Bose, 1995).

The network sensitivity factor methods, like as shift distribution factor generation (Soman et al., 2015), and Jacobian-based distribution factor (JBDF) (Huang and Yao, 2012), have been suggested so as to progress the computation of speed running programs and reduce of iterations. The applied of this access overcomes the impairment of Newton Raphson and Gauss-based load flow algorithms in economic dispatch. General optimum algorithms in economic dipatch and unit commitment are based on non-linear Lagrange multiplier methods (Sun et al., 2015) and meta-heuristic approaches (Marlon and Osvaldo, 2013). Soroudi and Rabiee approached a new model to solve the problem of dynamic multiple-zone ED by studying uncertainties in wind power generation, energy fuel costs and power system demands. Optimal state analysis is also used to verify the proposed approach to real-time operation of process power systems (Soroudi and Rabiee, 2013).

This paper study the optimal economic dispatch in electrical power system based on artificial neural network optimization technique program by using Matlab software program and find total power losses and total cost generations.

2. PROBLEM FORMULATION

The standard of optimal power flow problem can be written as:

Minimization of the objective function F(x)

which subject to equality constraints{ $g_i(x) = 0$ }

and inequality constraints { $a \leq h_i(x) \leq b$ }

The major factor play an effective role of the optimum dispatch of generation is power transmission loss. The transmission line loss PL formula of ED load problem consider as below.

Minimize of objective function:

$$C_{totol} = C_1 + C_2 + C_3 + \cdots + C_{ng} \quad \$/hr \qquad (1)$$

$$where \quad C_i = \propto_i + \beta_i P_i + \gamma_i P_i^2 \qquad (2)$$

C_i is the incremental fuel cost for the i[th] generating unit; and $\propto_i$, β_i and γ_i represents fuel constant coefficients.

Subject to

$$P_{i\,min} \leq P_i \leq P_{i\,max} \qquad (3)$$

Here, $P_{i\,min}$ and $P_{i\,max}$ represent lower and higher power generation limits for the ith generating unit

$$\sum_{i=1}^{ng} P_i = P_D + P_L \qquad (4)$$

Here, P_D is power system demand and P_L is transmission power losses.

Transmission power loss is considered to be quadratic function, which is given as:

$$P_L = \sum_{i=1}^{ng}\sum_{j=1}^{ng} P_i B_{ij} P_j + \sum_{j=1}^{ng} B_{0j} P_j + B_{oo} \qquad (5)$$

Here, B_{ij} , B_{0j} , and B_{00} are loss constant coefficients of systems.

The generalized objective function C_{total} is a non-linear function, increasing of the generation bus of power systems leads to increase the number of the equality and inequality constraints. Applications of an optimization technique such as the Lambda Iterative algorithm by using Matlab program are very suitable to solve the problem of a large power distribution system with a more non-linear objective functions and great number of constraints.

3. TRAINING THE NETWORK BY ANN

Artificial Neural Networks are made up of large interconnected neural numerating elements of a parallel distributed network processing. These networks have the ability to learn and store the acknowledgements. These acknowledgements make neural network to solve any problems (Aree, 2018). The learning of ANN may be either supervised or unsupervised. During the training the actual outputs for each input signal are made availability to the network (Tarik and Nian, 2016). The aim of ED is to minimizing the generation cost rate simultaneously at appropriate interval while satisfying various constraints. The constrained optimization can be modified as:

$$C_T = \sum_{k=1}^{T}\sum_{i=1}^{ng}[\alpha_i + \beta_i P_i^k + \gamma_i (P_i^k)^2] \quad (6)$$

The interconnection between the artificial neurons in an Artificial Neural Network (ANN) gave it the flexibility to adapt and copy any mathematical model (Eisa, 2013). In the last decades, it's been found that the nonlinear relationship between the inputs and the outputs in any black-box system can be replaced with ANN. This modeling is depicted as a supervised training procedure. This procedure gives the ability of the network's interconnections to adjust using the error signal in a way that the network output tries to track the desired output. Providing data to the network continues until the error is reduced to a predefined value. Network training was achieved using the method of Levenberg-Marquardt backpropagation (LMBP) due to its fast training process (Tommy and Siu, 2007). This method has the property of approaching to second-order training speed with no computation of the Hessian matrix H.

$$H = J^T J \quad (7)$$

where J is the Jacobian matrix that contains first derivatives of the network error with respect to the weights and biases. The LMBP algorithm uses the following approach to minimize the total error e:

$$x_{k+1} = x_k - [J^T J + \mu I]^{-1} J^T e \quad (8)$$

The topology of this ANN shows in Fig. 1(a). The hyperbolic tangent (tanh) as an activation function used for the hidden units, the identity function has been used for the output ones.

$$y = \sum_{n=1}^{N_h} w_n^{output} \tanh\left(\sum_{m=0}^{N_i} w_{mn}^{hidden} x_m\right) + w_0^{output} \quad (9)$$

Once the multilayer perceptron MLP topology is fixed, the ANN learns the relationship between input and output elements. For that, the network must be trained. The target values are a set of patterns training data consisting of input and corresponding output values. For each entire training pattern process, the weights are updated. This updating is done in such a way that a measure of the error in the network's results is minimised as shown in Fig. 1(b) for this work.

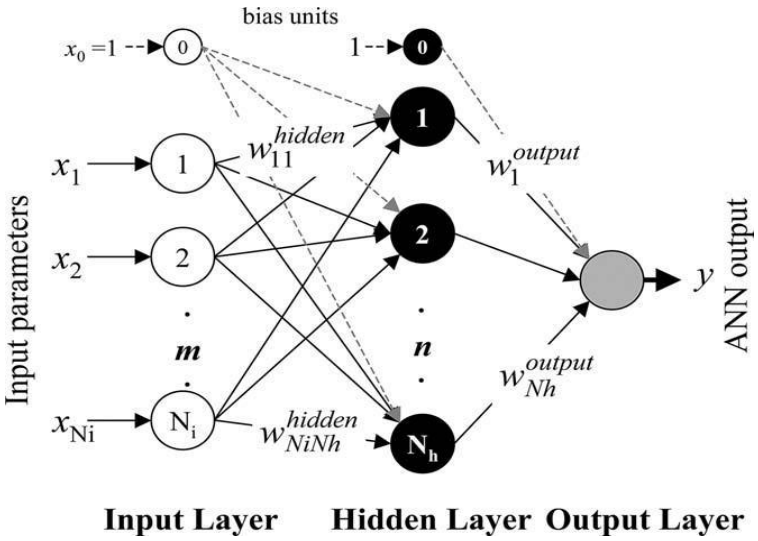

(a)

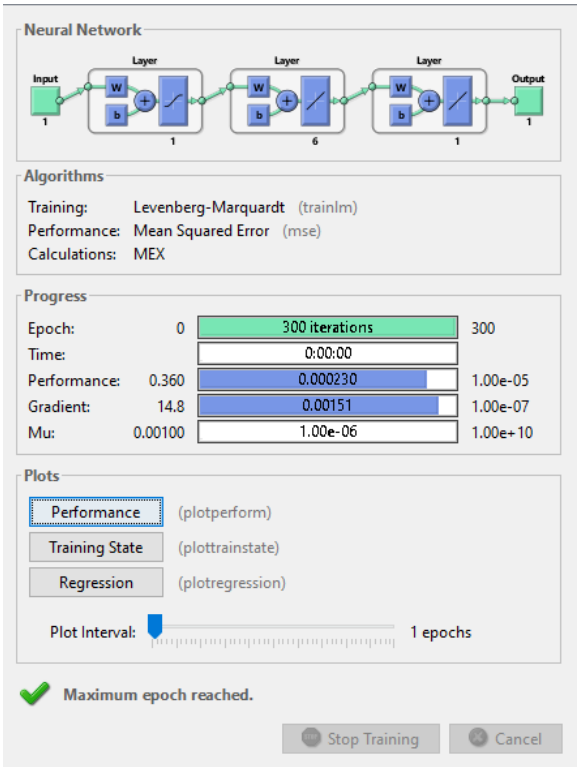

(b)

Figure 1. (a) Topology of the multilayer perceptron. (b) Neural Network Training

4. METHOD ALGORITHM

Step 1. Initialization

Initialize Lambda λ0 guess

Step 2. ELD approach

Using Lagrangian multiplier to calculate optimal power dispatch of this matrix

$$\begin{bmatrix} \frac{\gamma_1}{\lambda}+B_{11} & B_{12} & \cdots & B_{1n} \\ B_{21} & \frac{\gamma_2}{\lambda}+B_{22} & \cdots & B_{2n} \\ \vdots & \vdots & \ddots & \vdots \\ B_{n1} & B_{n2} & \cdots & \frac{\gamma_n}{\lambda}+B_{nn} \end{bmatrix} \begin{bmatrix} P_1 \\ P_2 \\ \vdots \\ P_n \end{bmatrix} = \frac{1}{2} \begin{bmatrix} 1-B_{01}-\frac{\beta_1}{\lambda} \\ 1-B_{02}-\frac{\beta_2}{\lambda} \\ \\ 1-B_{0n}-\frac{\beta_n}{\lambda} \end{bmatrix} \quad (10)$$

and total transmission line power losses PL by solving equation(5).

Step 3. Apply ANN based Lambda Iterative

Evaluate the fitness function Δλ.
Step 4. Repeat the step 2 and step 3 until the process has been converged or it satisfies the stopping criteria.
Step 5. Limiting Power generation
If optimal power under not maximum and minimum limits, fix that generate power and repeat the step 2, 3 and 4.
Step 6. Find total fuel cost
Step 7. Stop

Fig. 2 shows the Flowchart of economic dispatch using ANN based Lambda iterative technique.

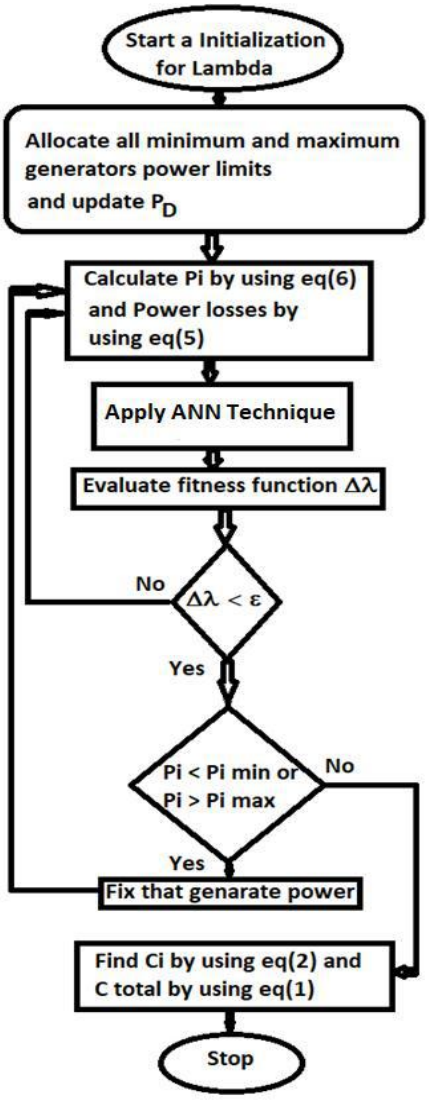

Figure 2. Economic dispatch flowchart using ANN based Lambda iterative technique

5. CASE STUDY

The ANN based Lambda iterative method is a very effective tool for the linear optimization problems that are able to handle both equalities constrained and inequality constrained linear optimization problems. Numerous computational programming methods, such as the barrier method, inner point and the Lambda iterative method have been developed and punished based on the basic rules of the Lambda iterative method. The Lambda iterative method and its extensive methods are widely applied in science, engineering, economics and our daily life.

In addition the optimal total cost of a test system been calculated for a various particular power demand. IEEE 30-bus model system have been employed to carried out various case studies, a proposed approach system with six generating as shown in Fig. 3. units is optimized and simulated by using Intel Core i7-3612QM, 2.10 GHz, 8 GB memory. The proposed algorithm was applied in MATLAB R2018a program.

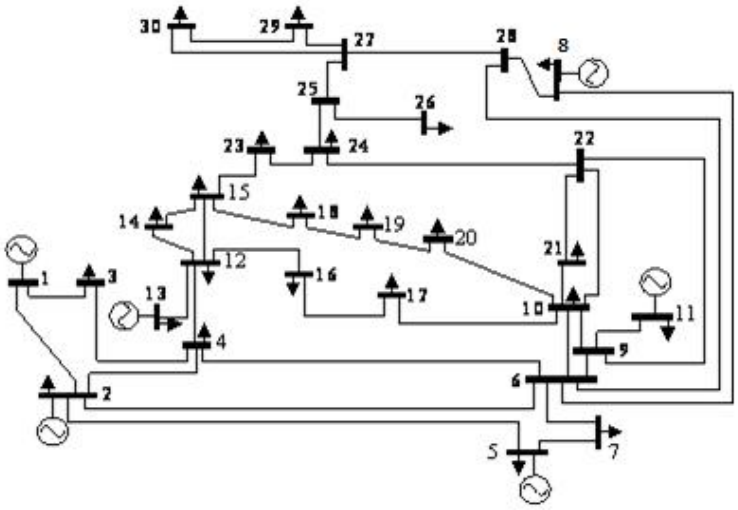

Figure 3. Topology of the IEEE 30-bus model system

Table 1 shows the minimum and maximum active power limits of six generators of the proposed system and constant coefficients of the quadratic cost functions. The full algorithm of optimum solution of total fuel cost for a proposed six-unit generating system shown in Fig. 2. Losses coefficient B are given in Table 3.

Table 1: Generators parameters of the IEEE 30-bus Electrical Network

Bus Number	Pg_i^{min} [MW]	Pg_i^{max} [MW]	a [$/hr]	b [$/MWhr]	c [$/MW^{2}hr]
Bus 1	50	200	0	2.00	$37.5 \cdot 10^{-4}$
Bus 2	20	80	0	1.75	$175 \cdot 10^{-4}$
Bus 5	15	50	0	1.00	$625 \cdot 10^{-4}$
Bus 8	10	35	0	3.25	$83 \cdot 10^{-4}$
Bus 11	10	30	0	3.00	$250 \cdot 10^{-4}$
Bus 13	12	40	0	3.00	$250 \cdot 10^{-4}$

6. SIMULATION RESULTS

The ED program is an effective code in the Matlab environment according to the system model and solving algorithms. The proposed method employed to solve the ED problem of the original system of the IEEE 30-bus model and verify the accuracy and effectiveness of the proposed method, and the relevant parameter of the ED and power flow are obtained. The numerical and ANN results (Table 2) demonstrate all results of the developed ED program. Matlab Software code were using to generate the output power in MW/hr, fuel cost of generators in $/hr and the total operational cost against the multiple power demand in MW. Fig. 4 and Fig. 5 show optimum output power and fuel cost of each six generating unit system with change of power demand respectively. Fig. 6 shows the minimum total cost of the proposed system with and without ANN against change of power demand.

Table 2: The simulation results of the traditional ANN based Lambda Iterative technique method for the ED of the original IEEE 30-bus test system.

P_D = 320MW		$P_D \leq$ 260MW in case P_D = 250 MW		$P_D \geq$ 380 MW In case P_D = 400 MW	
$P_{1\ actual}$	188.6354 MW	$P_{1\ actual}$	155.533 MW	P_{1} (Fixed) $_{actual}$	200.00 MW
$P_{1\ ANN}$	188.6362 MW	$P_{1\ ANN}$	155.5307 MW	P_{1} (Fixed) $_{ANN}$	200.00 MW
$P_{2\ actual}$	51.4141 MW	$P_{2\ actual}$	43.3428 MW	$P_{2\ actual}$	79.891 MW
$P_{2\ ANN}$	51.4149 MW	$P_{2\ ANN}$	43.3417 MW	$P_{2\ ANN}$	79.905 MW
$P_{5\ actual}$	21.9275 MW	$P_{5\ actual}$	19.005 MW	$P_{5\ actual}$	39.378 MW
$P_{5\ ANN}$	21.9282 MW	$P_{5\ ANN}$	19.0046 MW	$P_{5\ ANN}$	39.389 MW
$P_{8\ actual}$	29.5766 MW	$P_{8\ actual}$	11.662 MW	P_{8} (Fixed) $_{actual}$	35.00 MW
$P_{8\ ANN}$	29.5779 MW	$P_{8\ ANN}$	11.6595 MW	P_{8} (Fixed) $_{ANN}$	35.00 MW
$P_{11\ actual}$	14.8047 MW	P_{11}(Fixed) $_{actual}$	10.00 MW	$P_{11\ actual}$	24.601 MW
$P_{11\ ANN}$	14.8055 MW	P_{11}(Fixed) $_{ANN}$	10.00 MW	$P_{11\ ANN}$	24.615 MW
$P_{13\ actual}$	13.719 MW	P_{13}(Fixed) $_{actual}$	12.00 MW	$P_{13\ actual}$	21.234 MW
$P_{13\ ANN}$	13.7195 MW	P_{13}(Fixed) $_{ANN}$	12.00 MW	$P_{13\ ANN}$	21.244 MW
$P_{L\ actual}$	0.169 MW	$P_{L\ actual}$	0.1298 MW	$P_{L\ actual}$	0.2495 MW
$P_{L\ ANN}$	0.163 MW	$P_{L\ ANN}$	0.103 MW	$P_{L\ ANN}$	0.241 MW
$C_{total\ actual}$	898.1143 $/hr	$C_{total\ actual}$	663.2001 $/hr	$C_{total\ actual}$	1225.9 $/hr
$C_{total\ ANN}$	885.47 $/hr	$C_{total\ ANN}$	652.51 $/hr	$C_{total\ ANN}$	1210.7 $/hr

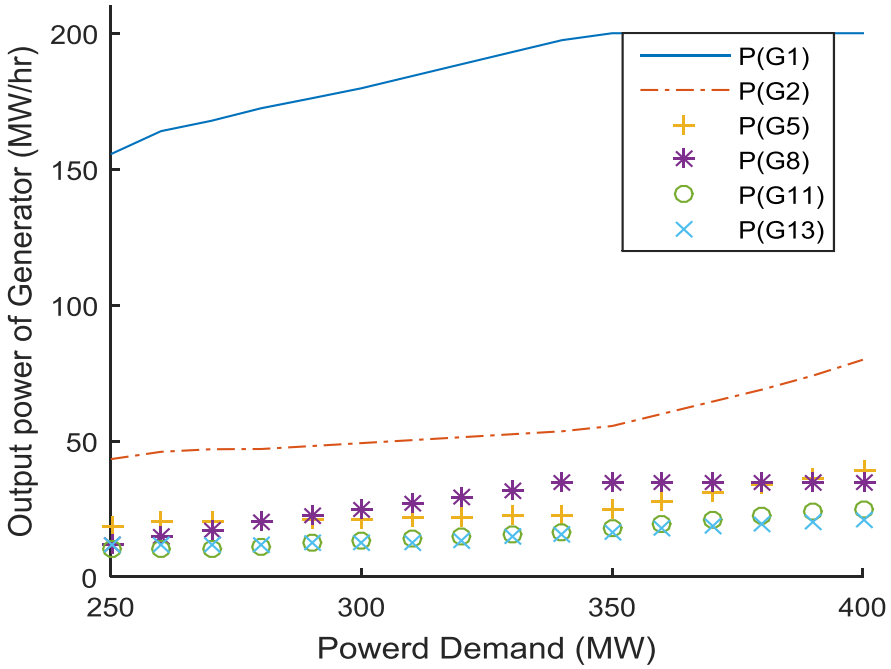

Figure 4. Relationship between all optimal output powers with power demand

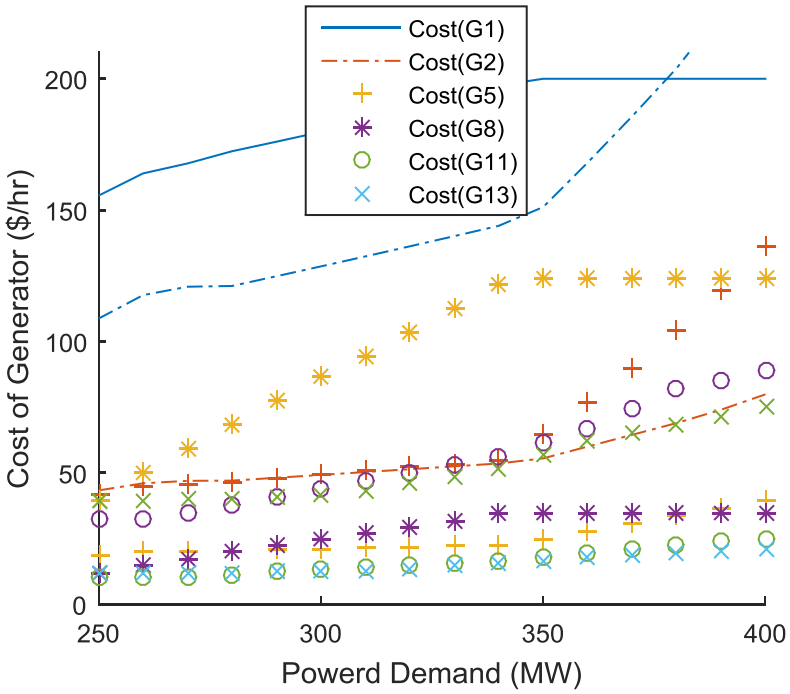

Figure 5. Relationship between all minimum costs of generators with power demand

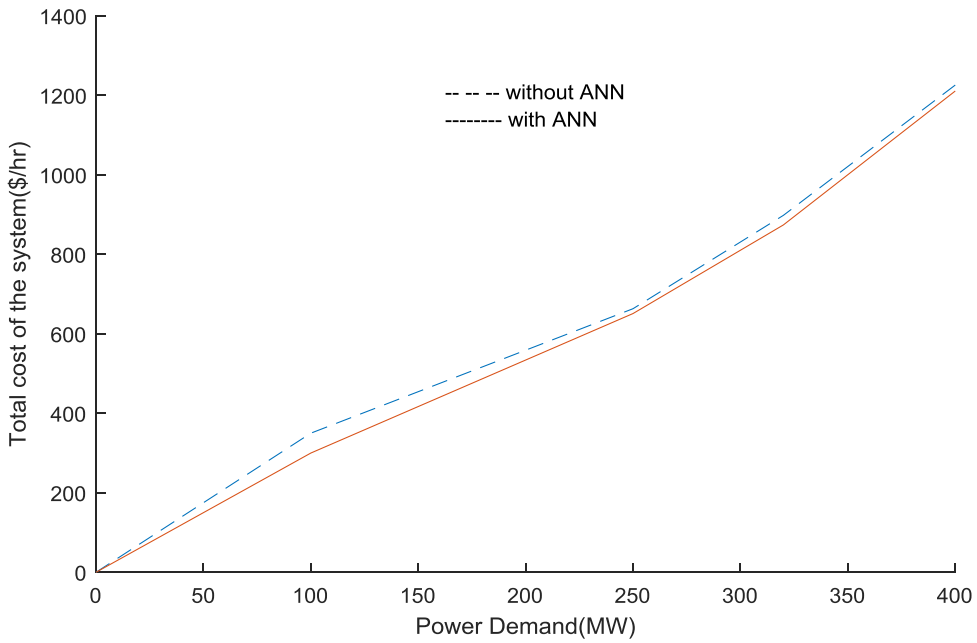

Figure 6. Relationship between minimum total costs of the system with and without ANN against power demand

7. CONCLUSIONS

The focus of this economic dispatch paper is to analysis power systems so as to get the optimal economic utility while reducing cost. The cost reduction process makes the system more efficient. The modeling and simulation process was also used to demonstrate the effectiveness of using Artificial Neural Network by Matlab software as a tool for quick, clear, accurate and explicit decision when planning the economic dispatch process as an engineering system.

This paper also focused on power demand, when power demands less than 265MW output power of at generator-11 and generator-13 should fix at minimum and for power demand greater than 350MW output power of at generator-1 and generator-8 should fix at maximum. The total cost reduce 12.6643 $/hr at 320MW power demand and also reduce to 15.2 $/hr at 400MW power demand.

Table 3: Generalized loss coefficients data for IEEE-30 bus system

$$B_{ij} = \begin{bmatrix} 0.000218 & 0.000103 & 0.000009 & -0.000010 & 0.000002 & 0.000027 \\ 0.000103 & 0.000181 & 0.000004 & -0.000015 & 0.000002 & 0.000030 \\ 0.000009 & 0.000004 & 0.000417 & -0.000131 & -0.000153 & -0.000107 \\ -0.000010 & -0.000015 & -0.000131 & 0.000221 & 0.000094 & 0.000050 \\ 0.000002 & 0.000002 & -0.000153 & 0.000094 & 0.000243 & -0.000000 \\ 0.000027 & 0.000030 & -0.000107 & 0.000050 & -0.000000 & 0.000358 \end{bmatrix}$$

$$B_{0i} = [-0.000003 \quad 0.000021 \quad -0.000056 \quad 0.000034 \quad 0.000015 \quad \mathbf{0.000078}]$$

$$B_{00} = [0.000014]$$

REFERENCES

Acha E. & Kazemtabrizi B., 2013. "A New STATCOM Model for Power Flows Using the Newton-Raphson Method". *IEEE Trans. Power Syst*., 28, 2455–2465.

Aree A. Muhammad, 2018. "Fault Location Estimation of Kurdistan Power System
using ANN". *ZANCO Journal of Pure and Applied Sciences, ZJPAS*: 2016, 28(2): s137-145.

Chai R., Zhang B., Dou J., Hao Z., & Zheng T., 2015. "Unified Power Flow Algorithm Based on the NR Method for Hybrid ACIDC Grids Incorporating VSCs". *IEEE Trans. Power Syst*., 31, 4310–4318.

Eisa Bashier M Tayeb, 2013. "Faults Detection in Power Systems Using Artificial
Neural Network", *American Journal of Engineering Research*
(AJER).Volume-02, Issue-06, pp-69-75.

Foley M., & Bose A., 1995. "Object-orientated on-line network analysis". *IEEE Trans. On Power Systems*, Vol. 10, pp.125-132.

Gomez Sanz, J. J., Garcia Rodriguez S., Cuartero Soler, N. Hernandez & Callejo L., 2014. "Reviewing Microgrids from a Multi-Agent Systems Perspective". *Energies* 2014, 7, 3355–3382.

Guo Y., Wu W., Zhang B. & Sun H., 2014. "A Fast Solution for the Lagrange Multiplier-Based Electric Power Network Parameter Error Identification Model". *Energies*, 7, 1288–1299.

Huang W. T. & Yao K. C., 2012. "New Network Sensitivity-Based Approach for Real-Time Complex Power Flow Calculation". *IET Gener. Transm. Distrib*., 6, 109–120.

Kim S., 2016. "Accuracy Enhancement of Mixed Power Flow Analysis Using a Modified DC Model". *Energies*, 9, 776.

Marlon C. & Osvaldo A., 2013. "Economic Dispatch of Energy and Reserve in Competitive Markets Using Meta-heuristic Algorithms". *IEEE Latin Am. Trans*., 11, 473–478.

Neyer A. F., F. F. Wu & K. Imhof., Aug. 1990. "Object-oriented programming for flexible software; example of a load flow". *IEEE Trans. on Power Systems*, Vol. 5, No.3.

Raygani S.V., Tahavorgar A., Fazel S. S. & Moaveni B., 2012. "Load flow analysis and future development study for an AC electric railway". IET Electr. Syst. Transp., 2, 139–147.

Soman S., Thomas P., George J. & Ganesh M., 2015. "Prevention of blackout by an effective forced islanding and restoration scheme". *In Proceedings of the International Conference on Emerging Research in Electronics, Computer Science and Technology (ICERECT)*, Mandya, India, 17–19 December 2015; pp. 298–303.

Soroudi A. & Rabiee A., 2013. "Optimal multi-area generation schedule considering renewable resources mix: A real-time approach". *IET Gener. Transm. Distrib.*, 7, 1011–1026.

Sun B., Luh P. B., Jia Q. S. & Yan B., 2015. "Event-Based Optimization within the Lagrangian Relaxation Framework for Energy Savings in HVAC Systems". *IEEE Trans. Autom*. Sci. Eng., 12, 1396–1406.

Tarik A. Rashid & Nian Kh. Aziz, 2016. "Student Academic Performance Using Artificial Intelligence". *ZANCO Journal of Pure and Applied Sciences, ZJPAS*: 2016, 28(2): 56-59.

Tommy W. S. Chow & Siu Y. Cho, 2007. "Neural Networks and Computing", *Imperial College Press.*

Zhihang Li, Wenchuan Wu & Boming Zhang, Nov 2013. "Dynamic economic dispatch using Langrangian relaxation with multiplier updates based on a Quasi Newton Method" *IEEE Transaction on power system*, Vol 28, No 4.

ZANCO Journal of Pure and Applied Sciences
The official scientific journal of Salahaddin University-Erbil
https://zancojournals.su.edu.krd/index.php/JPAS

ISSN (print):2218-0230**, ISSN (online):** 2412-3986**, DOI: http://dx.doi.org/10.21271/zjpas**

RESEARCH PAPER

The $1:-1:1$ Resonance Integrable Problem for a Cubic Lotka-Volterra Systems.

Hersh M. Saber[1], Waleed H. Aziz[2]

[1]Department of Physic, College of Education Shaqlawa, Salahaddin University-Erbil, Kurdistan Region, Iraq
[2]Department of Mathematic, College of Science, Salahaddin University-Erbil, Kurdistan Region, Iraq

A B S T R A C T:

This paper is devoted to investigate the integrability and linearizability problems around a singular point at the origin of a cubic three-dimensional Lotka-Volterra differential system with $(1:-1:1)$-resonance. A complete set of necessary conditions for both integrability and linearizability are given. For sufficiency part, we show that the system has two analytic first integrals at the origin. In particular, we use Darboux method of integrability, linearizable node and transformation technique to show that the system admits two independent first integrals.

KEY WORDS: Integrability; Linearizability; First integral; Lotka-Volterra; Darboux method.
DOI: http://dx.doi.org/10.21271/ZJPAS.31.4.11
ZJPAS (2019) , 31(4);103-113 .

INTRODUCTION :

In the past decades some works have been devoted to investigate the existence of first integrals in qualitative theory of differential systems as this subject has strongly related with various subjects in applied mathematics and physics. This paper deals with integrability and linearizability of the following three-dimensional Lotka-Volterra system of the form

$$\dot{x} = x(1 + ax + by + cz + L_1x^2 + V_1z^2) = P(x, y, z),$$

$$\dot{y} = y(-1 + dx + ey + fz + L_2x^2 + V_2z^2) = Q(x, y, z),$$

$$\dot{z} = z(1 + gx + hy + kz + L_3x^2 + V_3z^2) = R(x, y, z).$$

* **Corresponding Author:**
Hersh Mohammed Saber
E-mail: Hersh.Saber@su.edu.krd
Article History:
Received: 06/05/2018
Accepted: 10/07/2018
Published: 28/10 /2018

The classical Lotka-Volterra system is traced back of the works (Lotka, 1956, Volterra, 1931), that involved in many applications on various subjects such as biological models, neural networks, laser physics and chemical kinetic (Murza and Teruel, 2010, Noonburg, 1989), etc. In particular, authors in (Cairó, 2000, Cairó and Llibre, 2000a, Christodoulides and Damianou, 2009, Llibre and Valls, 2011b) considered integrability problems for this kind of systems and gave conditions on first integrals.

For our interest, we chose the eigenvalues to be 1, -1 and 1, so one can obtain two independent resonance and in this case the origin is in the Siegel domain, that is the convex hull of the eigenvalues with the origin located inside itself or on its boundary.

For two dimensional quadratic Lotka-Volterra systems

$$\dot{x} = x(\lambda + ax + by), \quad \dot{y} = y(\mu + cx + dy),$$

where $\lambda, \mu \in \mathbb{Z}$, $\lambda\mu < 0$. Some works have been devoted to investigate this problem for

instance (Christopher et al., 2004, Gravel and Thibault, 2002, Liu et al., 2004). For more general quadratic systems the authors in (Christopher et al., 2003, Fronville et al., 1998, Żołądek, 1997), characterize the existence of a local analytic first integral by using a simple generalization of the Poincaré center-focus problem and necessary conditions were given. Where $\lambda + \mu = 0$, the system have a complexified version of the classical center-focus problem. Other works for $(p: -q)$-resonance on integrability and linearizability of Lotka-Volterra systems were considered in (Chen et al., 2012, Giné et al., 2011, Giné and Romanovski, 2009, Giné and Romanovski, 2010, Hu et al., 2008, Romanovski and Shafer, 2008, Wang and Liu, 2008).

Whereas, for cubic systems integrability and linearizability for some families of systems are studied in (Chavarriga and Giné, 1998, Fercec et al., 2011, Han et al., 2016, Malkin, 1964), despite these authors, others have thought and attempted for working on three dimensional systems to give necessary and sufficient conditions for both integrability and linearizability for instance (Cairó and Llibre, 2000a, Cairó, 2000, Hu et al., 2013).

Recently (Aziz, 2014, Aziz and Christopher, 2012) investigated local integrability and linearizability of a quadratic three-dimensional Lotka-Volterra and a particular case in a general quadratic three-dimensional differential systems.

In this paper, we generalize the work in (Aziz and Christopher, 2012) by considering three-dimensional cubic Lotka-Volterra differential systems and give necessary and sufficient conditions for integrability and linearizability at the origin.

1. PRELIMINARY

In this section, we give a brief review of some definitions and known results. Consider the cubic three dimensional Lotka-Volterra system

$$\begin{aligned}\dot{x} &= x(1 + ax + by + cz + L_1x^2 + V_1z^2) = P(x, y, z),\\ \dot{y} &= y(-1 + dx + ey + fz + L_2x^2 + V_2z^2) = Q(x, y, z),\\ \dot{z} &= z(1 + gx + hy + kz + L_3x^2 + V_3z^2) = R(x, y, z).\end{aligned} \quad (1)$$

The associate vector field of system (1) is denoted by

$$\mathcal{X} = P(x, y, z)\frac{\partial}{\partial x} + Q(x, y, z)\frac{\partial}{\partial y} + R(x, y, z)\frac{\partial}{\partial z}. \quad (2)$$

Definition 1.

We say that system (1) is *integrable* at the origin if and only if there is a change of coordinates

$$(X, Y, Z) = \big(x + o(x, y, z), y + o(x, y, z), z + o(x, y, z)\big),$$

which transform system (1) into

$$\begin{aligned}\dot{X} &= X\zeta(X, Y, Z),\\ \dot{Y} &= -Y\zeta(X, Y, Z),\\ \dot{Z} &= Z\zeta(X, Y, Z),\end{aligned}$$

where $\zeta = 1 + o(X, Y, Z)$. Then XY and YZ are first integrals of system (1).

Definition 2.

System (1) is linearizable at the origin if and only if there is a change of coordinates

$$(\mathrm{X}, \mathrm{Y}, \mathrm{Z}) = \big(\mathrm{x} + \mathrm{o}(\mathrm{x}, \mathrm{y}, \mathrm{z}), \mathrm{y} + \mathrm{o}(\mathrm{x}, \mathrm{y}, \mathrm{z}), \mathrm{z} + \mathrm{o}(\mathrm{x}, \mathrm{y}, \mathrm{z})\big),$$

which transform system (1) into

$$\begin{aligned}\dot{\mathrm{X}} &= \mathrm{X},\\ \dot{\mathrm{Y}} &= -\mathrm{Y},\\ \dot{\mathrm{Z}} &= \mathrm{Z}.\end{aligned}$$

Definition 3.

A non-constant function $\Psi(\mathrm{x}, \mathrm{y}, \mathrm{z})$ of the differential system (1) is said to be a first integral, if it is constant for all its solutions. This means that, $\Psi(\mathrm{x}, \mathrm{y}, \mathrm{z})$ is first integral if and only if satisfy the following partial differential equation

$$\mathcal{X}\Psi = \mathrm{P}\frac{\partial \Psi}{\partial \mathrm{x}} + \mathrm{Q}\frac{\partial \Psi}{\partial \mathrm{y}} + \mathrm{R}\frac{\partial \Psi}{\partial \mathrm{z}} = 0.$$

Definition 4.

A non-zero function M is said to be an inverse jacobi multiplier for system (1) if satisfies the equation

$$\mathcal{X}(\mathrm{M}) = \mathrm{M}\,\mathrm{div}(\mathcal{X}).$$

Note that, if we have one first integral, Φ and an inverse jacobi multiplier, we can find another first integral.

Theorem 1. (Aziz and Christopher, 2012)

Suppose that the analytic vector field

$$\mathrm{x}\left(\lambda + \sum_{|\mathrm{I}|>0} \mathrm{A}_{\mathrm{xI}}\mathrm{X}^{\mathrm{I}}\right)\frac{\partial}{\partial \mathrm{x}} + \mathrm{y}\left(\mu + \sum_{|\mathrm{I}|>0} \mathrm{A}_{\mathrm{yI}}\mathrm{X}^{\mathrm{I}}\right)\frac{\partial}{\partial \mathrm{y}} + \mathrm{z}\left(\nu + \sum_{|\mathrm{I}|>0} \mathrm{A}_{\mathrm{zI}}\mathrm{X}^{\mathrm{I}}\right)\frac{\partial}{\partial \mathrm{z}} = 0,$$

has a first integral $\Phi = \mathrm{x}^{\alpha}\mathrm{y}^{\beta}\mathrm{z}^{\gamma}(1 + \mathrm{o}(\mathrm{x}, \mathrm{y}, \mathrm{z}))$, with at least one of $\alpha, \beta, \gamma \neq 0$, and an inverse jacobi multiplier $\mathrm{M} = \mathrm{x}^{\mathrm{r}}\mathrm{y}^{\mathrm{s}}\mathrm{z}^{\mathrm{t}}\big(1 + \mathrm{o}(\mathrm{x}, \mathrm{y}, \mathrm{z})\big)$, and suppose that the cross product of $(\mathrm{r} - \mathrm{i} - 1, \mathrm{s} - \mathrm{j} - 1, \mathrm{t} - \mathrm{k} - 1)$, and (α, β, γ), is bounded away from zero for any integer $\mathrm{i}, \mathrm{j}, \mathrm{k} \geq 0$. then $\mathcal{X}$ has a second analytic first integral of the form $\Psi =$

$x^{1-r}y^{1-s}z^{1-t}(1+o(x,y,z))$. Hence system (1) is integrable.

Theorem 2. (Aziz and Christopher, 2012)

If system (1) is integrable and there is a function $\zeta = x^{\alpha}y^{\beta}z^{\gamma}(1+o(x,y,z))$, such that $\mathcal{X}(\zeta) = k\zeta$, for some constant $k = \alpha - \beta + \gamma$, then the system is linearizable.

2. REDUCTION TO THE POINCARÉ DOMAIN (Aziz and Christopher, 2012)

A singular point whose eigenvalues lie in the Poincaré domain (that is, the convex hull of the eigenvalues does not contain the origin) can be brought to normal form via an analytic change of coordinates. In particular, a node with two analytic separatrices can have no resonant terms in its normal form and so must be analytically linearizable.

3. DARBOUX METHOD FOR INTEGRABILITY

Darboux method is a method that can be used to contract first integrals and inverse Jacobi multipliers for planar and higher differential systems if the system possess an adequate number of invariant algebraic curves (surfaces) and exponential factors. In this sense, the first integrals and inverse Jacobi multipliers can express as a product of these curves (surfaces) with exponential factors.

Definition 6.

Let a polynomial $F \in \mathbb{C}[x,y,z]$. If the algebric surface $F = 0$, is invariant by a vector field $\mathcal{X}$, then C_F is a polynomial of degree at most 2. In this case we say that $F = 0$ is invariant algebric surface of $\mathcal{X}$ and C_F is its cofactor. This means that

$$\dot{F} = \mathcal{X}F = P\frac{\partial F}{\partial x} + Q\frac{\partial F}{\partial y} + R\frac{\partial F}{\partial z} = C_F F,$$

for some polynomial $C_F \in \mathbb{C}[x,y,z]$.

Definition 7.

An exponential function E of the form $E(x,y,z) = \exp(f(x,y,z)/g(x,y,z))$, where $f,g \in \mathbb{C}[x,y,z]$, is called exponential factor if satisfy the following equation

$$\mathcal{X}E = C_E E,$$

where C_E is a cofactor of E and has one degree less than the vector field (2).

Definition 8.

A Darboux function is a function of the form

$$D = E\prod F_i^{\lambda_i},$$

where the F_i are invariant algebraic surfaces of the system, and $E = \exp(f/g)$, is an exponential factor.

Theorem 3. (Darboux Theorem) (Christopher and Li, 2007)

Assume a three dimensional system of degree m that has p distinct invariant algebraic surfaces $f_i = 0$ for $i = 1,\dots,p$, with cofactor C_{f_i} and q independent exponential factors E_j for $j = 1,\dots,q$, with cofactors C_{E_j}, then the following satisfies:

1. The function
$$IJM = f_1^{\lambda_1}\dots f_p^{\lambda_p}E_1^{\mu_1}\dots E_q^{\mu_q},$$
is an inverse jacobi multiplier provided that the condition
$$\sum_{i=1}^{p}\lambda_i C_{f_i} + \sum_{j=1}^{q}\mu_j C_{E_j} = \mathrm{div}\mathcal{X},$$
is satisfies for certain complex numbers $\lambda_i, i = 1,\dots,p$, and $\mu_j, j = 1,\dots,q$,
2. There exists $\lambda_i, \mu_j \in \mathbb{C}$ not all zero such that
$$\sum_{i=1}^{p}\lambda_i C_{f_i} + \sum_{j=1}^{q}\mu_j C_{E_j} = 0,$$
if and only if the (multi-valued) function
$$\Phi = f_1^{\lambda_1}\dots f_p^{\lambda_p}E_1^{\mu_1}\dots E_q^{\mu_q},$$
is a first integral of the vector field $\mathcal{X}$.

4. MECHANISMS FOR INTEGRABILITY AND LINEARIZABLITY

In this section, we present the mechanism that will be used for finding the integrability conditions for system (1).

Let H_1 and H_2 be two independent first integrals of the form

$$H_1 = xy\big(1+o(x,y,z)\big),$$

and

$$H_2 = yz\big(1+o(x,y,z)\big),$$

such that

$$\dot{H}_1 = \sum_{n_1,n_2\geq 0}\xi_{n_1,n_2}x^{n_1}y^{n_1+n_2}z^{n_2},$$

$$\dot{H}_2 = \sum_{n_1,n_2\geq 0}\kappa_{n_1,n_2}x^{n_1}y^{n_1+n_2}z^{n_2},$$

The coefficients ξ_{n_1,n_2} and κ_{n_1,n_2} are polynomials in parameters of (1) and they also are the obstruction of the existence of such first integrals H_1 and H_2. We denote by $I = \langle \xi_{n_1,n_2}, \kappa_{n_1,n_2}\rangle$ the ideal generated by such polynomials ξ_{n_1,n_2} and

κ_{n_1,n_2} and its varaiety by V(I). Moreover, we calculate such polynomials to a given degree using Maple. The degree have been used 16.

Hence we calculate the irreducible decomposition of the variety V by computing a factorized Gröbner basis using the Routine mianAssGTZ in Singular (Decker et al., 2011, Greuel et al., 2012). In particular the conditions on parameters that make ξ_{n_1,n_2} and κ_{n_1,n_2} vanish. This will be correspond to nesessary and sufficient conditions for integrability of (1) at the origin.

5. INTEGRABILITY AND LINEARIZABILITY CONDITIONS

The Lotka-Volterra system (1) has a property that $x = 0, y = 0, z = 0,$ are always invariant algebraic surfaces with respective cofactors

$$L_x = 1 + ax + by + cz + L_1x^2 + V_1z^2,$$
$$L_y = -1 + dx + ey + fz + L_2x^2 + V_2z^2,$$
$$L_z = 1 + gx + hy + kz + L_3x^2 + V_3z^2.$$

5.1 The $(1:-1:1)$ −Resonance

In this case, we are looking for two independent analytic first integrals

$$H_1 = xy(1 + O(x, y, z)),$$

and

$$H_2 = yz\big(1 + O(x, y, z)\big).$$

For finding resonant terms we written H_1 and H_2 as power series of order 16 then we point out the obstruction terms for the existences of two analytic first integrals, we denote them by $\xi_{n,n}$ and $\kappa_{n,n}$ for $n = 1, \dots, 5$ then

$$\chi(H_1) = P\frac{\partial H_1}{\partial x} + Q\frac{\partial H_1}{\partial y} + \mathrm{R}\frac{\partial H_1}{\partial z} = \sum_{\substack{j=2,3 \\ i=0,\dots,j}} \xi_{n,n}x^{j-i}y^jz^i, \quad n = 1, \dots, 5,$$

and

$$\chi(H_2) = P\frac{\partial H_2}{\partial x} + \mathrm{Q}\frac{\partial H_2}{\partial y} + \mathrm{R}\frac{\partial H_2}{\partial z} = \sum_{\substack{j=2,3 \\ i=0,\dots,j}} \kappa_{n,n}x^{j-i}y^jz^i, \quad n = 1, \dots, 5,$$

The expressions for $\xi_{n,n}$ and $\kappa_{n,n}$ for $n = 1, \dots, 5$ are presented and will no present the others as the size of these polynomial dramatically increases.

$\xi_{1,1} = ab - ed.$

$\xi_{2,2} = bf - hf - hc + ef.$

$\xi_{3,3} = -8a^2b^2 - 6a^2be - 9ab^2d + 6ade^2 + 9bd^2e + 8d^2e^2 + 2b^2L_1 + beL_1 - beL_2$

$\xi_{4,4} = 2b^2cf + 4b^2f^2 + b^2fk - 2bc^2h + 6bcef - 4bcfh - 2bchk + 12bef^2 + 3befk - 2bf^2h - 2bfhk - 3c^2eh - 2c^2h^2 + 4ce^2f - 6cefh - 3cehk - 4cfh^2 - 2ch^2k + 8e^2f^2 + 2e^2fk - 3ef^2h - 3efhk - 2f^2h^2 - 2fh^2k - 2bhV_2 + ehV_1 - ehV_2 + 2h^2V_1 + 2h^2V_2.$

$\xi_{5,5} = -9ab^2c - 2ab^2f - 9abce - 12abch + 6abef - 8abfh - 9aceh - 3ach^2 + 8ae^2f - 6aefh - 2afh^2 - 3b^2cd - 3b^2cg + 10b^2df - b^2fg + 9bcde - 12bcdh - 3bceg - 4bcgh + 42bdef - 8bdfh + 3befg - 4bfgh + 12cde^2 - 9cdeh - 3cdh^2 - 3cegh - cgh^2 + 32de^2f - 6defh - 2dfh^2 + 4e^2fg - 3efgh - fgh^2.$

$\kappa_{1,1} = ef - hk.$

$\kappa_{2,2} = -bd - bg + de + dh.$

$\kappa_{3,3} = 8e^2f^2 + 6e^2fk + 9ef^2h - 6ehk^2 - 9fh^2k - 8h^2k^2 - ehV_2 + ehV_3 + 2h^2V_3$

$\kappa_{4,4} = -2ab^2d - 2ab^2g - 3abde - 2abdh - 3abeg - 2abgh + 2ade^2 + 3adeh + adh^2 - 2b^2d^2 - 4b^2dg - 2b^2g^2 - 3bd^2e - 2bd^2h - 6bdeg - 4bdgh - 3beg^2 - 2bg^2h + 8d^2e^2 + 12d^2eh + 4d^2h^2 + 4de^2g + 6degh + 2dgh^2 + 2b^2L_2 + 2b^2L_3 - beL_2 + beL_3 - 2bhL_2.$

$\kappa_{5,5} = -b^2cd - b^2cg - 2b^2df - 2b^2dk - 3b^2fg - 3b^2gk - 3bcde - 4bcdh - 3bceg - 4bcgh - 6bdef - 6bdek - 8bdfh - 8bdhk - 9befg - 9begk - 12bfgh - 12bghk + 4cde^2 + 3cdeh - cdh^2 - 3cegh - 3cgh^2 + 32de^2f + 8de^2k + 42defh + 6dehk + 10dfh^2 - 2dh^2k + 12e^2fg + 9efgh - 9eghk - 3fgh^2 - 9gh^2k.$

The integrabilty conditions then can be summarized in the theorem below.

Theorem 4.

System (1) is integrable at the origin with $(1:-1:1)$-resonance if and only if one of the following conditions:

1) $b = e = h = 0.$

2) $b = d = f = h = 0.$

3) $a = d = f = g = h = L_1 = L_2 = L_3 = 0.$

3*) $b = c = d = f = k = V_1 = V_2 = V_3 = 0.$

4) $a = 2b + e = d = f = g = h = L_2 = 0.$

4*) $b = c = d = e + 2h = f = k = V_2 = 0.$

5)$a = 2b - e = d = f = g = h = 2L_1 - L_2 = L_3 = 0.$

5*)$b = c = d = e - 2h = f = k = V_1 = V_2 - 2V_3 = 0.$

6)$a - d = b - e = f = g = h = L_1 = L_2 = L_3 = 0.$

6*)$b = c = d = e - h = f - k = V_1 = V_2 = V_3 = 0.$

7)$2a-g=b+e=c=2d+g=f=h=3L_1-L_3=3L_2+L_3=0$.
7*)$b=c-2k=d=e+h=f+k=g=V_1-3V_3=V_2+V_3=0$.
8)$a=2b+e=c=d=f=g=k=L_2=V_1=V_2=V_3=0$.
8*)$a-2d-2g=c=d=e+2h=f=g=k=L_1=L_2=L_3=V_2=0$.
9) $a=2b+h=2c+k=d=e-h=f-k=g=L_2=V_1=V_2=V_3=0$.
9*)$a-2d-2g=c=e+2h=f=k=l1=l2=l3=v2=b+2h=d+2g=0$.
10)$a=b-h=c=d=e+2h=f=g=k=L_2=V_2=0$.
11)$a=b+h=c=d=e+2h=f=g=k=L_1+L_3=L_2+2L_3=V_2=0$.
11*)$a=b+h=c=d=e-2h=f=g=k=L_2=V_1+V_3=V_2-2V_3=0$.
12)$ab-de=ef-hk=ac-2ak+gk=ae+ah-de-eg=af+ak-dk-gk=bk-ce+ek-hk=bf-ch-fh+hk=bd+bg-de-dh=cd+cg-2dk+fg-gk=4bL_1-eL_2+eL_3-hL_1=2aL_1+2aL_3-4gL_1=aV_1-3aV_3+2gV_3=4cL_1-6kL_1+2kL_3=2cV_3-kV_1-kV_3=eV_2-eV_3-2hV_3=2fV_3-kV_2+kV_3=2L_1V_1-4L_1V_3+2L_3V_3=aL_2+aL_3+2dL_3-2gL_2=aV_2+aV_3-2dV_3-2gV_3=2bV_3-eV_1+eV_3-2hV_3=cV_2-cV_3-fV_1-fV_3=dL_1+dL_3+gL_1-gL_2=2eL_1-eL_2-eL_3+2hL_1=2fL_1+2kL_1-kL_2-kL_3=L_1V_2+L_1V_3-L_2V_3-L_3V_3=2bL_2+2bL_3-eL_2+eL_3-2hL_2=bV_2-bV_3-hV_1-hV_2+2hV_3=2cL_2+2cL_3+2fL_3-3kL_2-kL_3=dV_1-3dV_3+gV_1+gV_2-2gV_3=L_2V_1-2L_2V_3+L_3V_1+L_3V_2-L_3V_3=dL_2V_3+dL_3V_2+2dL_3V_3-gL_2V_2+gL_3V_3=deL_2+3deL_3+2dhL_3-egL_2+egL_3-2ghL_2=2dfL_3+dkL_2+3dkL_3-2fgL_2-gkL_2+gkL_3=0$.
Furthermore, the origin of system (1) is linearizable if and only if it satisfies one of the conditions ((1) − (11) except condition (7)) or one of the following holds:
12.1) $a=2b-e=c=d=f=g=k=2L_1-L_2=V_1=V_2=V_3=eL_3-hL_2=0$.
12.1*)$a=c=d=e-2h=f=g=k=L_1=L_2=L_3==V_2-2V_3=bV_3-hV_1=0$.
12.2)$a=2b-h=2c-k=d=e-h=f-k=g=2L_1-L_3=L_2-L_3=V_1=V_2=V_3=0$.
12.2*)$a-2g=b-2h=c=d-2g=e-2h=f=k=L_1=L_2=L_3=V_1-2V_3=V_2-2V_3=0$.
12.3)$a=b-h=c=d=e-2h=f=g=k=L_1-L_3=L_2-2L_3=V_1-V_3=V_2-2V_3=0$.

Proof:

Since 3*, 4* ,5*, 6*, 7*, 8*, 9*, 11*, 12.1* and 12.2* are dual with 3, 4, 5, 6, 7, 8, 9, 11 ,12.1 and 12.2 respectively under the transformation $(x,y,z)\to(z,y,x)$, then we do not consider them separately. Then other cases are considered below

Case 1. In this case we have

$$\dot{x}=x(1+ax+cz+L_1x^2+V_1z^2),$$
$$\dot{y}=y(-1+dx+fz+L_2x^2+V_2z^2),$$
$$\dot{z}=z(1+gx+kz+L_3x^2+V_3z^2).$$

The subsystem

$$\dot{x}=x(1+ax+cz+L_1x^2+V_1z^2),$$
$$\dot{z}=z(1+gx+kz+L_3x^2+V_3z^2),$$

is independent in y, then they are linearizable node the linearizing changing is given

$$X=x\big(1+O(x,z)\big),\ \text{and}\ Z=z(1+O(x,z)),$$

such that

$$\dot{X}=X,\quad \dot{Z}=Z.$$

The second equation can be written by

$$\dot{y}=y\big(-1+dx(X,Z)+fz(X,Z)+L_2x^2(X,Z)+V_2z^2(X,Z)\big).$$

We seek a function $\ell(X,Z)$ such that

$$\dot{\ell}(X,Z)=\big(dx(X,Z)+fz(X,Z)+L_2x^2(X,Z)+V_2z^2(X,Z)\big). \quad (3)$$

Then the transformation $Y=ye^{-\ell}$, can linearize equation (3) and gives $\dot{Y}=-Y$.

Writing

$$\ell(X,Z)=\sum_{i+j>0} b_{i,j}X^iZ^j,$$

$$\dot{\ell}(X,Z)=\frac{\partial\ell(\mathrm{X},\mathrm{Z})}{\partial\mathrm{X}}+\frac{\partial\ell(X,Z)}{\partial Z}$$

$$\dot{\ell}(X,Z)=\sum_{i+j>0} i\,b_{i,j}X^{i-1}\,\dot{X}\,Z^j+\sum_{i+j>0} j\,b_{i,j}X^i\,Z^{j-1}\,\dot{Z},$$

$$\dot{\ell}(X,Z)=\sum_{i+j>0} i\,b_{i,j}X^i\,Z^j+\sum_{i+j>0} j\,b_{i,j}X^i\,Z^j,$$

Since

$$\dot{\ell}(X,Z)=\big(dx(X,Z)+fz(X,Z)+L_2x^2(X,Z)+V_2z^2(X,Z)\big),$$

Then

$$\dot{\ell}(X,Z) = \sum_{i+j>0} (i+j) b_{i,j} X^i Z^j$$
$$= \big(dx(X,Z) + fz(X,Z) + L_2 x^2(X,Z) + V_2 z^2(X,Z)\big)$$
$$= \sum_{i+j>0} a_{i,j} X^i Z^j.$$

Then there is no obstruction of the existence of ℓ. Hence the required first integrals are

$$H_1 = xy(1 + O(x,y,z)),$$

and

$$H_2 = zy\big(1 + O(x,y,z)\big).$$

Case 2. System (1), reduce to

$$\dot{x} = x(1 + ax + cz + L_1 x^2 + V_1 z^2),$$
$$\dot{y} = y(-1 + ey + L_2 x^2 + V_2 z^2),$$
$$\dot{z} = z(1 + gx + kz + L_3 x^2 + V_3 z^2).$$

First and third equations give a linearizable node. Hence the changing the coordinates

$$X = x\big(1 + O(x,z)\big), \text{ and } Z = z(1 + O(x,z)),$$

gives

$$\dot{X} = X, \quad \dot{Z} = Z.$$

The second equation can be linearized if we can find an invariant algebraic surface of the form $\ell + \xi y = 0$ with cofactor $ey + L_2 x^2 + V_2 z^2$ where $\ell = \ell(X,Z)$, $\xi = \xi(X,Z)$, and $\ell(0) = 1$. The transformation $Y = \frac{y}{\ell + \xi y}$, will linearize the second equation.

The differentiation of $\ell + \xi y = 0$, gives $\dot{\xi} y - \xi y = \ell(ey + L_2 x^2 + V_2 z^2) - \dot{\ell}$.

To show that there is no obstruction for existence ℓ and ξ, we solve the following differential equations

$$\dot{\xi} - \xi = e\ell, \tag{4}$$
$$\dot{\ell} = \ell(L_2 x^2 + V_2 z^2), \tag{5}$$

Suppose

$$\ell = \textstyle\sum_{i+j>0} b_{i,j} X^i Z^j,\ \xi = \sum_{i+j>0} a_{i,j} X^i Z^j\ , \tag{6}$$

and by substitution (6) in (4) we get that

$$\sum_{i+j>0} (2i + j - 1) a_{i,j} X^i Z^j = \sum_{i+j>0} e b_{i,j} X^i Z^j,$$
$$\sum_{i+j>0} a_{i,j} X^i Z^j = \sum_{i+j>0} \frac{e}{2i + j - 1} b_{i,j} X^i Z^j,$$
$$\xi = \textstyle\sum_{i+j>0} \frac{e}{2i+j-1} b_{i,j} X^i Z^j.$$

Thus, equation (4) has a solution as long as $2i + j - 1 \neq 0$. If $2i + j - 1 = 0$ then $2i + j = 1$ as we know that indexes must be $\mathbb{Z}^+ \cup \{0\}$, this means that only solution of the equation is $i = 0$ and $j = 1$. So to prevent that will not happen it must be the value of $b_{0,1} = 0$ (that means, that ℓ contains no terms of Z).

$\ell = e^{\psi}$ and solve $\dot{\psi} = L_2 x^2 + V_2 z^2$. So if we let $\psi = \sum_{i+j>0} c_{i,j} X^i Z^j$, then

$$\dot{\psi} = \sum_{i+j>0} i c_{i,j} X^{i-1} \dot{X}\, Z^j + j c_{i,j} X^i Z^{j-1} \dot{Z},$$
$$\dot{\psi} = \sum_{i+j>0} (i+j) c_{i,j} X^i Z^j$$
$$= L_2 x^2(X,Z) + V_2 z^2(X,Z).$$

Suppose that $x^2(X,Z) = \sum_{i+j>0} d_{i,j} X^i Z^j$ and $z^2(X,Z) = \sum_{i+j>0} k_{i,j} X^i Z^j$. Thus, we can calculate the value of ψ by the following

$$c_{1,0} = L_2 d_{1,0} + V_2 k_{1,0},$$
$$c_{0,1} = 0,$$

because ℓ contains no terms of Z.

Thus,

$$\psi = (L_2 d_{1,0} + V_2 k_{1,0}) X + \textstyle\sum_{i+j>1} \frac{d_{i,j}}{2i+j} X^i Z^j.$$

Hence

$$\ell = 1 + (L_2 d_{1,0} + V_2 k_{1,0}) X + O(2).$$

Case 3. System (1) can be written as

$$\dot{x} = x(1 + by + cz + V_1 z^2),$$
$$\dot{y} = y(-1 + ey + V_2 z^2),$$
$$\dot{z} = z(1 + kz + V_3 z^2).$$

In this case we have invariant algebraic surfaces $\ell_{1,2} = 1 + \left(\frac{1}{2}k \pm \frac{1}{2}\sqrt{k^2 - 4V_3}\right) z = 0$ with cofactors $L_{\ell_{1,2}} = (\frac{1}{2}k \pm \frac{1}{2}\sqrt{k^2 - 4V_3})\mathrm{z} + V_3 z^2$. This allow us to find a first integrals and inverse jacobi multiplier of the forms

$$\Phi = x^{-\frac{e}{b}} y z^{1+\frac{e}{b}} \ell_1^{\eta_1} \ell_2^{\theta_1},$$

and

$$IJM = x^{1+\frac{e}{b}} y z^{1-\frac{e}{b}} \ell_1^{\eta_2} \ell_2^{\theta_2},$$

where $\eta_1 = \frac{1}{2}\left(\frac{1}{\sqrt{k^2-4v3}\ bv3}\right)\Big(\big((-b-e)v3 - v2b + v1e\big)\sqrt{k^2-4v3} + \Big(-kb + 2e\Big(c - \frac{1}{2}k\Big)v3 + k(bv2 - ev1)\Big)\Big)$,

$\theta_1 = -\frac{1}{2}\left(\frac{1}{\sqrt{k^2-4v3}\ bv3}\right)\Big(\big((b+e)v3 + v2b - v1e\big)\sqrt{k^2-4v3} + \Big(-kb + 2e\Big(c - \frac{1}{2}k\Big)v3 + k(bv2 - ev1)\Big)\Big)$, $\eta_2 = \left(\frac{1}{\sqrt{k^2-4v3}\ bv3}\right)\Big(\Big(\big(b + \frac{1}{2}e\big)v3 - \frac{1}{2}ev1\Big)\sqrt{k^2-4v3} - e\Big(\Big(c - \frac{1}{2}k\Big)v3 -$

$\frac{1}{2}kv1\Big)\Big)$, $\theta_2 = \Big(\frac{1}{\sqrt{k^2-4v3}\ bv3}\Big)\Big(\Big(\Big(b+\frac{1}{2}e\Big)v3 - \frac{1}{2}ev1\Big)\sqrt{k^2-4v3} + e\Big(\Big(c-\frac{1}{2}k\Big)v3 - \frac{1}{2}kv1\Big)\Big)$.

By Theorem 1 we can find the second first integral of the form

$$\Psi = x^{-\frac{e}{b}}z^{\frac{e}{b}}\big(1+O(x,y,z)\big).$$

Thus, first integrals of the required form are

$$H_1 = \Phi\Psi^{-1-\frac{b}{e}} = xy(1+\cdots),$$

and

$$H_2 = \Phi\Psi^{-1} = yz(1+\cdots).$$

Since $\zeta = z(\ell_2)^{\frac{2(V_3z+k)}{-2V_3z-k+\sqrt{k^2-4V_3}}}$ satisfies $\dot{\zeta} = \zeta$, then the system must be linearizable by Theorem 2.

Case 4. This case gives

$$\dot{x} = x(1+by+cz+L_1x^2+V_1z^2),$$
$$\dot{y} = y(-1-2by+V_2z^2),$$
$$\dot{z} = z(1+kz+L_3x^2+V_3z^2).$$

The change of coordinates $(X,Y,Z) = (x^2, x^2y, z)$, the system becomes

$$\dot{X} = 2X+2bY+2cXZ+2L_1X^2+2V_1XZ^2,$$
$$\dot{Y} = Y(1+2cZ+2L_1X+2V_1Z^2+V_2Z^2),$$
$$\dot{Z} = Z(1+kZ+L_3X+V_3Z^2).$$

The origin is in the poincaré domain then by Dulac-poincaré Theorem there is a change of the coordinates to

$$(\tilde{X},\tilde{Y},\tilde{Z}) = (X-2bY+O(2), Y(1+O(1)), Z(1+O(1))),$$

that linearize the equations. Two independent first integrals of the linear system pull back first integrals to the original variables $\Psi = \tilde{X}^{-\frac{1}{2}}\tilde{Y} = (x^2)^{-\frac{1}{2}}x^2y(1+O(1)) = xy(1+O(1))$ and $\Phi = \tilde{X}^{-1}\tilde{Y}\tilde{Z} = (x^2)^{-1}x^2y\,z\big(1+O(1)\big) = yz(1+O(1))$, hence first integrals of required form are

$H_1 = xy\big(1+O(1)\big)$ and $H_2 = yz\big(1+O(1)\big)$.

Case 5. We obtain the system

$$\dot{x} = x(1+by+cz+L_1x^2+V_1z^2),$$
$$\dot{y} = y(-1+2by+2L_1x^2+V_2z^2),$$
$$\dot{z} = z(1+kz+V_3z^2).$$

Note that $\ell_{1,2} = 1+\Big(\frac{1}{2}k \pm \frac{1}{2}\sqrt{k^2-4V_3}\Big)z = 0$, are invariant algebric surfaces with respective cofactors $L_{\ell_{1,2}} = (\frac{1}{2}k \pm \frac{1}{2}\sqrt{k^2-4V_3})\mathrm{z} + V_3z^2$, that gives

$$\Phi = x^{-\frac{2}{3}}y^{\frac{1}{3}}z\ell_1^{\eta_1}\ell_2^{\theta_1},$$

and

$$IJM = x^{\frac{5}{3}}y^{\frac{5}{3}}z\ell_1^{\eta_2}\ell_2^{\theta_2},$$

where $\eta_1 = \frac{1}{3}\Big(\frac{1}{\sqrt{k^2-4v3}\ v3}\Big)\Big(\Big(-\frac{3}{2}\sqrt{k^2-4v3}+2c-\frac{3}{2}k\Big)v3+\Big(v1-\frac{1}{2}v2\Big)\big(\sqrt{k^2-4v3}-k\big)\Big)$, $\theta_1 = \frac{1}{3}\Big(\frac{1}{\sqrt{k^2-4v3}\ v3}\Big)\Big(\Big(-\frac{3}{2}\sqrt{k^2-4v3}-2c+\frac{3}{2}k\Big)v3+\Big(v1-\frac{1}{2}v2\Big)\big(\sqrt{k^2-4v3}+k\big)\Big)$, $\eta_2 = -\frac{1}{3}\Big(\frac{1}{\sqrt{k^2-4v3}\ v3}\Big)\Big((-3\sqrt{k^2-4v3}+2c)v3+(v1+v2)\big(\sqrt{k^2-4v3}-k\big)\Big)$, $\theta_2 = -\frac{1}{3}\Big(\frac{1}{\sqrt{k^2-4v3}\ v3}\Big)\Big((-3\sqrt{k^2-4v3}-2c)v3+(v1+v2)\big(\sqrt{k^2-4v3}+k\big)\Big)$.

Theorem 1, guarantee that there is another first integral of the form

$$\Psi = x^{-\frac{2}{3}}y^{-\frac{2}{3}}\big(1+O(x,y,z)\big).$$

Then, the required first integrals are

$$H_1 = \Psi^{-\frac{3}{2}} = xy(1+\cdots),$$

and

$$H_2 = \Phi\Psi^{-1} = yz(1+\cdots).$$

Since $\zeta = z(\ell_2)^{\frac{2(V_3z+k)}{-2V_3z-k+\sqrt{k^2-4V_3}}}$ satisfies $\dot{\zeta} = \zeta$, then the system must be linearizable by Theorem 2.

Case 6. The corresponding system of (1) is

$$\dot{x} = x(1+ax+by+cz+V_1z^2),$$
$$\dot{y} = y(-1+ax+by+V_2z^2),$$
$$\dot{z} = z(1+kz+V_3z^2).$$

There are two invariant algebraic surfaces of the forms $\ell_{1,2} = 1+\Big(\frac{1}{2}k \pm \frac{1}{2}\sqrt{k^2-4V_3}\Big)z = 0$ with cofactors $L_{\ell_{1,2}} = (\frac{1}{2}k \pm \frac{1}{2}\sqrt{k^2-4V_3})\mathrm{z} + V_3z^2$. One can find a first integral and an inverse jacobi multiplier of the forms

$$\Phi = x^{-1}yz^2\ell_1^{\eta_1}\ell_2^{\theta_1},$$

and

$$IJM = xy^2z^2\ell_1^{\eta_2}\ell_2^{\theta_2},$$

where

$\eta_1 = -\left(\frac{\left(-\frac{1}{2}v1+\frac{1}{2}v2+v3\right)\sqrt{k^2-4v3}+(c-k)v3-\frac{1}{2}k(v1-v2)}{\sqrt{k^2-4v3}\ v3}\right)$, $\theta_1 = \left(\frac{\left(\frac{1}{2}v1-\frac{1}{2}v2-v3\right)\sqrt{k^2-4v3}+(c-k)v3-\frac{1}{2}k(v1-v2)}{\sqrt{k^2-4v3}\ v3}\right)$, $\eta_2 =$

$-\frac{1}{2}\left(\frac{(v2-v3)\left(-k+\sqrt{k^2-4v3}\right)}{\sqrt{k^2-4v3}\ v3}\right)$,
$\theta_2 = \left(\frac{(v2-v3)\left(k+\sqrt{k^2-4v3}\right)}{\sqrt{k^2-4v3}\ v3}\right)$.

By Theorem 1, we can find the second first integral of the form

$$\Psi = y^{-1}z^{-1}(1 + O(x, y, z)).$$

Therefore, the required first integrals are of the form

$$H_1 = \Phi^{-1}\Psi^{-2} = xy(1 + \cdots),$$

and

$$H_2 = \Psi^{-1} = yz(1 + \cdots).$$

Since $\zeta = z(\ell_2)^{\frac{2(V_3 z+k)}{-2V_3 z-k+\sqrt{k^2-4V_3}}}$ satisfies $\dot{\zeta} = \zeta$, then the system must be linearizable by Theorem 2.

Case 7. By substitution integrability condition, system (1) reduce to

$$\dot{x} = x(1 + ax + by + L_1x^2 + V_1z^2),$$
$$\dot{y} = y(-1 - ax - by - L_1x^2 + V_2z^2),$$
$$\dot{z} = z(1 + 2ax + kz + 3L_1x^2 + V_3z^2).$$

The substitution $u = xy$, implies

$$\dot{x} = x(1 + ax + L_1x^2 + V_1z^2) + bu,$$
$$\dot{u} = Vuz^2,$$
$$\dot{z} = z(1 + 2ax + kz + 3L_1x^2 + V_3z^2),$$

where $V = V_1 + V_2$, for this case we define a function ψ as

$$\psi = \psi_0 + u\psi_1 + u^2\psi_2 + \cdots,$$

provided that $\dot{\psi} = z^2$, $\psi_i = \psi_i(x, z)$, for all i. It clear that $\Phi = ue^{-V\psi}$ is a first integral. The associated vector filed is separated as

$$\chi = \chi_0 + \chi_1 + \chi_u,$$

where

$$\chi_0 = x(1 + ax + L_1x^2 + V_1z^2)\frac{\partial}{\partial x} + z(1 + 2ax + kz + 3L_1x^2 + V_3z^2)\frac{\partial}{\partial z}$$
$$\chi_1 = bu\frac{\partial}{\partial x},$$
$$\chi_u = Vuz^2\frac{\partial}{\partial u},$$

by using our assumption $\chi\psi = z^2$, we rewritten the formula

$$\chi_0\psi_0 = z^2,$$

and

$$\chi_0\psi_i + kVz^2\psi_i = -\chi_1\psi_{i-1}, \quad \forall i > 0. \quad (7)$$

These two statements must be clearify

1) We need to show that there is no obstruction terms in (7).
2) We have to show that the equation (7) for all ψ_i is divisible by z^2.

So first we want to show that for all $B = \sum_{i+j>0} b_{i,j}x^iz^j$, there exist an $A = \sum_{i+j>0} a_{i,j}x^iz^j$ such that $(\chi_0 + kVz^2)A = B$. Since

$$\begin{aligned}(\chi_0 + kVz^2)A = &\sum_{i+j>0}(i+j)a_{i,j}x^iz^j + \sum_{i+j>0}(i + 2ja)a_{i,j}x^{i+1}z^j \\ &+ \sum_{i+j>0}(i+3j)L_1a_{i,j}x^{i+2}z^j \\ &+ \sum_{i+j>0}(iV_1 + jV_3)a_{i,j}x^iz^{j+2} \\ &+ \sum_{i+j>0}(jk)a_{i,j}x^iz^{j+1} \\ &= \sum_{i+j>0} b_{i,j}x^iz^j,\end{aligned}$$

we can find $a_{i,j}$ that must satisfy

$$\begin{aligned}(i+j)a_{i,j} + (((i-1) + 2ja)a_{i-1,j}) + ((i-2) &+ 3j)L_1a_{i-2,j} + (iV_1 + (j \\ &- 2)V_3)a_{i,j-2} + (j-1)ka_{i,j-1} \\ &= b_{i,j}, \quad \forall i, j > 2,\end{aligned}$$

where $a_{1,0} = \frac{b_{1,0}}{1+V_1}$ and $a_{0,1} = b_{0,1}$, though it is clear that there is no obstruction for solving these equation recursively, and standard mojrization technique imply that the resulting series is convergent. Now for second requirement we notice that for solving the equation term by term yield that the right hand side has no constant term. Although, we observe that every ψ_i in the equation (7) is divisible by z^2. To show this we use, mathematical induction. We suppose that z^2 is divides the right hand side of (7) (for $i = 0$ this is immediate), this implies that

$$x(1 + ax + L_1x^2 + V_1z^2)\frac{\partial\psi_i}{\partial x},$$

is divisible by z^2, this shows that $\frac{\partial\psi_i}{\partial x}$, is divisible by z^2. Therefore, $\psi_i = g(x) + z^2h(x, z)$, hence $g'(x) = 0$, (that means g is constant), clearly $\psi_i - g$ also satisfies (8) and proceed by induction. thus after standard majorization argument, we find a first integral $\Phi = ue^{-V\psi}$, and inverse jacobi multiplier

$$IJM = u^{1+\frac{V_1+V_3}{V}}z^2,$$

By Theorem 1 the second first integral is

$$\begin{aligned}\Psi &= xu^{-\frac{V_1+V_3}{V}}z^{-1}(1 + O(1)), \\ &= x^{1-\frac{V_1+V_3}{V}}y^{-\frac{V_1+V_3}{V}}z^{-1}(1 + O(1)).\end{aligned}$$

The required first integrals are

$$H_1 = xye^{-V\psi} = xy(1 + \cdots),$$

and

$$H_2 = \Phi^{1-\frac{V_1+V_3}{V}}\Psi^{-1} = yz(1 + \cdots).$$

Case 8. In this case the system is

$$\dot{x} = x(1 + by + L_1x^2),$$
$$\dot{y} = y(-1 - 2by),$$
$$\dot{z} = z(1 + hy + L_3x^2).$$

In this case, there are invariant algebric surfaces $\ell_1 = 1 + 2by = 0$ and $\ell_2 = 1 + 2by + L_1x^2 = 0$ with repective cofactors $L_{\ell_1} = -2by$ and $L_{\ell_2} = 2L_1x^2 - 2by$. The change of coordinates

$$(X, Y, Z) = (x\ell_1\ell_2^{-\frac{1}{2}}, y\ell_1^{-1}, z\ell_1^{\frac{h}{2b}+\frac{L_3}{2L_1}}\ell_2^{\frac{-L_3}{L1}}).$$

will linearize the equations. The first integrals are $H_1 = XY$, and $H_2 = YZ$, and then pull back these integrals to the original variables x, y and z

$$H_1 = xy(1 + O(x, y, z)),$$

and

$$H_2 = zy\big(1 + O(x, y, z)\big).$$

Case 9. By integrability condition system (1) becomes

$$\dot{x} = x(1 + by + cz + L_1x^2),$$
$$\dot{y} = y(-1 - 2by - 2cz),$$
$$\dot{z} = z(1 - 2by - 2cz + L_3x^2).$$

The change of the coordinate

$$(X, Y, Z) = (x^2, x^2y, x^2z),$$

gives

$$\dot{X} = 2X + 2L_1X^2 + 2bY + 2cZ,$$
$$\dot{Y} = Y(1 + 2L_1X),$$
$$\dot{Z} = Z(3 + (2L_1 + L_3)X).$$

Notice that the origin is in the poincaré domain this means that the system is linearizable by the change of variables

$$(\tilde{X}, \tilde{Y}, \tilde{Z}) = (X - 2bY + 2cZ + O(2), Y(1 + O(1)), Z(1 + O(1))).$$

The functions $\Psi = \tilde{X}^{-\frac{1}{2}}\tilde{Y}$ and $\Phi = \tilde{X}^{-2}\tilde{Y}\tilde{Z}$ are first integrals of the linear system and can pull back to first integrals of the original system in the form

$$H_1 = \tilde{X}^{-\frac{1}{2}}\tilde{Y} = (x^2)^{-\frac{1}{2}}x^2y\big(1 + O(1)\big) = xy\big(1 + O(1)\big),$$

and

$$H_2 = \tilde{X}^{-2}\tilde{Y}\tilde{Z} = (x^2)^{-2}\,x^2y\,x^2z(1 + O(1)) = yz(1 + O(1)).$$

Case 10. System (1) become

$$\dot{x} = x(1 + hy + L_1x^2 + V_1z^2),$$
$$\dot{y} = y(-1 - 2hy),$$
$$\dot{z} = z(1 + hy + L_3x^2 + V_3z^2).$$

The change of coordiantes

$$(X, Y, Z) = (\frac{x^2}{1 + 2hy}, y, \frac{z^2}{1 + 2hy})$$

Gives

$$\dot{X} = X(2 + 2L_1X + 2V_1Z)(1 + 2hY),$$
$$\dot{Y} = -Y(1 + 2hY),$$
$$\dot{Z} = Z\big(2 + (2L_3X^2 + 2V_3Z^2)\big)(1 + 2hY).$$

By re-scaling the system by $(1 + 2hY)$, we have $\dot{Y} = -Y$, it is clear the first and third equations gives a linearizable node. Therefore, the changing the variables

$$X = x\big(1 + O(x, z)\big), \text{ and } Z = z(1 + O(x, z)),$$

gives

$$\dot{X} = X, \quad \dot{Z} = Z.$$

Case 11. The subsystem in this case is

$$\dot{x} = x(1 - hy - L_3x^2 + V_1z^2),$$
$$\dot{y} = y(-1 - 2hy - 2L_3x^2),$$
$$\dot{z} = z(1 + hy + L_3x^2 + V_3z^2).$$

The transformation $(X, Y, Z) = (x^2z^2, yz^2, z^2)$ will change the the system into

$$\dot{X} = X(4 + 2(V_1 + V_3)Z),$$
$$\dot{Y} = Y(1 + 2V_3Z),$$
$$\dot{Z} = 2Z + 2L_3X + 2V_3Z^2 + 2hY.$$

Notice that the critical point of system is in the poincaré domain this means that the system is linearizable via an analytic change of coordinates

$$(\tilde{X}, \tilde{Y}, \tilde{Z}) = \Big(X\big(1 + O(1)\big), Y\big(1 + O(1)\big), Z + L3X - 2hY + O(2)\Big).$$

The two first integrals $\Psi = \tilde{X}^{\frac{1}{2}}\tilde{Y}\tilde{Z}^{-\frac{3}{2}} = (x^2z^2)^{\frac{1}{2}}\,y\,z^2\,(z^2)^{-\frac{3}{2}}(1 + O(1)) = xy(1 + O(1))$ and $\Phi = \tilde{Y}\tilde{Z}^{-\frac{1}{2}} = yz^2(z^2)^{-\frac{1}{2}}(1 + O(1)) = yz(1 + O(1))$. Hence the two first integrals of the original system are

$$H_1 = xy\big(1 + O(1)\big) \text{ and } H_2 = yz(1 + O(1)).$$

Case 12. If $e \neq 0$ the conditions reduce to

$$\begin{aligned} ab - de = ef - hk = ae + ah - ab - eg \\ = bk - ce + ek - hk \\ = eV_2 - eV_3 - 2hV_3 \\ = 2bV_3 - eV_1 + eV_3 - 2hV_3 \\ = eL_3 + 2bL_1 - eL_1 - 2hL_1 \\ = 2bL_1 - eL_2 + eL_1. \end{aligned}$$

The invariant algebraic surface in this case is $\ell = 1 + ax - ey + kz + L_1x^2 + V_3z^2 = 0$ with cofactor $L_\ell = ax + ey + kz + 2L_1x^2 + 2V_3z^2$. This gives two independent first inegrals of the form

$$H_1 = xy\ell^{-1-\frac{b}{e}} \quad \text{and} \quad H_2 = yz\ell^{-1-\frac{h}{e}}.$$

If $e = 0$ we consider several cases as follows.

1. If $b = h = 0$, this is a sub-case of case 1.

2. If $h, b \neq 0$, in this case,we have $a = k = L_1 = V_3$, we can find an exponential factor $\ell = \exp(x - \frac{b}{d}y + \frac{fb}{dh}z + \frac{1}{2}\frac{L_2}{d}x^2 + \frac{1}{2}\frac{V_2 b}{dh}z^2)$, with cofactor

$$L_\ell = x + \frac{b}{d}y + \frac{fb}{dh}z + \frac{L_2}{d}x^2 + \frac{V_2 b}{dh}z^2,$$

so two independent first integrals of this case are

$$H_1 = xy\ell^{-d} \quad \text{and} \quad H_2 = yz\ell^{-\frac{dh}{b}}.$$

3. $b = 0, h \neq 0$. In this case, we have $a = b = c + f = d = k = L_1 = L_2 = V_1 + V_2 = V_3 = 0$. We can get an exponential factor of the form $\ell = \exp(-\frac{g}{h}x + y - \frac{f}{h}z - \frac{1}{2}\frac{L_3}{h}x^2 + xy - \frac{1}{2}\frac{V_2}{h}z^2)$, with cofactor $L_\ell = -\frac{g}{h}x - y - \frac{f}{h}z - \frac{L_3}{h}x^2 - \frac{V_2}{h}z^2$. The first integrals are

$$H_1 = xy \quad \text{and} \quad H_2 = yz\ell^h.$$

4. $h = 0, b \neq 0$. In this case, we have $a = d + g = f = k = L_1 = L_2 + L_3 = V_2 = V_3 = 0$ and an exponential factor $\ell = \exp(x + \frac{b}{g}y - \frac{c}{g}z + \frac{1}{2}\frac{L_3}{g}x^2 + yz - \frac{1}{2}\frac{V_1}{g}z^2)$ with cofactor $L_\ell = x - \frac{b}{g}y - \frac{c}{g}z + \frac{L_3}{g}x^2 - \frac{V_1}{g}z^2$. The first integrals

$$H_1 = xy\ell^g \quad \text{and} \quad H_2 = yz.$$

Case 12.1. In this case, the system becomes

$$\dot{x} = x(1 + by + \frac{1}{2}L_2x^2),$$
$$\dot{y} = y(-1 + 2by + L_2x^2),$$
$$\dot{z} = z(1 + hy + \frac{hL_2x^2}{2b}).$$

The invariant algebraic surface of the system is $\ell = 1 - 2by + \frac{1}{2}L_2x^2 = 0$ with cofactor $L_\ell = 2by + L_2x^2$, the change of the coordinates $(X, Y, Z) = \left(x\ell^{-\frac{1}{2}}, y\ell^{-1}, z\ell^{\frac{h}{2b}}\right)$, will linearize the system. When $b = 0$ we can find invariant algebric surface of the form $\ell = 1 + \frac{1}{2}L_2x^2 = 0$ with cofactor $L_\ell = L_2x^2$ also this invariant algebric surface will linearize the reduce system.

Case 12.2. In this case, the system becomes

$$\dot{x} = x(1 + \frac{1}{2}hy + \frac{1}{2}kz + \frac{1}{2}L_3x^2),$$
$$\dot{y} = y(-1 + hy + kz + L_3x^2),$$
$$\dot{z} = z(1 + hy + kz + L_3x^2).$$

The surface $\ell = 1 - hy + kz + \frac{1}{2}L_3x^2 = 0$ is invariant of the given system with cofactor $L_\ell = hy + kz + L_3x^2$, the system will linearize by a transformation

$$(X, Y, Z) = (x\ell^{-2}, y\ell^{-1}, z\ell^{-1}).$$

Case 12.3. The remain system is

$$\dot{x} = x(1 + hy + L3x^2 + V3z^2),$$
$$\dot{y} = y(-1 + 2hy + 2L3x^2 + 2V3z^2),$$
$$\dot{z} = z(1 + hy + L3x^2 + V3z^2).$$

The linearized change is given by $(X, Y, Z) = \left(x\ell^{-\frac{1}{2}}, y\ell^{-1}, z\ell^{-\frac{1}{2}}\right)$, where $\ell = 1 - 2hy + L_3x^2 + V_3z^2$.

REFERENCES

AZIZ, W. 2014. Integrability and linearizability of three dimensional vector fields. *Qualitative theory of dynamical systems*, 13**,** 197-213.

AZIZ, W. & CHRISTOPHER, C. 2012. Local integrability and linearizability of three-dimensional Lotka–Volterra systems. *Applied Mathematics and Computation*, 219**,** 4067-4081.

CAIRÓ, L. 2000. Darboux first integral conditions and integrability of the 3D Lotka-Volterra system. *Journal of Nonlinear Mathematical Physics*, 7**,** 511-531.

CAIRÓ, L. & LLIBRE, J. 2000a. Darboux integrability for 3D Lotka-Volterra systems. *Journal of Physics A: Mathematical and General*, 33**,** 2395.

CHAVARRIGA, J. & GINÉ, J. 1998. Integrability of cubic systems with degenerate infinity. *Differential Equations and Dynamical Systems*, 6**,** 425-438.

CHEN, X., GINÉ, J., ROMANOVSKI, V. G. & SHAFER, D. S. 2012. The 1:− q resonant center problem for certain cubic Lotka–Volterra systems. *Applied Mathematics and Computation*, 218**,** 11620-11633.

CHRISTODOULIDES, Y. T. & DAMIANOU, P. A. 2009. Darboux polynomials for Lotka–Volterra systems in three dimensions. *Journal of Nonlinear Mathematical Physics*, 16**,** 339-354.

CHRISTOPHER, C. & LI, C. 2007. *Limit cycles of differential equations*, Springer Science & Business Media.

CHRISTOPHER, C., MARDEŠIĆ, P. & ROUSSEAU, C. 2003. Normalizable, Integrable, and Linearizable Saddle Points for Complex Quadratic Systems in $\mathbb{C}^2$. *Journal of Dynamical and Control Systems*, 9**,** 311-363.

CHRISTOPHER, C., MARDEŠIĆ, P. & ROUSSEAU, C. 2004. Normalizability, synchronicity, and relative exactness for vector fields in C 2. *Journal of dynamical and control systems*, 10**,** 501-525.

DECKER, W., G. PfiSTER & H. SCHÖNEMANN. 2011. primdec.lib. AS INGULAR 3-1-3 library for primary decomposition and radicals of ideals

FERCEC, B., CHEN, X. & ROMANOVSKI, V. G. 2011. Integrability conditions for complex systems with homogeneous quintic nonlinearities. *J. Appl. Anal. Comput*, 1**,** 9-20.

FRONVILLE, A., SADOVSKI, A. & ŻOŁĄDEK, H. 1998. Solution of the 1:− 2 resonant center problem in the quadratic case. *Fundamenta Mathematicae,* 157**,** 191-207.

GINÉ, J., KADYRSIZOVA, Z., LIU, Y. & ROMANOVSKI, V. G. 2011. Linearizability conditions for Lotka–Volterra planar complex quartic systems having homogeneous nonlinearities. *Computers & Mathematics with Applications,* 61**,** 1190-1201.

GINÉ, J. & ROMANOVSKI, V. G. 2009. Linearizability conditions for Lotka–Volterra planar complex cubic systems. *Journal of Physics A: Mathematical and Theoretical,* 42**,** 225206.

GINÉ, J. & ROMANOVSKI, V. G. 2010. Integrability conditions for Lotka–Volterra planar complex quintic systems. *Nonlinear Analysis: Real World Applications,* 11**,** 2100-2105.

GRAVEL, S. & THIBAULT, P. 2002. Integrability and linearizability of the Lotka–Volterra system with a saddle point with rational hyperbolicity ratio. *Journal of Differential Equations,* 184**,** 20-47.

GREUEL, G. M., G. PfiSTER & H. SCHÖNEMANN. 2012. *SINGULAR 3-1-5 – a computer algebra system for polynomial computations.*

HAN, M., ROMANOVSKI, V. G. & ZHANG, X. 2016. Integrability of a family of 2-dim cubic systems with degenerate infinity. *Rom. Journ. Phys,* 61**,** 1-2.

HU, Z., HAN, M. & ROMANOVSKI, V. G. 2013. Local integrability of a family of three-dimensional quadratic systems. *Physica D: Nonlinear Phenomena,* 265**,** 78-86.

HU, Z., ROMANOVSKI, V. G. & SHAFER, D. S. 2008. 1:− 3 resonant centers on C2 with homogeneous cubic nonlinearities. *Computers & Mathematics with Applications,* 56**,** 1927-1940.

LIU, C., CHEN, G. & LI, C. 2004. Integrability and linearizability of the Lotka–Volterra systems. *Journal of Differential Equations,* 198**,** 301-320.

LLIBRE, J. & VALLS, C. 2011b. Polynomial, rational and analytic first integrals for a family of 3-dimensional Lotka-Volterra systems. *Zeitschrift für angewandte Mathematik und Physik,* 62**,** 761-777.

LOTKA, A. J. 1956. Elements of mathematical biology.

MALKIN, K. 1964. Criteria for center of a differential equation. *Volg. Matem. Sbornik,* 2**,** 87-91.

MURZA, A. C. & TERUEL, A. E. 2010. Global dynamics of a family of 3-D Lotka–Volterra systems. *Dynamical Systems,* 25**,** 269-284.

NOONBURG, V. 1989. A neural network modeled by an adaptive Lotka-Volterra system. *SIAM Journal on Applied Mathematics,* 49**,** 1779-1792.

ROMANOVSKI, V. G. & SHAFER, D. S. 2008. On the Center Problem for p:-q Resonant Polynomial Vector Fields. *Bulletin of the Belgian Mathematical Society-Simon Stevin,* 15**,** 871-887.

VOLTERRA, V. 1931. Théorie mathématique de la lutte pour la vie.

WANG, Q. & LIU, Y. 2008. Linearizability of the polynomial differential systems with a resonant singular point. *Bulletin des sciences mathematiques,* 132**,** 97-111.

ŻOŁĄDEK, H. 1997. The problem of center for resonant singular points of polynomial vector fields. *Journal of differential equations,* 137**,** 94-118.

ZANCO Journal of Pure and Applied Sciences
The official scientific journal of Salahaddin University-Erbil
https://zancojournals.su.edu.krd/index.php/JPAS

ISSN (print):2218-0230**, ISSN (online):** 2412-3986**, DOI: http://dx.doi.org/10.21271/zjpas**

RESEARCH PAPER

Analyses of Storage Coefficient for a Production Well

Dana Khider Mawlood

Department of Civil Engineering, College of Engineering, Salahaddin University-Erbil, Kurdistan Region, Iraq.

A B S T R A C T:

In case of Production or (single) well pumping tests the Storativities are overestimated, it depends on radial distance between effective well bore radius in single well test. The objective of the paper proposed to drive the diffusion equation to find out the effective radial distance. Applying AQTISOLVE and Aquifer win 32 software via Jacob method for well testing , we can obtain the Storativity value and the Transimissivity using specific capacity data to check the Transimissivity value . The advantage of this method reducing the cost by having single well test (production well) without observation well. Justification the parameters of aquifer is require because turbulent velocity and the screen of well (aquifer losses and well losses). Application of single well test lead to understand aquifer layer and the management of reservoir.

KEY WORDS: Diffusion equation, Single well test, Aquifer parameters, Effective radius.
DOI: http://dx.doi.org/10.21271/ZJPAS.31.4.12
ZJPAS (2019), 31(4); 114-122 .
.

INTRODUCTION :

Groundwater plays a major role in water supply and irrigation worldwide. With the growth of the population, the abstracting water increases and the water level decreases, these may lead to effect on the groundwater management, and change the characteristics of the aquifer. The withdrawal water from the aquifer required to testing of the aquifer in order to estimate the capacity of the well and determine the accurate aquifer properties. The test data were analyses through many methods according to the situation of each location.

Estimating the accurate values of aquifer parameters required conducting pumping test on the production well and measuring drawdown in the monitoring well .but it needed high cost of economy, so in order to decrease cost of other well ,it is regarded to used many methods for that test which is known as single well test.

Single-well aquifer tests consist of monitoring water-level changes in a well before, during, and after a known volume of water is either injected or removed from a formation open to the well. Single-well aquifer tests are described in this report, including pumping and slug tests. Water is typically removed from the well (pumped) at a constant rate during pumping tests (Kruseman et al., 1970).

The first scientist was (Theim, 1906) that developed a method for both confined and unconfined aquifer according to the Dupuit assumptions in 1863, who governed the equation for flow in water table aquifer for steady state

* **Corresponding Author:**
Dana Khider Mawlood
E-mail: dana.mawlood@su.edu.krd
Article History:
Received: 12/11/2018
Accepted: 10/06/2019
Published: 10/09/2019

(equilibrium conditions). Later, (Theis, 1935) based on heat transfer derived a method for transient groundwater flow in confined aquifer, then (Cooper Jr and Jacob, 1946) simplified Theis solution for long time of pumping test and small radial distance, both previous equations are applicable for unconfined aquifer type, if the drawdown is very small compared to the saturated thickness of the aquifer. Since the last decade there are many experiences that are tried to discover a method to estimate the aquifer parameters through analyzing single well test data such as by using single well test with the Cooper-Jacob method shows overestimate of transmissivity for unconfined aquifer while, for confined aquifer near to the known value (Keith J. Halford, et al, 2006). Moreover, (Anomohanran & serhien-Emekeme , 2014) performed a pumping test data to estimate aquifer parameters using Cooper-Jacob straight line method. and the method of (P. N. Ballukraya, et al,1991) it derived an equation to estimate Storativity by recovery test, Also (M. Razack, et al, 1991) tried to determine Transmissivity through specific capacity data, then aquifer Parameters and Well Efficiency Estimation for Selected Site in Erbil Governorate (Mawlood and Mustafa, 2017).

Now, Aquifer Test, AQTISOLVE and Aquifer win 32 software which calculates the parameters of the pumping test by computer, these software's are specifically used for the analysis of data of pumping test, data processing, analysis and research of obtaining parameters graphically. It can be applied to calculate the data of the pumping test and complete the display and printing of the process and get the result of parameters.

2. METHOLOGY

2.1.1 Derivation of Diffusion Equation for x-axis:

Storativity for a single well test, such as effective well bore storage (Choi, 2007), Recovery test (Ballukraya and Sharma, 1991), slug test, etc. In this case due to the absence of the observation well the application of diffusion equation is selected for ground water flow in the vicinity of the well. The pumping test is conducted by pumping water from the well itself at a constant rate and measuring the drawdown in the well as a function of time. The test data are used to understand how water.

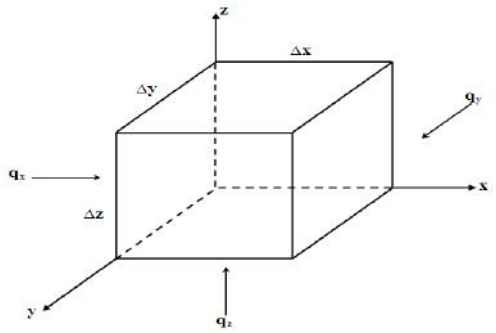

Figure 1 : Representative control volume (RCV**)**

The difference between inflow and outflow=change of storage

Flow in-flow out=change of storage

qin-qout=Δs

$$qin - \left(qin + \frac{dq}{dx}dx\right) = \Delta s \qquad (1)$$

since:

By substituting Darcy equation in terms of x-direction obtain the equation below:

$$-\frac{dq}{dx}dxA = \mathrm{SA}\frac{\mathrm{dh}}{\mathrm{dt}} \qquad (2)$$

$$-\frac{d\left(-K\frac{dh}{dx}\right)}{dx}dx(dydz) = S(dxdy)\frac{dh}{dt} \qquad (3)$$

horizontal area vertical area

$$dzK\frac{d^2h}{dx^2} = S\frac{dh}{dt} \qquad (4)$$

where:

dz is equal to the aquifer thickness T=Kb=Kdz, So:

$$T\frac{d^2h}{dx^2} = S\frac{dh}{dt} \quad (5)$$

$$\frac{T}{S}\frac{d^2h}{dx^2} = \frac{dh}{dt} \quad (6)$$

$$\eta\frac{d^2h}{dx^2} = \frac{dh}{dt} \quad (7)$$

The above equation is 1D diffusion equation in x-direction.

2.1.2 Derivation of Diffusion Equation for y-axis:

$$qin - \left(qin + \frac{dq}{dy}dy\right) = \Delta s \quad (8)$$

$$-\frac{dq}{dy}dyA = \mathrm{SA}\frac{\mathrm{dh}}{\mathrm{dt}} \quad (9)$$

Then replacing Darcy's equation for y-direction

$$-\frac{d\left(-K\frac{dh}{dy}\right)}{dy}dy(dxdz) = S(dxdy)\frac{dh}{dt} \quad (10)$$

$$dzK\frac{d^2h}{dy^2} = S\frac{dh}{dt} \quad (11)$$

$$T\frac{d^2h}{dy^2} = S\frac{dh}{dt} \quad (12)$$

$$\frac{T}{S}\frac{d^2h}{dy^2} = \frac{dh}{dt} \quad (13)$$

$$\eta\frac{d^2h}{dy^2} = \frac{dh}{dt} \quad (14)$$

The above equation is diffusion equation for y-direction.

2.1.3 Derivation of Diffusion Equation for z-axis:

$$qin - \left(qin + \frac{dq}{dz}dz\right) = \Delta s \quad (15)$$

$$-\frac{dq}{dz}dzA = \mathrm{SA}\frac{\mathrm{dh}}{\mathrm{dt}} \quad (16)$$

Then replacing Darcy's equation for z-axis, it will be:

$$-\frac{d\left(-K\frac{dh}{dz}\right)}{dz}dz(dxdy) = S(dxdy)\frac{dh}{dt} \quad (17)$$

$$dzK\frac{d^2h}{dz^2} = S\frac{dh}{dt} \quad (18)$$

$$T\frac{d^2h}{dz^2} = S\frac{dh}{dt} \quad (19)$$

$$\frac{T}{S}\frac{d^2h}{dz^2} = \frac{dh}{dt} \quad (20)$$

$$\eta\frac{d^2h}{dz^2} = \frac{dh}{dt} \quad (21)$$

The above equation is diffusion equation for z-direction, And for 3D diffusion equation the it will be:

$$\eta\frac{d^2h}{dx^2} + \eta\frac{d^2h}{dy^2} + \eta\frac{d^2h}{dz^2} = \frac{dh}{dt} \quad (22)$$

$$\eta\left\{\frac{d^2h}{dx^2} + \frac{d^2h}{dy^2} + \frac{d^2h}{dz^2}\right\} = \frac{dh}{dt} \quad (23)$$

The above equation 3D Transient Groundwater flow for isotropic homogeneous confined aquifer ,and it can be written in other form such as:

$$\eta\nabla^2 h = \frac{dh}{dt} \quad (24)$$

Where:

q : is Darcy flux(L/T).
K : is Hydraulic conductivity(L/T)
s : is aquifer storage (unitless)
T : is Transmissivity (L^2/T).
S : is Storativity(unit less).
η : is diffusivity (L^2/T).
x,y,z : is axis in the direction of x, y and z respectively.
t: is time (T).

∇:is lamda or lacplacian
By using the dimension of the equations:

η length/length²=length/time
(25)

Simplify the equation:
η 1/l²=1/T (26)
l^2=4ητ (27)
L=2√ητ (28)
Where:

L: is radial distance from pumping well to monitoring well (L).
$\mathcal{T}$: is time (T).
2: Geometric term.
η: is aquifer diffusivity(L²/T) which is equal to :

$$\eta = \frac{T}{S} = \frac{Kb}{Ssb} \quad (29)$$

The equation of (27) can be used to find out the radial distance at time of pumping, then substituting this distance as a radial distance from cooper-Jacob's time -drawdown equation to estimate Storativity (S).

2.2 Cooper-Jacob Straight Line Equation

Jacob (1946) derived a method based on Theis (1935) equation for large values of time (t) and small value of u and for time versus drawdown after considering Jacob's assumptions:

$$s = \frac{2.3Q}{4\pi T}\log_{10}\frac{2.25Tt_o}{r^2S} \quad (30)$$

To calculate the value of Transmissivity through Jacob's equation:

$$T = \frac{2.3Q}{4\pi\Delta s} \quad (31)$$

The above equation is used to estimate Transmissivity ,the slope of the line(Δs) on the semi logarithmic plot are taken by measuring the difference between two drawdown per one log cycle ,and the intercept of the straight line at zero drawdown determines the initial pumping test time(t_o) ,then using it to estimate storage coefficient(S) in the equation below:

$$S = \frac{2.25Tt_o}{r^2} \quad (32)$$

Where:

r: radial distance from pumping well to observation well (calculated from diffusion equation) (L).

2.3Application of Diffusion Equation:

The first step to finding the values of diffusivity by dividing equivalent hydraulic conductivity (K) on specific storage (Ss):
η=Kb/Ssb
η=k/Ss
η=0.1m²/s
[The value of aquifer diffusivity (η) determined according to the geological formation in the vicinity of the well during borehole test and sampling Fig.2and Table 1]. For soils and unconsolidated materials, the skeleton compressibility dominates fluid compressibility .Fracture wespecially have very small storage and potentially very high T, hence fractured rocks.

L=2√0.1*0.4*60
L=60m

After taking out the value of radial distance within diffusivity equation and estimating the value of Storativity, then the test data Table2 should be plot on semi-log paper. To determine the values of Δs and t_o on plot, see Fig.3
Although the following steps should be taken into account during the calculation in order to get the values of both Transmissivity and Storativity as the following calculations:

$$T = \frac{2.3 * 0.029}{4 * \pi(0.4)} = 0.013 m^2/s$$

And Storativity:

$$S = \frac{2.25 * 0.013 * 0.4 * 60}{60^{2}} = 0.0001$$

The value of Storativity for confined aquifer type is within the range of (0.001-0.00001) according to (Michael et al.,2006)

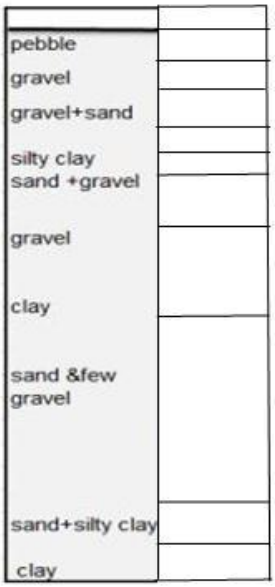

Figure 2: Geological profile taken from borehole test.

Table 1 Ranges of storitivity and diffusivity according to geological information

	∝	β	n	k	Ss	η
	1/pa			m/s	1/m	m^2/s
Clay	1.00e-07	4.40E-10	0.25	1.00E-10	9.81E-04	1.0E-07
Silt	5.00E-07	4.40E-10	0.25	1.00E-07	4.90E-03	2.0E-05
Sand	1.00E-08	4.40E-10	0.25	1.00E-05	9.91E-05	1.0E-01
Gravel	1.00E-08	4.40E-10	0.25	1.00E-03	9.91E-05	1.0E+01
Jointed Garnite	1.00E-11	4.40E-10	0.0001	1.00E-07	9.84E-08	1.0E+00
Facture Zone	1.00E-11	4.40E-10	0.001	1.00E-05	1.02E-07	9.8E+01

$Ss=\rho g(\propto+n\ _{\beta})(1/L)$

$\propto$= Solid skeleton compressibility (1/pressure)

$_{\beta}$= fluid compressibility

n=porosit

2.4 Transmissivity from specific capacity data

We can also fine Transmissivity by

- Specific capacity = yield/drawdown.
- $T = Q/ (h_0\text{-}h)\ 2.3/4\pi\log (2.25Tt/ (r^2S))$.
- $T = 15.3\ [Q/(h_0\text{-}h)]^{0.67}$ [m,d]
- $T = 0.76\ [Q/(h_0\text{-}h)]^{1.08}$ [m,d]

Study Area

Salah al-Din district is one of the districts of Shaqlawa district in Erbil province in Iraq, with a total area of 796 km 2, while the villages belonging to it have 56 villages and 25% lands, 35% hills and 40% mountains.

The pumping test exercise was carried out on a single well within the Salahaddin area, with a constant discharge of 177 Gpm (1146.96 m^3/day). The pumping well has a depth of 150 m. The aquifer saturated thickness is 138 m and the original static water level is 12 m, coordination number 38s0423770, UTM 4033138 with elevation :756m.

Figure 2: Satellite image of salahaddin area

Well depth: 150 m	**Length of pipe test:** 120 m
Static water level: 12 m	**Radius of pipe test:** 3 in
Dynamic water level: 18 m	**Type of test equipment:** 30-SP46 4 in
Discharge: 177(gal/min), 1146.96 (m^3/day)	**Inside raduis of pipes:** 8 in

Table(2) Pumping test data results from Directorate of Erbil Groundwater

Time (min)	**Depth to water level (meter)**	**Drawdown (meter)**	**Time (minute)**	**Depth to water level (meter)**	**Drawdown (meter)**	**Time (minute)**	**Recovery (meter)**
0	12	0	60	18	6	0.5	18
0.5	16.5	4.5	80	18	6	1	18
1	16.8	4.8	100	18	6	1.5	18
1.5	17.2	5.2	120	18	6	2	18
2	17.4	5.4	140	18	6	3	18
3	17.6	5.6	160			4	18
4	17.8	5.8	200			5	18
5	17.9	5.9	280			6	18
6	18	6	300			7	18
7	18	6	360			8	18
8	18	6	420			9	18
9	18	6	480			10	18
10	18	6	540			15	18
15	18	6	600			20	18
20	18	6	660			25	18
25	18	6	780			30	18
30	18	6	900			40	18
40	18	6	1020			50	18
50	18	6	1140			60	18
			24 hours				

3. RESULTS AND DISCUSSION

Table 3 presents aquifer parameters results from Salahaddin area by Jacob method. During the comparison between the calculated and standard range of Transmissivity, The calculated value of Transmissivity of Salahaddin well which can be classified according to (Table 3) from high to intermediate.

Figure 3 : Cooper-Jacob solutions by AQTISOLVE program

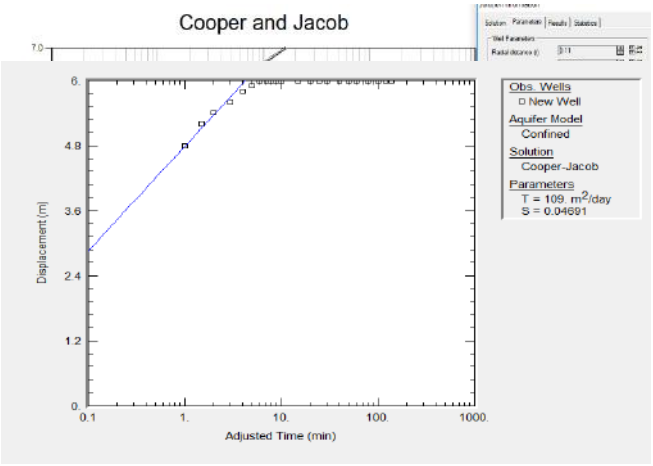

Figure 4: Cooper-Jacob solutions by aquifer test program

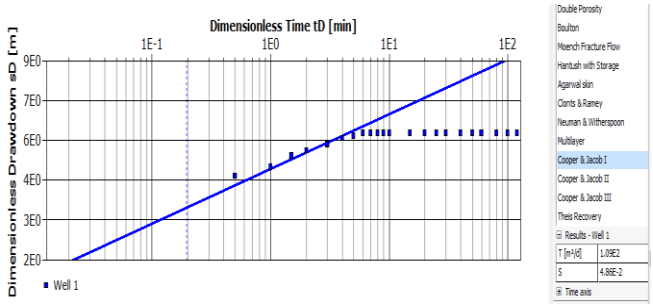

Figure 5 : Cooper-Jacob solutions by aquifer win 32 program

Table 3 Result of Transmissivity and Storativity by Jacob (1946) method

Jacob (1946) method	Transmissivity (m^2/day)	Storativity
AQTESOLVE program	109	0.04691
Aquifer test program	109	0.0486
Aquifer win 32 program	112.59	0.0410
Transmissivity from specific capacity data	221	-

Table 4 Transmissivity classification (Jirikrasny et al., 1993).

Coefficient of Transmissivity (m^2/day)	class of Transmissivity magnitude	Designation of Transmissivity magnitude
>1000	I	very high
100 to 1000	II	High
10 to 100	III	Intermediate
1 to 10	V	Low
0.1 to 1	IV	Very low
<0.1	VI	Imperceptible

CONCLUSION

The presented method can be used to analyses Storativity , according to the results ,the value of the Storativity is within the standard range for confined aquifer type which is between 0.001 to 0.00001, thus the paper satisfied that the values of the aquifer parameters especially Storativity can be find out from single well test by finding the radial distance through diffusivity equation and using this distance to calculate Storativity without existing monitoring well, however , it is obvious that the values of Storage coefficient cannot be accurate in case of have a single-well test because of two reasons first : it depends on radial distance between pumping well to point of measuring drawdown, we need observation well, second: Have a well loss and aquifer loss, which give inaccurate data of storativity. Monitoring well has no screen and the velocity of screen wells laminar by single well which have a submerging pump lead to turbulent velocity in the vicinity of the well, but this article proved that the suggested method succeeded in providing radial distance. This may lead to reduce the cost of drilling of observation well as well. Aquifer Test, AQTISOLVE and Aquifer win 32 software have been used for determine confined aquifer parameters. Using specific capacity data in order to obtain the Transimissivity to be compared with all programs that applied in research

REFERENCES

ANOMOHANRAN, O. AND ISERHIEN-EMEKEME, R.E., 2014. Estimation of aquifer parameters in Erho, Nigeria using the Cooper-Jacob evaluation method. American Journal of Environmental Sciences, 10(5), p.500.

BALLUKRAYA, P. & SHARMA, K. 1991. Estimation of storativity from recovery data. *Groundwater,* 29**,** 495-498.

CHOI, B.-S. 2007. A method for storativity compensation in single well test analysis. *Journal of Soil and Groundwater Environment,* 12**,** 36-43.

COOPER JR, H. & JACOB, C. E. 1946. A generalized graphical method for evaluating formation constants and summarizing well- field history. *Eos, Transactions American Geophysical Union,* 27**,** 526-534.

KEITH J.HALFORD,WILLIS D.WEIGHT, AND ROBERT P. SCHREIBER.(2006), Interpretation of Transmissivity
Estimates from single well pumping aquifer test,GROUNDWATER.Vol.44,3. (pp. 467-473).

KRUSEMAN, G. P., DE RIDDER, N. A. & VERWEIJ, J. M. 1970. *Analysis and evaluation of pumping test data*, International institute for land reclamation and improvement The Netherlands.

M. RAZACK AND DAVID HUNTLEY,(1991),Assessing Transmissivity from specific capacity in a large and Heterogeneous Alluvial Aquifer, GROUNDWATER, V.29. 6.

MAWLOOD, D. K. & MUSTAFA, J. S. 2017b. The Way of Improvement of Cooper-Jacob solution for different wells in Erbil surrounding. ZANCO Journal of Pure and Applied Sciences, 29, 120-127.

Michael Kasenow.(2006). AQUIFER TEST DATA: ANALYSIS AND EVALUATION. Water resources publications.

THEIM, G. 1906. Hydrologische methoden. *Gebhardt, Leipzig,* 56.

THEIS, C. V. 1935. The relation between the lowering of the piezometric surface and the rate and duration of discharge of a well using ground- water storage. *Eos, Transactions American Geophysical Union,* 16**,** 519-524.

ZANCO Journal of Pure and Applied Sciences
The official scientific journal of Salahaddin University-Erbil
https://zancojournals.su.edu.krd/index.php/JPAS

ISSN (print):2218-0230**, ISSN (online):** 2412-3986**, DOI: http://dx.doi.org/10.21271/zjpas**

RESEARCH PAPER

Assessment the Clean Index and Fertilizing Index of Some Imported Composts to Erbil City

Shakar Jamal Aweez[1] Sadeq , Dalshad Azeez Darwesh[2]

1,2 Department of Environmental sciences , College of Science, Salahaddin University-Erbil, Kurdistan Region, Iraq.

A B S T R A C T:

This study was carried out for assessing the clean and fertilizing indices of diverse composts from various countries imported to Erbil city. The compost samples included 4 most common compost kinds (Indian, Dutch, Estonia and local produced) with five replications were bought in different local agrochemical market and shopping. The experimental designed completely randomized design (CRD). The results revealed that the fertilizer index (FI) of imported and local compost was varied from 4.13 to 4.47 where as the clean index(CI) was varied from 3.20 to 3.93, all composts have a fertilizer potential value >4, however the clean index value of compost has medium heavy metals content, the statistical analysis in the present study indicated that imported and local compost has a good quality and proper for agriculture land.

KEY WORDS: Compost, Fertilizing index, Clean index, Heavy Metals
DOI: http://dx.doi.org/10.21271/ZJPAS.31.4.13
ZJPAS (2019) , 31(4);123-128 .

INTRODUCTION

Compost is resulting from the decomposition of organic matter. The compost involved garden waste, house holed solid waste, kitchen scraps, manure, leaves, grass clippings, and compost bears slight physical similarity to the raw material from which it originated. Composting of degradable wastes is seen as a method of diverting organic waste materials from landfills and creating a product, relatively effective in cost that is suitable for agricultural purposes. In addition to its potential beneficial components some waste materials may also contain nonessential elements, persistent organic compounds and microorganisms that may be harmful to the plants and environment. Heavy metals released from various sources may finally reach to the surface soil, and their further fate depends on soil physical and chemical properties such as pH, redox potential, (Mora, 2006). The presence of heavy metals in compost raises significant concern about its adverse impact on the environment as a result of excessive compost application to agricultural lands. High and excessive accumulation of heavy metals in the soil may eventually contaminate both human and animal food chain. Heavy metals can affect the growth, morphology, and metabolism of soil microorganisms, and diminish both the population and activity of microbial pools, therefore decrease soil fertility. Heavy metals uptake by plants and successive accumulation in human tissues and bio magnifications through the food chain causes both human health and environment concerns (Singh and Kalamdhad, 2012). Several studies were carried out around the world for estimating the compost quality index, particularly the fertilizing and clean index by (Torkshvand,2010; Saha et al., 2010; Bera et al., 2013; Dolui et al., 2014; Mandal et al., 2014 and Jalal,2016). The rapid increases in application of compost to the soil specially in the nursery at 15 last years in Kurdistan region increasing the demand of composed, therefore a huge amount of several kinds of compost from

* **Corresponding Author:**
Dalshad Azeez Darwesh
E-mail: dalshas.darwesh@su.edu.krd
Article History:
Received: 07/01/2019
Accepted: 09/05/2019
Published: 10/09 /2019

various countries imported to this region without quality control and prehistoric analyses, thus this study aimed to assesses the clean and fertilizing index of some common and widely used composts that imported to Erbil city, Kurdistan region-Iraq.

1. MATERIALS AND METHODS

1.1. Experimental design

This study was carried out for assessing the clean and fertilizing indices of diverse composts from various countries imported to Erbil city. The compost samples included 4 most common compost kinds (Indian C1, DutchC2, Estonia C3 and C4 locally produced) with five replications were bought in different local agrochemical market and shopping. The samples were dried at 65°C and then wet digested in H_2O_2 and H_2SO_4 acid (1/1, v/v) mixture using the producer of (Allen , 1974). The N content was measured by the distillation method of (Ryan et al., 2001) the P content was determined by the molybdenum blue colorimetric by spectrophotometric method, while the flame photometric method was used to determined K (Allen et al., 1974). The digested samples were used for determination the concentration of Cr, Cd, Pb,Cu, Ni and Zn by atomic absorption flame emission spectrophotomery and ICP (indicative coupled plasma) as described by (Pansu and Gautheyrou, 2006). The total Organic carbon and matter were determinate according to Walkly and Black method as described by (Richards, 1954).

The Fertilizing index of the composts is computed using the formula 1 as described by (Saha et al ., 2010):

$$FI = \frac{\sum_{j=i}^{n} Sj*Wj}{\sum_{j=1}^{n} Wj} \text{.....(1)}$$

Where S_j is score value of analytical data and W_j is weighing factor of the j^{th} fertility parameters as present in (Table 1). The clean index was also calculated using heavy metal concentrations (Zn, Cu, Cd, Pb, Ni, Cr) . Score values were given to each analytical value of the heavy metals as per scheme mentioned in (Table 2). Clean index' value was calculated by the following formula 2

$$CI = \frac{\sum_{j=i}^{n} Sj*Wj}{\sum_{j=1}^{n} Wj} \text{.....(2)}$$

where Sj is score value of analytical data and Wj is weighing factor of the j^{th} heavy metals as present in (table 2)

1.2Statistical analysis

The experimental designed in completely randomized design (CRD). Data was statistically analyzed using SPSS version 24. All data expressed as mean value. The difference among the means of compost types were compared by applying Duncan multiple comparison tests at level of significant 5%. (Steele and Torrie, 1969).

Table 1: Criteria for weighing factor to fertility parameters and score value to compost. From *(Saha et al., 2010.*

Fertility parameters	Score value(*Sj*)					Weighting factor(*Wj*)
	5	4	3	2	1	
TOC%	>20	15.1-20.0	12.1-15	9.1-12	<9.1	5
TN%	>1.25	1.01-1.25	0.81-1.00	0.51-0.20	<0.51	3
TP%	>0.60	0.41-0.60	0.21-0.40	0.11-0.20	<0.11	3
TK%	>1.00	0.76-1.00	0.51-0.75	0.26-0.50	<0.26	1
C:N	<10.10	10.1-15	15.1-20	20.1-25	>25	3

Table 2:Criteria for assigning weighing factor to heavy metals parameters and score value to analytical data of compost. From *(Saha et al., 2010)*.

Heavy metals mg.Kg^{-1}	Score value(*Sj*)						Weighting factor(*Wj*)
	5	4	3	2	1	0	
Zn	<151	151-300	301-500	501-700	701-900	>900	1
Cu	<51	51-100	101-200	201-400	401-600	>600	2
Cd	<0.3	0.3-0.6	0.7-1.0	1.1-2.0	2.0-4.0	>4.0	5
Pb	<21	51-100	101-150	151-250	251-400	>400	3
Ni	<10.1	21-40	41-80	81-120	121-160	>160	1
Cr	<51	51-100	101-150	151-250	251-350	>350	3

2. RESULTS AND DISCUSSION

The characterization of compost and its comparison with FCO (Fertilizer Control Order) standard prescribed by Indian government and the standard of Hong kong are presented in (Table 3). The mean values of electrical conductivity revealed a significant difference among compost types as well as were lower than permissible limit of Indian standard which is <4 dS.m^{-1} .The total organic carbon is indicator of organic matter content of the compost, therefore the statistical analysis showed a significant different among the compost $p \leq 0.05$ The average value of total organic carbon (TOC) of both Dutch and Estonia were higher than the permissible limit of Indian standard which is >16, while the Percentage of TOC in local compost was 12.5% less than permissible limit of Indian standard. The TOC% was 16.5 for Indian compost is close to the permissible limit of Indian standard. The total organic matter (TOM) is important to compost quality parameters generally the total organic carbon values in all imported and local compost is greater than the permissible limit of Hon Kong standard which is ≥20, the higher percentage is 36.65 estimated from Dutch compost. Carbon and nitrogen ratios are a very important characteristics for estimation the compost maturity with respect to the organic matter and the nitrogen cycle, the carbon nitrogen ratio is directly related to the plant growth, because when the plant cultivated in soil amended with a compost have higher carbon nitrogen ratio the plant growth stunted and often yellow in color due to nitrogen deficiency arising out of nitrogen immobilization in that soil. Although the data analysis in this study refer to significant difference among the studied compost the carbon and nitrogen ratios are less than the permissible limit of Indian standard which is <20. The mean pH values of the composts were (6.63, 5.7, 6.01 and 7.15) for Indian, Dutch, Estonia and Local compost respectively, which were varied from the almost slightly acid and slightly alkaline , the pH vales of Dutch and Estonia were low as compared to FCO standard as recommended range 6.5-7.5, this result may related to the total organic matter% in both the Dutch and Estonia compost, because the organic matter decomposition released a organic acid such as humic acid which responsible on the pH lowering in compost. (Mandal *et al.*, 2014)

The nitrogen, phosphorus and potassium are important macronutrients of plant growth, however play important role in compost quality determination. The statistical analysis in (Table 3) show a significant difference among the compost for nitrogen, phosphorus and potassium. The higher values (2.9, 3.28 and 0.5%) for nitrogen, potassium and phosphorus were recorded in Dutch, Indian and local compost respectively, the Nitrogen % is higher than permissible limit of Indian standard, however the K% was more than permissible limit of Indian standard except in Dutch compost was less, while the phosphorus% in all compost are lower than permissible limit of Indian standard except in local compost was equal to the 0.5min in the FCO standard.

Non essential trace metals detection in compost is great important for the quality, not only because these elements necessary for protect the soil and water resource from pollution, but also their impact on human health. In general the average concentration of all heavy metals were lower than permissible limit of Indian standard except the average concentration of Hg in all compost was exceeded permissible limit of German and Hong Kong standards as well as the concentration of Cd in Estonia and local compost was higher than permissible limit of Indian standard ,particularly its concentration in Estonian is very higher, thus its unsuitable to agriculture use, because the exceeded heavy metals content limited the use of compost to the agriculture land, the impact of contaminated of compost by pollutants on environmental health is varies cording to soil properties such as texture and the plant species.(Zhao *et al.*, 2011).

The grades and marketability of compost depended largely on the fertilizer index and clean index, also these two indices provide the information about the quality of compost before its application for different purpose. The classification of compost based on marketability and use in accordance to fertilizer index (FI) and clean index (CI) are presented in (Table 4). The fertilizer index and clean index of imported and local compost are shown in (Fig1). The fertilizer index of compost was varied from 4.13 to4.47 where as the clean index was varied from 3.20 to 3.93, all compost has a fertilizer potential value >4 however the CI value of compost has medium heavy metals content, the statistical analysis in the present study indicated that imported and local compost has a good quality and proper for agriculture land.

Table 3 : Chemical characteristics of composts.

Compost types / Properties		Indian (C1)	Dutch (C2)	Estonia (C3)	Local production (C4)	FCO Indian standard	a Hong Kong Standard
EC dS.m^{-1}		0.80c	1.20b	1.10b	3.60a	<4.0	--
TOC%		16.50b	21.31a	18.90b	12.50c	16min	≥12%
TOM%		28.38b	36.65a	a32.51	21.50c	--	≥20%
C:N ratio		6:1	8:1	7:1	6:1	20max	≤25
pH		6.63b	5.70c	6.01c	7.15a	6.5-7.5	5.5-8.5
N %		2.74b	2.90a	2.67b	1.97c	0.5min	≥4%
K %		3.28a	0.90d	1.79c	2.61b	1.0min	
P %		0.33c	0.36c	0.42b	0.50a	0.5min	
Heavy metals mg.kg^{-1}	**As**	2.86a	0.83d	1.96b	1.52c	15-25c	≤13
	Cr	33.32b	43.21a	23.18c	36.38b	50	≤201
	Cd	1.80c	1.18c	28.40a	6.61b	5	≤3
	Pb	4.30c	19.90a	12.60b	6.40c	100	≤150
	Hg	14.50b	43.20a	3.90c	14.00b	1.0b	≤1
	Cu	2.18b	2.32b	3.02a	2.11b	300	≤700
	Ni	46.70a	39.90b	50.10a	33.70b	50	≤62
	Zn	27.20c	13.60d	41.90a	33.10b	1000	≤1300
Clean index		**3.87**	**3.93**	**3.20**	**3.27**		
Fertilizing index		**4.27**	**4.53**	**4.47**	**4.13**		

a :General agriculture use, b:Germeny standard, c:Netherland standard

The same letter are not significantly different among mean value at 0.05probabilty levels

The result of heavy metal indicated that the compost contain higher concentration of Hg when compared to the permissible limit of heavy metals standard in USA, UK, Australia and all E urope countries that produce and use compost, this may be due to the present of some electronic or textile waste during preparation these compost, thus attention should focused on the heavy metals particularly the As and Hg which has great impact on the environmental health particularly the soil health.

Table 4 : Classification of MSW compost for their marketability and use in different area. From (*Saha et al.,2010).*

Class	Fertilizer index	Clean index	Quality control compliance	Remark
A	>3.5	>4.0	Complying for heavy metal parameters	Best quality. High manurial value potential and low heavy metal content and can be used for high value crops, such as in organic farming
B	3.1-3.5	>4.0	Complying for heavy metal parameters	Very good quality. Medium fertilizing potential and low heavy metal content
C	>3.5	3.1-4.0	Complying for heavy metal parameters	Good quality. High fertilizing potential and medium heavy metal content
D	3.1-3.5	3.1-4.0	Complying for heavy metal parameters	Medium quality. Medium fertilizing potential and medium heavy metal content
RU-1	<3.1	-	Complying for heavy metal parameters	Should not be allowed to market due to low fertilizing potential. However, these can be used as soil conditioner
RU-2	>3.5	>4.0	Not complying for heavy metal parameters	"Restricted use. Should not be allowed to market. Can be used for growing non-food crops. Requires periodic monitoring of soil quality if used repeatedly"
RU-3	>3.5	-	Not complying for heavy metal parameters	Restricted use. Should not be allowed to market. Can be used only for developing lawns/gardens (with single application), rehabilitation of degraded land

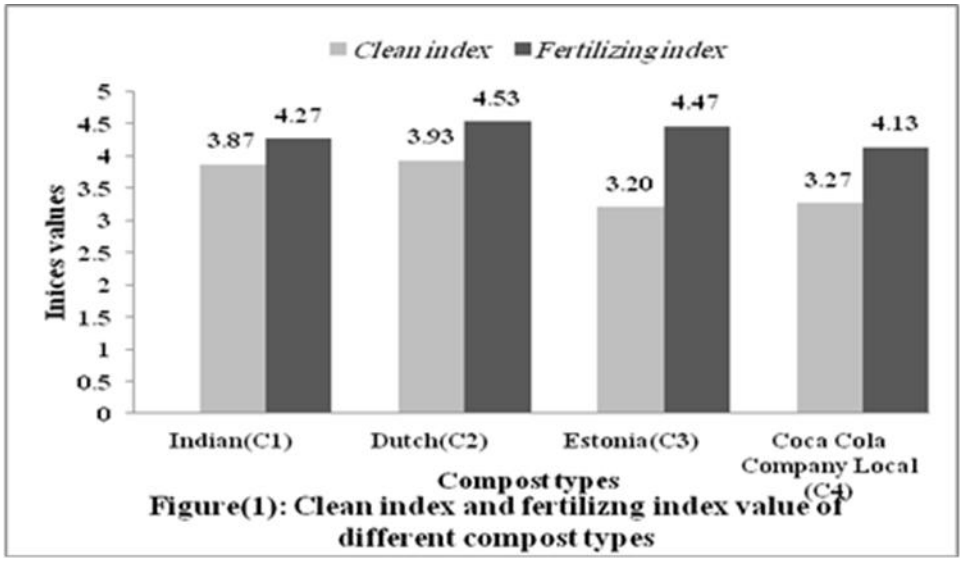

Figure(1): Clean index and fertilizng index value of different compost types

2. CONCLUSIONS

According to the fertilizer index and clean index the compost that imported and that which produce locally had high fertilizer potential and serves as nutrients source as well as the clean index refers to the present of the heavy metals as medium concentration, while the result of present study indicated that the compost contain high concentration of Hg when compared to the permissible limit of heavy metals standard in USA, UK, Australia and all Europe countries that produce and use compost, thus attention should concentrated on this manner before marketing and use of these compost, thus the present study suggested that the clean index equation must involved the Hg metals because there toxicity and harmful to environment and human via soil pollution.

Conflict of Interest

There is no conflict of interest.

References

ALLEN, S. E. 1974. Chemical analysis of ecological materials. Black well scientific publication Osney Mead, Oxford. pp: 64-214

BERA, R., DATTA, A., BOSE, S., DOLUI, A. K., CHATTERJEE, A. K., DEY, G. C., BARIK, A. K., SARKAR, R. K., MAJUMDAR, D. and SEAL, A. 2013. Comparative evaluation of compost quality, process convenience and cost under different composting methods to assess their large scale adoptability potentials also complemented by compost quality index, International Journal of Scientific and Research Publications, 3(6): p.1–11.

DOLUI, A. K., BANERJEE, S., BERA, R., DATTA, A., SAHA, S. and SEAL, A. 2014. Assessment of novcom composting method as an effective bio-degradation process and its impact on acid tea soils under various management practices, Journal of Recent Advances in Agriculture, 2(2): p.181–191.

JALAL S. Y. 2016. Applied Compost Quality indices for Assessment Different Composting Methods by Using Household Solid Waste. M.Sc thesis of College of Science, Salahaddin University-Erbil.

MANDAL, P., CHATURVEDI, M. K., BASSIN, J. K., VAIDYA, A. N. and GUPTA, R. K. 2014. Estimating the quantity of solid waste generation in oyo, Int J Recycl Org Waste Agricult., 3: p.133–139.

MORA, A. P.; BURGOS, P.; MADEJO´N, E.; CABRERA ,R.; JAECKEL, P.; SCHLOTER, M. 2006. Microbial Community Structure and Function in a Soil Contaminated By Heavy Metals: Effects of Plant Growth and Different Amendments. Soil biology and biochemistry. 38:327-341.

PANSU,M, and GAUTHEYROU,J. 2006 .Handb ook of soil Analysis.Springer-velageBerlin Heidelberg.3:1-38.

RICHARDS, L. A. 1954. Diagnosis and Improvement of Saline and Alkaline Soils United States Salinity Laboratory Staff, USA. Hand Book No.60

SAHA, J. K., PANWAR, N. and SINGH, M. V. 2010 . An assessment of municipal solid waste compost quality produced in different cities of India in the perspective of developing quality control indices, Waste Management, 30: p.192–201.

SINGH, J. and KALAMDHAD, A. S. 2012 . Reduction of Heavy Metals during Composting. International Journal of Environmental protection. 2(9):36-43.

STEEL, R.G.D and TORRIE, J.H. 1969. Principle and Procedures of Statistics. McGraw Hill, New York.481pp

TORKASHVAND, A. M. 2010 . Improvement of compost quality by addition of some amendments, Australian Journal of Crop Science, 4(4): p.252–257.

ZHAO S,I,JAN and, DUO,I. 2011. EDTA associated phytoextraction of heavy metals by turf grass from municipal solid waste compost using permeable barriers and potential leaching risk. Bioresour.Tech.102:621-626.

ZANCO Journal of Pure and Applied Sciences
The official scientific journal of Salahaddin University-Erbil
https://zancojournals.su.edu.krd/index.php/JPAS

ISSN ():, ISSN ():, DOI: http://dx.doi.org/10.21271/zjpas

RESEARCH PAPER

Interrelation ship between honey bee workers activity and artificial foods

Azad h. Saleh[1], Abdulbaset M. Amin[2], Khalis A. H. Ameen[3]

1- Deparment of Plant Protection ,College of agriculture , Salahaddin University-Erbil, Kurdistan region, Iraq.

2- Department of Forestry ,College of Agriculture,Salahaddin University-Erbil, Kurdistan region, Iraq.

3-Ministry of Agriculture and Water Resources-Kurdistan region of Iraq

A B S T R A C T:

This study was conducted in March 2015 during seasonal period; spring, early summer, late summer and autumn respectively at the apiary of the Grdarasha research station of Agriculture College, Salahaddin University - Erbil / Kurdistan Region- Iraq. The result showed that the highest numbers of workers prefer fed on dry yeast was 529.000 workers inside the hives and 252.333 workers outside the hives. The highest average age of longevity was 31.5 days when fed on dry yeast and the lowest average was 26.0 days fed on bean. The highest percentage of protein content in workers body was 48.922% fed with dry yeast and the lowest was 40.915% fed with bean. The workers fed on dry yeast gave the higher resistant to cooling at 15°C for 14 days, at 12°C for 11days at 8°C for 8 days and at 4°C 6 days for both dry yeast and broad bean. The workers fed with bean and sugar solution gave the lower resistant to cooling at 15°C for 11 days, at 12°C for 10 days, at 8°C for 6 days, at 4°C for 5 days. The highest average of body weights of mature larvae fed on dry yeast was 106.20 mg but the lowest was 79.45 mg fed on bean in spring season. The highest body weight of ten day old workers was 121.15 mg fed on broad bean and the lowest was 102.95 fed on bean in spring season.

KEY WORDS: honey bee, Supplementary food, activity, worker bee.
DOI: http://dx.doi.org/10.21271/ZJPAS.31.4. 14
ZJPAS (2019) , 31(4);129-138 .

INTRODUCTION :

Beekeeping and honey production were well known to the ancient Kurdish people, the honey has become one of the important foods in Kurdistan. In northern part of our country Erbil governorate, summer season is so longer and hot as compared to other parts. The natural bee flora starts disappearing for the months causing dearth of food (pollen and nectar) for bees.

* **Corresponding Author:**
Khalis A Hamad Ameen
e.mail: Khalisahmed2006@yahoo.com
Article History:
Received: 03/10/2018
Accepted: 12/05/2019
Published: 10/09/2019

The periodical dearth periods of pollen result into low nutritional reserves which adversely affect the colony performance due to stoppage or reduction of egg laying, brood rearing and low honey production.

The necessity of artificial diets to honey bees has been long-standing interest to the beekeeping industry. Pollen grains, nectar and honey are the necessary constituent for the growth and development of the honey bee. (Haydak 1967).Heinrich (1979) indicated that honey bees drop into a cold comatose condition when the temperature decreased below 10 C° and could not voluntary recover without external warming. Dietz et al., (1989) found that both Africanized and European honey bee colonies died when exposed to the temperature

0C°. Targany (2008) found that the workers tolerated cold temperature dependent on different types of foods. Daly and Morse, 1991; Shamdin ,2003 and Bas ,2013. Mentioned that the amount foods of honey bee larvae had effects on adult body weight

1. MATERIALS AND METHODS

This study was conducted at the apiary of the Grdarasha research station of agriculture college, 10 km south of the college of Agriculture – salahaddin university in Erbil in march, 2015 in order to study the effect of some supplemental foods on the honey bees activities and production of (broods, honey, wax and pollen) during spring, early summer, late summer and autumn seasons under field condition. At the beginning of the research sixteen colonies of *Apis mellifera* were selected from apiary depending on the following characters:

For measurement, two langstroth frames were prepared, first then changed in way by dividing each frame in to 17 inch (43.2 cm) in length and 8 inch in width, holes made to each frame fastening wires (silk) which was across of two wires equal in length and wide with one square inch in a way that the total number of the inch were equal to 136inch.(Targany, 2008 and Bas, 2013).

Sugar solution (control) : Sugar solution was prepared by dissolving one kilo gram of crystal sugar in one liter of water after the water was heated to 70°C, each colony was supplied with one liter of sugar solution at the same concentration weekly during different season (spring, early and late summer and autumn). The ratio of concentration was 1:2 in summer 1:1in spring and autumn (Targany, 2008 and Bas, 2013).

The prepared food was given to the bees by using plastic bottles which was put on the frames in the hive. The bottle cover was pierced circularly in an appropriate way to allow the food came down gradually and the bottle were put on two pieces of wood to allow the bees reach the food and eat them, the wood under the bottle was 10cm long and 1.5cm wide.(Targany,2008).

Samples were taken from experimental colonies containing a considerable number of labeled workers with known ages on colony inspection (Bas, 2013).

Studying the food preference and acceptance by the honey bees for all the replicates and for a period of four continuous days at three different times (9-10,12-1,3-4) hourly of the day and calculated the number of honey bee worker coming to feed on the food inside and outside the hives in the each replicate for 45minutes at the day (Targany, 2008).

For determination of honey bee longevity were numbers of honey bee workers caged for each treatment contained (60 workers) of different ages in small cages with small empty piece of comb used for water and fed on the same prepared food the caged worker bees with the food were put in the hive to determine their longevity monitoring calculating the dead bees and adding food to them when needed to avoid bee death during shortage of food (Abou-EL-Enain *et al*, 2006 and Targany 2008).

The climatic information was taken from Erbil General Directorate of Metrology and Seismology.

The results were analyzed statistically using factorial design with four replicate.

Statistical analysis was performed using SAS program (2002-2003), version 9.1; Duncan's multiple range Test was used to determine the differences between means at P= 0.05.

2. RESULTS AND DISCUSSION

Table (1) shows that the worker bees prefer feeding on dry yeast plus sugar solution inside and outside the hive then sugar solution, broad bean plus sugar solution and finally bean plus sugar solution. The highest numbers of workers prefer fed on dry yeast were 529.000 workers inside the hives but outside the hives was 252.333 workers. Statistical analysis showed significant difference at level 0.05 between treatments and prefer the foods where the superiority of dry yeast plus sugar solution in comparison with other treatments. The result agreed with Al-Sharhy and Al-Ghamdi (٢٠٠٦) who indicated that honey bee colonies fed on a mixture of yeast meals with gluten or yeast has

a high palatability by bees similar to palatable natural commercial pollen, with Hayes (1984) who recommended that the soybean flour and yeast added to candy as the food to be given to colonies in the spring. AL-Ghamdi (2002) who observed that the Carniola bee colonies which were fed on pollen supplementary feeding during the experiment period indicated to the highest level of population density, brood rearing, pollen and honey storage compared with the control colonies which were only fed on natural food sources and the number of combs covered with bees in colonies supplement with patty increased gradually. Al-anssari(1998) stated that the beekeepers often feed their colonies by alternative food or complementary food during the summer to make up for the shortage of both pollen and nectar.

Table (1): Food preference by honey bee workers in and outside the hives during different times of day /2015.

Food	Times of day (9-10, 12-1, 3-4) hours		Means
	Inside	Outside	
Sugar solution	502.333 B	229.333 f	365.833 b
Broad bean	455.667 C	144.000 g	299.833 c
Dry yeast	529.000 A	252.333 e	390.667 a
Bean	349.333 D	93.000 h	221.167 d
Means	459.083 A	179.667 b	

Means with the same letter are not significantly different at the level 0.05.

Table (2) shows the effect of some supplemental food on the caged honey bee workers in the hive and fed on sugar solution was 26.500 days and the longevity ranged between 13-40 days, while the average age of the workers fed on broad bean plus sugar solution was 29.500 days and the longevity ranged between 16-43 days, but the workers fed on dry yeast plus sugar solution reaged 31.500 days and the longevity ranched between 18-45 days and the workers fed on bean plus sugar solution was 26.00 days and the longevity ranged between 13-39 days. The highest average age was 31.500 days treated with dry yeast and compared with the lowest average was 26.00days fed on bean. Statistical analysis showed significant differences at level 0.05 between dry yeast and other treatments. The results agreed with El-banby and Gorgui (1970) who revealed that the average age of the longevity of workers when fed on the sugar syrup was (23.42) days while fed corn flour and sugar syrup is 31.35 days and fed a mixture of skim milk, corn flour and sugar syrup (1:2) lived (29.63) days and the average age of workers fed on brewers yeast with skim milk and corn flour and sugar solution was (34.47) days and with Abdullah (1988) who found the effect of nutrition on longevity of caged workers bee was less than the average age of 27.8 days when feeding honey, while the average age of the worker bees fed on soybeans, sugar syrup, sucrose syrup plus soybean and skim milk were (53.28, 29.16, 34.22) days respectively while Jevral protein was (50.55) days. Abou El- Enain, *et al*., (2006) stated that the age rates for the cages bee it were (15.07, 28.94, 23.0, 15.13, 16.31) days for all deist soybeans, wheat germ, dry yeast, palm dates and sugar syrup respectively, and wheat germ treatment superior of incorporeally the rest of the treatments, said that the cause this is due to the protein content of wheat germ. Targany (2008) who recorded the average age of caged workers bee in the hive when fed on sugar syrup, apricot juice plus sugar syrup, feramil plus sugar syrup and corn flour plus skim milk plus sugar syrup amount to (27.510,36.220, 42.720, 45.310) days respectively and showed the superior of apricot and feramil on other diets. El-Hady, (2012) who showed the longest mean of age at (16 –18 days) when the newly emergence workers fed on soybean cake. Irandoust and Ebadi (2013) showed that the highest longevity of caged honey bees was (61 days) fed with Wheat gluten supplement and lowest (9.2 days)

longevity fed with lentil substitute of bees in 50% mortality, while in 100% morality pollen and lentil substitutes caused the highest (143.5 days) and lowest (20.7 days) longevity of bees, respectively.

Table (2): Effect of some supplemental food on longevity of worker bees in the hives /2015.

Food	Number of workers	Range of dates	Means of workers longevity
Sugar solution	60	13-40	26.500 b
Broad bean	60	16-43	29.500 ab
Dry yeast	60	18-45	31.500 a
Bean	60	13-39	26.00 b

Means with the same letter are not significantly different at the level 0.05.

The temperature 15°C: The percentage mortality started among all workers of all treatment at the 24 hours 1day to reach 6.66%, 8.33%, 6.66% and 6.66% respectively as shown in table (3/A). The percentage of mortality rate was reached 100% at the 11 days for treatment of sugar solution and bean, at the 12 days for treatment of broad bean, at the 14 days for treatment of dry yeast. The treatment of dry yeast gave the high energy for tolerant than other treatments.

The temperature 12°C: The percentage mortality started among all workers of all treatment at the 24 hours 1day to reach 8.33%, 6.66%, 6.66 % and 6.66 % respectively as shown in table (3/B). The percentage of mortality rate was reached 100% at the 10days for treatments of sugar solution and bean, at the 11 days for both treatment of broad bean and dry yeast.

The temperature 8°C: The percentage mortality started among all workers of all treatment at the 24 hours 1day to reach 18.33%, 11.66%, 6.66%, and 11.66 % respectively as shown in table (3/C). The percentage of mortality rate was reached 100% at the 6days for both treatments of sugar solution and bean, at the 7 days for treatment of broad bean, at the 8days for treatment of dry yeast. The treatment by dry yeast was more tolerant the cool temperature of other treatments at the 8°C.

The temperature 4°C: The percentage mortality started among all workers of all treatment at the 24 hours 1day to reach 18.33%, 23.33%, 26.66% and 26.66% respectively as shown in table (3 /D). The percentage of mortality rate was reached 100% at the 5days for treatments of sugar solution and bean, at the 6days for treatments of broad bean and dry yeast. The treatment of dry yeast and broad bean gave more tolerant the cool temperature at 4°C. These results agreed with Shamdin (2003) who recorded that the workers in caged which fed by vitamin C with sugar solution remained on lived at the 5°C for 5days, at the 10 °C for 7days and at the 15°C for 16 days. Villa and Rinder (1993) who found that the worker in caged lower significantly amounts of sucrose syrup at 15 °C. Bas (2013) who recorded that the caged workers bee fed on vitamin C tolerated the cold temperature when exposed to 15°C for 15 days, 10°C for 7 days , 5°C for 7 days, on other hand disagreed with Targany (2008) who found that the workers tolerated cold temperature dependent on different types of foods the workers when exposed at 15 C. for longer period of cold temperature about 156 hours fed of apricot juice, feramil, sugar solution and corn flour respectively while about 120 hours at 8°C. ,72 hours at 6°C and 60 hours at 4°C while workers fed on apricot juice and feramil for longer period to tolerated cold temperature when exposed at 0°C for 24 hours, at 4°C for 60 hours, at 8 °C for120 hours, at 15°C for 156 hours.

Table (4) shows the effect of some supplemental food on body weights of mature larvae supplemented with sugar solution, broad bean, dry yeast and bean in spring season were 83.00, 96.95, 106.20 and 79.45 mg respectively. The highest average was 106.20 mg fed on dry yeast while the lowest average was 79.45 mg fed on bean. Statistically significant difference at level 0.05 between treatments and body weight of mature larvae fed on dry yeast where superior compared with other treatments.

The average of body weights of mature larvae supplemented with sugar solution, broad bean, dry yeast and bean in early summer season were 85.30, 91.20, 99.80 and 77.85 mg respectively. The highest average was 99.80 mg fed on dry yeast while the lowest average was 77.85 mg fed on bean. Statistically shows significant difference at level 0.05 between treatments and body weight of mature larvae fed on dry yeast where superior compared with other treatments.

The average of body weights of mature larvae supplied with sugar solution, broad bean, dry yeast and bean in late summer season were 87.20, 93.65, 100.80 and 76.80 mg respectively. The highest average was 100.80 mg fed on dry yeast while the lowest average was 76.80 mg fed on bean. Statistically, there was significant difference at level 0.05 between treatments and body weight of mature larvae fed with dry yeast where superior compared with other treatments.

The average of body weights of mature larvae supplemented with sugar solution, broad bean, dry yeast and bean in autumn season were 81.85, 86.90, 98.50 and 75.90 mg respectively. The highest average was 98.50 mg fed on dry yeast while the lowest average was 75.90 mg fed on bean.

Statistically, there was significant difference at level 0.05 between treatments and body weight of mature larvae fed on dry yeast where superior compared with other treatments. Statistically had significant differences at level 0.05 between treatments and body weight of mature larvae in four seasons fed on dry yeast where the superiority in comparison with other treatments. Statistically the effect of supplemental foods there were a significant difference between the body weight and foods, dry yeast considered as a best food compared with other treatments as shown in table (4). These results agreed with Shamdin (2003) who recorded that the highest rates of weights was (126.58mg) of the mature larvae fed with soya bean. Bas (2013) record highest rate of body weights (mg/larva) of mature larvae fed with gevral protein were 121.50, 116.20 and 112.03 in spring, summer and autumn respectively.

Table (5 /A, B, C and D) shows the effect of some supplemental food on body weights of workers from four treatments with four ages in spring, early summer, late summer and autumn seasons. The comparison among the body weight in each ages showed significant differences at level 0.05 between treatments in all seasons. Highest weight of one day old workers was 111.45 mg fed on dry yeast in autumn season while the lowest weight was 83.02 mg fed on bean in early summer. The highest mean of body weight was 104.91 mg fed on dry yeast and lowest was 86.85 mg fed on bean. The highest body weight of ten day old workers was 121.15mg fed on broad bean in spring season while the lowest body weight was 81.32 mg fed on bean in early summer and the highest mean of body weight was 112.76mg fed on dry yeast and lowest was 89.17mgfed on bean. The highest body weight of twenty day old workers was 98.60 mg fed on dry yeast in early summer season while the lowest body weight was 70.55 mg fed on bean in early summer. Also the highest mean of body weight was 94.33mg fed on dry yeast and lowest was 73.28mgfed on bean. The highest body weight of thirty day old workers was 94.32 mg fed on dry yeast in spring season while the lowest body weight was 66.62 mg fed on bean in late summer. The highest mean of body weight was 87.60 mg fed on dry yeast and lowest was 69.04mg fed on bean. Figure 1, 2, 3, and 4 shows the effect of supplemental food on the body weight in different seasons.

The results agreed with Daly and Morse (1991) who mentioned that the amount foods of honey bee larvae had effects on adult body weight. Shamdin (2003) found highest rate body weight of one day old was (109.15mg) and (91.14mg) thirty day old workers when fed on soy bean.

De Groot (1953) who observed that the mean dry weight of worker bees 28 days old lower than worker bees 14 days old was (20.7 and 22.4 mg).

Ayoub (2011) who found that the weight of 10 days old workers higher than the body weight of newly emerged and forager workers. Bas (2013) who recorded the highest rate of body weight of newly emerged workers

in colonies fed with gevral protein was 113.60 mg/ workers in autumn season and The highest body weight of seven day old workers in colonies fed with gevral protein was 123.97 mg. in spring season, The highest body weight of twenty one day old workers in colonies fed with apricot juice was 97.33 mg in summer season and the highest body weight of twenty eight day old workers in colonies fed with gevral protein was 96.73 mg. in spring season. Disagreed with Winston (1987) who stated the weight of honey bee workers ranged from 81-140 mg.

Table (6) shows the effect of some supplemental food on length and width of body dimension of the mature larvae fed on sugar solution, broad bean, dry yeast and bean in different seasons. In spring season, the length were 8.77, 9.28, 9.65 and 8.75 mm respectively. The width were 4.11, 4.13, 4.29 and 4.10mm respectively. Highest average length was 9.65 mm fed with dry yeast while the lowest average length was 8.75 mm fed with bean. In early summer season the length were 8.59, 9.35, 9.42 and 8.65 mm respectively. The width were 4.12, 4.14, 4.20 and 4.11 mm respectively. The highest average length was 9.42 mm fed with dry yeast while the lowest average length was 8.59 mm fed with sugar solution. In late summer season the length were 8.51, 8.99, 9.25 and 8.57 mm respectively. The width were 4.11, 4.43, 4.50 and 4.16 mm respectively. The highest average length was 9.25 mm fed on dry yeast while the lowest average length was 8.51 mm fed on sugar solution. In autumn season the length were 8.48, 8.95, 9.21 and 8.45 mm respectively. The width were 4.10, 4.13, 4.20 and 4.10 mm respectively. The highest average length was 9.21 mm fed on dry yeast while the lowest average length was 8.45 mm fed on bean.

The effect of foods on body dimensions the highest length of dry yeast was 9.38 mm where superior in compare with the lowest average length was 8.59mm in sugar solution. The highest average width was 4.29 mm fed with dry yeast where the superior in comparison with the lowest average width was 4.11 for each of the sugar solution and bean. Statistically there were insignificant difference between treatments and average length and width except bean and sugar solution. The effect of season on body dimensions the highest average length in spring season compared with other seasons and the highest width in late summer season. The result agreed with Bas (2013) who recorded highest rates of length of body dimensions of mature larvae were 9.93, 9.57 and 9.20 mm. in colonies fed with apricot juice in spring, gevral protein in summer and autumn seasons respectively. Shamdin (2003) who recorded that the highest rate of length was 12.16mm and the highest rate of width was 4.27mmbut without significant difference between treatments and body dimension.

Table (3/A): The percentage of mortality of the workers fed on some supplemental food at 15°**C**.

Food	Mortality of workers %													
	1st day	2nd day	3rd day	4th day	5th day	6th day	7th day	8th day	9th day	10th day	11th day	12th day	13th day	14th day
Sugar Solution	6.66	7.14	9.61	12.76	14.64	20.00	25.00	28.57	33.33	60.00	100			
Broad bean	8.33	7.27	7.84	10.63	14.28	16.66	20.00	25.00	27.77	38.46	75.00	100		
Dry yeast	6.66	7.14	7.69	8.33	13.63	15.78	12.50	14.28	16.66	20.00	25.00	33.33	62.50	100
Bean	6.66	9.92	11.76	13.33	17.94	21.87	24.00	26.31	35.71	66.66	100			

Table (3/B): The percentage of mortality of the workers fed on some supplemental food at 12°**C**.

Food	Mortality of workers %										
	1st day	2nd day	3rd day	4th day	5th day	6th day	7th day	8th day	9th day	10th day	11th day
Sugar solution	8.33	9.09	12.00	13.63	18.42	22.58	29.16	47.05	77.77	100	
Broad bean	6.66	7.14	7.69	8.33	9.09	22.50	22.58	29.16	41.17	60.00	100
Dry yeast	6.66	7.14	9.61	12.76	14.63	17.14	24.13	31.81	46.66	75.00	100
Bean	6.66	7.14	15.38	18.18	25.00	37.03	41.17	50.00	80.00	100	

Table (3/C): The percentage of mortality of the workers fed on some supplemental food at 8°**C**.

Food	Mortality of workers %							
	1st day	2nd day	3rd day	4th day	5th day	6th day	7th day	8th day
Sugar solution	18.33	20.40	35.84	52.00	58.33	100		
Broad bean	11.66	20.75	21.42	36.36	42.85	58.33	100	
Dry yeast	6.66	12.50	16.32	24.39	35.48	50.00	60.00	100
Bean	11.66	22.64	26.82	43.33	64.70	100		

Table (3/D): The percentage of mortality of the workers fed on some supplemental food at 4°**C**.

Food	Mortality of workers %					
	1st day	2nd day	3rd day	4th day	5th day	6th day
Sugar solution	18.33	24.48	45.94	75.00	100	
Broad bean	23.33	30.47	34.37	42.85	66.66	100
Dry yeast	26.66	29.54	48.38	50.00	62.50	100
Bean	26.66	36.36	46.42	66.66	100	

Table (4): Effect of supplemental food on the body weight of mature larvae (mg)

Food	Weight of mature larvae(mg)				Means
	Spring season	Early summer season	Late summer season	Autumn season	
Sugar solution	83.00 fg	85.30 f	87.20 ef	81.85 f-h	84.33 c
Broad bean	96.95 bc	91.20 de	93.65 cd	86.90 ef	92.17 b
Dry yeast	106.20 a	99.80 b	100.80 b	98.50 bc	101.35 a
Bean	79.45 g-i	77.85 g-i	76.80 hi	75.90 i	77.50 d

Means	91.40 a	88.53 b	89.61 ab	85.78 c	

Means with the same letter are not significantly different at the level 0.05.

Table (5/A): Effect of some supplemental food on body weight of one day old workers (mg).

Food	weight of one day old worker(mg)				Means
	Spring season	Early summer season	Late summer season	Autumn Season	
Sugar solution	99.15 ef	90.32 h	95.27 g	95.02 g	94.94 c
Broad bean	103.65 bc	96.65 fg	100.12 de	101.67 c-e	100.52b
Dry yeast	102.65 b-d	100.32 de	105.22 b	111.45 a	104.91 a
Bean	94.12 g	83.02 j	84.25 ij	86.02 i	86.85d
Means	99.89 a	92.58 c	96.21 b	98.54 a	

Means with the same letter are not significantly different at the level 0.05.

Table (5/B): Effect of some supplemental food on body weight of ten day old workers (mg).

Food	weight of ten day old worker(mg)				Means
	Spring season	Early summer season	Late summer season	Autumn Season	
Sugar solution	112.30 cd	98.22 i	100.18 hi	105.15 fg	103.96 b
Broad bean	121.15 a	101.65 g-i	106.83 ef	113.17 b-d	110.70a
Dry yeast	116.75 a-c	106.77 ef	110.22 de	117.32 ab	112.76a
Bean	102.95 f-h	81.32 k	83.07 k	89.35 j	89.17c
Means	113.28 a	96.99 d	100.08 c	106.25 b	

Means with the same letter are not significantly different at the level 0.05

Table (5 /C): Effect of some supplemental food on body weight of twenty day old workers (mg).

Food	weight of twenty day old worker(mg)				Means
	Spring season	Early summer season	Late summer season	Autumn season	
Sugar solution	80.75 d	79.12 de	80.82 d	83.65 cd	81.08 c
Broad bean	91.15 b	92.02 b	82.27 cd	85.75 c	88.80 b
Dry yeast	95.17 ab	98.60 a	93.23 b	94.35 ab	94.33a
Bean	75.60 ef	70.55 g	72.40 fg	74.60 fg	73.28 d
Means	85.66 a	85.07 a	82.18 b	84.58 a	

Means with the same letter are not significantly different at the level 0.05.

Table (5 /D): Effect of some supplemental food on body weight of thirty day old workers(mg).

Food	weight of thirty day old worker(mg)				Means
	Spring season	Early summer season	Late summer season	Autumn season	
Sugar solution	71.57 gh	76.65 f	70.82 gh	80.12 e	74.79 c
Broad bean	83.07 de	81.72 de	75.35 f	84.97 cd	84.09 b
Dry yeast	94.32 a	90.17 b	87.77 bc	89.37 b	87.60 a

Bean	68.02 hi	68.37 hi	66.62 i	73.15 fg	69.04 d
Means	79.25 b	79.23 b	75.14 c	81.90 a	

Means with the same letter are not significantly different at the level 0.05.

Table (6): Effect of some supplemental food on body dimension of mature larvae.

Food	Body dimensions of mature larvae (mm)								Food effect	
	Spring season		Early summer season		Late summer season		Autumn season			
	Length	Width	Length	Width	Length	Width	Length	Width	L	W
Sugar solution	8.77 de	4.11 cd	8.59 e-g	4.12 c	8.51 fg	4.11 cd	8.48 G	4.10 cd	8.59 c	4.11 c
Broad bean	9.28 b	4.13 bc	9.35 b	4.14 bc	8.99 cd	4.43 a	8.95 D	4.13 bc	9.14 b	4.20 b
Dry yeast	9.65 a	4.29 b	9.42 ab	4.20 bc	9.25 b	4.50 a	9.21 Bc	4.20 bc	9.38 a	4.29 a
Bean	8.75 d-f	4.10 d	8.65 d-f	4.11 c	8.57 e-g	4.16 bc	8.45 G	4.10 cd	8.60 c	4.11 c
Season effect	9.11 a	4.15 b	9.00 a	4.14 b	8.83 b	4.30 a	8.77 b	4.13 b		

Means with the same letter are not significantly different at level 0.05.

REFERENCES

Abdulla, M.A.(1988).Effect of diet with high protein content on the activity of honeybee (*Apis Mellifera* L.).M.Sc.Thesis, Mosul.University.155. (cited by Targany,2008).

Abou-EL-Enain, H.T.,Omer, R.E., Khattap, M.M., Azap, M.M. and Younis,M.S.(2006). Effect of pollen substitutes on some different activities in honey beecolonies. J, Agric.Sci.Mansoura Univ.,31(8):5407-5416.

Al-Anssari, O.M.N.(1998).The bees in honey production and crops pollination.AL-Askandaria University, Egypt, 1336.(in Arabic).

Al-Ghamdi, A. (2002).The effect of pollen supplementary feeding on someactivities of honey bee colonies during summer season in Riyadh, Saudi Arabi.Saudi J.Biolo.Sci.,9: 85-93.

Al-Sharhy, M.M.and Al-Ghamdi, A. (2006).The effect of summer feeding withpollen substitute on the honey bee colony activation in brood rearing and honey production.Plant protection. College of foods and agriculture sciences, SaudiArabia, king Saud. Univ.,1-20.(in Arabic).

Ayoub, Z. N. (2011). Workers ontogeny in queen less or brood less colonies ofhoney bees (*Apis mellifera* L.). Ph.D. Thesis, Faculty of Biology and Earth Science, Jagiellonian University, Poland.,: 92.

Bas, S. M. A (2013) A study of the effect of some pollen supplemental food on body organs of honey bee workers and their activities *Apis mellifera* L. (Hymenoptera: Apidae). M.Sc. Thesis, College of Agriculture.Univ ofDohuk. 139.

Daley, H.V. and Morse, R. A. (1991). Abnormal sizes of workers honey bees (*Apismellifera* L.). reared from drone comb (Hymenoptera: Apidae). J. KansasEntomol. Soc., 64: 193-196.

De Groot , A.P. (1953). Protein and amino acid requirements of the honeybee (*Apismellifica* L.).

Laboratory of Comparetive Physiology, University,Utrecht. 197-285.

Dietz, A., Leitner, J. F.,Vergara, C. and Mejia, M. (1989). Effect of prolonged confinement in a refrigerator chamber on the survival of Africanized and European honey bee colonies. Amer.Bee J.,129: 815.

El-banby, M.A. and Gorgui,W.A. (1970) Development of trany bees whose coloniesare fed on sugar syrup utrition and pollen substitutes. Apiacta 1: 3-8.

Hayes, J.V. (1984). Supplemental feeding of honey bees.Amer.Bee J.1: 35-37.

Heinrich, B.(1979). Thermoregulation of African and European honey bees duringforaging, attack and hive exist and returns.J.Exp.Biol.80: 217-229.

Irandoust, H. and Ebadi, R. (2013).Nutritional effects of high protein feeds ongrowth, development, performance and overwintering of honey bee (*Apismellifera* L.).Int. J. Adv. Biol. Biom. Res.,1(6):601-613.

SAS.Statistical analysis system.(2002-2003) User's guide for personal computer. Release V.9.1 SAS institute inc. Cary, NC, USA.

Shamdin,Z.N. (2003). Effect of supplemental protein and vitamins on the development of specific tissues with and different kinds of pollen substitutes. Res. Bull.FacAgric., Ain shams. Uni., 610: 1-22.

El-Hady, A. M. E. (2012). Influence of some pollen substitutes on brood rearing of honey bee and workers longevity.J. Plant Prot. Path., Mansoura Univ., 3(3): 299 – 306**.**

Haydak , M. H. (1967).Bee n

special concern to their fine structures inrelation to the activity of honey bee workers *Apis mellifera* L. (Hyminoptera:Apidae).M.Sc.Thesis, College of Agriculture. Univ.of Dohuk.101.

Targany, Y. M.A. (2008). Effect of rich proteins diet on the activities of honey beeColonies *Apis mellifera* L.(Hymenoptera:Apidae) M.Sc. Thesis. College of Agriculture .Univ of Salahaddin, Erbil.,126.

Villa, J. D. and Rinder, T. E. (1993). Cold room thermoregulation, store consumptionand survival of Africanized and European honey bees (Apis mellifera L.). Honeybees breeding. Genetics physiology research.Apidologia., 24(4): 411- 423.

Winston, M. L. (1987).The biology of the honey bees.cambridge. Harvard university press.

ZANCO Journal of Pure and Applied Sciences
The official scientific journal of Salahaddin University-Erbil
https://zancojournals.su.edu.krd/index.php/JPAS

ISSN (print):2218-0230**, ISSN (online):** 2412-3986**,DOI: http://dx.doi.org/10.21271/zjpas**

RESEARCHPAPER

Effect of different cadmium levels on growth and biochemical parameters of Cyprinus carpio fingerlings reared in a close system.

Marwa A. Yaseen [1], Siraj M. A. Goran [2]

[1,2]Department of Environmental Science, College of Science, Salahaddin University-Erbil, Kurdistan Region, Iraq

A B S T R A C T:

Five experimental diets were formulated to feed *Cyprinus carpio* fingerlings. The diet contained $CdCl_2.H_2O$ as a source of pollutant with levels 0, 0.5, 1, 2 and 3 mg /KgDW as well as the feed contained 28% crude protein and 8% crude lipid. The experiment last for 71 days in Aquaculture breeding unit in College of Science, University of Salahaddin, Erbil. The diets were hand-fed to fish twice a day at 3 % of fish body weight. Fish exposure to 0.5, 1 and 3 mg/kg Cd for 71-days caused an increase in the levels of both Alanine Transaminase (ALT) and Aspartate Aminotransferase (AST) enzymes of *C. carpio*. Negative correlation was found among High Density Lipoprotein (HDL) with triglyceride, amylase, Glutamic-Pyruvic Transaminase (GPT), Glutamic oxaloacetic transaminase (GOT) and Alkaline phosphatase level (ALP). by increasing Cd concentration, serum cholesterol levels were decreased. Significant Positive correlation were observed between mass gain and fish growth rate, body final weight and survival, while negative correlation found between fish growth rate, mortality and feed conversion ratio (FCR) during this study.

Water samples were collected weekly from the experimental tanks for evaluation of physical and chemical properties. The range of temperature and turbidity of studied water samples during the study period were (22.75 to 25.47 ^{o}C) and (0.4 to 4.2 NTU) respectively. The minimum values of total hardness, reactive phosphorus (PO_4^{-3}), ammonia (NH_3) and nitrate (NO_3) for measured water samples were 220 mg.$CaCO_3$.l^{-1}, 4.063 mg.l^{-1}, 0.067 mg.$l^{-1}$and 37.088 mg.l^{-1}, while the maximum values were 277.5 mg.$CaCO_3$.l^{-1}, 15.05 mg.l^{-1}, 1.356 mg.l^{-1} and 45.622 mg.l^{-1} respectively.

KEYWORDS: Cadmium; Growth; Biochemical Parameters; *Cyprinus carpio*.
DOI: http://dx.doi.org/10.21271/ZJPAS.31.4.15
ZJPAS (2019) , 31(4);139-152 .

INTRODUCTION :

Water is one of the most essential necessities for fish farming (Mohammed and Bamarni, 2019). Quality and quantity of water is important for aquaculture (Summerfelt, 2000). Fish species discharge various waste products, such as ammonium, carbon dioxide, and organic material containing nutrients.

***Corresponding Author:**
Marwa A. Yassen
E-mail: marwa_chalabi@yahoo.com
Article History:
Received: 03/04/2019
Accepted: 22/05/2019
Published: 10/09 /2019

Feeding will affect the physical and chemical state of water and pollute the water through left-overs of feed, excrements, supplied organic matter to the water, which, consume oxygen and release ammonia (Val *et. al.*, 2006).

The most serious danger to fish production is poor water quality and deficiency of acceptable quantity of water (Bert, 2007).

Biological and physico-chemical properties of water offers appropriate conditions for the survival of fish as well as other organisms which create essential components of the food chain and affects survival and growth of

organisms (Gupta and Gupta, 2006; Aziz and Rasheed, 2017).

Heavy metals carry a wide variety of challenges to aquatic organisms, especially to fish. These pollutants are uncommon and make disturbance (Clarke, 1993), because of their toxicity, persistence and tendency for bio-accumulation in food chains (Wani, 1986).

Cadmium is toxic and derives from the natural reservoirs, production activities (Foulkes, 1986; EPA, 2007), and participates in both toxicological and ecotoxicological risks (Waisberg *et al*., 2003 and WHO, 1992). The natural level of cadmium in fresh water is 0.1 to 10 µg/l, while in discharged water can fluctuate from 50 µg/l to 10,000,000 µg/l due to the anthropogenic processes (Singhal and Abusaria, 1990; Ringwood, 1992).

The physiological influence of prolonged exposure to cadmium in fish species are reduction in growth (Ricard *et al*., 1998; Ting *et al*., 2013) and change in biochemical blood parameters, such as cortisol and triglyceride that reveal the stress response in fish (Brodeur *et al*.,1998; Lacroix and Hontela, 2004).

The survival of many aquatic species depends on the health status of the hosts, type/length of exposure to toxicants (Silvestre *et al*., 2006).

Scientists use growth function to provide dependable source of information for repeatable results and as a foundation for managing decisions on systems related to aquaculture field (Dumas *et al*., 2010).

Blood biochemical parameters were measured as indexes for the physiological state of fish (Edsall, 1999) and checking the physiological status and health condition of fish (Svetina *et al*., 2002).

The most important purposes of this research are to determine the impacts of Cd at different concentrations on biochemical parameters and the growth performance of common carp fingerlings in addition to the quality of water during the entire period of experiment.

1. MATERIALS AND METHODS

Five experimental diets were formulated with $CdCl_2.H_2O$ as a source of pollutant in the feed of *C. carpio* fingerlings as follows; 0 (control), 0.5, 1, 2 and 3 mg /Kg, as well as the feed contains 28% crude protein and 8% crude lipid (Goran *et al*., 2016). The research was carried out in Aquaculture breeding unit in a close system, which located near the green house in the college of science (Environmental Science Department), Salahaddin University, Erbil, Kurdistan Region -Iraq, (Plate 1).

Plate 1: Close system design for current study

Common carp (*C. carpio*) were took from Daqooq fish Farm and adapted for three weeks before the experiment. At the starting of the trial, groups of 27 fish with average weight (4.2 ± 0.4 g for each) were casually distributed into the cages of the system (8 rectangular cages; 30 cm× 38 cm× 65 cm; 74 litre volume for each individual cage) containing a closed system of recirculation and biofiltration section. Flow-through aeration was provided for each cage separately by electrical aerator (HAIBAO, Submersible water pump, HB-1400, China) at a rate of 14.16 L/min. The diets were hand-fed to the fish twice a day at 9:00 am and 5:00 pm, at 3 % of fish body weight to guarantee that the food will completely consume by the carp fish to avoid any accumulation of foods in the system. All the treatments are implemented in duplicate (with replication) for 71 days.

Water samples were collected weekly from the experimental tanks for assessment of physical

and chemical water properties according to typical procedures of APHA (1998) and Maiti (2004).

Samples of water are collected by 1.5 litre washed polypropylene containers and taken to the lab for water quality analysis. Water sampling last for 10 weeks from 18th June 2018 to 20th August 2018. Water samples were tested for electrical conductivity (EC), pH, total dissolved solids (TDS), turbidity, chloride (Cl^-), total hardness, sodium (Na^+), potassium (K^+), magnesium hardness and calcium (Ca^{+2}). TDS, hydrogen ion concentration (pH) and electrical conductivity were measured by portable device directly in the field (Hanna, HI98123; Made in thailand) (APHA, 1998), water temperature via mercury thermometer, dissolved oxygen measured by DO-meter model (AZ 8404) (electrometric method) (APHA, 1998), and total ammonia by portable device (Milwaukee, ammonia medium range meter-MI405, Romania). Turbidity was measured by a Turbidimeter HACH. 2101N, chloride measured by argentometric way (APHA, 1998). Sodium, Potassium and Calcium were detected by (Jenway PEP8; Flame Photometer) (Goran *et al*., 2016).

Hardness was analyzed by titration method and nitrate by Ultraviolet (UV) Spectrophotometric Screening Method model (Cecil instruments, CE 7200) (Maiti, 2004).

Fish were weighted weekly after feed deprivation day (7th day) and daily retaining of food was adjusted according to the new fish weight. At the last stage of the trial, the similar weighting process have been used and the parameters growth performance were evaluated by weight gain (WG), specific growth rate (SGR), feed conversion ratio (FCR), mortality (%) and survival (%) according to Davies and Gouveia (2010) and Ahmed *et al.* (2012).

The blood was gotten from the caudal vein from ventral body (Campbell, 2015). The blood samples were taken in gel vials for biochemical analysis. Blood samples then centrifuged at 3000 rpm for five minutes and then the serum used for determination of biochemical parameters. Total Cholesterol, Total Triglycerides (TG), Lipase, Amylase, Glutamic-Pyruvic Transaminase (GPT), Aspartate Aminotransferase (AST), High Density Lipoprotein (HDL), Low Density Lipoprotein (LDL), Urea, Creatinine, bilirubin total, bilirubin Direct, Alkaline phosphatase level (ALP), Bilirubin indirect and Very-Low-Density Lipoprtein (VLDL) were analysed by Accent 200 (CORMAY) in Alfa Medical laboratory for Disease Diagnosis in Erbil city.

The obtained data during the period of this study were statistically analyzed and correlation tested by SPSS program (Version 21) using one way ANOVA with replication for comparisons among means of water and fish measurements of studied treatments at p-value of <0.05 which considered significant.

1.1. Description of the study area

C. carpio is accepting to a range of conditions but usually prefer large water systems with adequate flowing. Carp can survive temperatures between 3 and 35^{o}C, and can thrive in large turbid water. They are omnivorous fish species, feeds on aquatic plants and animals. The optimal pH range for *C. carpio* is 6.5 to 9.0 and can survive low values of oxygen (0.3-0.5 ppm) as well as super saturation (Billard, 1995). *C. carpio* is adapted to drastic environments mainly physical and chemical parameters of water body (Moyle and Cech, 2004) .

2. RESULTS AND DISCUSSION

Temperature of the studied water samples (for all treatments) were ranged between 22.75^{o}C in cage 3mg/kg during 25-Jun and 25.47^{o}C in control cage during 23-Jul, (Table 1), whereas DO concentrations were ranged from 5.65 mg.l^{-1} was recorded at cage 3 mg/kg during 25-Jun to 10.27 mg.l^{-1} recorded at cage 1 mg/kg during 23-Jul (Table 2). Dissolved oxygen content not significantly differs ($p \leq 0.05$) between the control water and treatment samples. pH and dissolved oxygen concentrations had been depend upon water temperatures (Sawyer *et al.*, 2003) .

The parameters of water quality were analysed in the investigational cages showed an increase throughout metal exposure period. In the present study the results showed that dissolved oxygen level was increased in water cages throughout the entire period of study. The reason for thatis the influence of heavy metal caused changes in the function of respiratory system in carp. Increasing in oxygen level might impair the respiratory factors. The huge discharge of mucus

and inflammation around the gill of *C. carpio* noticed in present research, this may be due to the damage in respiratory role. Higher level of dissolved oxygen in water have effects on fish by producing a major stress around the gills and reduction in carp metabolism (Vinodhini and Narayanan, 2009).

The maximum turbidity value in studied water samples throughout 10 weeks was 4.2 NTU which recorded at 0.5 mg/kg cage during 25-Jun, while the minimum value was 0.4 NTU found at 1 mg/kg cage during 6-Aug (Table 1).

The highest chloride concentration was recorded at (0.5 and 3 mg/kg cage) during July with value 29 $mg.l^{-1}$, while sulfate was high in (0.5 mg/kg cage) during Jun with value 134 ppm, (Table 3). The minimum values of total hardness, reactive phosphorus (PO_4^{-3}), ammonia (NH_3) and nitrate (NO_3) for measured water samples were 220 $mg.CaCO_3.l^{-1}$, 4.063 $mg.l^{-1}$, 0.067 $mg.l^{-1}$ and 37.088 $mg.l^{-1}$, while the maximum values were 277.5 $mg.CaCO_3.l^{-1}$, 15.05 $mg.l^{-1}$, 1.356 $mg.l^{-1}$ and 45.622 $mg.l^{-1}$ respectively (Table 3).

In addition, the maximum concentrations of sodium and potassium in the studied water samples were 1.66 $mg.l^{-1}$at (1 mg/kg cage) during 6-Aug and 0.57 $mg.l^{-1}$ at (1 mg/kg cage) during 23-Jul respectively (Table 2). Magnesium ion was greater than calcium ion in all studied samples (Table 3). Calcium and magnesium values were decreased in cages, because it is necessary for nutrition and is an crucial component of fish Bones and structure (APHA, 1998). Levels of sodium and potassium were decreased in cages. The internal sodium and chloride are regularly being exchanged by simple diffusion (Shulman *et al.*, 1999).

Table (1) Weekly variation of water's physical parameters in the treatment cages during 71 days of study.

Parameters	Treatments	Weeks									
		18-Jun	25-Jun	02-Jul	09-Jul	16-Jul	23-Jul	30-Jul	06-Aug	13-Aug	20-Aug
Temperature (^{o}C)	Control	24.25	23.65	23.925	24.875	24.675	25.475	24.725	24.525	24.725	24.675
	Cd 0.5 mg	23.2	22.8	22.95	23.6	23.5	24.45	23.5	23.4	23.5	23.5
	Cd 1 mg	23.15	22.8	22.95	23.5	23.4	24.4	23.45	23.4	23.5	23.45
	Cd 2 mg	23.35	22.95	23.1	23.85	23.65	24.7	23.75	23.5	23.75	23.65
	Cd 3 mg	23.2	22.75	22.95	23.75	23.8	24.5	23.75	23.9	23.75	23.75
Turbidity (NTU)	control	2.8	3.75	3.25	1.925	2	3.2	2.575	0.85	1.45	1.25
	Cd 0.5 mg	2.85	4.2	3.5	1.6	1.9	2.6	2.2	1.2	0.75	2.35
	Cd 1 mg	2.9	3.6	3.25	2.2	1.2	2.05	1.6	0.4	1.3	0.9
	Cd 2 mg	2.8	4	3.35	1.6	2.15	3.15	2.65	1.2	1	1.15
	Cd 3 mg	1.6	1.9	1.7	1.4	1.1	1.5	1.3	0.75	1.65	1.25

Table (2) Weekly variation of water's chemical parameters in the treatment cages during 71 days of study.

Parameters	Treatments	Weeks									
		18-Jun	25-Jun	02-Jul	09-Jul	16-Jul	23-Jul	30-Jul	06-Aug	13-Aug	20-Aug
pH	**Control**	8.1	8.1	8.1	8.2	8	8.05	8	8	8.05	8
	Cd 0.5 mg	8.1	8.1	8.1	8.2	8.05	8.05	8.05	8.1	8.05	8.05
	Cd 1 mg	8.1	8.1	8.1	8.1	8	8	8	8.05	8	8
	Cd 2 mg	8.1	8.1	8.1	8.15	8	8	8	8.1	8	8
	Cd 3 mg	8.1	8.1	8.1	8.15	8	8	8	8.1	8	8
Electrical Conductivity (µs/cm)	**Control**	366.25	372.5	369	360	360	360	360	360	360	360
	Cd 0.5 mg	372.5	380	376	365	362.5	360	361	365	361	360
	Cd 1 mg	375	380	377	370	362.5	360	361	365	311	310
	Cd 2 mg	370	380	375	360	360	360	360	360	360	360
	Cd 3 mg	370	375	372	365	360	365	362.5	355	362.5	360
Dissolved Oxygen	**Control**	6.6	5.745	6.17	7.46	9.1225	9.8225	9.47	8.425	8.095	8.14

(DO) ($mg.l^{-1}$)	**Cd 0.5 mg**	6.87	6.01	6.435	7.735	9.605	10.18	9.89	9.035	8.585	7.71
	Cd 1 mg	6.96	6.005	6.48	7.915	9.325	10.27	9.795	8.385	8.805	8.315
	Cd 2 mg	6.905	5.92	6.41	7.895	9.205	9.535	9.37	8.88	8.18	9.02
	Cd 3 mg	6.52	5.65	6.08	7.395	9.34	9.92	9.625	8.77	8.235	8.235
Biochemical Oxygen Demand (BOD_5) ($mg.l^{-1}$)	**Control**	5.3625	4.655	5.01	6.065	5.53	5.6425	5.5875	5.4125	5.7775	4.5975
	Cd 0.5 mg	4.25	2.67	3.455	5.825	5.53	6.035	5.78	5.025	4.92	3.72
	Cd 1 mg	4.5	2.85	3.675	6.145	4.825	5.755	5.29	3.895	5.59	5.035
	Cd 2 mg	4.575	2.92	3.745	6.225	5.09	5.42	5.255	4.76	5.145	5.945
	Cd 3 mg	3.28	2.5	2.885	4.06	5	5.535	5.265	4.47	4.83	4.575
Total Dissolved solids (TDS) ($mg.l^{-1}$)	**control**	180	182.5	181.75	180	180	180	180	180	192.75	180
	Cd 0.5 mg	185	190	187	180	180	180	180	180	199.5	180
	Cd 1 mg	185	190	187	180	177.5	180	178.5	175	196	178
	Cd 2 mg	185	190	187	180	180	180	180	180	197.5	180
	Cd 3 mg	185	190	187	180	180	180	180	180	198.5	180
Sodium ($mg.l^{-1}$)	**Control**	1.422	1.301	1.286	1.543	1.573	1.543	1.558	1.604	1.452	1.437
	Cd 0.5 mg	1.316	1.271	1.271	1.362	1.589	1.573	1.581	1.604	1.475	1.468
	Cd 1 mg	1.331	1.301	1.286	1.362	1.604	1.543	1.573	1.664	1.468	1.437
	Cd 2 mg	1.331	1.271	1.271	1.392	1.573	1.543	1.558	1.604	1.437	1.422
	Cd 3 mg	1.347	1.301	1.286	1.392	1.558	1.513	1.536	1.604	1.460	1.437
Potassium ($mg.l^{-1}$)	**control**	0.222	0.184	0.203	0.260	0.468	0.547	0.507	0.388	0.507	0.311
	Cd 0.5 mg	0.230	0.204	0.217	0.256	0.456	0.547	0.501	0.364	0.501	0.302
	Cd 1 mg	0.226	0.187	0.206	0.265	0.469	0.577	0.523	0.360	0.523	0.302
	Cd 2 mg	0.236	0.208	0.222	0.265	0.449	0.555	0.502	0.343	0.502	0.308
	Cd 3 mg	0.223	0.200	0.212	0.247	0.417	0.477	0.447	0.356	0.447	0.299

Table (3) Monthly variation of water's chemical parameters in the treatment cages during the study period.

Parameters	**treatments**	**Control**	**Cd 0.5 mg**	**Cd 1 mg**	**Cd 2 mg**	**Cd 3 mg**
Ammonia ion ($mg.l^{-1}$)	Jun	1.064	1.356	1.259	1.034	1.021
	Jul	0.192	0.067	0.116	0.14	0.109
	Aug	0.572	0.201	0.207	0.073	0.158
	mean±SD	0.609±0.437	0.541±0.709	0.527±0.635	0.415±0.536	0.43±0.513
Nitrate (NO_3) ($mg.l^{-1}$)	Jun	39.679	40.542	40.602	39.618	39.237
	Jul	40.1	40.341	40.582	38.514	40.02
	Aug	42.962	37.088	45.622	45.191	44.598
	mean±SD	40.914±1.786	39.324±1.939	42.269±2.904	41.108±3.579	41.285±2.896
Phosphate (PO_4) ($mg.l^{-1}$)	Jun	4.063	5.85	8.375	7.075	7.325
	Jul	9.138	8.05	7.5	10.6	11.425
	Aug	14.5	13.55	13.3	14.95	15.05
	mean±SD	9.233±5.219	9.15±3.966	9.725±3.127	10.875±3.945	11.267±3.865
Total hardness ($mg.CaCO3.l^{-1}$)	Jun	241.25	277.5	241	243	220
	Jul	250.75	254.5	259.5	255.5	254
	Aug	245.75	265.5	250	249	236.5
	mean±SD	245.917±4.752	265.833±11.504	250.167±9.251	249.167±6.252	236.833±17.002
Calcium ion ($mg.l^{-1}$)	Jun	25	25	25	25	24.8
	Jul	23	23	23	22.7	23
	Aug	23.675	24	24	23.8	23.75
	mean±SD	23.892±1.017	24±1	24±1	23.833±1.15	23.85±0.904
Sulphate (SO_4^{-2}) ($mg.l^{-1}$)	Jun	122.25	134	123.5	118	130.5
	Jul	102.75	103.5	122.5	111	92.5
	Aug	112.25	118.5	123	114	111
	mean±SD	112.417±9.751	118.667±15.251	123±0.5	114.333±3.512	111.333±19.002
Chloride (Cl^{-1}) ($mg.l^{-1}$)	Jun	24.5	22	21	25	20
	Jul	25.75	29	23	28.5	29
	Aug	25	25	21.5	26.5	24.5
	mean±SD	25.083±0.629	25.333±3.512	21.833±1.041	26.667±1.756	24.5±4.5
Magnesium ion ($mg.l^{-1}$)	Jun	43.428	52.235	43.367	43.853	38.387
	Jul	46.951	47.862	49.077	48.287	47.741
	Aug	45.19	50.049	46.222	46.07	43.064
	mean±SD	45.19±1.761	50.049±2.187	46.222±2.855	46.07±2.217	43.064±4.677

Significant difference in the levels of ALP and GOT were detected between the control and different concentrations of cadmium chloride. The lowest value of serum cholestrol was 55 mg/dL recorded in fish treated with Cd (3 mg/kg), while the highest serum cholestrol was 100 mg/dL recorded at treatment (0.5 mg/kg). With increasing Cd concentration, serum cholesterol in blood was decreased. HDL values in control and treatment cages were lower than LDL values, (Table 4).

Triglyceride is one of the blood parameters used for evaluation the metabolism of lipid in fish species; higher levels of TG may happen with nephritic syndrome (Bernet *et al*., 2001). Oral exposure of metals especially cadmium in the current research induced significant rise in the level of blood TG in carp juveniles and agreed with results obtained by Mohiseni (2016). The levels of blood Cholestrol were significantly increased in the animals treated with metal while the level of increased in cages treated with 0.5 and 1 ppm and decreased at cages treated with higher cadmium levels, and not agreed with results obtained by Mohiseni (2016). High levels of cholesterol may led to weaknesses in fish body and the capability of swimming (Brake, 1997) was detected in present research.

Glutamic oxaloacetic transaminase (GOT), glutamic-pyruvic transaminase (GPT) and alkaline phosphatase level (ALP) are plasma enzymes considered significant plasma indicators to investigate the health of animal. Likewise, other plasma biomarkers such as urea and triglyceride usually are used to identify animal health (Mohiseni, 2016). Tietz (1987), Campbell and Dickinson (1984) described that these enzymes release to the blood stream when the hepatic parenchyma cells are injured. De smet and Blust (2001) described that there is an increase in GOT and GPT activities in *C. carpio* exposed to cadmium. Continuous exposure of *C. carpio* to sub-lethal cadmium levels lead to higher levels of ALT and AST enzyme, treated with 0.5, 1 and 3 mg/kg Cd of 71-days (Oner *et al.,* 2008). ALT and AST have an important role in amino acid and protein metabolism, also they discharge into the blood plasma after tissue impairment. El-Naga *et al.* (2005) revealed that transaminases like AST and ALT were significantly affected by Cd and after a temporary reduction during the first two days, enzymatic activity raised and their values were similar to the control. Thirumavalavan (2010) revealed that the activity of GOT and GPT enhanced in *Oreochromis mossambicus* tissues treated with $CdCl_2$ and the reason is that, permeability of cell membrane increases causing in the impairment of tissues after seven and fourteen days.Various factors such as exposure period and cadmium dosage influence the activity of ALP. Bonda *et al*. (2007) reported that after long-term exposures to low concentration of this metal-induced disfunction of kidneys.

Negative correlation was found between HDL with triglyceride, amylase, GPT, GOT and ALP (Table 5). Creatinine values in control cages were lower than treatment cages, (Table 4). Values obtained for various blood biochemical parameters in the current study for *C. carpio* fingerlings were found to be normal and showing healthy condition and thriving well in the aquatic body with favorable environmental conditions. Results of present study presented negative correlation between direct Bilirubin with HDL and LDL, (Table 5).

High levels of amylase were recorded in blood of *C. carpio* treated with cadmium particularly in cages treated with 2 ppm with values of 984 U/L if compared with control blood samples with a value of 108 U/L (Table 4). After 71 days of fish exposure to heavy metal the blood of *C. carpio* exhibited a major rise in amylase, while at 3 mg/kg amylase levels decreased, this is due to the vulnerable stress produced by heavy metals and lead to hyperglycemia which in turn increase in amylase levels till 2 mg/kg exposure. Earlier researchs showed that, the carbohydrate metabolism altered by metal cadmium, which led to hyperglycemia (high blood suger) through provoking the glycogenolysis in some types of fish (Levesque *et al.*, 2002). The same status of hyperglycemia was detected in *C. carpio* during the present research and the research of Vinodhini and Narayanan (2009). Hyperglycaemic response in this study is asign of metabolic disturbance of carbohydrate probably because of the liver glycogen breakdown and interceded possibly through adrenocortical hormones, also reduced insulin secretory activity (Parvathi *et al*., 2011). Indeed, prolonged stress after metal toxicity exerts weakness and hypoxic condition with the inability of hepatocytes to propagate the regular cellular metabolism (Heath, 1995), (Plate 2). The decreased glycogen content in fish, which was also observed during the present study, alters the

enzymes of carbohydrate metabolism and might be utilized in the formation of glycoproteins and lipids (Levesque *et al*., 2002), (Table 4).

Plate 2: A. Effect of different cadmium doses on *C. carpio*

Plate 2: B. Effect of different cadmium doses on *C. carpio*

Plate 2: C. Effect of different cadmium doses on *C. carpio*

Table (4) values of biochemical parameters of *C. carpio* blood during 71 days of study.

Biochemical Analysis						
Test names	Unit	**Treatments**				
		control	Cd 0.5 mg	Cd 1 mg	Cd 2 mg	Cd 3 mg
Cholestrol	mg/dL	93	100	99	57	55
TG	mg/dL	239	246	215	276	281
HDL-D	mg/dL	29.2	32.3	25.3	8.2	8.4
LDL-D	mg/dL	33	38.1	43.3	16.9	12.1
Urea	mg/dL	13	17	12	19	14
Bilirubin total	mg/dL	0.76	0.88	0.8	0.89	0.62
Bilirubin Direct	mg/dL	0	0.05	0.01	0.07	0.07
ALP	U/L	70	79	45	235	526
Creatinine	mg/dL	0.38	0.58	0.43	0.46	0.41
Lipase	U/L	13	56.1	13.6	9.1	10.5
Amylase	U/L	108	369	101	984	211
Bilirubin indirect	mg/dL	0.76	0.83	0.79	0.96	0.69
VLDL	mg/dL	48	49	43	55	56
GOT	U/L	208	28	1872	166	1741
GPT	U/L	139	284	132	227	197

Table (5) Correlation coefficient between biochemical parameters in fish treated with different concentrations of ($CdCl_2$)

Parameters	Chol.	TG	HDL-D	LDL-D	Urea	Bil total	Bil-D	ALP	Crea.	Lipase	Amyl.	Bilirubin ind.	VLDL	GOT	GPT
Cholestrol	1														
TG	-0.909	1													
HDL-D	0.971	-0.796	1												
LDL D	0.977	-0.956	0.900	1											
Urea	-0.414	0.602	-0.336	-0.406	1										
Total Bilirubin	0.355	-0.255	0.331	0.422	0.611	1									
Bilirubin Direct	-0.770	0.871	-0.721	-0.761	0.724	-0.021	1								
ALP	-0.868	0.835	-0.822	-0.895	0.126	-0.684	0.728	1							
Creatinine	0.294	-0.005	0.332	0.281	0.599	0.632	0.371	-0.259	1						
Lipase	0.546	-0.194	0.630	0.463	0.306	0.447	0.083	-0.367	0.902	1.000					
Amylase	-0.554	0.582	-0.540	-0.485	0.919	0.580	0.659	0.151	0.319	-0.055	1				
Bilirubin indirect	-0.116	0.126	-0.148	-0.018	0.788	0.877	0.278	-0.333	0.415	0.089	0.877	1			
VLDL	-0.910	1.000	-0.795	-0.960	0.592	-0.264	0.858	0.834	-0.025	-0.208	0.575	0.118	1		
GOT	-0.140	-0.152	-0.298	-0.046	-0.658	-0.656	-0.057	0.389	-0.438	-0.443	-0.496	-0.584	-0.156	1	
GPT	-0.162	0.484	-0.054	-0.214	0.819	0.429	0.719	0.158	0.867	0.718	0.546	0.410	0.468	-0.521	1

Correlation is significant at the 0.05 level

The initial body weight values of *C. carpio* in (control, 0.5mg, 1mg, 2mg, 3mg cages) were 4.412, 4.035, 4.15, 4.17, 4.235 gm respectively, while the final body weight were changed to 10.350, 9.805, 11.085, 6.70 and 11.155 gm respectively. The final weight of fish body, growth rate and weight gain of *C. carpio* in 2 mg cage lower than other treatment and control cages in contrast, feed conversion ratio of *C. carpio* in 2 mg cage higher than other groups (Table 6). Generally, the survival rate of fish was higher than mortality rate. The results of the present study showed positive relationship between fish growth rate and weight gain, final body weight and survival, while negative correlation were found between the growth rate, FCR and mortality during the study period (Table 7).

Cadmium exposure not stimulate significant growth in fish species as noticed by Ossana *et al*. (2009) and came in agreement with current study. Specific growth rate reduction in *C. carpio* after exposure to cadmium was stated in many literatures (Hans *et al*., 2006).

The obtained data of the present study observed that cadmium affected on the growth even at 0.5 ppm, (Plate 2). On the other hand, lower cadmium doses may cause increase the rate growth in several types of fish (Sloman *et al.*, 2003) which not agreed with results of current study. Researches on this field are changing according to exposure period, way of exposure, fish species and parameters of water quality.

Cadmium has an adverse effect on anabolic hormone metabolism and can retard the expression of hormone which responsible in fish growth (Jones *et al.*, 2005). Cadmium is a major stressor factor for fish. Stress has many impacts on fish growth rate in many ways (Jentoft *et al*., 2005). The interface of cadmium with other elements like calcium and zinc, which are important for growth in fish, has been revealed previously by Witeska *et al.* (1995). Conforming to some study, heavy metal (cadmium) led to impair bone metabolism of *C. carpio* and decrease the growth of fish. Cadmium can also destroy the beta cells in pancreas and drop the insulin hormone, which has a role in cytoplasmic growth (Heath, 1987). Cadmium may prevent the uptake of essential nutrients and some important amino acid for fish growth (Witeska *et al.*, 1995).

Table (6) Growth performance and feed utilization of *C. carpio* fed the experimental diets for 10 weeks.

Growth Performance					
Parameters	**Treatments**				
	Control	Cd 0.5mg	Cd 1mg	Cd 2mg	Cd 3mg
EBW(g)	4.413	4.035	4.150	4.170	4.235
FBW(g)	10.350	9.805	11.085	6.700	11.155
weight gain(g)	5.938	5.770	6.935	2.530	6.920
SGR (%day^{-1})	1.202	1.250	1.384	0.668	1.364
FCR	0.371	0.456	0.317	0.898	0.289
Mortality (%)	0.000	35.541	7.479	53.241	46.296
Survival (%)	100.000	64.459	92.521	46.759	53.704

Table (7) Correlation coefficient between growth performance parameters in fish treated with different ($CdCl_2$) concentrations.

Parameters	EBW	FBW	weight gain	SGR %	FCR	Mortality (%)	Survival (%)
EBW	1						
FBW	0.189	1					
weight gain	0.115	0.997	1				
SGR %	0.029	0.985	0.995	1			
FCR	-0.218	-0.998	-0.992	-0.982	1		
Mortality (%)	-0.479	-0.551	-0.520	-0.499	0.564	1	
Survival (%)	0.479	0.551	0.520	0.499	-0.564	-1.000	1

Correlation is significant at the 0.05 level

3. CONCLUSION

1- Nitrate and phosphate levels increase toward the higher concentration proceeding time of experiment.
2- Biochemical parameters like GPT, GOT, Amylase and triglyceride (TG) were found to be increased.
3- Growth and serum biochemical parameters could reflect environmental metal stress concerning the effects of metal contamination and fish health.
4- The present study has demonstrated that the effects of sublethal concentration of heavy metal for the exposure period of 71 days proved to be toxic to common carp (*C. carpio* L.).

REFERENCES

AHMED, A. R., JHA, A. N. & DAVIES, S. J. 2012. The efficacy of chromium as a growth enhancer for mirror carp (*Cyprinus carpio* L): an integrated study using biochemical, genetic and histological responses. *Biol Trace Elem Res*, p. 187–197.

AMERICAN PUBLIC HEALTH ASSOCIATION (APHA) 1998. Standard Methods for the examination of water &wastewater, 20th Edition. American Public Health Association, Washington, 2671 pp.

AZIZ, F. H. & RASHEED, R. O. 2017. Heavy metals in water, fishes and sediments in Derbendikhan reservoir, kurdistan Region-Iraq. Zanco.J. of Pure and Appli. Sci. Salahaddin Univ. 29(3): p.19-27.

BERNET, D., SCHMIDT, H., WAHLI, T. & BURKHARDT-HOLM, P. 2001. Effluent from a sewage treatment works causes changes in plasma chemistry of brown trout (*Salmotrutta* L.). *Ecotoxicol Environ Saf*.48: p.140–147.

BERT, T. M. 2007. Ecological and Genetic Implications of Aquaculture Activities. Springer, 545pp.

BILLARD, R. 1995. Carp Biology and Culture. Springer in association with Praxis-Paris: 342pp.

BONDA, E., WŁOSTOWSKI, T. & KRASOWSKA, A. 2007. Cadmium metabolism and toxicity in human and animals. KosmosProblemyNaukBiologicznych,56: p.87–97.

BRAKE, I. 1997. Immune status role of vitamins. Feed Mix, 5(1):p. 21-24.

BRODEUR, J. C., DANIEL, C., RICARD, A. C. & HONTELA, A. (1998). In vitro response to ACTH of the interrenal tissue of rainbow trout (*Oncorhynchusmykiss*) exposed to cadmium. *Aqua Toxicol*, 42: p.103–113.

CAMPBELL, E. J. & DICKINSON, C. J. 1984. *Clinical physiology*. Bulter and Tanner Ltd. London, 315 pp.

CAMPBELL, T. W. 2015. *Exotic Animal Hematology and Cytology*. John Wiley & Sons, Inc, 402 pp.

CLARKE, G. M. 1993. Fluctuating assymetry of invertebrate population as a biological indicator of environmental quality. *Environ Pollut*, 82: p. 207-211.

DAVIES, S. J. & GOUVEIA, A. 2010. Response of common carp fry fed diets containing a pea seed meal (*Pisum sativum*) subjected to different thermal processing methods. Aquaculture, 305: p.117–123

DE SMET, H. & BLUST, R. 2001. Stress responses and changes in protein metabolism in carp *Cyprinuscarpio* during cadmium exposure. *Ecotoxicol Environ Saf*, 48: p. 255–262

DUMAS, A., FRANCE, J. & BUREAU, D. 2010. Modelling growth and body composition in fish nutrition: where have we been and where are we going? *Aquaculture Researc*, 41: p. 161–181.

EDSALL, C. C. 1999. A blood chemistry profile for lake trout. *J. Aquat. Anim. Health*. 11.p. 81-86.

EL-NAGA, E. H., EL-MOSELHY, K. M. & HAMED, M. A. 2005. Toxicity of cadmium and copper and their effects on some biochemical parameters of marine fish Mugil seheli. *Egypt Aquat*, 2: p.60–71.

ENVIRONMENTAL PROTECTION AGENCY (EPA) 2007. *Framework for Metals Risk Assessment*, Office of the Science Advisor, Risk Assessment Forum, EPA, 257pp.

FOULKES, E.C. 1986. *Cadmium (Handbook of Experimental Pharmacology)*. Vol. 80, Springer-Verlag, Berlin, 400 pp.

GORAN, S.M., OMAR, S.S.& ANWER, A.Y. 2016. Water Quality and Physiological Parameters of Common Carp Fingerling Fed on Jerusalem artichoke Tubers. *Polytechnic J*. university of polytechnic, 6 (3): p.502-516.

GUPTA, S. K. & GUPTA, P. C. 2006. General and Applied Technology (Fish and Fisheries), Chand and Company, New Delhi, 1130 pp.

HANS, R., KAREN, V.C., LIEVEN, B., WIM, D.M. & RONNY, B. 2006. Dynamics of cadmium accumulation and effects in common carp (*Cyprinuscarpio*) during simultaneous exposure to water and food (Tubifextubifex). *Environmental Toxicology and chemistry*, 25: p. 1558–1567.

HEATH, A.G. 1987. Water pollution and fish physiology. CRC Press, Florida, USA, 245 pp.

HEATH, A.G. 1995. Water Pollution and Fish Physiology, CRC Press Inc., Boca Raton, Florida, 201 pp.

JENTOFT, S., AASTVEIT, A. H., TORJESEN, P. A. & ANDERSEN, O. 2005. Effects of stress on growth, cortisol and glucose levels in non-domesticated Eurasian perch (*Percafluviatilis*) and domesticated rainbow trout (*Oncorhynchusmykiss*). *Comparative Biochemistry and Physiology*, 141: p. 353–358.

JONES, I., KILLE, P. & SWEENEY, G. 2005. Cadmium delays growth hormone expression during rainbow trout development. *Journal of Fish Biology*, 59(4): p.1015– 1022.

LACROIX, A. & HONTELA, A. 2004. A comparative assessment of the adrenotoxic effects of cadmium in two teleost species, rainbow trout, *Oncorhynchusmykiss*, and yellow perch, *Percaflavescens*. *AquatToxicol*, 67: p.13–21.

LEVESQUE, H. M., MOON, T.W., CAMPBELL, P. G. C. & HONTELA, A. 2002. Seasonal variation in carbohydrate and lipid metabolism of yellow perch (*Perca flavescens*) chronically exposed to metals in the field. *Aquat. Toxicol*, 60: p. 257-267.

MAITI, S. K. 2004. Handbook of Methods in Environmental Studies, Vol. 1: *Water & Wastewater Analysis*. 2nd edition, ABD Publisher, Oxford Book Company, 307 pp.

MOHAMMED, N. & BAMARNI, K.2019.Water quality monitoring of Duhok Dam (Kurdistan Region of Iraq). Zanco.J. of Pure and Appli. Sci. Salahaddin Univ, 31(1): p.7-16.

MOHISENI, M. 2016. Biochemical Alteration Induced by Cadmium and Lead in Common Carp via an Experimental Food Chain. *Iranian Journal of Toxicology*, 10 (4): p.25-32.

MOYLE, P. B. & CECH, J. J. 2004. Fishes, an introduction to Ichthyology. 5th edition, Pearson Benjamín Cummings, 726 pp.

ONER, M., ATLI, G. & CANLI, M. 2008. Changes in serum parameters of freshwater fish *Oreochromis niloticus* following prolonged metal (Ag, Cd, Cr, Cu, Zn) exposures. *Environ Toxicol Chem*, 2: p.360–366.

OSSANA, N.A., EISSA, B.L. & SALIBIAN, A. 2009. Short communication: Cadmium bioconcentration and genotoxicity in the common carp (*Cyprinuscarpio*). *International Journal of Environment Health*, 3: p. 302– 309.

PARVATHI, K., SIVAKUMAR, P. & RAMESH, M. 2011. Sublethal effects of chromium on some biochemical profiles of the fresh water teleost *Cyprinus carpio*.*International Journal of Applied Biology Tech*, 2: p.295-300.

RICARD, A.C., DANIEL, C., ANDERSON, P. & HONTELA, A. 1998. Effects of subchronic exposure to cadmium chloride on endocrine and metabolic functions in rainbow trout *Oncorhynchus mykiss*. *Arch Environ Contam Toxicol*, 34: p.377–381.

RINGWOOD, A.N. 1992. Effects of chronic cadmium exposure on growth of larvae of Hawaiian bivalve *Isognomon californium*. *Mar EcolProgSer*, 83: p.63-70

SAWYER, C. N., MCCARTY, P. L. & PARKIN G. F. 2003. Chemistry for Environmental Engineering & Science. 5th Edition, McGraw-Hill Companies. New York, U.S.A, 752 pp.

SHULMAN, G. E., MALCOLM, L. R., SOUTHWARD, A. J., TYLER, F. A. & YOUNG, C. M. 1999. Advances in Marine Biology, the Biochemical Ecology of Marine Fishes. Academic Press, 36: 351pp.

SILVESTRE, F., DIERICK, J., DUMONT, V., DIEU, M., RAES, M. & DEVOS, P. 2006. Differential protein expression profiles in anterior gills of *Eriocheirsinensis*during acclimation to cadmium. *Aquatic Toxicology*, 76: p. 46– 58.

SINGHAL, R. N. & ABUSARIA, S. R. 1990. Effects of industrial effluents on aquatic animals. M Phil dissertation, Kurukshetra University, Kurukshetra, India, 3: p. 456 –462

SLOMAN, K.A., SCOTT, G.R., DIAO, Z., ROULEAU C., WOOD, C.M. & MCDONALD, D.G. 2003. Cadmium affects the social behaviour of rainbow trout, *Oncorhynchusmykiss*. *Aquatic Toxicology*, 65: p. 171–185.

SUMMERFELT, R. C. 2000. Water Quality Considerations for Aquaculture. Department of Animal Ecology. Iowa State University, Ames, USA, p. 348-356.

SVETINA, A., MATAŠIN, Z., TOFANT, A., VUEEMILO, M. & FUAN, N. 2002. Haematology and some blood chemical parameters of young carp till the age of three years. *Acta. Vet. Hung.J.*, 50: p. 459-467.

THIRUMAVALAVAN, R. 2010. Effect of cadmium on biochemical parameters in fresh water fish, *Oreochromis mossambicus*. *Asia J Sci Tech*, 4: p.100–104.

TIETZ, N. W. 1987. Fundamentals of clinical chemistry. Saunders WB Co: p.221-234.

TING, Z., YU, Z., DELIANG, L.I., TIAO, X. & LI, J. 2013. Exposure of silver carp (*Hypophthalmichthysmolitrix*) to environmentally relevant levels of cadmium: hematology, muscle physiology, and implications for stock enhancement in the Xiangjiang River (Hunan, China). Sci China (Life Sci), 56: p.66–72.

VAL, A. L., DE ALMEIDA-VAL, V. M. F. & RANDALL, D. J. 2006. The Physiology of Tropical Fishes. Vol. 21, Academic Press is an imprint of Elsevier, 634 pp.

VINODHINI R. & NARAYANANM. 2009. The Impact of Toxic Heavy Metals On The Hematological Parameters In Common Carp (*Cyprinus Carpio L.)*. *Iran. J. Environ. Health. Sci. Eng.*, 6 (1): p. 23-28

WAISBERG, M., JOSEPH, P., HALE, B. & BEYERSMANN, D. 2003. Molecular and cellular mechanisms of Cadmium carcinogenesis, *Toxicology*, 192: p.95–117.

WANI, G. P. 1986. Toxicity of heavy metals to embryonic stages of *Cyprinuscarpio*. Poll Res, 5: p.47-51.

WITESKA, M., JEZIERSKA, B. & CHABER, J. 1995. The influence of cadmium on common carp embryos and larvae. *Aquaculture*, 129 (4): p. 129–132.

WORLD HEALTH ORGANIZATION (WHO) 1992. Environmental Health Criteria : *Cadmium: Environmental aspects*, 280 pp.

ZANCO Journal of Pure and Applied Sciences
The official scientific journal of Salahaddin University-Erbil
https://zancojournals.su.edu.krd/index.php/JPAS

ISSN (print):2218-0230**, ISSN (online):** 2412-3986**, DOI: http://dx.doi.org/10.21271/zjpas**

RESEARCH PAPER

Twenty- five new records of algae in eight artificial fish ponds in Erbil

Farhad H. Aziz [1], Sara A. Yasin [2]

[1,2]Department of Environmental Science, College of Science, Salahaddin University-Erbil, Kurdistan Region, Iraq

A B S T R A C T:
This study was carried out from March to October 2018 in eight artificial fish ponds within Erbil province Kurdistan region of Iraq which is the first work in such ponds. A total of 116 algal species belong to 58 genera, 31 families, 19 orders, 9 class and 8 divisions were identified. The dominant division was Chlorophyta with 58 species (50%), followed by Cyanophyta with 31 species (26.72%), Euglenophyta with 19 species (16.37%), Chrysophyta with 4 species with (3.45%) and each of Charophyta, Pyrrophyta, Rhodophyta and Cryptophyta was with one species (0.58%). The dominant species were *Euglena, Cosmarium, and Oscillatoria*. Among identified taxa, 25 species were new records to Iraqi algal flora.

KEY WORDS: Algae; new records; Ponds; Erbil; Iraq
DOI: http://dx.doi.org/10.21271/ZJPAS.31.4.16
ZJPAS (2019) , 31(4);153-166 .

INTRODUCTION:

Algae are an important component of aquatic ecosystems because they reflect environmental health through their distribution and abundance (Stevenson, 1996). The algal diversity in an ecosystem depends upon the physical and chemical water properties (Aziz and Rasheed, 2017). The presence of algae in the fresh pond is extremely important as it is a source of food for the aquatic organisms (Bellinger and Sigee, 2010). In Iraqi Kurdistan Region phyco-limnological studies were carried out from 1978 to 2012. A total of 1341 species were recorded and reported in the algal checklist of Kurdistan region (Aziz, 2011).

* **Corresponding Author:**
Sara Abdulkhaliq Yasin
E-mail: sara.ayasin@yahoo.com
Article History:
Received: 05/04/2019
Accepted: 26/05/2019
Published: 10/09 /2019

More recently, a number of algae added to Iraqi algal flora (Rasoul, 2013, Toma, 2013, Bilbas, 2014, Goran, 2014, Aziz, 2015, Hamadamen, 2015, Sdiq, 2015, Ahmed, 2016, Sharif, 2016, Aziz and Rasoul, 2016, Aziz and Muhammed, 2016, Najmadden, 2017) etc. Since there is no study on artificial fish ponds in Kurdistan, this study was carried out to known algal composition, abundance, distribution, spatial variation and periodicity as affected by related environmental conditions.

1. MATERIALS AND METHODS

1.1. Study area

Erbil district is situated on a plain area with a chain of hills from East. On the west side of the region, there is Greater Zab River, which separates Erbil from Dahuk province. Ainkawa, Qushtapa, Bahrka, Bnaslawa, and Khabat are the major towns. The study area consists of two sub-districts around Erbil province which are: Bahrka and Qushtapa. Bahrka sub-district consists of

three villages which are: Jazhnikan, Grdaraq and Kawrasor. It is an open area located about 14 km from northwest of Erbil city; its height reaches about 472 m.a.s.l., $36^{o}32^{'}02.8^{''}$ N latitude and $44^{o}03'88.2''$ E longitudes and is characterised by agriculture. Qushtapa district located about 23 Km from south of Erbil city at $36^{o}00'09.7''$ N latitude and $44^{o}03'40.4''$ E longitudes and it has an elevation of 393 m.a.s.l.(Erbil Governorate, 2018).

The study areas were comprised of 8 sites, four sites (1, 2, 3 and 4) are located within Bahrka sub-districts which are Jazhnikan-concrete pond, Jazhnikan-soil pond, Grdaraq and Kawrasor , and other sites (5, 6, 7 and 8) were selected from Qushtapa sub-districts which are Masi xweyy-concret pond, Masi xweyy-soil pond, Baban, Kani. All sites are built of soil except site number one and five was constructed of concrete. The source of water is from deep well (see figure 1) (KRSO, 2018).

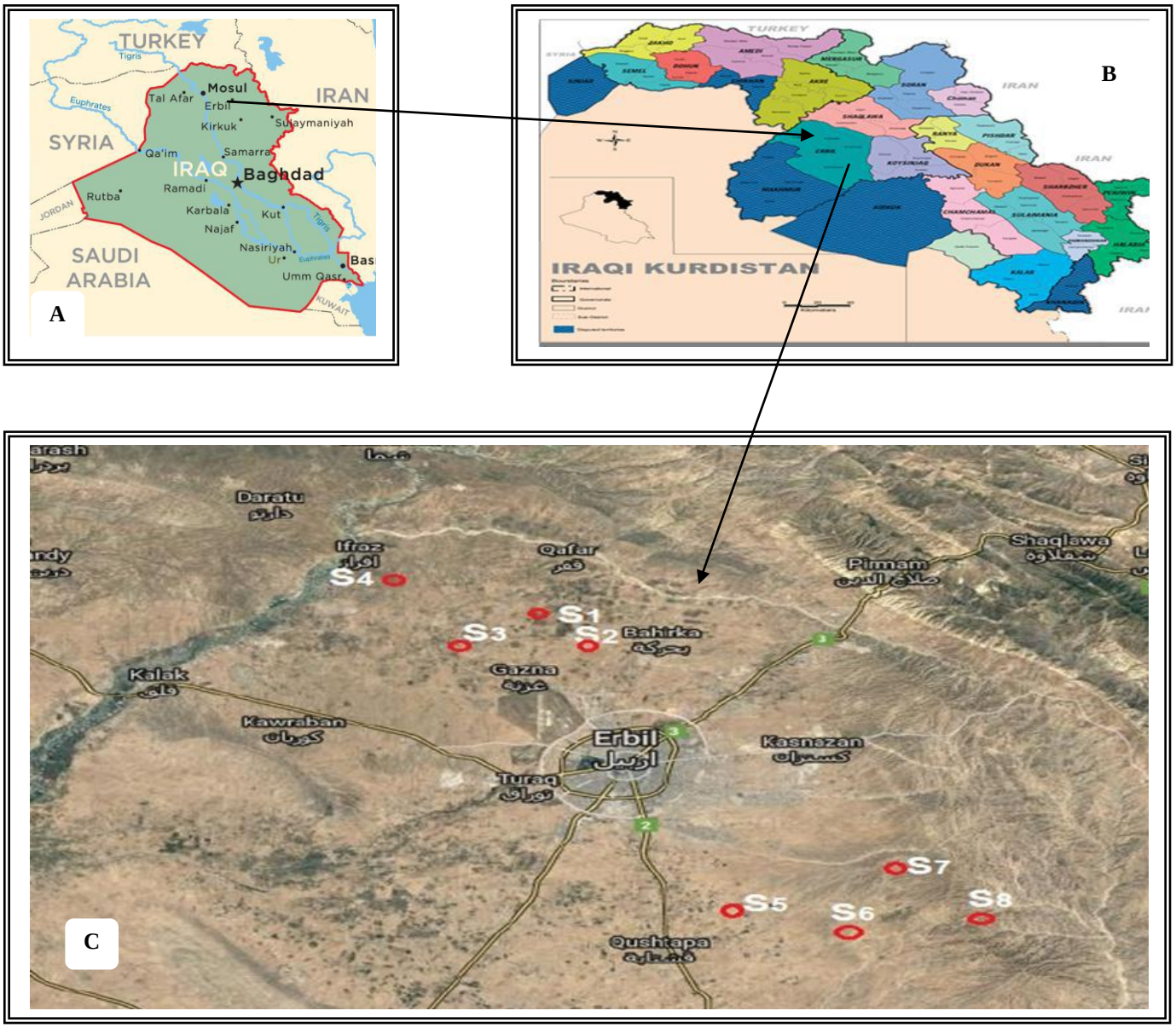

Figure 1: Erbil City, Kurdistan of Iraq .

Table (1) The percentage of studied algal division (Boldand Wynne, 1985)

Division	Classes	Orders	Families	Genera	Species	%
Cyanophyta	1	3	5	17	31	26.724
Chlorophyta	1	8	18	30	58	50
Charophyta	1	1	1	1	1	0.862
Euglenophyta	1	1	1	4	19	16.379
Chrysophyta	2	3	3	3	4	3.448
Pyrrophyta	1	1	1	1	1	0.862
Rhodophyta	1	1	1	1	1	0.862
Cryptophyta	1	1	1	1	1	0.862
Total	9	19	31	58	116	100

1.2. Sample collection and algal identification

Algal samples were collected monthly in special containers by phytoplankton network. Whereas, algal forms were identified before algal fixation as soon as possible because of their loss of taxonomic characters. Using the most common and new available references (West and West, 1908, West and West, 1912, Desikachary, 1959, Randhawa, 1959, Ramanathan, 1964, Prescott, 1968, Prescot, 1970, Prescott, 1975, Benson, 1975, Lang *et al.*, 1987, Komarek, 2005, John *et al.*, 2011, Wehr *et a.*, 2015) and supported by Google websites. The classification and arrangement of algal taxa done according to (Bold and Wynne, 1985) and the new records determined according to the last checklist of Iraqi and Kurdistan algal flora (Maulood *et al.*, 2013).

2. RESULTS AND DISCUSSION

In the current study, as shown in Table (1) a total of 116 species were recorded belong to 58 genera, 31 families, 19 orders, 9 class and 8 divisions in the studied sites. Moreover; among identified algal species, the Chlorophyta was dominant division in species composition 58 species with 50%, followed by Cyanophyta 31 species with 26.72% and Euglenophyta 19 species with 16.37%, Chrysophyta 4 species with 3.45% and each of Charophyta, Pyrrophyta, Rhodophyta and Cryptophyta was with one species (0.58%). In the present study, 25 species of algal flora were new records for Iraqi algal flora according to (Maulood *et al.*, 2013), four belong to Cyanophyta, eleven belong to Chlorophyta, seven belong to Euglenophyta, two belong to Chrysophyta, and one belongs to Pyrrophyta. As in this study, the dominancy of Chlorophyta over Cyanophyta was also observed by (Aziz, 1997, Al-Saadi *et al.*, 2000, Bapper, 2004, Goran, 2006, Zewayee, 2011, Hamadamen, 2015) this is may be due to the environmental condition and water properties of the area which is hard and alkaline toward neutrality and the recording of such new species contributed to the habitat and nature of the study ponds, which was the first study carried out in the area (Aziz, 2011). However, a contrast sequence observed by (Al-Barzingy, 1995) which recorded the dominancy of Cyanophyta due to environmental stress especially temperature.

3. DESCRIPTIONS OF ALGAL NEW RECORDS

***Gloeocapsa alpina* (Naeg.) Brand 1900 (Plate 1, Fig 1):**

Colonies microscopic, 2-8-celled, but frequently aggregated in to macroscopic, irregular blackish mass. Cells of (sub) colony lamellate, with the mucilage blue to dark violet; (sub) colony up to 40 µm (John *et al.*, 2013). Recorded in May, June and July at sites three, four and six.

***Arthrospira jenneri* (Kuetz.) Stizen. 1852 (Plate 1, Fig 2):**

Trichome width 4-8 µm, width of spiral 9-17 µm; distance between spirals 12-25(-31) µm. Frequently with granules at cross walls; trichome end cell rounded (John *et al.*, 2013). Recorded at sites four, six and eight in May, June and August.

***Cylindrospermum lichenforme* {(Bory 1825) Kuetz. 1847} (Plate 1, Fig3):**

Colony mucilaginous, dark green. Cells 3.5-4.2(-4.8) µm wide, slightly longer than wide, quadratic to cylindrical, narrowed at the cross wall. Heterocyst elongate, (-4)-5-6 µm wide, 7-12 µm long.Akinete 10-14 µm wide, 20-30(-40) µm long (John *et al.*, 2013). This species was recorded at sites one, seven and eight in March, April, August and October.

***Homoeothrix fusca* Starmach 1934 (Plate 1, Fig 4):**

Filaments unbranched, straight or flexuous, 4.5-7.5µm wide at base, 48-85µm long, forming clumps up to 1 cm or single among other blue-green algae. Sheath thick, fimbriated at the apex, dark brown. Trichome 2-3.5 µm wide near the base, 1.5-2.5 µm in the middle, usually ending in hair (John *et al.*, 2013). Recorded at sites three, four and seven in March, May and July.

***Haematococcus pluvialis* (Flotow) Wille 1903 (Plate 1, Fig 5):**

Cells spherical to ellipsoid, (8-)-10-30(-51) µm wide, (10-)15-50(-63)µm long, up to 1.5 times as long as broad, papilla absent; protoplasmic

detail was not visible within them (John *et al.*, 2013). This species was presented in sites one and eight during June and August.

***Pectodictyon cubicum* Taft 1945 (Plate 1, Fig 6):**

Colony microscopic, an eight-celled unfilled cube, cells situated at the corners of the mucilage outline, cells inter-connected by stout gelatinous strands, often forming complex coenobia. Cells spherical, 3.5–7 µm in diameter; chloroplast parietal with single pyrenoid (Lang *et al.*, 1987). Recorded at sites one and six during June and July.

***Sphaerocystis planktonica* (Korshikov) Bourr. 1966 (Plate 2, Fig 1):**

Coenobia of 4, 8 or 16 (-32) cells within a spherical mucilaginous envelope (35-)50—124(-150) µm wide) which sometimes becomes indistinct with age; cells 4-9 µm wide and sporangia up to 12.5 µm wide (John *et al.*, 2013). Recorded at all sites except seven in April, May, June and August.

***Tetraspora lacustris* Lemm. 1898d (Plate 2, Fig 2):**

Thallus is free –floating, spherical, or elongate and irregularly shaped, microscopic gelatinous colony containing relatively few spherical cells, the long pseudocilia usually clearly evident. Cells arranged in groups of 2 or 4; 7-10 µm in diameter (Prescot, 1970). Recorded at sites three, four and seven in May, July and September.

***Chlorococcum minutum* (R.C.Starr 1955) (Plate 2, Fig 3):**

Cells 4-10(-20) µm wide,spherical to avoid; walls thicker in older cells; chloroplast a hollow sphere with a lateral pore, often 2 contractile vacuoles present in opening, pyrenoid eccentric and covered by a continuous starch sheath; zoospores, alpanospores and gametes produced by successive bipartition, zoospores ellipsoid-ovoid, 3-5µm wide and 6-7µm long (John *et al.*, 2013). This species was recorded at the sites one, three, six, seven and eight during May and June.

***Oedogonium porrectum* Nordst.&Hirn 1900 (Plate 2, Fig 4):**

Macrandrous; dioecious.Vegetative cells cylindric, 5.8-8-(10) µm in diameter, 23-29-(55) µm long.Oogonia solitary; ellipsoid or oblong-ellipsoid; operculate; division superior; 19.5-22-(27)µm in diameter, (27.3)-39-44-(53) µm long. Oospores ellipsoid; not filling the oogonia; wall smooth; (17.5)-18-24 µm in diameter, 25-27.3-(28) µmlong. Antheridia 6-7µm in diameter, 6-8 µmlong (Prescot, 1970). Recorded at sites seven and eight in June.

***Oedogonium mexicanum* Wittrock 1878 (Plate 2, Fig 5):**

Macrandrous; dioecious. Vegetative cells cylindric, 34-41µm diameter, 60-140 µm long. Oogoniacylindric-ovoid; opening by a superior pore; 53-63 µm in diameter, 76-110 µm long. Oospores cylindric-ovoid; filling the oogonia; wall smooth; 51-60 µm in diameter, 63-80 µm long.Antheridia 28-35 µm in diameter, 70-17 µm long (Prescot, 1970). Recorded at sites two and three in March.

***Closterium praelongum* var. *brevius* (Nordst.)Willi Krieger 1935 (Plate 2, Fig 6):**

Cells significantly shorter and mostly narrower than the type variety, 12-24.6 µm wide, 250-441 µm long, outer margin with curvature similar to the type variety, inner margin straight or slightly tumid, with ends very slightly reflexed, apices 3-7 µm wide; walls with striae, 14-17 in 10, even more indistinct than the type variety (John *et al.*, 2013). Recorded in May at sites two, three, four, five and seven.

***Cosmarium tetragonum* var. *ornatum* Willi Krieger et Ger. 1965 (Plate 3, Fig 1):**

Cells vertically oblong or rectangular, 25-28 µm wide, 43-47 µm long, considerably longer than broad (1.55-1.76 times longer than broad), with a deep sinus open inwardly; semi-cells more or less quadrate, with narrowly rounded basal angles, 2-undulte sides and subtruncate apices having 4 small undulation (John *et al.*, 2013). Recorded in April and August at sites one, five and six.

***Cosmarium zonatum* P.Lundell 1871 (Plate 3, Fig 2):**

Cells (22-)25.4-28.5 µm wide, (43.5-)52-54(-58) µm long, 1.8-2.06 times longer than

broad, with a deep widely open sinus; semi cells subovate, basal margins broadly convex, lateral margins slightly refuse, with apices broadly convex and having an internal thicken (John *et al.*, 2013). Recorded in May and October at sites one and two.

***Mesoetanium caldariorum* (Lager.) Hansgirg 1886 (Plate 3, Fig 3):**

Cells narrow cylindrical, mostly narrowing abruptly toward the apices so that they appear as sub truncate cones, somewhat curved, 10.5-13 µm wide, 42-64 µm long, chloroplast single, ribbon-like, with 2-4 pyrenoids, mostly extending from end to end of cell but sometimes with a gap between their ends and the apices (John *et al.*, 2013). Recorded at sites seven and eight in May and June.

***Euglena adhaerens* Matvienko 1938 (Plate 3, Fig 4):**

Cells 7.5-12 µm wide, 100-165 µm long, longitudinal cylindrical to spindle-shaped, anterior end narrowed and bluntly; posterior end tapering; pellicle slightly striated; flagellum not visible (John *et al.*, 2013). This species recorded at sites five, six, seven and eight during May and September.

***Euglena contabrica* E. G. Pringshiem 1956 (Plate 3, Fig 5):**

Cells 20-25 µm wide, 54-62 µm long, spindle-shaped and twice attenuated towards the posterior end, cylindrical in middle part of cell; euglenoid movement present; chloroplast numerous (John *et al.*, 2013). Recorded in July and October at sites one, five and eight.

***Euglena fusiformis* H. J. Carter 1901 (Plate 3, Fig 6):**

Cells 15-32.5 µm wide, (15-)35-42.5 µm long, lemon shaped, widely oval, anterior end conically narrowing and small concavity at apex, posterior end narrowing to a short, colourless to yellow (John *et al.*, 2013). Recorded at sites two and three in May and June.

***Lepocinclis acus* (O. F. Muller) Marin et Mel. 2003 (Plate 4, Fig 1):**

Cells 7-28.3 µm wide, (52-)60-180(-311) µm long, needle-shaped, elongate spindle shaped, sometimes bent and sometimes assuming an S-shape, anterior end narrowed and apically truncate, posterior end tapered to a long fine point (John *et al.*, 2013). This species was recorded at sites three, six and seven in June, August and October.

***Phacus helicoides* Pochmann 1941 (Plate 4, Fig 2):**

Cells 30-45 µm wide, 70-120 µm long, elongated or spindle-shaped to pear shaped, margins with 2 or 3 bluges, strongly spirally twisted through 1.5-7 times, usually 3; anterior end narrowing and bilobed, posterior end tapering in to a twisted (John *et al.*, 2013). Recorded during July and October at site eight.

***Trachelomonas armata* (Her.) F.Stein 1878 (Plate 4, Fig 3):**

Lorica 29-32 µm wide, (28-)30-45 µm long, widely ellipsoid to ovoid, thickened around apical pore (6-8 µm in diameter) or with a low and toothed, spiny collar, posterior end widely rounded (John *et al.*, 2013). Recorded at sites one and seven during April and May.

***Trachelomonas horrida* Palmer 1905 (Plate 4, Fig 4):**

Test oval, flagellum aperture with a short broad collar; wall uniformly beset with long, stout, bluntly pointed spines interspersed by short, sharp spines; test 27.5 µm in diameter, 35-40 µm long (Prescot, 1970). Recorded in April and September at sites six, seven and eight.

***Ophiocytium cochleare* (Eichw.) A.Braun 1855 (Plate 4, Fig 5):**

Cells free-foating, cylindrical, strongly arched and spirally twisted, one end truncate, the other with astout, sharp spine; cells 5-9.5 µm in diameter (Prescot, 1970). Recorded in May and June at sites three and four.

***Pseudokephyrion undulatum* (G. A. Klebs) Pascher 1913 (Plate 4, Fig 6):**

Lorical ovoid to barrel-shaped, undulate because of 2-4 transverse constrictions, 18-25 µm long; brownish; chloroplasts parietal, 2 per cell, one with eyespot (John *et al.*, 2013) . Recorded in April, June and July at sites three, six, seven and eight.

***Ceratium furcoides* (Levander) Langhans 1925 (Plate 4, Fig 7):**

Cells narrowly spindle-shaped, strongly dorsiventrally flattened, 28-42(-56) µm wide, 123-222 µm long; epitheca formed in to a narrow horn whithout shoulders, hypotheca broad and short, drawn out in to 2 posterior horns of different length (John *et al.*, 2013). Recorded at site four in May and August.

4. CONCLUSIONS

1. Present study provides base line information about the water quality of artificial fish ponds.
2. A total of 116 algal species belong to 58 genera, 31 families, 19 orders, 9 classes and 8 divisions were identified.
3. Chlorophyta (58 species) was the dominant group in the number of identified species, followed by Cyanophyta (31 species), and Euglenophyta (19 species).
4. Among Chlorophyta *Scenedesmus*, *Cosmarium* and *closterium* were dominant, while among Cyanophyta and Euglenophyta *Oscillatoria*, *Euglena* and *Trachelomonas* were domonant.
5. Among 116 taxa of recorded algal species, 25 species were new records to Iraqi algal flora, 4 belonged to Cyanophyta, 11 belonged to Chlorophyta, 7 belonged to Euglenophyta, 2 belonged to Chrysophyta and 1 belonged to Pyrrophyta.

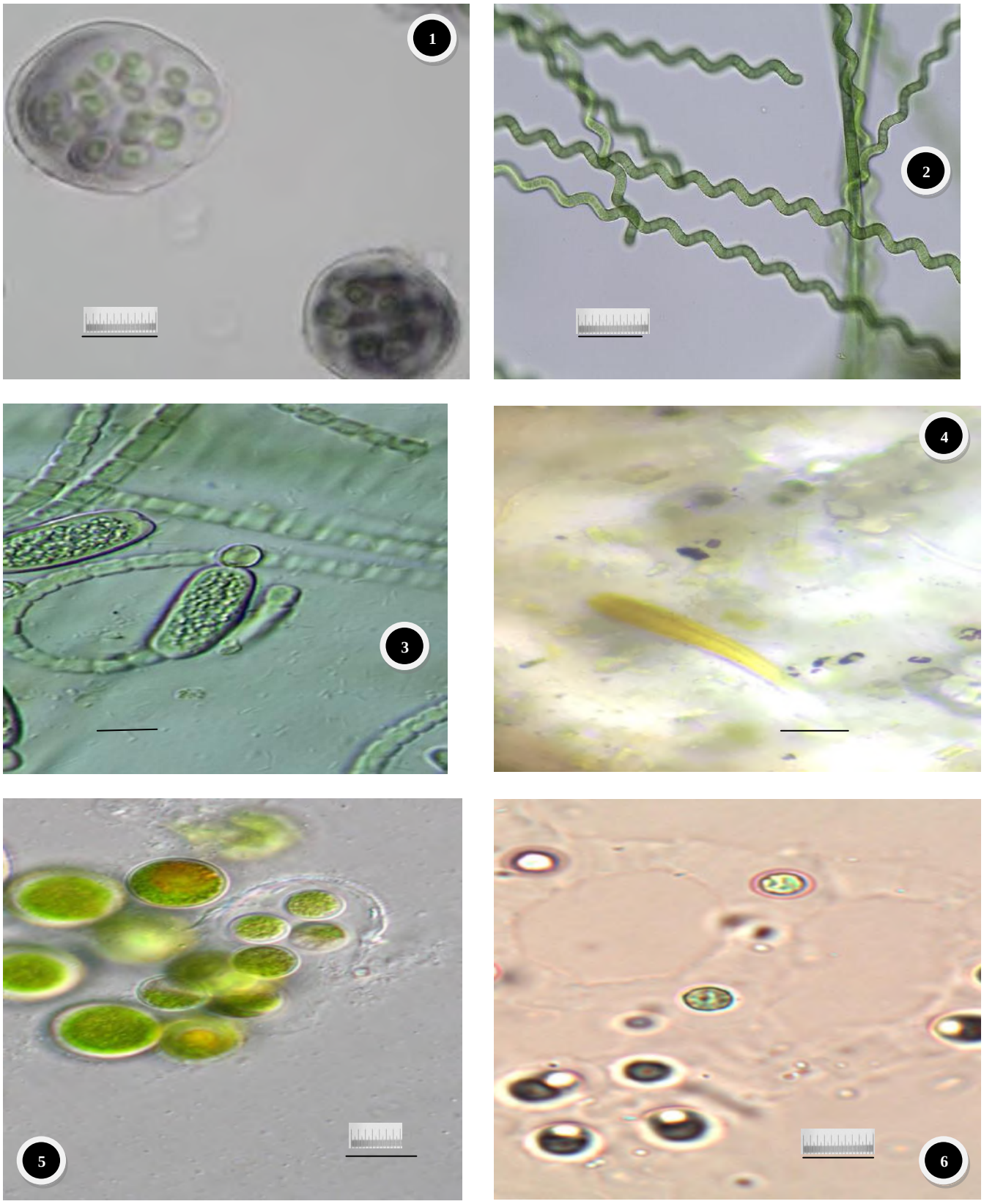

Plate (1): 1.*Gloeocapsa alpine*, 2. *Arthrospira jenneri*, 3. *Cylindrospermum lichenforme*, 4. *Homoeothrix fusca*, 5. *Haematococcus pluvialis*, 6 . *Pectodictyon cubicum*. Scale bars: 10 µm

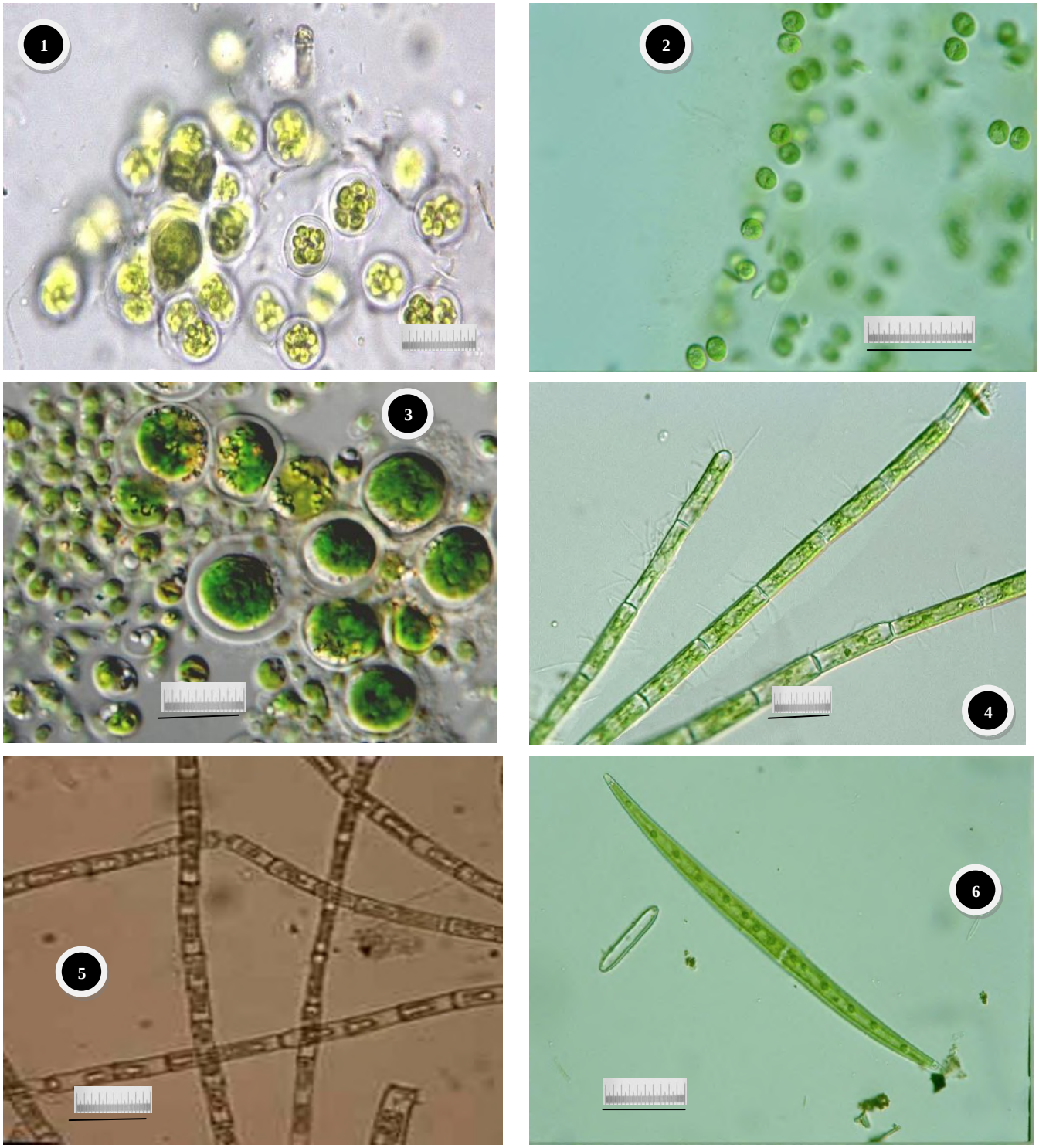

Plate (2): 1. *Sphaerocystis planktonica*, 2. *Tetraspora lacustris*, 3.*Chlorococcum minutum*, 4. *Oedogonium porrectum*, 5. *Oedogonium mexicanum*, 6. *Closterium praelongum* var. *brevius.* Scale bars: 10 µm

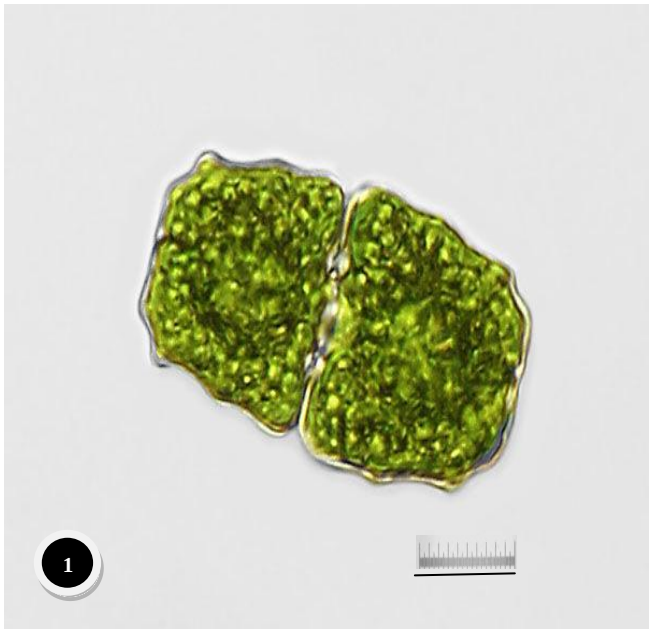
1

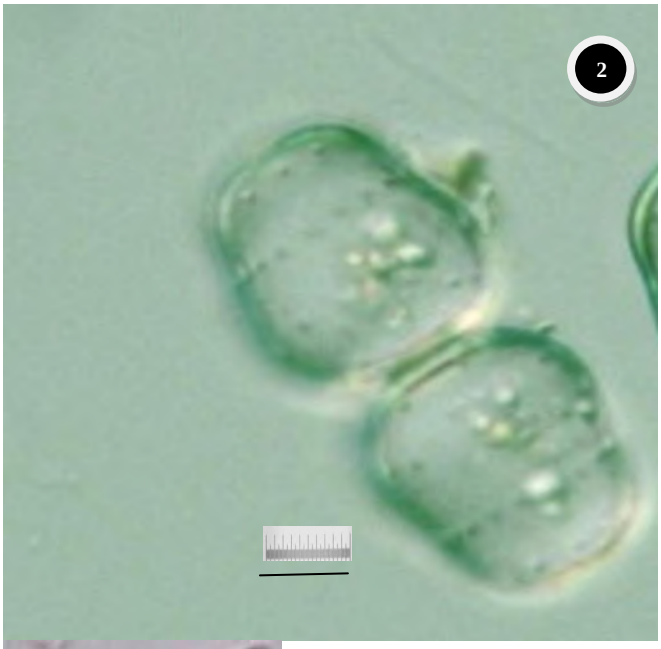
2


3


4

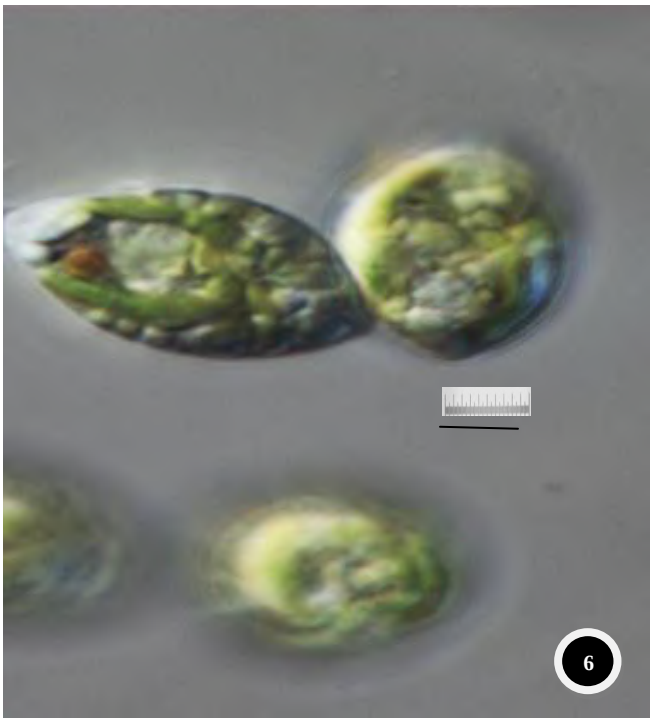

Plate (3): 1. *Cosmarium tetragonum* var. *ornatum,* 2. *Cosmarium zonatum*, 3. *Mesoetanium caldariorum*, 4. *Euglena adhaerens*, 5. *Euglena contabrica*, 6. *Euglena fusiformis.* Scale bars: 10 µm

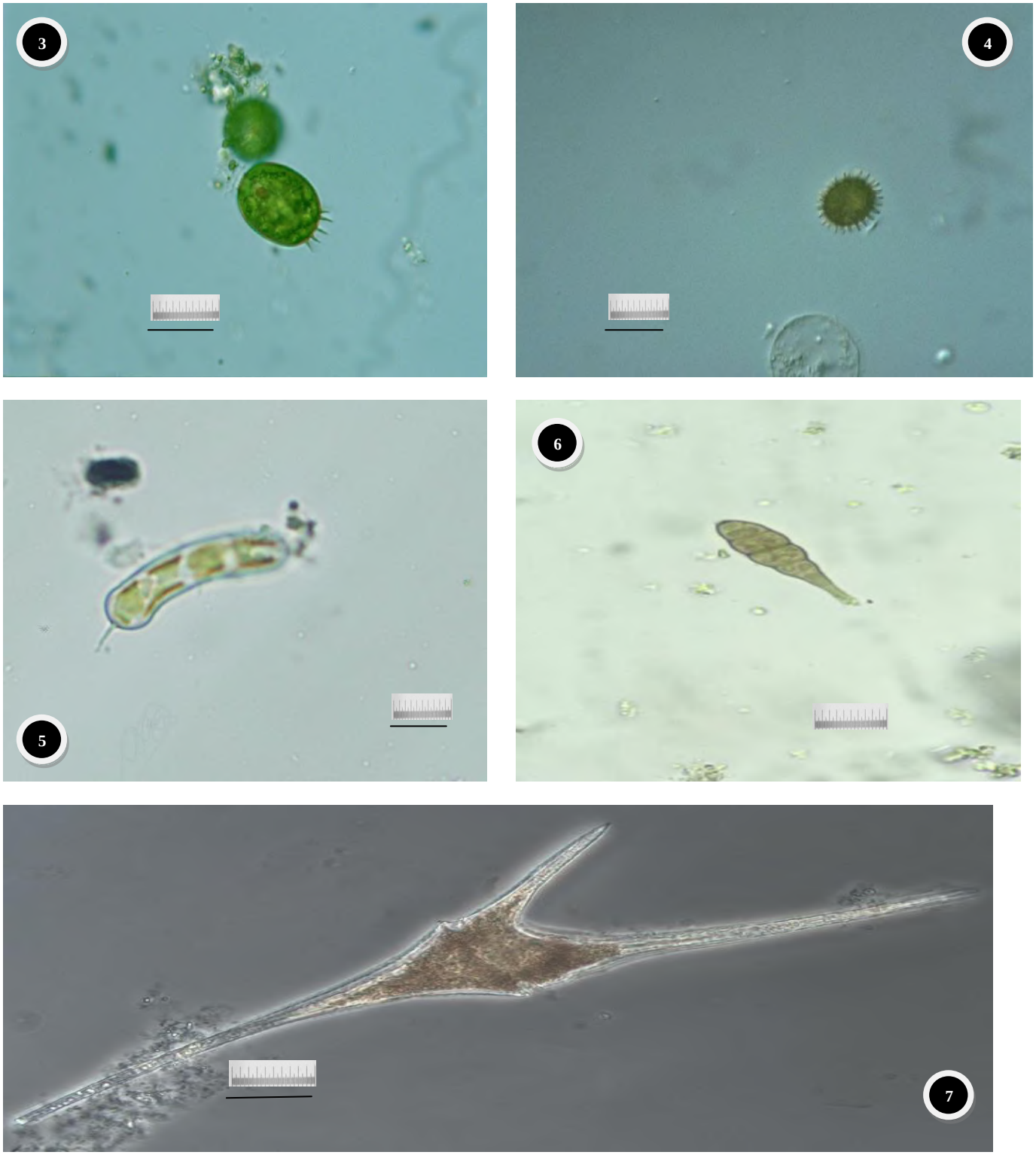

Plate (4): 1. *Lepocinclis acus,* 2. *Phacus helicoides,* 3. *Tachelomonas armata,* 4. *Trachelomonas horrida,* 5. *Ophiocytium cochleare,* 6. *Pseudokephyrion undulatum,* 7. *Ceratium furcoides.* Scale bars is10 µm and each bar is 1 µm

REFERENCES

AHMED, A. Q. 2016. Phyco-limnological Study on Some Springs around Safeen Mountain Area. M.Sc. Thesis, Univ. of Salahaddin-Erbil, Iraq.

AL-BARZINGY, Y. O. M. 1995. Phycological study within Erbil province. Master Thesis. University of Salahaddin, Erbil, Kurdistan Region-Iraq.

AL-SAADI, H., KASSIM, H., AL-LAMI, A. & SALMAN, S. 2000. Spatial and Seasonal Variations of Phytoplankton Population in the Upper Region of the Euphratis River, Iraq. Limnologica, 30(1).p. 83-90.

AZIZ, F. H. & MUHAMMED, A. Q. 2016. Twenty new Records of Algae in Some Springs around Safeen Mountain Area. Journal of Advanced Laboratory Research in Biology. Society of Open Science, 7(3).p. 17- 23.

AZIZ, F. H. & RASHEED, R. O. 2017. Heavy metals in water, fishes and sediments in Derbendikhan reservior, Kurdistan region-Iraq. Zanco.J. of Pure and Appli. Sci. Salahaddin Univ. 29(3).p.19-27.

AZIZ, F. H. & RASOUL, B. H. 2016. Thirty two algae new records reported in ponds at gwer sub-district, erbil - Kurdistan region, Iraq. Bull. Iraq nat. Hist. Mus. 14 (1).p. 27-42.

AZIZ, F. H. 2015. New Record of the Genus *Porphyridium purpureum* from Kurdistan. *Journal of Advanced Laboratory Research in Biology*. 4 (2). P. 54- 57.

AZIZ, F. H. 2011. Checklist of the algal survey in Iraqi Kurdistan region – Iraq with particular references to habitats. Zanco.J. of Pure and Appli. Sci. Salahaddin Univ. 23(3).p. 30-72.

AZIZ, F. H. 1997. A Phycological study with particular reference to Rawanduz River path within Erbil province, Iraq. Ph.D. Thesis. University of Salahaddin, Erbil, Kurdistan Region-Iraq.

BAPPER, U. H. K. 2004. Ecological study on the distribution of alage in different aquatic habitats within Erbil province. Ph.D. Thesis. Salahaddin University, Erbil, Kurdistan Region-Iraq.

BELLINGER, E. G. & SIGEE, D. C. 2010. Freshwater algae: Identification and Use as Bioindicators. 1st ed. Chichester, West Sussex, UK: Wiley-Blackwell.

BENSON, C. E. & RUSHFORTH, S. R. 1975. The algal flora of Huntington Canyon, Utah, USAVaduz: J. Cramer.,.18.333.

BILBAS, A. H. A. 2014. *Ecosystem Health Assessment of Dukan Lake, Sulaimani, Kurdistan Region of Iraq.* Ph.D. Thesis. Univ. of Salahaddin. Erbil. Iraq.

BOLD, H. C. & WYNNE, M. J. 1985. Introduction to the algae. 2nd ed. Englewood Cliffs, N.J.: Prentice-Hall.

DESIKACHARY, T. V. 1959. Cyanophyta. 1st ed. New Delhi: Indian Council of agriculture research.

ERBIL GOVERNORATE, ERBIL GEOGRAPHY. [ONLINE] HAWLERGOV.ORG., 2016. Available at: http://hawlergov.org/en/page.php?id=1329120973 [Accessed 13 Jan. 2018].

GORAN, S. M. A. 2006. Limnology and Non- diatom Phytoplankton Composition of Dilope spring and Kesnezan impoundment Hawler-Kurdistan Region of Iraq. Master Thesis. Salahaddin University, Erbil, Kurdistan Region-Iraq.

GORAN, S. M. A. 2014. *Ecological study on Dukan Lake with particular Reference To bioaccumulation of some Heavy Metals PAH_S in fish and Gull Tissues-sulaimani, Kurdistan Region of Iraq*. Ph.D. Thesis, Univ. of Salahaddin-Erbil, Iraq.

HAMADAMEN, A. R. 2015. A Phycological study of the Qandil mountain streams/ Sulaimani. Master Thesis. Salahaddin University, Erbil, Kurdistan Region-Iraq.

JOHN, D. M., WHITTON, B. A. & BROOK, A. J. 2011. The freshwater algal flora of the British Isles. 1st ed. Cambridge: Cambridge University Press.

KOMAREK, J. & ANAGNOSTIDIS, K. 2005. Süsswasserflora von Mitteleuropa. Cyanoprokaryota: 2. Teil/2nd Part: Oscillatoriales. 1st ed. nchen Elsevier SpektrumAkademischerVerlag.

KRSO (KURDISTAN REGIONAL STATISTICS OFFICE), HAWLER MAP. [ONLINE] KURDISTAN REGION STATISTICS OFFICE, 2015. Available at: http://www.krso.net/Default.aspx?page=category&c=hawler [Accessed 16 Jan. 2018].

LANG, N. J., KRUPP, J.M. & KOLLER, A. L. 1987.Culturing, ultrastructure and colony formation in Pectodictyon cubicum (Chlorophyceae, Chlorococcales). Journal of Phycology 23:457464. Available from http://www.algaebase.org/search/species/detail/?species_id=X63b103d9203c3bc0

MAULOOD, B. K., HASSAN, F. M., AL -LAMI, A. A., TOMA, J. J. & ISMAIL, A. M. 2013. Checklist of Algal Flora in Iraq. 1st ed. Baghdad: Ministry of Environment, Republic of Iraq.

NAJMADDEN, S. K. 2017. Study a range of physical, chemical and biological parameters of selected water bodies within Erbil city. M.Sc. Thesis, Univ. of Salahaddin-Erbil, Iraq.

PRESCOTT, G. W. 1968. Algae of the Western Great Lakes. Dubuque, Iowa: WC Brown Company.

PRESCOTT, G.W. 1970. Algae of the Western Great Lakes Area. 6th. Ed. William C. Brown Co., Publishers. Dubuque, Lowa. Aw dwaylagarrefrensakani de dadaneyn la identification of algae.

PRESCOTT, G. W. 1975. How to know the freshwater alga. WC Brown: McGraw-Hill Science.

RAMANATHAN, K. R. 1964.Ulotrichales. 1st ed. New Delhi: Indian Council of Agricultural Research.

RANDHAWA, M. S. 1959. Zygnemaceae. 1st ed. New Delhi: Indian Council of Agricultural Research.

RASOUL, B. H. R. 2013. *A phycolimnological study in ponds near Greater Zab River in Gwer area –Erbil.* M.sc. Thesis, Univ. of Salahaddin, Iraq.

SDIQ, K. H. 2015. *Ecological and Physiological Study on Some Algae Species growth in Dukan Lake. Kurdistan region of Iraq*. M.Sc. Thesis, Univ. of Slemani.

SHARIF, C. M. 2016. Phyco-limnological study on some springs within Zrarati area in Erbil province. Kurdistan Region, Iraq.

STEVENSON, R.L., BOTHWELL, M.L. & LOWE, R.L. 1996. Algal Ecology: Freshwater benthic ecosystems. Academic Press. New York.

TOMA, J. J. 2013. Limnological study of Dokan, Derbendikhan and Duhok lakes, Kurdistan region of Iraq. *Open Journal of Ecology*. 3 (1). P. 23-29.

WEST, G. & WEST, W. 1908. A monograph of the British Desmidiaceae.Vol III. 1st ed. London: The Ray Society.

WEST, G. & WEST, W. 1912. A monograph of the British Desmidiaceae.Vol IV. 1st ed. London: The Ray society.

WEHR, J., SHEATH, R. & KOCIOLEK, J. 2015. Freshwater algae of North America: Ecology and Classification. 2nd ed. San Diego, USA: Academic Press.

ZEWAYEE, F. Q. 2011. Aphycolimnological study on some springs and streams within Erbil province. Master Thesis. Salahaddin University, Erbil, Kurdistan Region-Iraq.

ZANCO Journal of Pure and Applied Sciences
The official scientific journal of Salahaddin University-Erbil
https://zancojournals.su.edu.krd/index.php/JPAS

ISSN (print):2218-0230**, ISSN (online):** 2412-3986**, DOI: http://dx.doi.org/10.21271/zjpas**

RESEARCH PAPER

Description of red-legged ham beetle, *Necrobia rufipes* De Geer, 1775 (Coleoptera : Cleridae) From Kurdistan region- Iraq

Zayoor Z. Omar[1] , Shatha H. Ahmmed[2] ,Nabeel A. Mawlood[2]

1- Department of Plant Protection, Khabat Technical Institute, Erbil Polytechnic University, Erbil, Kurdistan Region, Iraq.

2- Department of Plant Protection, College of Agriculture, Salahaddin University-Erbil, Kurdistan Region, Iraq.

A B S T R A C T:

Red-legged ham beetle, *Necrobia rufipes* De Geer is described from Kurdistan region- Iraq. The specimens were collected from the carrion and carcasses in contact with soil during January and March- 2018. Some important taxonomic parts especially male genitalia have been photographed. In comparison with other Cleridae , The body mostly entirely is metallic green. legs and antennae are red . Localities and date of the collection have been reported.

KEY WORDS: Description , Coleoptera, Cleridae , Necrobia rufipes , Kurdistan region- Iraq .
DOI: http://dx.doi.org/10.21271/ZJPAS.31.4.17
ZJPAS (2019) , 31(4);167-172 .

1. INTRODUCTION :

Cleridae (also known as checkered beetles) is a small family of Coleoptera occurring worldwide but primarily in tropical and subtropical areas. According to Gerstmeier (2000) there are approximately 3600 species assigned to just over 300 genera, of which there are about 350 species in the Palaearctic region. The family has been sorted in seven subfamilies (Lawrence & Newton Jr., 1995). The family has a worldwide distribution, and a variety of habitats and feeding preferences. Ninety-one species have been described, of which 70 are from the Palaearctic (Corporaal,1950), 11 from Nearctic (Foster ,1976a) and 10 from the Afrotropical regions (Corporaal,1950).

* **Corresponding Author:**
Zayoor Z. Omar
E-mail: Zewarzainal@yahoo.com
Article History:
Received: 16/01/2019
Accepted: 26/05/2019
Published: 10/09 /2019

Most genera of the family are predaceous and feed on other beetles and larvae; however other genera are scavengers .Some feed upon pollen as adults whereas larvae are predaceous, bore into dry or smoked meats and do most damage. They are found on dried fish, skins and bones of dead animals, and other carrion which they are saprophagous and predaceous (Opitz, 2002, Triplehorn and Johnson, 2005). A few are considered pests of stored animal products, dry carrion, or stored meat products (Furniss and Carolin, 1977; Majka, 2006).Some species are consisting predominately of predators of hymenopteran larvae and orthopteran egg pods (Foster, 1976b). Another species are occasionally found on carrion in the later dry stages of decay. Also some species are pests and are found infesting many of the species are known as "flower visitors", that prey on other flower visiting insects and also feed on pollen. These species are found in moist, sunny environments where

flowering plants are found in abundance (Ronald, 1998) . Red-legged ham beetle, *Necrobia rufipes* De Geer, 1775 is commonly known as the copra beetle in tropical countries and red-legged ham beetle in the United States, *N. rufipes* is a species of predatory beetle, in the family , with a cosmopolitan distribution (Haines and Rees 1989). According to Nwana (1993) the red-legged ham beetle is a cosmopolitan pest, causing considerable damage to stored commodities such as copra (dried coconut), cheese, dried fish, ham and other products rich in protein content. In India, it is also recorded as a serious pest of cashew nuts (Sengupta et al.,1984). These beetles can subsist on a diet of copra alone but their development is slow; their diet is almost certainly a supplement by predation on other insects and can promote cannibalism when there is a super population (Ashman 1963). *N. rupifes* De Geer was identified by Carvalho et al., (2000) in a checklist of artropods associated with pig carrion and human corpses in southeastern Brazil. In Iraq there is no any taxonomic study of the family species except; Derwesh (1965) indicated 12 species in four genera. Abdul-Rassoul (1976) recorded two species, and Al-Ali (1977) recorded two species. The main aim of this paper is a detailed description of red-legged ham beetle, *N. rufipes* De Geer which collected from the carrion and carcasses in many localities of Kurdistan region - Iraq and to provide diagnoses of the species (including male genital characters).

2. MATERIALS AND METHODS

The present paper is based on 50 specimens collected from the carrion and carcasses in contact with soil during January and March / 2018 of many localities of Kurdistan region – Iraq (Garmian region , Sulimani and Erbil). The specimens were placed in boiling water for 10-15 minutes to soften their parts. Then the parts were separated and the lipids materials of the body were dissolved by using 10% KOH, then the parts were wished by distilled water for 2-3 minutes in order to neutralize the alkali. The habitus and important parts photographs were taken using a digital camera (Ucmas series microscope camera). The measured proportions of body parts are given in points of an eyepiece linear micrometer in a binocular microscope(Lane and Crosskey , 1993; Mawlood et al., 2016) (Each scale bar = 0.5m). The species were identified with the help of taxonomic key of (Carvalho et al., 2000).The species were confirmed by many the specialist Dr. Michael Geiser from Natural History Museum, London ; Dr, Jiri Hava , Czech University of Life Sciences Prague ; Zdenko Lucbauer (Bratislava, Slovakia) ; Petr Kresl from Bucknell University, Lewisburg (Janovice nad Úhlavou, Czech Republic). **3. RESULTS**

Description

Synonyms

***Necrobia rufipes* De Geer ,1775**

= *Tenebrio dermestoides* Piller and Mitterpacher, 1783

= *Corynetes glabra* Champollion, 1814

= *Necrobia amethystinae* Stephens, 1832

= *Necrobia mumiarum* Hope (in Pettigrew), 1834

= *Necrobia pilifera* Reitter, 1894

= *Necrobia foveicollis* Schenkling, 1900

= *Necrobia pilifera* var. *aeneipennis* Csiki, 1900

= *Necrobia pilifera* var. *cupreonitens* Lauffer, 1905

Body (Fig.1a,b and c) Male

Elongated oval, slightly convex, shiny metallic green or greenish blue in colour , sides subparallel, widest at apical fourth. Surface densely setose punctate. The legs and antennae are red (dark clubs). Length 4.2– 6.8 mm.

Head : Oval, shiny metallic bluish-green, sparsely punctate , the punctures large and small intermingled, median portion of frons and vertex with very few punctures. Pubescence sparse, erect, and black. Eyes blackish brown, coarsely granulated, slightly emargination approximate to the antennal insertion, surface sparsely short black setose, length 3.4-4.0 mm. Frons and vertex with densely black short setose, sparsely punctate. Labrum(Fig.2 a) Dark yellow, moderately emarginated, surface sparsely setose and punctate, anterior edge long setose. Epipharynx yellow, posterior edge with row of short yellow setae. Mandible (Fig. 2b) stout with 4 denticles, upper denticle is the longest, two times as long as of below, surface sparsely yellow brown setose. Maxilla (Fig.2 c) brown-dark brown, sparsely short dark yellow setose, apical maxillary palpomere which is oval and apically truncate, 2^{nd}-3^{rd} palpomeres glass shaped, 2^{nd} palpomere

1.2 times as long as 3rd , 4th palpomere elongated oval , 2.1 times as long as 3rd , apical part of lacinia and galae highly long brown setose. Labium (Fig. 2d) brown-dark brown, Labium palps ,four segmented ,sparsely short dark yellow setose,1st segment is the smallest , 3rd segment elongated oval, 1.3 times as long as the 2nd. Antennae 11 antennomeres ; capitate form, dark yellow - dark brown , sparsely brown short setose; length 1.5-1.9 mm. 1st antennomere thick, slightly bent; 2nd about one-third the length of 1st , equilateral; third almost twice the length of second but of equal thickness; 4th -7th antennomeres mutually equal in length, each just perceptibly wider than the one preceding; the eighth is transverse; 9-11 antennomeres formed club, 9th and 10th antennomeres strongly transverse, subequal, about one-half as long as broad; the eleventh almost square1.2 as long as 10th.

Thorax: Pronotum narrow, sides evenly curved from base to apex, basal and apical angles very obtuse, lateral cariniform margin distinct, finely serrulate. Surface rather sparsely setose with moderately coarse punctures; punctures much more dense at sides than on disc; pubescence as on head. Scutellum small, transverse. Elytra long, suture closed, lateral margin finely beaded, each with nine distinct rows of punctures, the normally occurring tenth row being confused with the ninth; rows obsolete just behind the middle, surface between puncture rows and of apical portion rather densely 'set with fine punctures from each of which a posteriorly directed subrecumbent black hair arises. Under parts and legs rather finely and densely punctured, clothed with pale fulvous pubescence with a few longer black hairs interspersed. Legs moderately long, femora not greatly enlarged, tibiae straight, tarsal formula is 5–5–5, subsegments on each leg is typically lobed, and the 4th tarsi is very small and concealed between the lobes of the third, normally difficult to distinguish, the first three segments with lamelliform pads beneath. Claws rather long, provided at base with a broad toothlike appendage. In the female each of the elytral punctures, which are arranged in rows, gives rise to a stiff black hair slightly inclined anteriorly; in the male these hairs are subrecumbent and directed posteriorly.

Abdomen: Black, five visible segmented , densely black short setose , densely punctate.1st-4th abdominal sternite rectangular , 1st segment 1.1 as long the 2nd , 3rd and 4th segments same length, 5th segment cup shaped. 8th abdominal sternite (Fig. 2f) dark brown – black, cup shaped, anterior angle rod like, surface moderately brown setose, posterior margin densely black long, a stiff curved setose. 9th abdominal sternite (Fig. 2g) spade like, apical part tubular, basal part bilobed ,triangular. 9th abdominal tergite(Fig. 2h) expanded, cup shaped , posterior margin moderately ivagenated , surface sparsely brown short setose with long stout seta at each side.

Male genitalia: Aedeagus (Fig. 2 I and j) brown . Length 1.7-2.1 mm. In dorsal view(Fig. 2i) Tegmen triangular, 0.9-1.3 mm ; phallus tubular shaped striate at posterior, 1.9 times as long as tegmen; median lobe very slightly sclerotized and almost parallel; phallobasic apodem tubular, 0.8 times as long phallus. In Lateral view(Fig.2 j) Tegmen triangular at posterior, slightly curving to the right; phallus slender, long, slightly arched at posterior; aedegal apodem slender and narrow based, slightly arched at 1/3 of posterior.

a

b

c

Fig. 1. *Necrobia rufipes* De Geer (Body : Male) Scale bar =15 X
a. Dorsal view b. Ventral view c. Lateral view

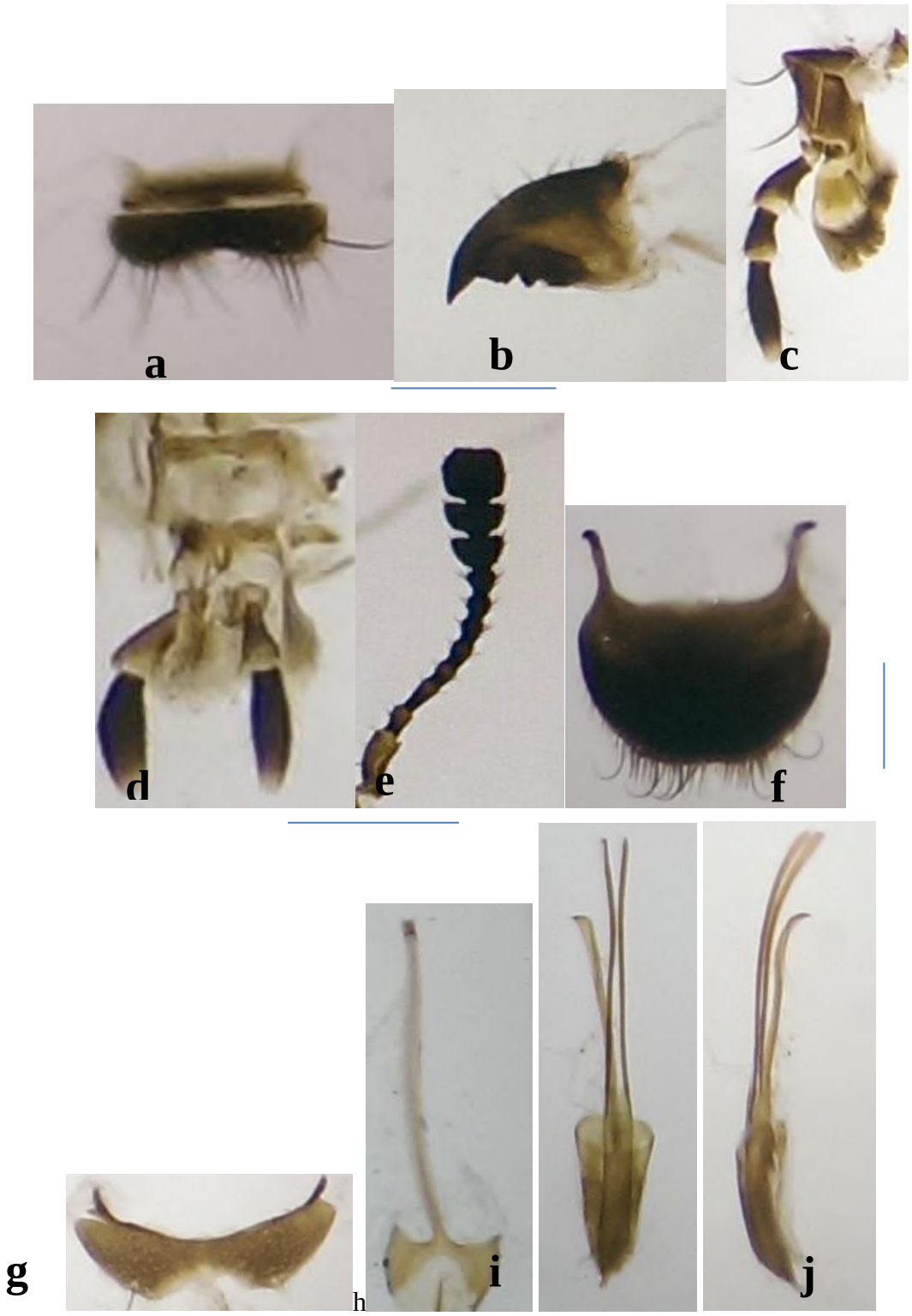

Fig .2. *Necrobia rufipes* De Geer
a. Labrum b. Mandible c. Maxilla d. Labium e. Antenna f. 8th abdominal sternite g.9th abdominal sternite h.^{9th} abdominal tergite i. Aedeagus(Dorsral view) g. Aedeagus (Lateral view) ; Scale bar = 0.5mm

AKOWNOLDEGMENTS

We sincerely thanks Dr. Michael Geiser the curators of Coleoptera (beetles) from Natural History Museum, London • Department of Life Sciences ; Dr, Jiri Hava , Czech University of Life Sciences Prague CULS., Department of Forest Protection and Entomology ; Zdenko Lucbauer (Bratislava, Slovakia) the interest of Opilo, Family Cleridae and Petr Kresl from Bucknell University, Lewisburg (Janovice nad Úhlavou, Czech Republic) for their assistance to identified the species.

REFERENCES

Al-Ali, A. S. (1977). Phytophagous and entomophagous insects and mites of Iraq. Natural History Research Center, Publishing 33:142 pp.

Ashman, F. (1963). Factors affecting the abundance of the copra beetle, *Necrobia rufipes* (Deg.) (Col, Cleridae). Bull. Entomol. Res., 53(4) : 671-680.

Carvalho, L.M.L., Thyssen, P.J., Linhares, A.X. and Palhares, F.A.B. (2000). A checklist of arthropods associated with pig carrion and human corpses in Southeastern Brazil. Mem. Inst. Oswaldo Cruz., 95(1):135-138.

Corporaal, L. B. (1950). Coleopterorum catalogus, pars 23 (editiosecunda) Cleridae. Uitgeveru Dr. Junk, The Hague, Netherlands, 373 pp.

Degeer, C. (1775). Mémoires pour servir a l'histoire des insectse, vol. 5. De l'impremiere de Pierre Hesselberg; Stockholm. 448 p.

Derwesh, A.I.(1965). A preliminary list of identified insects and arachnids of Iraq. Direct. Gen. Agr. Res. Proj. Baghdad. Bull., No. 121-123.

Foster, D. E. (1976a). Revision of North American *Trichodes* (Herbst) (Coleoptera: Cleridae). Special Publications, Museum Texas Tech University, Texas Tech Press, Lubbock, Texas.88 pp.

Foster, D. E.(1976b). North American Thaneroclerinae larvae (Coleoptera: Cleridae) Coleopterists Bulletin, 30(1): 75-80.

Furniss, R. L. and Carolin, V. M. (1977). Western forest insects.United States Department of Agriculture, Forest Service. Miscellaneous Publications 1339.654 pp.

Gerstmeier, R.(2000). Aktueller Stand der Buntkäfer-Forschung (Coleoptera, Cleridae, Thanerocleridae). Entomologica Basiliensia , 22, 169–178.

Haines, C.P. D. and Rees, D. P. (1989). *Necrobia rufipes* . A field guide to the types of insects and mites infesting cured fish. Food and Agriculture Organization.

Lane, R. P. and Crosskey, R. W. (1993). Medical insects and arachnids. The Natural History Museum. Chapman and Hall, London.

Lawrence, J.F. and Newton Jr., A.F. **(**1995). Families and subfamilies of Coleoptera (with selected genera, notes, references and data on family-group names). In: Pakulak J & Slipinski SA (eds.). Biology, phylogeny, and classification of Coleoptera: papers celebrating the 80th birthday of Roy A. Crowson.

Majka, C. G.(2006). The checkered beetles (Coleoptera: Cleridae) of the Maritime Provinces of Canada. Zootaxa, 1385: 31-46.

Mawlood, N.A., Hamad M.I. and. Abdullah ,Y.M. (2016). A new record of glaphyrid scarab beetles ,*Eulasia vitatta* (Fabricius , 1775) (Coleoptera, Glaphyridae) from Erbil Kurdistan region-Iraq . Zanco Journal of Pure and Applied Sciences .28 (3): 1-4 .

Nwana, I.E.A.(1993) . Survey of storage Coleoptera with attack dried cocoyam chips in Nigeria. J. Stored Prod. Res., 29, (95): p. 98.

Opitz, W. (2002). Cleridae. Pp. 267-728. In: American Beetles, Volume 2. Arnett, R. H and Thomas, M. C. (eds.). CRC Press, Boca Raton, lorida.861 pp.

Ronald, G. (1998). Checkered Beetles: Illustrated Key to the Cleridae and Thanero cleridae of the Western Palaearctic.Weikersheim,Germany: Margraf Verlag. pp. 12–15.

Sengupta, T., Mukhopadhyay, P. and Sengupta, R. (1984). Major beetle pest of stored food products in India. Records Zool. Surv. India Occas., 62, 65-66.

Triplehorn, C. A Johnson, N. F. (2005). Borror and DeLong's introduction to the study of insects (7th ed.). Belmont: Brooks/Cole. Pp.428–429.

ZANCO Journal of Pure and Applied Sciences
The official scientific journal of Salahaddin University-Erbil
https://zancojournals.su.edu.krd/index.php/JPAS

ISSN (print):2218-0230**, ISSN (online):** 2412-3986**, DOI: http://dx.doi.org/10.21271/zjpas**

RESEARCH PAPER

Effect of foliar application of Phosphorus on Growth and development of *Vicia faba L.* under Magnesium levels

Halalal R. Qader

Department of Environmental science, College of Science, Salahaddin University- Erbil, Kurdistan Region, Iraq.

A B S T R A C T:

The present experiment was done to study the interaction of foliar application effect of phosphorus and magnesium on faba bean plants. This study conducted in Biology Department in the College of Science- University of Salahaddin- Erbil during November 2, 2017 to February 20, 2018 in the greenhouse as pot experiment. The experiment consisted of combination treatments of foliar spray with different phosphorus (P) concentrations at doses (0, 100, 200, 300, 400, 500 ppm) and soil irrigation by two magnesium (Mg) concentrations (0, 200 ppm). This study consists of 12 treatments with three replications. The following parameters has been observed: plant height, leaf and branch numbers, water content and dry weight of shoot system, leaf area, stem diameter, yield components including pod and seed numbers, dry weight of 100 seeds and photosynthetic pigments. The results indicate that phosphorus and magnesium interactions significantly increase plant height, number of branches, water content, leaf area, number of pods per plant, carotenoid contents.

KEY WORDS: Phosphorus, Faba bean, Magnesium ,Leaf area ,Pigments .
DOI: http://dx.doi.org/10.21271/ZJPAS.31.4.18
ZJPAS (2019) , 31(4);173-179. .

1.INTRODUCTION :

Vicia faba L. (faba bean) is a herbaceous annual plant species belongs to Papilionaceae (Fabaceae) family, domesticated in the middle east, Mediterranean region, Ethiopia, and China. It is used as an important crop for human food as dried or fresh vegetables (Shakori & Sharifi, 2016). Nutritionally, it is a main source of potassium, iron and vitamins A and C. (Glow, 2010). Faba bean an important source of protein in plants for humans (Cazzato *et al.*, 2012). Faba bean is a famous winter leguminous crops in Iraq, it is cultivated in crop rotations to improve soil properties, through atmospheric nitrogen fixation and serve as cheap source of protein (Jasim, 2007 and Akibode and Maredia, 2007). Faba beans are rich of vitamins, sugar, carbohydrates, starch, lipids, fats, minerals especially calcium and iron. (Salih *et al.*, 1986).

Phosphorus is an essential mineral nutrient for some of the physiological functions in plants, they required for growth. Phosphorus has basic role in such processes in the plants including photosynthesis process, respiration, energy transfer and storage, important in the division of cell and cell enlargement, nutrients movement within the plant (Jin *et al.*, 2005 and Tang *et al.*, 2009). Phosphorus has their role in increasing growth of faba beans and has it role in increasing the number and size of a nodule which fixing the nitrogen, legumes need some amount of phosphorus for their growth (Hammayun *et al.*, 2011). Plants required uptake of phosphorus a

* **Corresponding Author:**
Halalal R. Qader
E-mail: halala.qader@su.edu.krd or halala.rahman@gmail.com
Article History:
Received: 7/01/2019
Accepted: 28/05/2019
Published: 10/09 /2019

nutrient for their growth for all stages from seed to adult plant.

Magnesium is an essential and important macronutrients for growth and development of plants (Cakmak and Kirkby, 2008). Magnesium has some physiological and biological roles in plants, photophosphorylation (formation of nucleic acid is a nucleotide used in cells as a coenzymes formation in chloroplasts) which took the leaves green color, plant respiration, photosynthetic carbon dioxide (CO2) fixation, protein synthesis, chlorophyll formation, phloem loading, photooxidation in leaf tissues, activating such enzymes which have role in process of photosynthesis (Cakmak and Atilla, 2010). Some plants required high amount of magnesium than others like legumes (Wayatt, 1967).

The main objectives of this study were to elucidate the interaction of foliar application of phosphate and soil application of magnesium effects on faba bean plants.

2. MATERIALS AND METHODS

This study was conducted in the glasshouse of the biology Department, College of Science, University of Salahaddin-Erbil, during November 2, 2017 to February 20, 2018 to investigate the interaction effects of phosphorus (P) and Magnesium (Mg) on growth and development of faba bean (Elisar). The study involved 36 plastic pots each pot with a diameter of 24 cm in length and 21 cm in dept. Each pot filled with 7kg of dry sandy loam soil of Askikalak area, the soil sieved through 2mm pore size sieves, add in each pot 3 seed were sown. This experiment consisted of combination treatments of foliar spray with different Phosphorus (NaH_2PO_4) concentrations at doses (0, 100, 200, 300, 400, 500ppm) and soil irrigation by two Mg ($MgSO_4$) concentrations (0, 200 ppm), and involved 12 treatments with three replications. The following measurements has been taken for each pot: plant height (cm), number of leaves.plant^{-1}, number of branches.plant^{-1}, shoot dry weight (g),water content of shoot system, leaf area(cm^2), stem diameter, yield components such a number of pods.plant^{-1}, number of seeds.pod^{-1}, dry weight of 100 seeds(g), and photosynthetic pigments.

Water content (g.plant^{-1}) of shoot system estimated as follows: firstly, fresh shoot has been weight, secondly shoot dried at 110°C for 1 hrs, and then at 70°C for 24 hrs, in an oven. After that cooled at room temperature, dry weight of shoot obtained for half an hour (He *at al.*, 2005).

Water content =F.wt.-D.wt.

F.wt. =fresh weight

D.wt. =dry weight

Chlorophyll content in leaves (mg.g^{-1}) estimated by taking 0.5g of fresh leaves left in 10 ml of absolute ethanol for 24 hrs. In dark condition, this process repeated three times to complete extraction of chlorophyll the final volume reached 30 ml were spectrophotometrically estimates on two wavelength 649and 665 nm as follows (Wintermans and Demote, 1967):

µg chlorophyll a/ml solution = (13.70) (A665nm)-(5.76) (A 649nm)

µg chlorophyll b/ml solution = (25.80) (A649nm)-(7.60) (A 665nm)

Total chlorophyll =chlorophyll a + chlorophyll b

µg Carotenoid/ml solution=(1000 A_{470} -2.13 C a-97.64*C b)/209

A=absorbance

m =nanometer

Statistical analysis

The data of this study designed according to Factorial Completely Randomized Designs (Factorial C.R.D) with three replications and tweleve treatments. Duncan Multiple Range Test used for the comparison of treatment means at 5% for greenhouse parameters and 1% levels for laboratory parameters (Muhummed, 2004). The statistical analysis was done by using Statistical Package for Social Sciences (SPSS version 16 software). For drawing charts, Excel 2007 software used.

3. RESULTS AND DISCUSSION

3.1. Vegetative growth characteristics

The data in table (1) shows that foliar application of phosphorus significantly ($p \leq 0.05$) increased plant height at doses (400 ppm) under (0 ppm) of magnesium after 45 days from application as compared with their controls, as well as there were significant differences between treatments (200, 400ppm) under (0ppm) of magnesium after 30 days from application. It was observed that there were significant differences between foliar application of phosphorus at doses

(500 ppm) under (200 ppm) of magnesium after 45 days from application in the number of branches as compared their control (table 3), as well as leaf area also significantly ($p \leq 0.05$) increased by phosphorus application at rate (400 ppm) under (0ppm) of magnesium as compared with their control. Water contents of shoot system significantly ($p \leq 0.05$) increased at doses (100ppm) under (0ppm) of magnesium as compared with their control table (4). These results partially agreed with those obtained by (Turk, 2003) that phosphorus increased plant height. (Ga, 2017) mentioned that phosphorus increased plant height in faba bean plants which increased nitrogen fixation due to growth and developments of plants. (Senbayram *et al.*, 2015) notice that magnesium have many roles in physiological process for plant growth and development.

3.2. Yield components

Table (5) shows that foliar application of phosphorus significantly ($p \leq 0.05$) increased number of pods at doses (200 ppm) under (0ppm) of magnesium as compared with their control, and there were significant difference between treatments (100, 300 ppm) under (200 ppm) of magnesium. These results agreed with those obtained by (Hamayun, 2011 and Kleiber *et al.*, 2012) that phosphorus and magnesium increased the plant yields. It was noticed that foliar application of phosphorus under magnesium levels increased yield components which due to increases products of plants.

3.3. Photosynthetic pigments

According to the results in table (6) there were significant differences between treatments at dose (100, 400ppm of phosphorus under (0ppm) of magnesium in carotenoid contents. These results partially agreed with those obtained by (Alam and Sheren, 2002) (Kleiber *at al*, 2012) showed that phosphorus and magnesium increased chlorophyll contents of leaves. As well as an increased in the photosynthetic pigments led to increased photosynthetic energy this led to increase process of photosynthesis and growth of plant. (Razaq *et al.,*) mentioned that biosynthesis of green pigments in leaves depend on P concentrations, and also increase production and biomass of carotenoid in plants.

Table 1: Interaction effects of phosphorus and magnesium on plant height at different stages of growth

Interaction treatments		Plant height (cm) after (days) from application		
Mg ppm	**P ppm**	**15 days**	**30 days**	**45 days**
0	0	43.00 c	59.33 ab	68.33 c
	100	46.00 abc	58.66 c	69.33 bc
	200	48.33 ab	67.66 a	76.00 ab
	300	43.66 c	51.66 c	61.66 d
	400	47.33 ab	66.33 a	76.66 a
	500	45.33 bc	61.00 ab	70.66 bc
200	0	43.33 c	60.00 ab	68.68 c
	100	44.66 bc	64.33 ab	72.00 abc
	200	43.66 c	64.66 ab	73.33 abc
	300	45.66 bc	59.66 ab	68.66 c
	400	46.33 bc	60.33 ab	67.66 cd
	500	46.66 bc	60.66 ab	70.00 bc

*Data presented as mean, the same letters mean not significant differences while the different letters mean significant differences $p \leq 0.05$

Table 2: Interaction effects of phosphorus and magnesium on number of leaves at different stages of growth

Interaction treatments		Number of leaves after (days) from application		
Mg ppm	**P ppm**	**15 days**	**30 days**	**45 days**
0	0	16.33 a	30.00 a	39.00 a
	100	16.66 a	33.66 a	41.66 a
	200	16.00 a	26.33 a	35.00 a
	300	16.16 a	33.00 a	41.00 a
	400	18.33 a	30.33 a	44.33 a
	500	18.00 a	31.00 a	39.00 a
200	0	17.66 a	32.66 a	41.00 a
	100	17.33 a	31.66 a	39.33 a
	200	17.00 a	35.00 a	43.66 a
	300	18.33 a	31.66 a	38.66 a
	400	16.33 a	33.33 a	42.33 a
	500	18.00 a	31.33 a	39.33 a

*Data presented as mean, the same letters mean not significant differences while the different letters mean significant differences $p \leq 0.05$

Table 3: Interaction effects of phosphorus and magnesium on number of branches at different stages of growth

Interaction treatments		Number of branches after (days) from application		
Mg ppm	**P ppm**	**15 days**	**30 days**	**45 days**
0	0	8.00 a	12.33 a	15.33 b
	100	8.66 a	13.00 a	16.00 b
	200	8.00 a	13.3 a	15.00 b
	300	8.00 a	15.00 a	17.66 ab
	400	8.33 a	13.00 a	16.00 ab
	500	8.66 a	13.66 a	14.66 b
200	0	7.66 a	13.33 a	16.00 ab
	100	9.00 a	12.66 a	16.00 ab
	200	8.00 a	12.33 a	16.33 ab
	300	7.99 a	13.33 a	16.66 ab
	400	8.33 a	12.66 a	17.66 ab
	500	8.66 a	14.33 a	18.33a

*Data presented as mean, the same letters mean not significant differences while the different letters mean significant differences $p \leq 0.05$

Table 4: Interaction effects of phosphorus and magnesium on some vegetative growth characteristics

Interaction treatments		vegetative growth characteristics			
Mg ppm	**P ppm**	**Shoot dry weight (g.plant^{-1})**	**Leaf area cm^2.plant^{-1}**	**Stem diameter (cm)**	**Water contents (g.plant^{-1})**
0	0	1.92 a	540.06 b	1.92 a	9.52 b
	100	2.01 a	676.09ab	2.01 a	10.13 ab
	200	2.20 a	627.53 ab	2.20 a	11.96 ab
	300	2.13 a	512.21 b	2.13 a	10.79 ab
	400	2.23 a	846.10 a	2.23 a	11.07 ab
	500	2.09 a	688.33 ab	2.09 a	11.81 ab
200	0	2.21 a	694.56 ab	2.22 a	13.38 ab
	100	2.04 a	592.30 ab	2.04 a	14.500 a
	200	1.87 a	652.18 ab	2.11 a	12.95 ab
	300	2.19 a	734.78 ab	2.24 a	10.68 ab
	400	2.15 a	623.97 ab	2.26 a	10.87 ab
	500	2.06 a	685.30 ab	2.06 a	13.0 b

*Data presented as mean, the same letters mean not significant differences while the different letters mean significant differences p≤0.05

Table 5: Interaction effects of phosphorus and magnesium on some yield components

Interaction treatments		yield components		
Mg ppm	**P ppm**	**Number of pods.plant^{-1}**	**Number of seeds.pod^{-1}**	**Dry weight of 100 seeds(g)**
0	0	7.00 b	3.66 a	62.33 b
	100	8.33 ab	4.33 a	68.33 ab
	200	10.66 a	4.66 a	61.33 b
	300	10.33 ab	5.00 a	62.00 b
	400	8.66 ab	4.66 a	65.00 ab
	500	9.00 ab	5.33 a	66.33 b
200	0	10.00 ab	4.66 a	69.33 ab
	100	9.33 ab	5.00 a	72.33 a
	200	8.33 ab	5.33 a	65.66 ab
	300	10.33 ab	5.66 a	72.00 a
	400	10.66 a	4.66 a	67.33 ab
	500	9.66 ab	4.33 a	68.33 ab

*Data presented as mean, the same letters mean not significant differences while the different letters mean significant differences p≤0.05.

Table 6: Interaction effects of phosphorus and magnesium on photosynthetic pigments of leaves (mg.g^{-1}fresh weight)

Interaction treatments		Photosynthetic pigments (mg.g^{-1}fresh weight)			
Mg ppm	**P ppm**	**Chlorophyll a**	**Chlorophyll b**	**Total chlorophyll**	**Carotene**
0	0	1.64 a	1.55 ab	3.19 bcd	0.83 abcd
	100	2.05 a	1.57 ab	3.62 abcd	0.91 a
	200	1.77 a	1.16 b	2.93 d	0.79 d
	300	1.99 a	2.10 a	4.10 a	0.90 abc
	400	2.01 a	1.76 ab	3.77 ab	0.92 a
	500	1.97 a	1.31 b	3.29 bcd	0.86 abcd
200	0	1.88 a	1.75 ab	3.64 abc	0.80 cd
	100	1.90 a	1.12 b	3.21 bcd	0.83 abcd
	200	1.97 a	1.31 b	3.28 bcd	0.81 cd
	300	1.92 a	1.30 b	3.04 cd	0.86 abcd
	400	1.88 a	1.34 b	3.22 bcd	0.84 abcd
	500	1.96 a	1.38 b	3.34 bcd	0.89 ab

*Data presented as mean, the same letters mean not significant differences while the different letters mean significant differences $p \leq 0.01$

4. CONCLUSIONS

According to the obtained results from the present study, the interaction effect of foliar application of phosphorus and soil irrigation of magnesium has effective role in growth and development of faba bean plants through significantly increased plant height, number of branches, leaf area, water content, dry weight of shoot system and yield characteristic number of pods per plant, dry weight of 100 seeds, as well as chlorophyll b, total chlorophyll and carotene pigments.

REFERENCES

AKIBODE, S. and M.MAREDIA 2011. Global and regional trends in production, trade and consumption of food legume crops. In: Report submitted to SPIA. Department of Agriculture, Food and Resource Economics, Michigan State University.

ALAM, S. A. AND SHEREEN. 2002. Effect of different levels of zinc and phosphorus on growth and chlorophyll content of leave. *Asian journal of plant Science*. Vol, 1:4, 364-366.

CAKMAK, I. AND A. M. YAZICI. 2010. Magnesium: A Forgotten Element in Crop Production. *Better crops*.vol:94, 23-25.

CAkMAK, I., E.A. KIRKBY . 2008. Role of magnesium in carbon partitioning and alleviating photooxidative damage. *Physiologia Plantarum*; 133, 692–704.

CAZZATO, E. V. TUFARELLI, C. E. STELLACCI AM. AND LAUDALIOV. 2012. Quality, yield and nitrogen fixation of faba bean seeds as affected by sulphur fertilization. *Acta Agriculturae Scandinavica. Section B-Soil and Plant Sci.* 62(8):732-738.

GLOW- WORM, PJ11 MAR. 2010. Benefits and dangers of the broad bean.

HAMAYUN, M., S. AFZAL KHAN, A. KHAN, Z. K. SHINWARI, N. AHMAD, Y. HAKIM AND I. LEE. 2011. Effect of foliar and soil application of Nitrogen, Phosphorus and Potassium on yield components of lentil. *Pak. J. Bot.*, 43(1): 391-396.

HE, Y.; Y. LIU; W. CAO; M. HUAI; B. X and B. HUANG. 2005. Effects of Salicylic Acid on Heat Tolerance Associated with Antioxidant Metabolism in Kentucky Bluegrass. *Am. Crop Sci. Soci.*, 45:988-995.

JASIM, A. H. 2007. Effect of foliar fertilization on growth and yield of broad bean *Vicia faba* L. Alanbar J.Agric. Sci., 5(2):177-182.

JIN, J., W, G. H., X. LIU , X. PAN AND H. SJ. 2005. Phosphorus application affects the soybean root response to water deficit at the initial flowering and full pod stages. *Soil Science and Plant Nutrition*, 51 (7):953–960.

KLEIBER, T., A. GOLCZ AND W. KREZESINSKI. 2012. Effect of Magnesium nutrition of Onion (*Allium*

cepa L.) Part 1 yields and nutrients status. *Ecol. Chem. Eng*. S.(19) 1, 97-105.

MAM RASUL, GA. 2017. Effect of Different Levels of Nitrogen and Phosphorus on Yield and Yield Components of Faba bean (*Vicia faba* L.) in Calcareous Soil from Kurdistan Region of Iraq. *Journal of A agricultural Research*, Vol: (2) 1, 1-6.

MUHAMMED, M.Q. 2004. Effect of zinc and its interaction with two auxins (IAA&NAA) on the growth and development of Pea (*Pisum sativum* L.)Var. Little Marvel.Thesis, Erbil. Iraq.

Razaq, M, P. Zhang, H. Shen and Salahuddin. 2017. Influence of nitrogen and phosphorus on the growth and root morphology of *Acer mono. journal pone*, 12 (2): 1-13

SALIH F. A., A.M. ALI AND A.A. ELMUBARAK. (1986). Effect of phosphorus application and time of harvest on the seed yield and quality of faba bean. FABIS Newsletter, 15: 32-35.

SENBAYRAM, MEHMET, ANDREAS GRANSEE, VERENA WAHLLE AND HEIKE THIEL. 2015. Role of magne sium fertilisers in agricu lture: plant–soil continuum. Crop and Pasure Sceinces, 66, 1219-1229.

SHAKORI, SHARAM AND PEYMAN SHARIFI. 2016. Effect of Phosphate Biofertilizer and Chemical Phosphorus Growth and Yield of Vicia faba L. electronic journal of biology. VolS1: 47-52.

TANG, C., H. XZ, O. YF AND Z. SJ. 2009. Phosphorus deficiency does not enhance proton release by roots of soybean (*Glycine max* (L.) Murr.). *Environmental and Experimental Botany;* 67(1):228–234.

TURK, M., A. TAWHA AND N. SAMARA. 2003. Effects of seeding rate and date and phosphorus application on growth and yield of narbon vetch (*Vicia narbonensis*). *Agronomie, EDP Sceinces*, 23 (4), pp.355-358.

Wayatt, F. A. 1967. Influence af calcium and magnesium compounds on plant growth". *Journal of Agricultural Research.*Vol: V1, No:6.

WINTERMANS, J.F AND A. DEMOTE. 1965. Spectrophotometry characterstics of chlorophyll (a) and (b) and their phynophytins in ethanol. *Bioch.BiophysiologyActa.,* 109:448-453.